

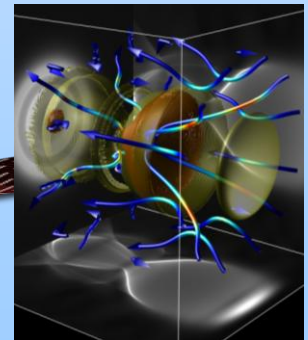
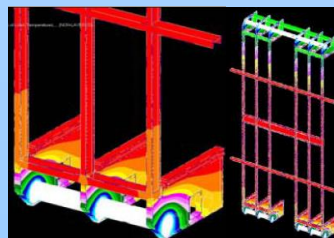
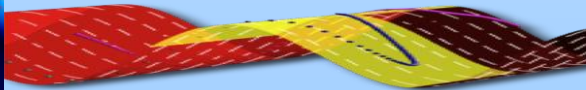
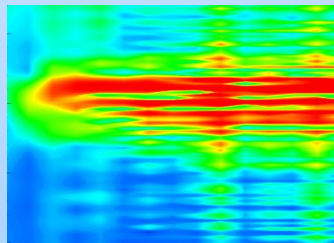
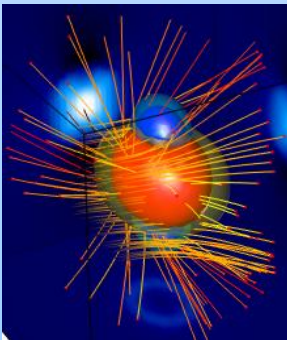


ipfn

INSTITUTO DE PLASMAS E FUSÃO NUCLEAR

ASSOCIATION EURATOM/IST
ASSOCIATED LABORATORY WITH FCT

2008 ANNUAL REPORT





ipfn

INSTITUTO DE PLASMAS E FUSÃO NUCLEAR

ASSOCIATION EURATOM/IST ASSOCIATED LABORATORY WITH FCT

2008 ANNUAL REPORT

Activities carried out in the frame of:

- **The Contract of Association EURATOM/IST on Plasma Fusion Research**
- **The Contract of Associated Laboratory with FCT on Plasma Physics and Engineering**

CONTENTS

	Page
<i>A. FOREWORD</i>	
1. Introduction	
1.1. Foreword	1
1.2. Organization	1
1.3. Activities on controlled nuclear fusion	1
1.4. Activities on technologies of plasmas and intense plasmas	2
<i>B. CONTROLLED NUCLEAR FUSION¹</i>	
2. Tokamak ISTTOK	
2.1. Introduction	5
2.2. Liquid metal limiter	5
2.3. Study of fusion relevant materials	6
2.4. Diagnostics	6
2.5. Real time control and data acquisition	7
2.6. Plasma physics studies	8
3. Participation in the use of the JET facilities by the EFDA Associates	
3.1. Introduction	11
3.2. Operation	11
3.3. Scientific exploitation	11
3.4. Performance enhancements	18
3.5. Management	21
4. Participation in the ITER project	
4.1. Introduction	23
4.2. Diagnostics	23
4.3. Control and data acquisition	24
4.4. Heating systems	25
4.5. Remote handling	26
5. Participation in the ASDEX-Upgrade programme	
5.1. Introduction	29
5.2. Microwave reflectometry	29
5.3. Plasma physics studies	30
6. Participation in the TJ-II programme	
6.1. Introduction	33
6.2. Microwave reflectometry	33
6.3. Edge physics	33
6.4. Heavy ion beam analyser	34
7. Participation in the TCV programme	
7.1. Introduction	35
7.2. X-ray diagnostics	35
7.3. Advanced plasma control system	37
8. Participation in the COMPASS project	
8.1. Introduction	39
8.2. Tokamak systems	39
8.3. FW-CW reflectometry system	39
8.4. Control and data acquisition	40

¹ Activities carried out in the frame of the Contract of Association EURATOM/IST and the Contract of Associated Laboratory.

9. Collaboration with the Association EURATOM/CEA	
9.1. Introduction	41
9.2. ITER-like PAM LH launchers	41
9.3. Microwave reflectometry	41
9.4. Motional stark effect diagnostic	42
9.5. Stochastic solutions of the poisson-Vlasov and Maxwell-Vlasov system	42
10. Other theory and modelling studies	
10.1. Introduction	43
10.2. Dynamical systems' description of ITB oscillations	43
10.3. Tokamak equilibria with toroidal current reversal	43
10.4. Noniterative reconstruction of tokamak equilibria	43
10.5. Signal processing	44
10.6. Integrated tokamak modelling task force	45
10.7. ITER scenario modelling	45
10.8. Other studies	46
11. Keep-in-touch activities in inertial fusion energy	
11.1. Introduction	47
11.2. Fast ignition	47
11.3. High intensity photonics	47
11.4. Plasma accelerators and intense radiation sources	47
11.5. Fast electron transport theory for the HiPER project	47
12. Participation in the fusion technology programme	
12.1. Introduction	49
12.2. Characterization of fusion materials using nuclear techniques	49
12.3. Socio-economic studies on nuclear fusion	50
13. Other fusion-related activities	
13.1. Introduction	51
13.2. Collaboration with Brazilian Institutions	51
13.3. Collaboration with W7-X project	51
13.4. Education and training	52
13.5. Organization of scientific meetings	52
13.6. Outreach activities	52
13.7. Participation in the management of international fusion programmes and projects	53
 <i>C. TECHNOLOGIES OF PLASMAS AND HIGH POWER LASERS²</i>	
14. Plasma theory and simulations	
14.1. Introduction	55
14.2. Laser-plasma accelerators with the next generation lasers	55
14.3. Radiation from self-injected beams of laser-plasma accelerators with the next generation lasers	55
14.4. One-to-one direct modelling of experiments and astrophysical scenarios:pushing the envelope on kinetic plasma simulations	55
14.5. Hardware acceleration of pic codes: tapping into the power of state of the art processing units	56
14.6. Selective trapping and acceleration of charged particles	56
14.7. All-optical ultrafast muon acceleration	57
14.8. Monte Carlo simulations of relativistic collisions in plasmas	57
14.9. Laser-driven nuclear fusion in homonuclear and heteronuclear clusters	57
14.10. Laser plasma interaction in the regime of the extreme light infrastructure	57
14.11. Migrating large output applications to grid environments	58
14.12. Streaming the boris pusher: a cuda implementation	58
14.13. Solar energetic particle acceleration in coronal mass ejection shock fronts	59
14.14. Non-resonant magnetic field amplification in supernova remnant shocks	59
14.15. One-to-one experimental modeling of self-guided propagation in LWFA	59
14.16. Generation of single cycle laser pulses in plasmas	60
14.17. Boosted frame pic simulations of LWFA: towards the energy frontier	60
14.18. Ion dynamics and acceleration in relativistic shocks	61

² Activities performed in the frame of the Contract of Associated Laboratory, out of the Contract of Association EURATOM/IST.

14.19. High-brilliance synchrotron radiation induced by the plasma magnetic mode	61
14.20. Fast ignition with ultrahigh intensity lasers	61
14.21. Post-processing radiation modeling	62
14.22. Betatron radiation in laser-wakefield accelerators	62
14.23. Ion acoustic instability	63
14.24. Hybrid simulations of high-energy ion interaction with mini-magnetospheres	63
15. Laser-plasma accelerators and applications	
15.1. Introduction	65
15.2. Pre-formed plasma channels using discharges in structured gas cells	65
15.3. The use of a simmer discharge to improve the quality of plasma channels	65
15.4. Improvements of the gas cell design and experimental setup	66
15.5. Compact free-electron-lasers (FEL)	67
15.6. Transverse dynamics of a plasma column created by field ionization	67
16. High intensity laser science and technology	
16.1. Introduction	69
16.2. Spatio-temporal distortion from beam propagation in grating compressors	69
16.3. Full front-end characterization	69
16.4. Supercontinuum generation in solid state media	69
17. Coherent soft-x-ray sources	
17.1. Introduction	71
17.2. Online tuning of the quasi-phase matched order	71
17.3. Polarization of high order harmonics in two-colored fields	71
17.4. Tunability of spectrally narrow high order harmonics	72
17.5. Optimization of soft x-ray amplifiers for seeded x-ray lasers	73
18. Generation of electromagnetic radiation in plasmas and diagnostics	
18.1. Introduction	75
18.2. The characterization and generation	75
18.3. Radiation sources based on a GEV laser wakefield accelerator and electro beam characterization ...	76
19. High density laser-plasma physics	
19.1. Introduction	79
19.2. Fast electron transport theory for the HiPER project	79
19.3. Laser-solid experiments	79
20. Environmental engineering plasma laboratory	
20.1. Introduction	81
20.2. Plasma torches for environmental issues	81
20.3. Extraordinary phenomena in hydrogen plasmas	83
20.4. Improvement of plasma diagnostic techniques	84
21. Non-equilibrium kinetics and simulations of plasmas and afterglow plasmas	
21.1. Introduction	85
21.2. Modelling of fundamental kinetic and radiative processes in low-pressure, high temperature plasmas	85
21.3. Study of N ₂ -O ₂ afterglow plasmas for plasma sterilization of thermosensitive medical instruments ..	87
21.4. Study of AR-O ₂ afterglow plasmas for plasma sterilization and insight into elementary processes ...	88
21.5. Simulation of surface atomic recombination	88
21.6. Kinetic modelling of low-pressure DC discharges in air	88
21.7. Study of N ₂ -O ₂ post-discharges when oxygen is added downstream a pure nitrogen microwave discharge	89
21.8. Simulation of titan's atmosphere using a N ₂ afterglow plasma with CH ₄ addition in the post-discharge	89
22. Modelling of plasma sources	
22.1. Introduction	91
22.2. Microwave-driven plasma reactor operated by an axial injection torch	91
22.3. Micro-plasma reactors	92

22.4. Capacitively coupled plasma reactors	95
23. Fundamental physics in space	
23.1. Introduction	97
23.2. Generalized chaplygin gas model	97
23.3. Braneworld models and Lorentz invariance	97
23.4. F(R) extensions to general relativity	97
23.5. Non-commutative quantum mechanics	97
23.6. Mission design of fundamental physics tests	97
23.7. Thermal modelling of the pioneer anomaly	98
24. Quantum plasmas	
24.1. Introduction	99
24.2. Plasma effects in magneto-optical traps (MOT)	99
24.3. Waves in quantum plasma	100
24.4. Theoretical methods	100
24.5. Electromagnetic diagnostics for weakly ionized plasma flows	100
25. Other activities of the research line on intense lasers and plasmas technologies	
25.1. Introduction	101
25.2. Outreach activities	101
25.3. Organization of scientific meetings	101
25.4. Participation in the management of international projects and programmes	101
<i>D. SCIENTIFIC OUTPUTS, PRIZES AND AWARDS</i>	
26. Publications, laboratorial prototypes, prizes and awards	
26.1. Magnetic fusion	103
26.2. Technologies of plasmas and lasers	113
<i>E. ANNEXES</i>	
27. Annex I - Composition of the management bodies in 2008	121

1. INTRODUCTION

C. Varandas¹, F. Serra², L.O. Silva³

1.1. FOREWORD

This document is the first Annual Report of “Instituto de Plasmas e Fusão Nuclear” (IPFN), a research unit of “Instituto Superior Técnico” (IST) created on January 1st 2008 from the previous “Centro de Fusão Nuclear” (CFN) and “Centro de Física de Plasmas” (CFP), two units with national and internationally well recognized expertise in several areas of magnetic and inertial nuclear fusion, plasma physics and engineering, lasers and photonics and advanced computing.

The activities described in this document were mainly carried out in the frame of:

- The Contract of Association (CoA) signed in 1990 between the “European Atomic Energy Community” (EURATOM) and IST, hereinafter referred to as Association EURATOM/IST;
- The Contract of Associated Laboratory signed in 2001 by “Fundação para a Ciência e a Tecnologia” (FCT), hereinafter mentioned as Associated Laboratory (AL).

The quality of our research and development activities is well expressed by the scientific output: 188 articles in referred journals (2,9 articles per Ph.D) and 10 laboratorial prototypes.

Finally, some events should be underlined by their relevance (i) the increase of our participation in the JET scientific campaigns (Figure 1.1); (ii) significant participation in the COMPASS project; (iii) an important role played in the negotiations of an Agreement between EURATOM and Brazil; (iv) the beginning of the participation of Portuguese research units and firms in the ITER construction; (v) the signature of the contracts for the Portuguese participation in HiPER and ELI, two important projects foreseen in the road map of the European Strategy Forum on Research Infrastructures (ESFRI).

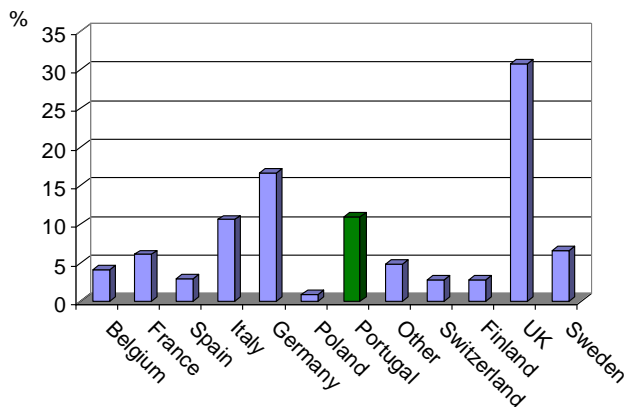


Figure 1.1 – Participation in the 2008 JET campaigns

1.2. ORGANIZATION

Figure 1.2 presents a block diagram of the IPFN organization. The scientific activity is organized in two Thematic Areas:

- Controlled Nuclear Fusion;
 - Technologies of Plasmas and Intense Lasers.
- and six Scientific Groups:
- Experimental Physics on Magnetic Confinement Fusion Devices;
 - Microwave Diagnostics for Fusion Plasmas;
 - Theory and Modelling of Magnetic Confinement Fusion Plasmas;
 - Control and Data Acquisition;
 - Lasers and Plasmas;
 - Gas Discharges and Gaseous Electronics.

1.3. ACTIVITIES ON CONTROLLED NUCLEAR FUSION

1.3.1. Introduction

These activities, carried out according to the Contract of Association EURATOM/IST are described in chapters 2 to 13.

The CoA frames the Portuguese participation in the EURATOM Specific Research and Training Programme in the Field of Nuclear Fusion Energy, hereinafter referred as Community Fusion Programme. This Programme has as its long-term objective the development of a prototype commercial fusion power plant. It is presently implemented through several Agreements, in particular: (i) Contracts of Association signed between EURATOM and Institutions of the Member States of the European Union (EU) and Switzerland (Associates); (ii) the European Fusion Development Agreement (EFDA) and the Mobility Agreement, both signed by EURATOM and its Associates; and (iii) the European Joint Undertaking for ITER and the Development of Fusion Energy (F4E), signed by EURATOM, the EU Member States and Switzerland.

1.3.2. Main projects of the Association EURATOM/IST

The work programme of the Association EURATOM/IST included activities carried out in Portugal (mainly related with the tokamak ISTTOK) and abroad related with the operation and scientific exploitation of large and medium-sized tokamaks and stellarator (JET, ASDEX-Upgrade, TCV, and TJ-II) as well as with the design and construction of the next generation fusion devices (ITER and W7-X). Its main projects in 2008 were:

¹President of IPFN.

²Vice-President of IPFN and Head of the Research Unit of the Contract of Association EURATOM/IST.

³Vice-President of IPFN.

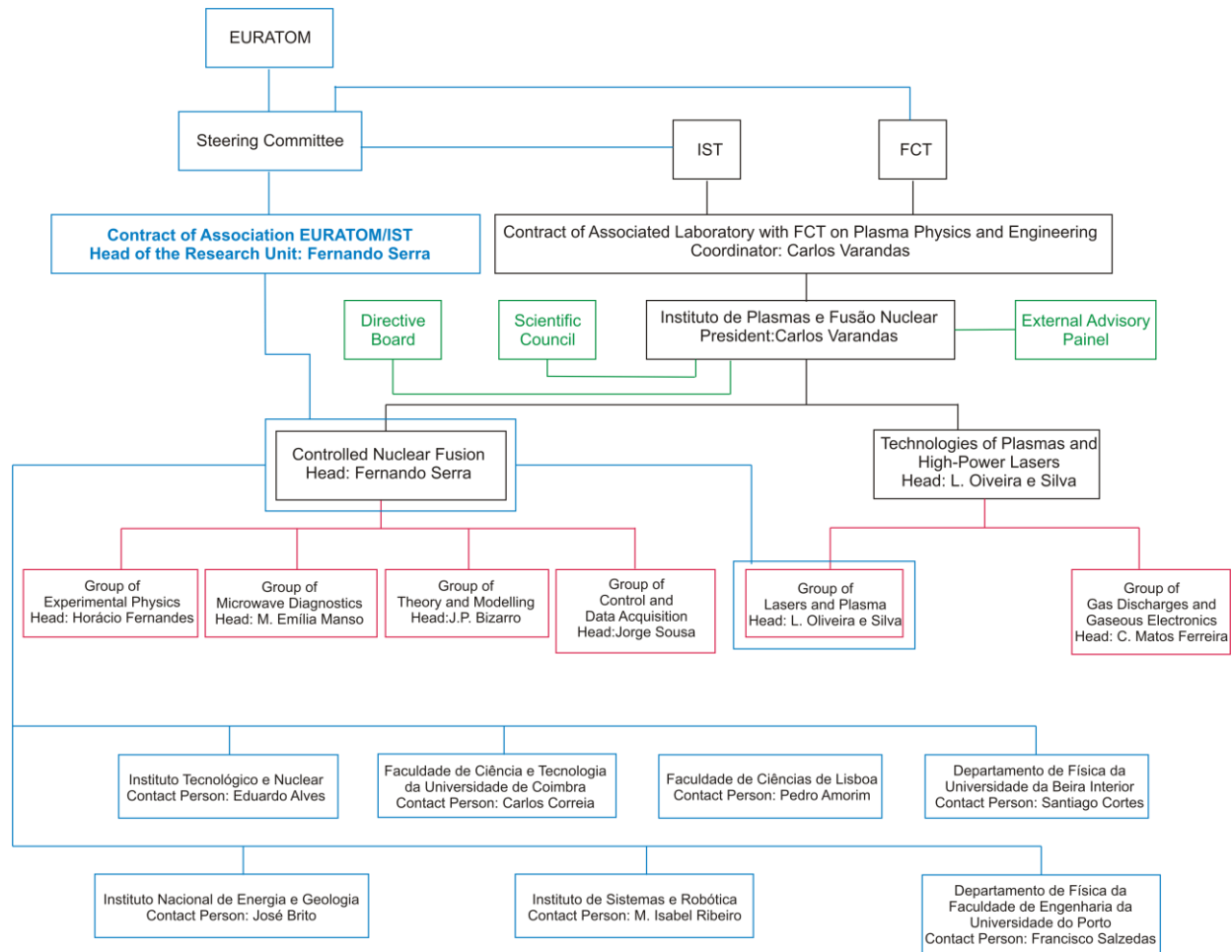


Figure 1.2 – Organization of IPFN

- Tokamak ISTTOK;
- Participation in the collective use of the JET facilities by the EFDA Associates;
- Participation in the ITER Project;
- Participation in the ASDEX-UPGRADE Programme;
- Participation in the TJ-II Programme;
- Participation in the TCV Programme;
- Participation in the COMPASS Project;
- Collaboration with the Association EURATOM/CEA
- Other activities on theory and modelling;
- Keep-in-touch activities on inertial fusion energy;
- Participation in the Fusion Technology Programme under EFDA;
- Other fusion-related activities.

Table 1.1 presents information about the responsible person(s) and the Institutions involved in each project.

1.4. ACTIVITIES ON TECHNOLOGIES OF PLASMAS AND INTENSE PLASMAS

The activities carried out in the frame of this thematic area are described in chapters 14 to 24. The main projects in 2008 were:

- Plasma theory and simulations;
- Laser-plasma accelerators and applications;
- High intensity laser science and technology;
- Coherent soft-x-ray sources;
- Generation of electromagnetic radiation in plasmas and diagnostics;
- High density laser-plasma physics;
- Environmental engineering plasma laboratory;
- Non-equilibrium kinetics and simulations of plasmas and afterglow plasmas;
- Modelling of plasma sources;
- Fundamental physics in space;
- Quantum plasmas.

Table 1.2 contains information about the responsible person(s) and the Institutions involved in each project.

Project	Responsible Person(s)	Collaborating Institutions	
		Portuguese	Other
Tokamak ISTTOK	Horácio Fernandes Carlos Silva	IPFN ⁵ UBI ⁶ CEI ⁷ , CFA ⁸	CIEMAT ⁹ , IPP-Kharkov ¹⁰ , UI ¹¹ , IFUR ¹² , IFUSP ¹³
Participation in the collective use of the JET Facilities by the EFDA Associates	Fernando Serra Bruno Gonçalves	IPFN, CEI, UBI	EFDA ¹⁴ CSU ¹⁵ Culham UKAEA ¹⁶
Participation in the ASDEX Upgrade programme	Maria Emília Manso Fernando Serra	IPFN	IPP-Garching ¹⁷
Participation in the ITER Project	Carlos Varandas Bruno Gonçalves	IPFN	EFDA CSU Garching
Participation in the TJ-II programme	Carlos Varandas Maria Emília Manso	IPFN	CIEMAT
Participation in the TCV programme	Carlos Varandas	IPFN	CRPP ¹⁸
Participation in the COMPASS Project		IPFN	IPP.CR ¹⁹
Collaboration with the Association EURATOM/CEA	J. Pedro Bizarro	IPFN	
Other studies on theory and modelling	J. Pedro Bizarro	IPFN	IFP ²⁰ , PT ²¹ , DFRC ²²
Keep-in-touch activities on inertial fusion energy	J.T. Mendonça	IPFN	
Participation in the Fusion Technology Programme	Carlos Varandas	ITN ²³ , IPFN	
Other fusion related activities	Carlos Varandas	IPFN	

Table 1.1 – Responsible person(s) and collaborating Institutions in the 2008 projects of the Association EURATOM/IST

Project	Responsible Person(s)	Collaborating Institutions	
		Portuguese	Other
Plasma theory and simulations	L.O. Silva	IPFN, ISCTE ²⁴ , INESC-ID ²⁵	UCLA ²⁶ , UR ²⁷ , IC ²⁸ , RAL ²⁹ , MPIQO ³⁰ , PT ³¹
Laser-plasma accelerators and applications	L.O. Silva N. Lopes	IPFN, FCUL ³²	US ³³ , RAL, USA ³⁴ , OU ³⁵
High intensity laser science and technology	L.O. Silva G. Figueira	IPFN	
Coherent soft-x-ray sources	L.O. Silva M. Fajardo	IPFN	LOA ³⁶ , PALS ³⁷
Generation of electromagnetic radiation in plasmas and diagnostics	L.O. Silva J.M. Dias	IPFN	US, RAL, OU
High density laser-plasma physics	L.O. Silva J. Davies	IPFN	RLA, UPM ³⁸ , OsU ³⁹ , URLS ⁴⁰ , LULI ⁴¹
Environmental engineering plasma laboratory	C.M. Ferreira	IPFN	PD-EU ⁴² , LANL ⁴³ , LPI ⁴⁴ , UPS ⁴⁵ , NU ⁴⁶ , BSTC ⁴⁷ , UNM ⁴⁸ , PDSU ⁴⁹ , DFUC ⁵⁰
Non-equilibrium kinetics and simulations of plasmas and afterglow plasmas	C.M. Ferreira	IPFN	UV-SA ⁵¹ , LSGS ⁵² , UP ⁵³ , LPTP ⁵⁴ , DFUM ⁵⁵ , RISSPO ⁵⁶ , IPT ⁵⁷ , FG ⁵⁸ , MU ⁵⁹ , BrU ⁶⁰
Modelling of plasma sources	C.M. Ferreira	IPFN, CFUM ⁶¹	DFUC, CSI ⁶² , LPGP ⁶³ , LPCE ⁶⁴ , LLAN ⁶⁵ , UV ⁶⁶ ,
Fundamental physics in space	Orfeu Bertolami	IPFN, CCTAE ⁶⁷ , UL ⁶⁸	ESA ⁶⁹ , JPL ⁷⁰ , ZARM BU ⁷¹
Quantum plasmas	J. Tito Mendonça	IPFN, UM ⁷²	RAL, UFF ⁷³ , UN ⁷⁴ , UAB ⁷⁵ , RUB ⁷⁶

Table 1.2 – Responsible person(s) and collaborating Institutions in the 2008 projects of the Associated Laboratory

⁵ IPFN means “Instituto de Plasmas e Fusão Nuclear”

⁶ UBI means “Universidade da Beira Interior”

⁷ CEI means “Centro de Electrónica e Instrumentação da Faculdade de Ciências e Tecnologia da Universidade de Coimbra”

⁸ CFA means “Centro de Física Atómica da Universidade de Lisboa”

⁹ CIEMAT means “Centro de Investigaciones Energeticas Medioambientales y Tecnologicas”

¹⁰ IPP- Kharkov means “Institute of Plasma Physics of the National Science Center” “Kharkov Institute of Physics & Technology”.

-
- ¹¹ UI means “University of Innsbruck”.
- ¹² IFUR means “Institute of Physics of the University of Riga”
- ¹³ IFUSP means “Instituto de Física da Universidade de São Paulo”
- ¹⁴ EFDA means “European Fusion Development Agreement”
- ¹⁵ CSU means “Close Support Unit”
- ¹⁶ UKAEA means “United Kingdom Atomic Energy Authority”
- ¹⁷ IPP-Garching means “Max-Planck-Institut für PlasmaPhysik”
- ¹⁸ CRPP means “entre de Recherches en Physique des Plasmas de École Polytechnique Fédérale de Lausanne”
- ¹⁹ IPP.CR means “Institute for Plasma Physics – Czech Republic”
- ²⁰ IFP means “Istituto di Física del Plasma”
- ²¹ PT means “Politécnico di Torino”
- ²² DFRC means “Department de Recherches sur la Fusion Controlée”.
- ²³ ITN means “Instituto Tecnológico e Nuclear”
- ²⁴ ISCTE means “Instituto Superior de Ciências do Trabalho e Empresas”
- ²⁵ INESC-ID means “Instituto Nacional de Engenharia de Sistemas e Computadores – Investigação e Desenvolvimento”
- ²⁶ UCLA means “University of California Los Angeles”
- ²⁷ UR means “University of Rochester”
- ²⁸ IC means “Imperial College”
- ²⁹ RAL means “Rutherford Appleton Laboratory”
- ³⁰ MPIQO means “Max Planck Institute for Quantum Optics”
- ³¹ PT means “Politécnico di Torino”
- ³² FCUL means “Faculdade de Ciências da Universidade de Lisboa”
- ³³ US means “University of Strathclyde”
- ³⁴ USa means “University of Salamanca”
- ³⁵ OU means “Oxford University”
- ³⁶ LOA means “LOA/École Polytechnique”
- ³⁷ PALS means “Prague Asterix Laser System”
- ³⁸ UPM means “Universidad Politécnica de Madrid”
- ³⁹ OsU means “Osaka University”
- ⁴⁰ URLS means “University of Rome La Sapienza”
- ⁴¹ LULI means “LULI/École Polytechnique”
- ⁴² PD-EU means “Physics Department, Eindhoven University of Technology”
- ⁴³ LANL means “Los Alamos National Laboratory”
- ⁴⁴ LPI means “Lebedev Physical Institute”
- ⁴⁵ UPS means “Université Paul Sabatier”
- ⁴⁶ NU means “Nagoya University”
- ⁴⁷ BSTC means “Bioethanol Science and Technology Centre”
- ⁴⁸ UNM means “University of New Mexico”
- ⁴⁹ PDSU means “Physics Department, Sofia University”
- ⁵⁰ DFUC means “Departamento de Física, Universidad de Córdoba”
- ⁵¹ UV-SA means “Université de Versailles-Service d’Aéronomie”
- ⁵² LSGS means “Laboratoire de Science et Génie des Surfaces”
- ⁵³ UP means “Université de Provence”
- ⁵⁴ LPTP means “Laboratoire de Physique et Technologie des Plasmas”
- ⁵⁵ DFUM means “Department de Physique, Université de Montréal”
- ⁵⁶ RISSPO means “Research Institute for Solid State Physics and Optics”
- ⁵⁷ IPT means “Moscow Institute of Physics and Technology”
- ⁵⁸ FG means “Fluid Gravity”
- ⁵⁹ MU means “Masaryk University”
- ⁶⁰ BrU means “Brno University of Technology”
- ⁶¹ CFUM means “Centro de Física da Universidade do Minho”
- ⁶² CSI means “Consejo Superior de Investigaciones Científicas”
- ⁶³ LPGP means “Laboratoire de Physique des Gazes et des Plasmas”
- ⁶⁴ LPCE means “Laboratoire Plasmas et Conversion d’Énergie”
- ⁶⁵ LLAN means “Laboratoire des Lésions des Acides Nucléiques”
- ⁶⁶ UV means “Université de Versailles”
- ⁶⁷ CCTAE means “Centro de Ciências e Tecnologias Aeronáuticas e Espaciais”
- ⁶⁸ UL means “Universidade Lusófona”
- ⁶⁹ ESA means “European Space Agency”
- ⁷⁰ JPL means “Jet Propulsion Laboratory”
- ⁷¹ BU means “Bremen University”
- ⁷² UM means “Universidade do Minho”
- ⁷³ UFF means “Universidade Federal Fluminense do Rio de Janeiro”
- ⁷⁴ UN means “Université de Nice”
- ⁷⁵ UAb means “University of Aberdeen”
- ⁷⁶ RUB means “Ruhr Universtat Bochum”

2. TOKAMAK ISTTOK¹

H. Fernandes, C. Silva (Heads), B.B. Carvalho, R. Coelho, B. Gonçalves, I. Nedzelskij, V. Plyusnin, C.A.F. Varandas, D. Alves, I. Carvalho, P. Carvalho, P.A. Carvalho, A. Duarte, P. Duarte, H. Figueiredo, J. Figueiredo, J. Fortunato, R. Gomes, T. Marques, A. Neto, T. Pereira, A. Soares, Y. Tashev, D. Valcárcel.

2.1. INTRODUCTION

This project has included, besides the normal tokamak maintenance activities, work in the following main research areas:

- Liquid metal limiter;
- Study of fusion relevant materials;
- Diagnostics;
- Real time control and data acquisition;
- Plasma physics studies.

2.2. LIQUID METAL LIMITER

The following tasks were performed in 2008²:

▪ *Study of the gallium jet deflection:* A deflection on the liquid gallium jet due to the plasma-jet interaction has been detected at a distance of 0.5 m from the main chamber (Figure 2.1). This phenomenon has been studied by varying a large set of discharge parameters. The main results were: (i) the deflection increases as the jet is inserted deeper into the plasma; (ii) no dependence on the amplitude or direction of the plasma current is observed; (iii) a linear dependence on the toroidal field amplitude is measured; and (iv) no dependence on the toroidal field direction is observed. This question needs to be further investigated in ISTTOK, being a detailed modelization of the experiment planned.

▪ *Measurements with high sensitivity infra-red sensors:* A new multichannel infra-red (IR) sensor detector with three separated channels has been acquired and tested. This IR system with high sensitivity sensors and 1/2" diameter germanium collection lens has a considerable better response than the one used previously, being more adequate for the ISTTOK experimental conditions (low temperature). A much higher spatial resolution has been achieved by using multi-channel sensors. It is now possible to follow the droplets along their trajectory due to the shift discussed in the previous section. Figure 2.2 clearly shows the shift of the droplet within the field of view (FOV). The first set of spikes depict the droplet moving forward (radially outward) and backwards (radially inward) at the end of the discharge. This system also allows the measurement of the jet temperature variation as it crosses the plasma. We can conclude therefore that this diagnostic will allow the

determination of the power extraction capability of the gallium jet once an absolute temperature calibration is performed.

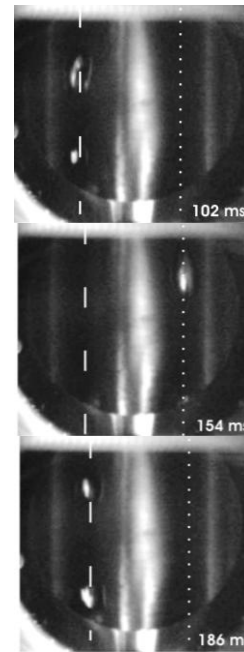


Figure 2.1 - Sequence of frames evidencing the droplets radial shift due to the influence of the plasma.

▪ *Construction of a multi-jet gallium system to increase its efficiency as a limiter:* A new multi-jet liquid metal curtain based on a 4×2.3 mm diameter gallium jets is being developed in Riga. This geometry has been chosen to ensure that the system will work as an effective limiter. The required experimental parameters (break-up length of 13 cm, 1 cm width screen and good stability) have however not been achieved yet. In the present setup configuration, with one single pipe and multi-nozzle output, this is only possible with a large flow rate (higher than 80 cm³/s), that cannot be safely handle by the gallium collector being therefore further developments needed prior to the installation on ISTTOK.

¹Activities carried out in the frame of the Contract of Association EURATOM/IST and the Contract of Associated Laboratory, by staff of the Groups of Experimental Physics, Theory and Modelling and Control and Data Acquisition.

²Work in collaboration with the Associations EURATOM/University of Latvia and EURATOM/ENEA-Frascati. Contact Persons are Olgerts Lielausis and Giuseffe Mazzitelli respectively.

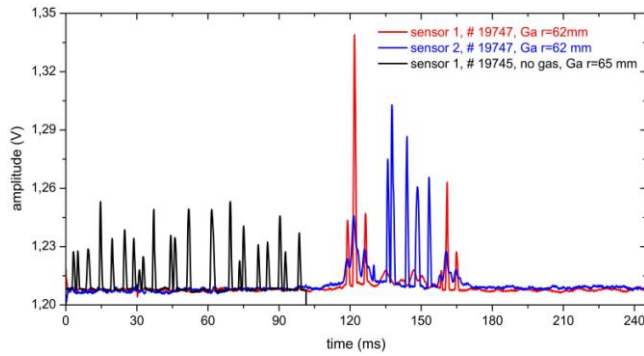


Figure 2.2 - New IR sensor response showing the increased signal amplitude and narrower FOV, when compared to previous measurements.

2.3. STUDY OF FUSION RELEVANT MATERIALS

The following tasks were performed in 2008³:

- *Development and study of nanostructured:* A novel material design for nuclear fusion reactors is proposed based on Cu-nDiamond and W-nDiamond composites. The proposed design involves the production of W/W-nDiamond/Cu-nDiamond/Cu functionally graded material (Figure 2.3). W, W-nDiamond, Cu-nDiamond and Cu layers were produced independently by mechanical alloying and subsequently consolidated/welded through spark plasma sintering. Modulation of processing parameters allowed controlling the extent of unfavourable conversion of nDiamond into tungsten carbide, as well as to overcome the copper to nDiamond intrinsically difficult bonding. Besides the achievement of a higher hardness, the aim of this research was to obtain W and Cu alloys with a very high thermal conductivity. Microstructural features and mechanical properties of the as-produced materials were performed.

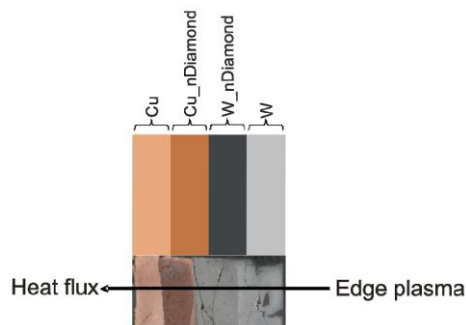


Figure 2.3 - Proposed design with W/W-nDiamond/Cu-nDiamond/Cu layers and image of the sample produced. The arrow indicates the material orientation at the reactor first wall.

- *Study of H retention on W, Cu and Mo probes:* W, Cu and Mo probes exposed to ISTTOK plasmas has been studied with an electronic microprobe, by X-ray diffraction, elastic recoil detection analysis and microindentation experiments. H retention was observed in all the studied samples. Severe intergranular bubble formation occurred in probes exposed to the ISTTOK edge plasma. Nucleation of these high pressure bubbles at grain boundaries and their coalescence seem to be closely associated with the recrystallization and grain growth processes, demonstrating that retention studies should consider the grain size distribution and its evolution over time. Additionally, it was observed the presence of bubble sites and corresponding slip bands (Figure 2.4) in two of the probes (W and a Cu). The occurrence of H retention, bubble formation, slips bands and abnormal grain growth evidences an H plasma exposure occurred in a long campaign at very high temperatures (above 1200° C). Elastic recoil detection analysis was used to measure H concentration profiles and significant long term H retention has been measured.

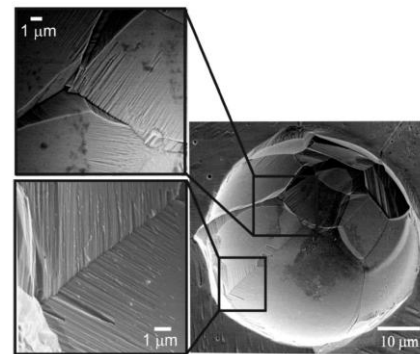


Figure 2.4 - Large bubble in W evidencing slip line bands at the internal surface.

2.4. DIAGNOSTICS

The following main activities were made in 2008:

- *Improvement of the Fourier-Bessel tomographic algorithm* by taking into account the finite width of the viewing cone of each sensor and using different radial basis functions that can be adapted to different magnetic configurations⁴. Tests have shown that this new algorithm with Bessel functions as radial basis functions is more reliable than the standard Fourier-Bessel. Figure 2.5 shows a comparison of the new Bessel method (Fgen) with the standard Fourier-Bessel and the time Minimum Fisher algorithms that is more accurate, but much lengthier. The phantom is the original emissivity profile used to determine artificial sensor data, with 3% Gaussian noise, which is the input to the algorithms. The Minimum Fisher yields the best reconstruction, but at the cost of a longer time. Fourier-Bessel and Fgen take the same time, but the latter yields a better result.

³Work performed in collaboration with “Departamento de Materiais e Tecnologias de Produção do Laboratório Nacional de Energia e Geologia”.

⁴Work in collaboration with the Associations EURATOM/IPP – Greiswald and EURATOM/HAS. Contact Person are Arthur Weller and Sandor Zoletnik respectively.

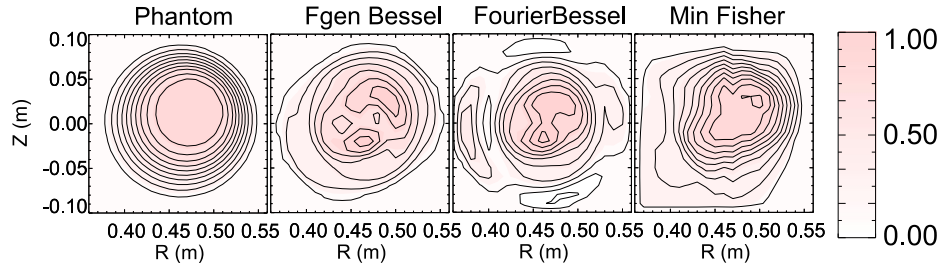


Figure 2.5 - The phantom of a shafranov shifted 2-dimensional emissivity profile and three reconstructions using the generic Bessel, Fourier-Bessel and Minimum Fisher algorithms.

- Installation of ion-electron converters in one channel of the time of flight energy analyzer (TOFEA) aiming at improving the signal-to-noise ratio of the diagnostic. Positive results were obtained particularly in the start signal with the suppression of the background signal and consequent improvement of the signal-to-noise ratio;
- Upgrade of the heavy ion beam diagnostic detection system by installing broad band amplifiers (400 kHz). This upgrade allowed the simultaneous measurements of the plasma density fluctuations in six sample volumes using the multiple cell array detector. A rich frequency spectrum have been observed with a low frequency component (15-20 kHz) that has been identified as GAM, and a high frequency band (100-200 kHz) that is well correlated with Mirnov oscillations. The plasma density fluctuations ($r = 5$ cm) in the GAM region are observed to be highly correlated with the ion saturation current fluctuations measured by electric probes ($r = 6.5$ cm);
- Study of the runaway electrons using Cherenkov-type detectors⁵. A detector of runaway electrons based on the Cherenkov radiation emitted at the interaction of energetic particles (electrons) with transparent medium has been extensively used in the ISTTOK edge plasma. The runaway generation regimes have been identified in the low current ISTTOK discharges confirming previous results obtained by the numerical analysis of macroscopic plasma parameters. The population of the runaway electrons with energy higher than 80 keV has been recorded, being their energy compatible with the critical energy for the runaway process in ISTTOK. The numerical evaluation of the experimental data has revealed that such electrons can be generated at the vicinity of the plasma centre and they can be detected at the probe position;
- Design and construction of a new new Gundestrup probe and development of codes to interpret the measurements. Both the parallel and perpendicular plasma flows have been determined for different direction of the plasma current and toroidal magnetic field and during edge biasing experiments;

- Development of analysis tools for cross-correlation studies using magnetic and heavy ion beam probe data aiming at a detailed characterization of MHD plasma instabilities.

2.5. REAL TIME CONTROL AND DATA ACQUISITION

The following main activities were performed in 2008:

- Development of a web-browser tool for data viewing and parameter searching using SDAS;
- Integration of the data access library SDAS on free and open-source data analysis tools Octave and Scilab;
- Parallelization of the Empirical Mode Decomposition and Hilbert-Huang Transform methods, using signal partition and SSH remote invocation in a joint numerical code that also encompasses parallel Cohen class time-frequency distributions. Communication between master and slave nodes based on reading, writing and polling files was implemented upon a common file system exported via NFS;
- Upgrade of the interferometer for real-time plasma density evaluation to be used in a feedback loop for controlling the gas puffing system;
- Development of a Java-server based FusionTalk to replace the Delphi based one.
- Creation of web tools, under IAEA contract, for the establishment of a small tokamak network. An internet wiki has been establishment for easier coordination between members and a SVN repository;
- Development of a real-time MHD mode number identification code using recursive filtering techniques. The MHD activity of the ISTTOK plasma is characterised by low m-number resistive modes lasting less than 1ms and with a broad frequency spectrum range. The challenges facing a reliable estimation of the poloidal/toroidal structure of such short-lived coherent signals have led to the development of alternative strategies beyond the Fourier paradigm, founded on recursive filtering techniques. A first prototype code, relying on the Kalman filtering technique and applicable to a real-time MHD mode number identification, has been developed and applied to the identification of bursty $m=2$

⁵Work carried out in collaboration with Institute for Nuclear Studies (IPJ), Poland. Contact Person: Andrzej Soltan and Marek Rabinsk.

MHD activity in ISTTOK plasmas (Figure 2.6). Also in the framework of mode structure analysis, preliminary cross-correlation analysis of MHD fluctuations using ISTTOK magnetic probe and heavy ion beam probe (providing local measurements of the density fluctuations) diagnostics has enlightened the prospects from the radial characterization of MHD plasma instabilities.

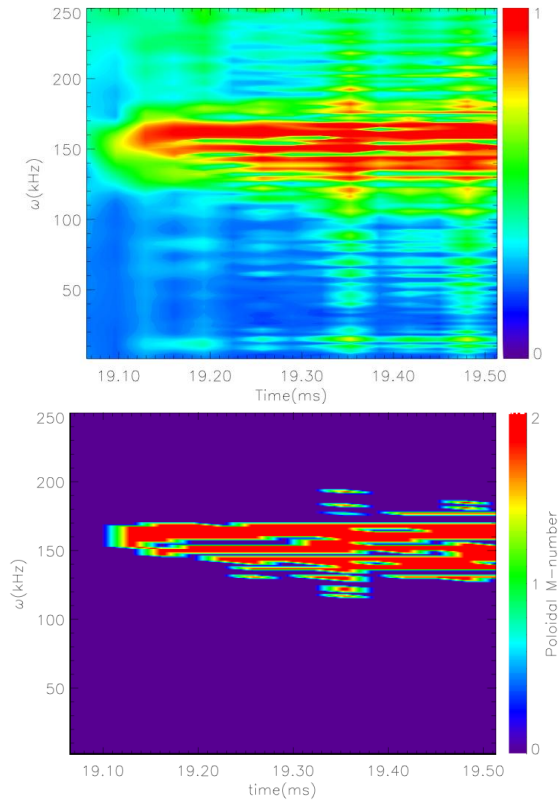


Figure 2.6 - Coherency and mode number analysis using 12 mirnov signals with 80% coherency threshold applied.

2.6. PLASMA PHYSICS STUDIES

Plasma physics studies have been carried out related with the study of long-range fluctuations, characterization of the edge plasma flows and AC discharges.

2.6.1 Study of long-range fluctuations in the ISTTOK edge plasma

Recently, the ISTTOK plasma physics studies were concentrated mainly on the characterization of the edge turbulence. The Portuguese tokamak is equipped with two probe systems that allow the investigation of the three dimensional characteristics of the edge fluctuations. It has been found that the ISTTOK fluctuations have distinct characteristics for $r > a$ (SOL) and $r \lesssim a$ (edge plasma). The characteristics of the potential fluctuations in the SOL are consistent with the typical broad band turbulent fluctuations

while in the edge plasma they are dominated by low frequency oscillations consistent with a symmetric structure in the poloidal and toroidal direction, characteristic of the geodesic acoustic mode.

Potential signals measured simultaneously at different toroidal locations show a striking similarity (Figure 2.7). To quantify the similarity between potential fluctuation probe signals the toroidal cross-correlation has been computed. Signals are dominated by a ~ 20 kHz oscillation with time varying amplitude (Figure 2.7b). As shown in Figure 2.7c, a high toroidal cross-correlation (up to .9) is found. As no significant phase shift is observed between signals measured by the probe systems poloidally and toroidally separated, results suggest that the potential has a $m = 0, n = 0$ structure compatible with GAM. Figure 2.7c also shows the amplitude of the V_f power spectrum in the range 15-25 kHz. Both long-range correlations and low frequency components show a significant degree of intermittency and a good correlation between them is found.

The toroidal correlation is proportional to the GAM amplitude and has the opposite behavior of the turbulent flux demonstrating that on ISTTOK the radial transport and the long-distance correlations are coupled. These findings provide the first direct evidence of multi-scale physics in the regulation of transport mechanisms in the edge of fusion plasmas.

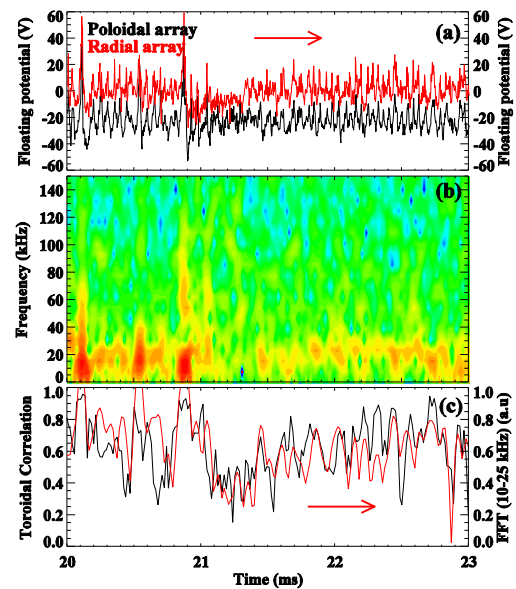


Figure 2.7 - Temporal evolution of: (a) V_f measured simultaneously in two toroidal positions at $r-a = -10$ mm; (b) V_f spectrogram; and (c) toroidal correlation between V_f signals together with the amplitude of the V_f power spectrum in the range 10-25 kHz.

2.6.2 Characterization of the edge plasma flows

The generation mechanisms of spontaneous parallel plasma flows are not fully understood. It has been shown that different tokamaks can have both co and counter toroidal magnetic field (B_T) and also co and counter plasma current momentum. A radially movable eight segment Gundestrup probe was used to measure both the parallel and perpendicular plasma flow under direct and reversed B_T (Figure 2.8). It was found that the parallel flow is not sensitive to the B_T direction, changing direction near the limiter radius ($y=85$ mm) in both configurations. In the scrape-off layer (SOL) the parallel momentum is due to the parallel electric field generated by the presence of the limiter and the measured velocity is in the direction of the closest plasma facing surface as expected.

The transverse plasma flow is symmetric in relation to the magnetic field direction in the boundary plasma (SOL and edge plasma), and was found to be related with the spontaneous radial electric field. However, for $r < 70$ mm the symmetric reversal of the flow is not observed, being roughly independent of the B_T direction at the probe innermost position.

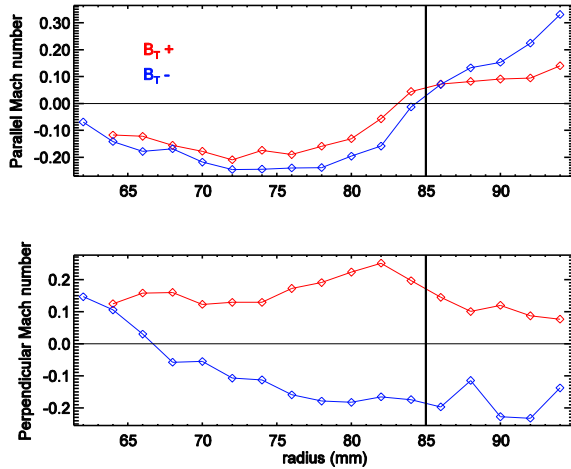


Figure 2.8 - Radial profile of the parallel and perpendicular Mach number for both toroidal field directions.

2.6.3. Study of AC discharges

One handicap of iron core tokamaks such as ISTTOK is the limitation in the discharge duration due to its saturation. Typically, 40 ms discharges can be achieved in DC ISTTOK operation. With the use of two new power supplies and their controllers, the plasma position could be controlled and long duration AC discharges achieved.

A 250 ms discharge with ten 25 ms half-cycles has been achieved (Figure 2.9). As shown, the plasma current is reduced in the later part of the discharge and the particle confinement degraded. Comparing the temporal evolution of the plasma density and H_α radiation it can be concluded

that recycling increases over the discharge time, possibly limiting its duration. The temperature increase of the first wall components due to the longer discharge duration can contribute significantly to an increase of this hydrogen wall influx. A real-time gas puffing system has been recently implemented that could help in the recycling control.

Other physics studies were carried out comparing the positive and negative plasma current half-cycles, such as edge fluctuations and asymmetries in the plasma current reversal. Fluctuations levels in the edge quantities were found to be higher in negative cycles in spite of the fact that plasma position tends to be slightly different in positive vs. negative cycles.

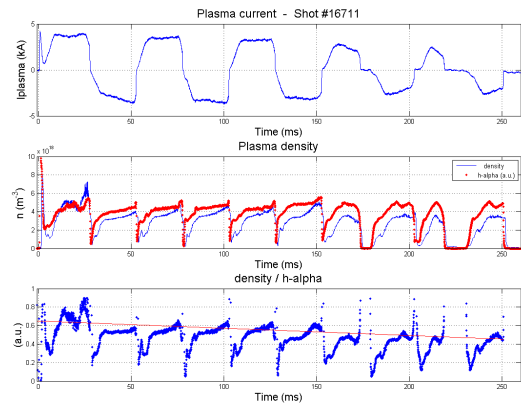


Figure 2.9 - Temporal evolution of the plasma current (top), plasma density and H_α radiation (center) and density over H_α (bottom).

3. PARTICIPATION IN THE COLLECTIVE USE OF THE JET FACILITIES BY THE EFDA ASSOCIATES¹

F. Serra (Head), B. Gonçalves (Deputy Head), J.P. Bizarro, D. Borba, R. Coelho, S. Cortes, L. Cupido, A. Figueiredo, A. Fonseca, M.E. Manso, F. Nabais, M.F. Nave, I. Nedzelski, I. Nunes, V. Plyusnin, T. Ribeiro, F. Salzedas, C. Silva, J. Sousa, C. Varandas, P. Varela, D. Alves, P. Belo, J. Bernardo, P. Carvalho, N. Cruz, A. Fernandes, J. Ferreira, J. Figueiredo, L. Meneses, A. Neto, R. Pereira.

3.1. INTRODUCTION

The Association EURATOM/IST has continued its participation in the collective use of the JET facilities, in the frame of EFDA through the “JET Operation Contract” and the “JET Implementing Agreement”.

The main activities in this project were related with:

- Operation;
- Scientific exploitation;
- Performance enhancements;
- Management.

3.2. OPERATION

Three members of the IST/IPFN staff have been working in the JET Operation Team:

- One Physicist has continued to work in the JET “Plasma Operation Group”, as a session Leader for the Campaigns;
- One Physicist has been working in the “Plasma Operation Group” as a Plasma Control expert in the framework of the Plasma Control Upgrade activities;
- One Physicist has carried on his work in the Reflectometry and LIDAR Diagnostic Group, being responsible by: (i) maintenance of the X-mode correlation reflectometer (KG8b); (ii) the analysis and validation of the signals of the KG8b X-mode correlation reflectometer and the KG3 O-mode fluctuation reflectometer.

In addition, during JET experimental campaigns one Physicist has been seconded to perform duties as Session Leader for the experiments.

3.3. SCIENTIFIC EXPLOITATION

3.3.1. Introduction

IST has proceeded with an important contribution to the JET scientific exploitation mainly through an active participation of twenty two scientists in the experimental Campaigns (C20-C25) and in the analysis/interpretation and modelling of the experimental data.

3.3.2. Fast ion losses in experiments with ³He in advanced tokamaks scenario

Experiments with ³He minority heating in advanced tokamaks scenario have been carried out in order to study fast ions redistribution. In these experiments, a variety of Alfvén eigenmodes was observed, namely Alfvén cascades,

Core-TAE and Global high-m TAE. The temporal evolution of fast ion losses was observed to depend on the energy and pitch angle, and bursts of losses were also observed to occur.

3.3.3. ITB oscillations in advanced tokamak scenarios with a dominant fraction of bootstrap current

The modelling of advanced tokamak scenarios with very large bootstrap currents has continued, namely in situations of truly steady-state tokamak discharges, meaning zero loop voltage. The benchmarking of JETTO in view of carrying out these studies has been systematized.

3.3.4. Perturbative toroidal momentum transport studies

Experiments have been carried out to confirm the existence of an inward momentum pinch and to characterize its dependence on plasma parameters. This work will provide a better understanding of the physics of momentum transport, and contribute to the theory, model and code validation efforts. An elaborate transport analysis method was used to study the effects of a periodic torque density perturbation on rotation for different plasma conditions. It was observed that it is possible to decouple the diffusion from the convection for the radial toroidal momentum transport, and to compare the dependence of the momentum pinch on plasma parameters such as rotation, magnetic helicity or electron density against results from gyro-kinetic codes.

3.3.5. Verification, validation and benchmark of ELM modules in the code JETTO

Progress was done in testing and benchmarking the transport code JETTO and the MHD models included in the code. A set of simulations for testing the main numerical modules of JETTO during a JAMS/ JETTO upgrade has been designed and developed. The input choices were chosen to be as broad as possible, covering the main choices for equilibrium, transport and heating. In addition, some more specialised choices such as pellet injection and a couple of simple sawtooth and ELM models have been included. Five catalogued simulations and documentation about the modules tested and input choices for each case, was delivered to the JET Code Management Group.

¹Activities carried out in the frame of the Contract of Association EURATOM/IST and the Contract of Associated Laboratory, by staff of the Groups of Experimental Physics, Theory and Modelling and Control and Data Acquisition.

3.3.6. Modelling ELM behaviour in JET discharges with gas puffing

The ELM behaviour in JET discharges with different levels of Deuterium gas puffing has been simulated using the 1.5D core transport code JETTO coupled to an ELM model based on linear ballooning theory. The objective of the study was to model discharges where the pressure at the top of pedestal and the ELM frequency remains unchanged following a step down in gas puffing. The sensitivity of the ELM behaviour with respect to different boundary conditions, transport assumptions and recycling was considered (Figure 3.1). Preliminary results have shown that a constant ELM frequency can be obtained by a combination of reduced boundary density and reduced recycling. The latter assumptions are being revised by using the EDGE2D/EIRENE code on a case to case basis to provide a more consistent estimate of the SOL plasma response.

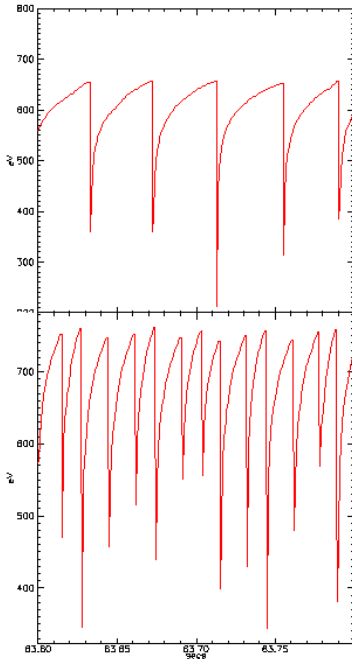


Figure 3.1- Simulations of the temperature at the top of the H-mode barrier, using the code JETTO coupled to a ballooning model for the ELMs. The ELM frequency increases from 30 Hz to 65 Hz, when the density boundary, i.e. the density at the scrap off layer, is halved from 5.0×10^{19} to $2.5 \times 10^{19} \text{ m}^{-3}$. The recycling coefficient is 1 in both cases.

3.3.7. Impurity transport modeling with GLF23

Simulations with the theoretical transport model GLF23 for impurities included in JETTO/SANCO transport code found that the anomalous convective term was inward directed in the plasma core for $\rho < 0.4$. These results are in contradiction with the experimentally observed hollow impurity profiles. The simulations also found that if neoclassical impurity transport occurs within the ETB, the neoclassical convective impurity velocity is outward for all high Z impurities while and inward for Helium (Figure 3.2).

This result indicates that it will be much harder to remove the Helium ash than higher Z impurities.

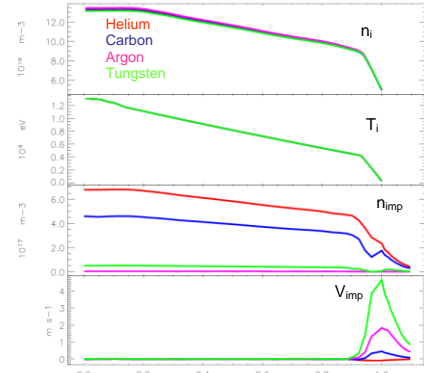


Figure 3.2 - Core transport simulations with JETTO/SANCO of: Helium (red), Carbon (blue), Argon (magenta) and Tungsten (green) for ITER Scenario2, for a prescribed electron density and electron and ion temperatures.

3.3.8. Impurity transport in the whole plasma using the transport code COCONUT

Simulations of the ELM free H-mode JET plasmas with COCONUT show that the Deuterium density increases with the deuterium puff rate and this change occurs almost immediately after the deuterium puff rate was switched on at the edge, while in the plasma core the change occurred hundred of milliseconds later, as it was observed experimentally (Figure 3.3). Although it is showed in these simulations that the radiated power

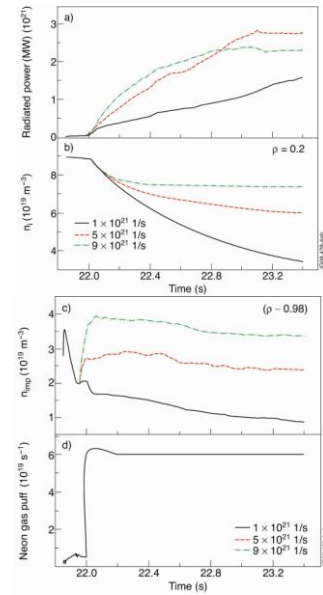


Figure 3.3 - Time traces of the: a) radiated power; b) Deuterium density at $\rho = 0.2$; c) Deuterium density at $\rho = 0.98$ and d) the Neon gas puff rate from the COCONUT simulations, with $\Gamma_D = 1.0 \times 10^{21}$ particles/s (blue line), $\Gamma_D = 5.0 \times 10^{21}$ particles/s (red line) and $\Gamma_D = 9.0 \times 10^{21}$ particles/s (green line).

increases with the deuterium density, this does not imply that there is an increase of the impurity concentration in the plasma core, because fully stripped impurities, which are inside the ETB, do not contribute to the radiated power. Indeed the impurity concentration in the plasma core decreases with the deuterium puff rate (Figure 3.4).

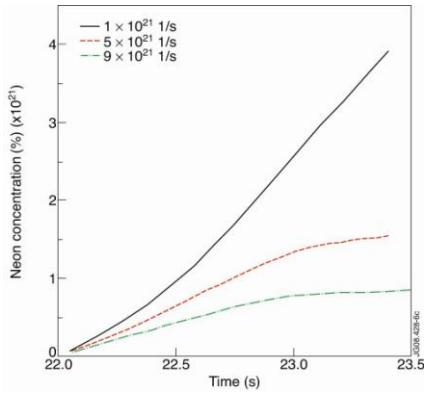


Figure 3.4 - Time evolution of Neon concentration in the plasma core for three Deuterium puffs rates, 1×10^{21} p/s; 5×10^{21} p/s and 9×10^{21} p/s for ELM free H-mode plasmas.

3.3.9. Modelling ITER H-mode scenarios with EDGE2D/EIRENE

Simulations performed for the ITER scenario 2 with the core transport code JETTO have shown that the $Q = 10$ was only achieved in H-mode plasmas. It was considered important to introduce an ETB in the SOL transport model. The perpendicular transport coefficients used in the EDGE2D/EIRENE code were determined, for a critical pressure gradient (ballooning limit) driven from MHD analysis. The initial results (Figure 3.5 and Figure 3.6) show fully attached plasmas and that the peak heat flux deposition should be expected to be much higher than the recommend by the ITER design (10MW/m^2 at the divertor targets). The introduction of extrinsic impurities is foreseen in order to reduce the heat flux. A combination of Neon and Deuterium has to be considered because it was observed numerically that Deuterium puff alone is not enough to reduce the power load.

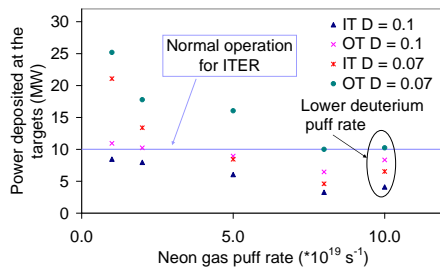


Figure 3.5 - Maximum power density deposited at the targets as a function of the Neon inlet puff rate

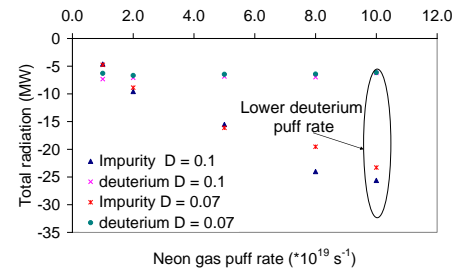


Figure 3.6 - Total radiation in the EDGE2D/EIRENE computational domain as a function of the Neon inlet puff rate.

3.3.10. Kalman filtering technique for MSE data processing

Extensive tests of the Kalman filtering based processing of the APD harmonics necessary for the magnetic field pitch angle calculation were performed. Successful ELMs and frequency/phase jitter mitigation were demonstrated and a fast C-code implementation was developed and installed on the JAC cluster (Figure 3.7).

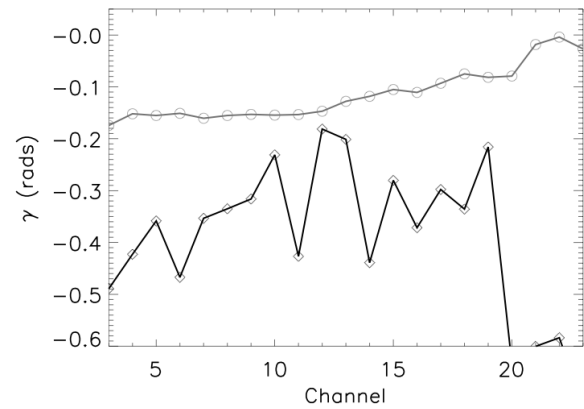


Figure 3.7 - Magnetic pitch angle during an ELM with (grey) and without (black) the Kalman algorithm

The method was also applied to Toroidal Alfvén Eigenmodes (TAEs) which are excited using an antenna whose input signal is driven at a varying frequency in the range of approximately 100 to 300 kHz. Whenever the TAE resonant frequency in the plasma matches the antenna frequency, TAEs are excited and the Mirnov pickup coils detect such activity. The study of the amplitude and phase of the TAE perturbation observed in Mirnov pickup coil signals provides extremely useful information about these important modes in the plasma. The work consisted of the Development of a software synchronous detector for extracting, from the Mirnov coil signals, only the spectral portion at the antennas' excitation frequency. The algorithm is based on flexible real-time recursive filtering techniques with high sampling rate outputs improving on the current hardware approaches installed at JET. The Mode number analysis of TAE modes excited by the TAE antenna was performed using a prototype two-fold recursive filter

implementation (in-phase and quadrature component detection in addition to a dual space-time mode number analysis) that takes advantage of the superior model-based estimation capabilities of the filter. Preliminary results indicate that optimal mode estimation requires mitigation of spatial aliasing interference with the mode numbers of interest (Figure 3.8).

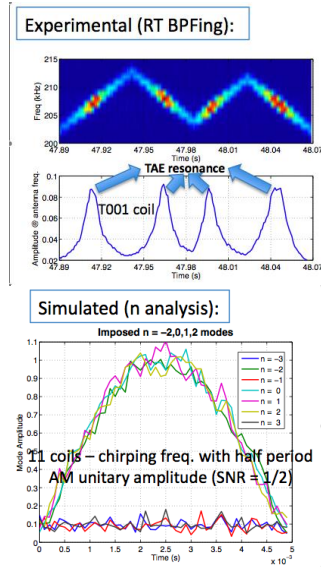


Figure 3.8 – Experimental excitation of TAEs and the simulated spectra of modes for a scenario with imposed $n = -2, 0, 1, 2$ modes.

3.3.11. ELM transport in the JET far-SOL

The ELM propagation in the SOL is investigated and the radial velocity estimated using different methods. Scrape-off layer parameters measured by the reciprocating probe clearly shows that both Type I and III ELMs are composed of a number of coherent structures or filaments propagating radially with velocities up to 6 km/s with lifetimes in the range 40 - 100 μ s (Figure 3.9). The large radial velocities observed at the beginning of Type I ELMs imply that filaments reach the wall with a significant fraction of the pedestal density and temperature. During ELMs a strong parallel flow ($M \sim 0.4$) is measured at the top of the machine towards the inner divertor that increases during filaments. These observations are in agreement with the ballooning nature of the ELM losses.

3.3.12. Mitigation of disruptions and runaway electrons

Recently massive gas injection (MGI) experiments have been started at JET. The experiments on disruption mitigation and runaway generation suppression using the disruption mitigation valve (DMV) were completed with pressure scans (5,17,27,36 bar) for different toroidal fields and plasma currents. Up to 2×10^{23} of Neon and Argon atoms have been injected into ohmic and neutral beam heated plasmas. Almost vanishing of runaway electrons (REs) was

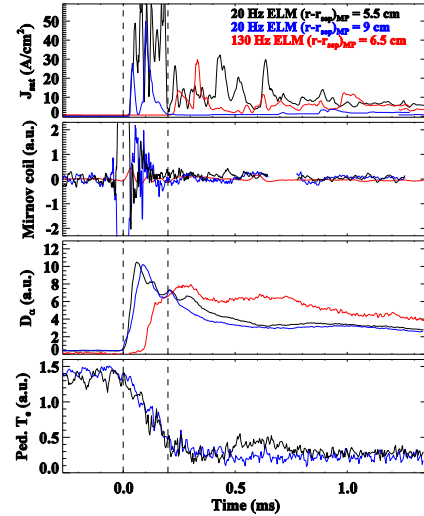


Figure 3.9 - Time evolution of J_{sat} , MHD activity (measured with Mirnov coils located near the outer midplane), outer divertor D_α radiation and pedestal temperature during a Type I. The J_{sat} measured by the probe during a Type III ELM is also shown for comparison.

observed at maximum DMV pressure. Basic assessment shows that about of 20% of the injected gas is mixed into the plasma during the thermal quench. The overall reaction time from the DMV activation to current quench varies between 9 and 15 ms, depending on gas amount and species, safety factor and plasma energy. The time delay between start of radiation phase and thermal quench was found to decrease with q_{95} . It was observed that the current quench rate is not strongly varying with Neon pressure.

RE generation was observed for argon injection caused by high toroidal electric fields up to 50 V/m at a modest density on the start of the current quench. This allows detailed studies of RE generation characteristics, like, for example, the dependence on the strength of the magnetic field. In particular, at argon injection, runaway electrons were observed for magnetic fields below 2 T, which was considered as the previous threshold for RE generation in many tokamaks (Figure 3.10).

The loss of these runaways occurs in several subsequent events of less than 100's and can lead to wall temperatures exceeding 1500 C in hot spots as observed by fast cameras in the infrared and visible range. The post-disruption runaway beam dynamics was studied, including analysis and comparison of the data from soft and hard X-rays, EFIT, visible imaging and magnetics for the modelling of RE beam dynamics (Figures 3.11 and 3.12).

Analysis of the data obtained allowed determination of the most probable zones of the interaction of runaway beams with plasma facing components together with the places of the maximal transient heat loads caused by runaway electrons.

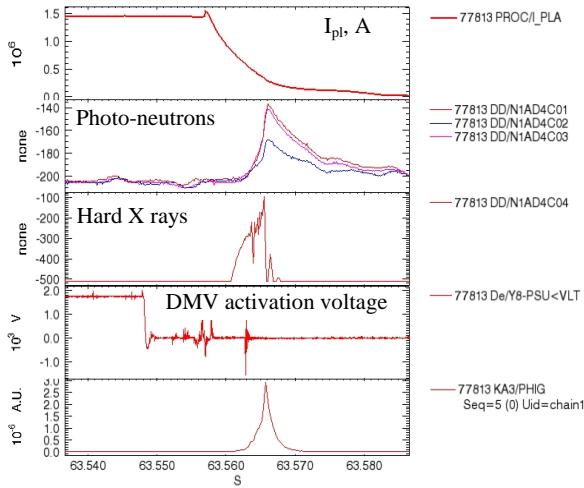


Figure 3.10 - Observation of runaway electrons during 1.5MA disruption at $B=1.2$ T with pure argon injection (bursts of photo-neutrons, hard X-rays and scintillating probe signals during current quench)

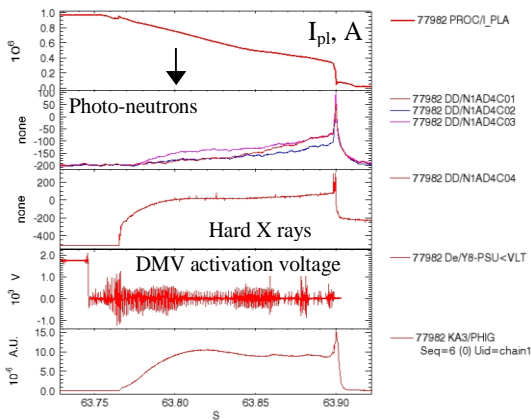


Figure 3.11 - #77982 – runaway generation in low current disruption.

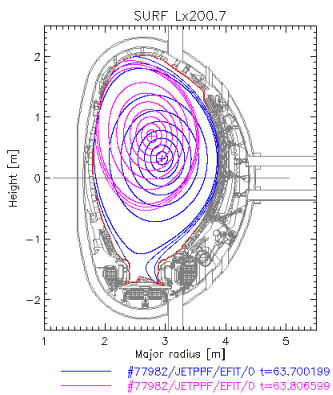


Figure 3.12 - Example of EFIT reconstruction of the current-carrying channel geometry: JET pulse #77982 (pink contours in temporal point marked on previous figure, blue contours – pre-disruption configuration).

Studies of fluctuations during disruptions were also performed. After minor disruptions significant changes in the LIDAR electron density profile are observed. These changes are particularly localized close to the $q=2$ rational surface. Since it is in this region that energy transport is fastest during the minor disruption, the two phenomena may be related. The microwave reflectometry KG8b channels were used in correlation mode, to probe the plasma radius in order to search for fluctuations that can be the cause of the above referred density fluctuations.

3.3.13. Rotation studies of JET discharges with low momentum input

The work on the JET Intrinsic rotation database and execution of experiments aimed at measuring and understanding rotation in JET plasmas with low momentum input, has continued. A database on rotation in ICRF, LH and Ohmic heated plasmas has been compiled in order to determine how rotation scales with various plasma parameters and heating details. Dedicated experiments to determine the effect of the toroidal field ripple on rotation in ohmic and ICRH plasmas has been carried out. Analysis of MHD modes frequency and direction of propagation has been extensively used as a method for determining poloidal and toroidal rotation. The effect of MHD modes and fast particles on rotation has been considered.

3.3.14. Toroidal field ripple effects on JET intrinsic rotation

Studies of rotation in plasmas with low momentum injection are important in predictions for ITER where toroidal momentum sources will be small. In addition, a toroidal field ripple of 0.5% is thought to break the plasma, further reducing rotation in ITER plasmas. Experiments to study the effect of toroidal field ripple on intrinsic rotation plasmas have been performed recently at JET. Ohmic and RF heated plasmas with $B_T=2.2$ T and $I_p=1.5$ MA and 2.1 MA were considered. Ripple levels ranged from the usual JET low value of 0.08% to an enhanced 1.5% (Figure 3.13). NBI experiments in previous JET ripple campaigns showed that ripple reduced rotation in plasmas with co-injected momentum. The object of the new experiment was to find out if ripple would also affect rotation in plasmas with no momentum input and, in the case of Ohmic plasmas without fast ions. Preliminary rotation analysis of charge exchange measurements (from short NBI pulses used for diagnostic purpose only) as well as MHD mode numbers and frequency data, shows that ripple indeed changes the rotation of both Ohmic and RF heated plasmas. In both cases ripple drives counter rotation (Figure 3.14), possibly indicating a strong torque due to non-ambipolar transport of thermal ions.

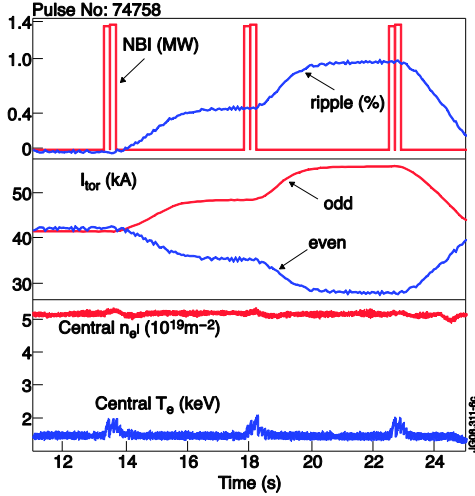


Figure 3.13 - Ohmic pulse (2.1 MA, 2.2 T) with an unbalanced toroidal current on odd and even toroidal coils to give three different ripple levels. Charge exchange rotation profiles are measured during the short NBI blips.

3.3.15. Toroidal velocity measurements in TF ripple experiments

The analysis of the toroidal velocity at the plasma edge, in discharges presenting Edge Localized Modes (ELMs) of type-I and type-III, with varying amounts of TF Ripple was performed. The aim is to determine the role of the toroidal rotation and/or its shear at the plasma edge in determining the ELM characteristics, as well as the effect

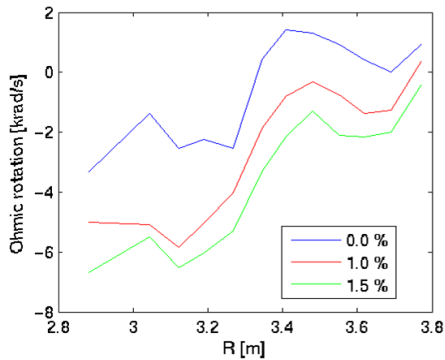


Figure 3.14 - Charge exchange toroidal rotation profiles showing that counter-rotation increases with ripple.

of the TF Ripple induced particle losses on the toroidal rotation of the plasma. The performed work focused on the relation of the variation of the toroidal rotation, and its shear, with the ELM frequency at the top of the pedestal; The effect of the TF ripple on localized measurements of edge plasma toroidal rotation, close to the top of the ion temperature pedestal (T_i^{ped}), and its influence on ELM frequency was therefore examined on JET. Detailed measurements of the edge plasma toroidal rotation and T_i have been carried out using the edge Charge eXchange Recombination Spectroscopy diagnostic system at JET with

temporal resolution of 50 ms and a spatial resolution generally up to 2 cm. The analysis has been performed for several Type-I ELMy H-mode plasmas with varying amounts of TF ripple (from the standard JET ripple $\delta r=0.08\%$ up to a maximum of 1%) and edge plasma densities. (Figure 3.15). Although more discharges have to be analyzed, preliminary results seems to indicate that the ELM frequency and toroidal rotation of the plasma are linked (Figure 3.16).

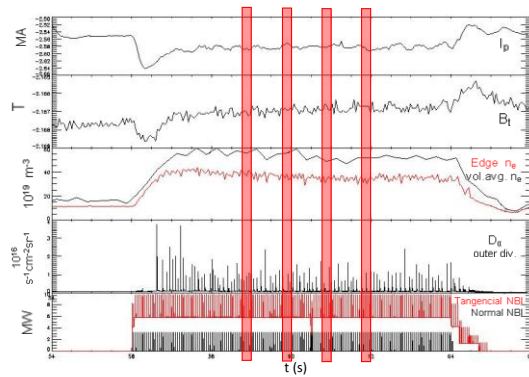


Figure 3.15 - Several parameters of JET discharge 69837. Red boxes indicate the selected time window of 0.5s for the analysis.

3.3.16. Toroidal momentum braking

The prospects for the ELM mitigation through externally driven magnetic fields at JET has prompted a series of experiments aiming at the assessment of both $n=1$ and $n=2$ effect on the ELM frequency and size and on the global confinement and plasma profiles evolution. Indeed, it is observed that a self-similar braking of plasma toroidal rotation occurs most notably at plasma core during error field correction coil (EFCC) ELM mitigation experiments (Figure 3.17) in both $n=1$ and $n=2$ configurations while stronger braking appears at the plasma edge near the pedestal. In addition to the density pump-out effect, similarly to previous experiments, no clear dependence of toroidal rotation braking on the plasma collisionality range $\nu=[0.004 - 0.012]$ has been observed.

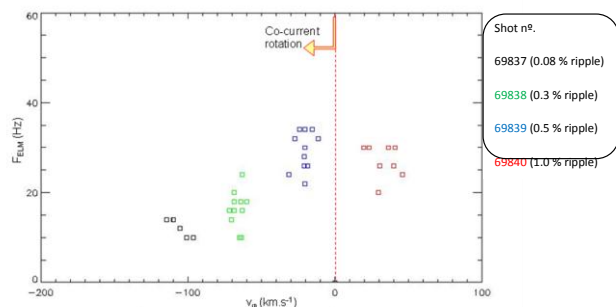


Figure 3.16 - Relation between the ELM frequency and the pedestal toroidal rotation velocity for several JET discharges with varying amount of TF ripple.

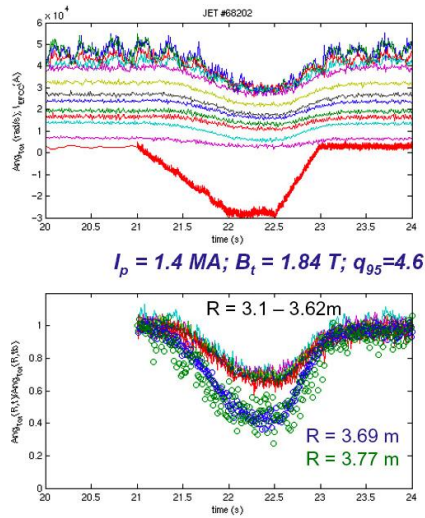


Figure 3.17 - Time evolution of (upper) plasma toroidal angle velocity, I_{EFCC} and (lower) normalized angular frequency to that before EFCC switched on. The signals in the upper figure from up to bottom are measured from different plasma radii from core to edge

3.3.17. Study of MHD effects on core rotation of ICRF heated plasmas

JET experiments to investigate toroidal rotation in purely ICRF heated plasmas have shown both peaked and hollow rotation frequency profiles. The hollow profiles suggested that the core of some ICRH plasmas might be counter-rotating. The origin of counter rotation is not understood. These observed profile differences have been thought to be associated to differences in MHD activity. At the low ICRH powers ($P_{ICRH} < 6$ MW) used in these L-mode discharges the main MHD instability observed was sawtooth activity. Although for $P_{ICRH} > 3$ MW core tae modes can be seen before monster sawtooth crashes. Charge exchange rotation profiles obtained during short NBI pulses taken in discharges with different ICRF powers were compared. Rotation profiles were found to be very different depending on the MHD activity observed. Profiles are more hollow and counter-rotating in the core when core tae modes are present (Figure 3.18) indicating the role of fast-ion losses in counter-rotation.

3.3.18. ITER-Like Antenna Commissioning

ILA commissioning was done in the areas of power handling, plasma loading, matching behaviour, and performance of arc protection systems. The ILA commissioning required both L-mode and H-mode pulses with different magnetic fields depending on the antenna operating frequency. H-mode pulses obtained by a combination of NBI and ICRF power were used to study coupling tolerance to ELMs. The ILA commissioning sessions were often combined with other high level commissioning of diagnostics, heating or plasma control systems.

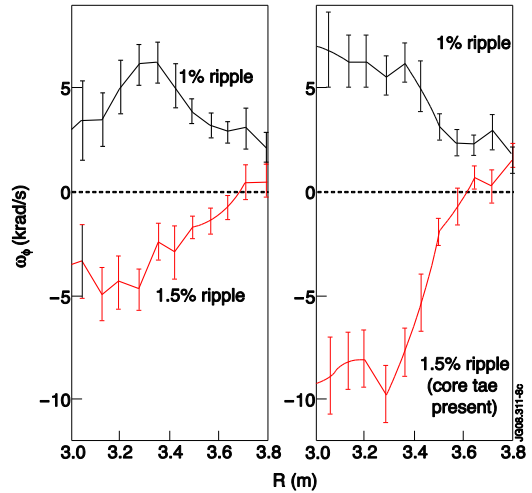


Figure 3.18 – Toroidal rotation profiles in discharges with ICRF heating for 1% ripple (black) and 1.5% ripple (red). Increasing ripple makes the plasma counter rotate (negative profiles, in red). Core counter rotation is larger when core-tae modes, that remove fast-ions from the core, are present.

Data analysis has revealed the first fast ions accelerated by new ITER-like antenna at approximately 4 MW of ICRF power. Studies were performed to determine the heating efficiency of the new ITER-like antenna. The first part of those studies has been dedicated to determination of processes responsible for increase of impurities during ICRH. It was found that the interaction of energetic ions with plasma surrounding surfaces could cause the enhanced impurity release. Furthermore, it was found that the interaction of energetic ions with plasma surrounding surfaces could cause the enhanced impurity release.

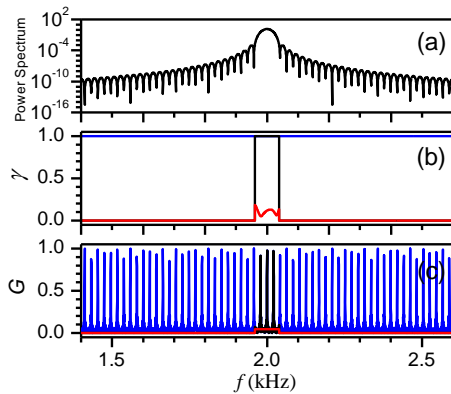
3.3.19. MHD analysis of DIII-D Quiescent H-Modes

Participation in DIII-D Quiescent H-mode experiments and data-analysis of DIII-D plasmas was performed as a contribution to the Edge Pedestal Physics ITPA group on the development of small ELM and quiescent H-mode (QHM) regimes. The following studies of MHD activity in QHM plasmas have been done: radial localization of edge MHD modes using the ECE analysis code ECEPOW; comparison of MHD observations in ELM-free and QHM phases and, cross correlation between the edge harmonic oscillator (EHO) and fast ion loss signals. A clear correlation between the EHO and fast-ion losses was obtained. A QHM pulse has been selected for transport and MHD modelling using codes in the JET JAMS code platform.

3.3.20. Radial correlation reflectometry software tool

Work on the coherence analysis software tool for the JET correlation reflectometry diagnostic has been concluded with verification and validation of the tool. Upgrades have been done to handle recent modifications in the VME control and data acquisition system and the KC1M

continuous data acquisition system, as well as to use the newly available HRTS density measurements and to include a relativistic correction in the calculations. Whenever possible, problems caused by several existing problems that have been detected in the new VME software when using the tool, have been handled by the analysis tool (Figure 3.19). Calculation of coherent reflection has been added to the tool, with the purpose of allowing a future integration with full wave modelling of the diagnostic, which would allow the physical interpretation of the measured correlation lengths and measurement of the level of density fluctuations. The analysis tool started to be used to analyse ongoing JET experiments with focus on transitions from L to H confinement and pedestal studies.



3.19 - Study of the effect of low-power zeroing, systematic phase correction and phase noise in the coherence and coherent reflection of test signals to verify the radial correlation analysis tool.

3.3.21. Use of short-time Fourier analysis versus wavelets to analyze ELMs and short-lived ELM precursors

A technical comparison was done on the use of wavelets as an alternative to the usual Fourier methods (used for instance in CATS analysis) to perform mode analysis in JET. The comparison shows that wavelets do not improve upon standard Fourier analysis. It was also highlighted that some JET codes need to be upgraded to fully benefit from the time-frequency resolution given by standard Fourier analysis methods.

3.3.22. Development of the software application for data display and analysis for JET fast visible camera

The display application for the IR camera KL8 was upgraded in order to be able to use magnetic geometry EFIT data and to input pellet's trajectory. The developed tool besides allowing the access to fast visible camera data plots a 3D model of the field of sight (Figure 3.20). The tool allows choosing a region of interest and wrapping the image into the 3D model.

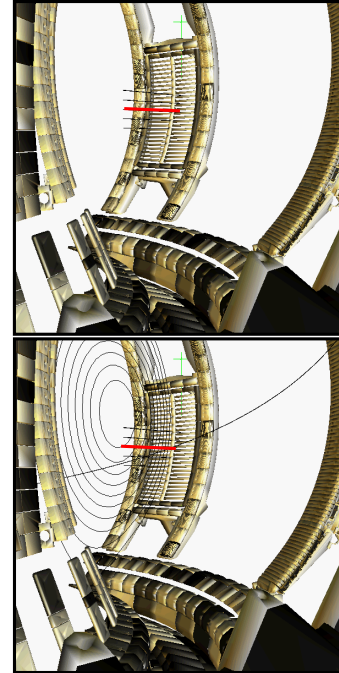


Figure 3.20 - KL8 tool: mapping the pellet injection geometry. (LFS Pellet trajectory + 10 cm spacing, EFIT, #76930, t=58.919s)

3.3.23. ELMs studies with microwave reflectometry

The one channel prototype KG8a diagnostic measuring the edge part of the JET density profile built by IPFN was equipped with a new acquisition system that enabled edge density profile data to be acquired on a routine basis.

Selection of a suitable algorithm for the automatic evaluation of the first cutoff layer localization was achieved. In figure 3.21a it is depicted the density evolution during the onset of an ELM, showing profiles acquired with 800 μ s separation before the ELM (t1, t2), during the ELM (t3) and after the ELM (t4, t5). A shift toward the antenna can be observed in t3 with a later recovering to the prior profile position. Figure 3.21b depicts the time evolution of four density layers along a 4 ms period displaying the change in the density profile gradient during the onset of an ELM.

3.4. PERFORMANCE ENHANCEMENTS

3.4.1. Introduction

The Association EURATOM/IST has been involved in several tasks carried out in the frame of the second stage of the JET Enhancement Projects (EP2):

- JET Fast Camera;
- JET reflectometer (KG10);
- Data acquisition for the neutron camera diagnostics enhancements (DNG-G);

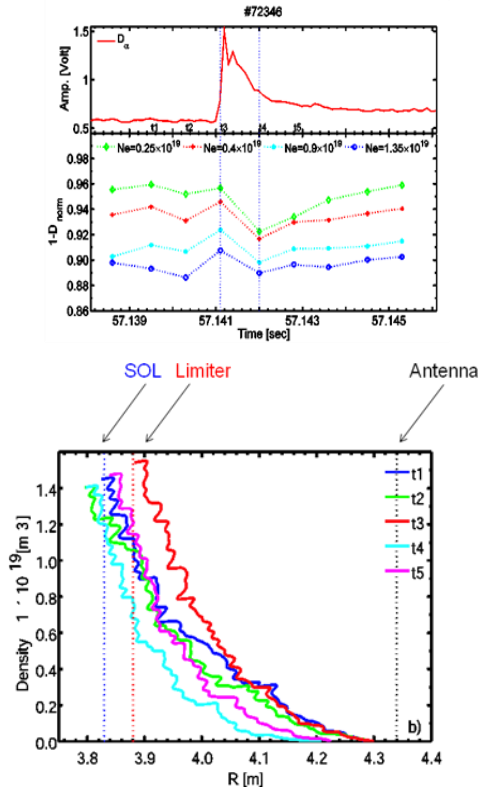


Figure 3.21 - Results from JET KG8a diagnostic: (a) - Density evolution during the onset of an ELM, showing profiles acquired with 800 μ s separation before the ELM (t_1 , t_2), during the ELM (t_3) and after the ELM (t_4 , t_5). A shift toward the antenna can be observed in t_3 with a later recovering to the prior profile position; (b) Evolution of four density layers along a 4 ms period displaying the change in the density profile gradient during the onset of an ELM

- Data acquisition for the gamma ray spectroscopy (GRS)
- ATCA hardware platform for the Plasma Control Upgrade project (PCU-VS);
- Development of a Digital Link for the Vertical Stabilization controller (PC2-VS);
- Real-Time Measurement & Control Diagnostics & Infrastructure (RTM).

IST has provided the project leader for the DNG-G and RTM projects.

3.4.2. JET Fast Camera

The main activities were related with the development of the interface between CODAS and the Fast Camera diagnostic (KL8). The TDC (Time digital converter) card was commissioned and some improvements requested by CODAS on the way data is retrieved from the internal memory were performed. The first channel was connected to the JET $t=0$ trigger, which acts as the time reference for all the other channels. It was also connected to the camera shutter output signal in order to measure the start and duration of each individual frame with a sub microsecond precision and to the ELM triggering signal. The first results

indicate that the accuracy of this fast time vector is in accordance with the information provided by other diagnostics, namely the fast D_{α} radiation from the divertor region.

3.4.3. JET reflectometer (KG10)

3.4.3.1. Basic configuration

The main activities concerned the development of a new 6-channel reflectometer for JET. The new JET diagnostic should be able to make high resolution measurements of the complete JET density profile aiming to improve the time-dependent transport analysis capabilities at JET, including evolution of transport barriers, pedestal survey, the study of fast transient events (ELMs, pellets...) and the coupling of RF heating. A proposal for a high performance multi channel reflectometer diagnostic [33 – 150 GHz] was presented. The proposal incorporates advanced microwave technologies developed at IPFN, compatible with the JET long and complex transmission line. IPFN constructed three of the six channels and is also developed a novel controllers with TCPIP connection all the 6 channels (including the 3 ones being developed by CEA). The new controller assembly displayed in Figure 3.22 is based on a PC104 platform equipped with a dedicated programmable IO board plus a fast function generator FPGA/DAC based board all together in a single module (Figure 3.22).

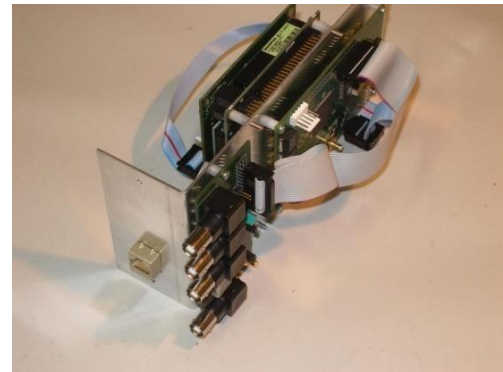


Figure 3.22 - The new controller assembly based on a PC104 platform equipped with a dedicated programmable IO board along with a fast function generator FPGA/DAC based board all together in a single module.

The schematic configuration of the reflectometry system is depicted in Figure 3.23. For highest performance the high sensitivity heterodyne receiver system uses a novel scheme for synchronous local oscillator generation by frequency conversion which includes the delay line that is necessary to compensate the large distance to the plasma; it provides phase and quadrature signal outputs for improved plasma signal discrimination. The electronics developments were concluded and all sub assemblies were tested. Partial assembly of parts is progressing according to the

planning. The control software was finalized and tested successfully on a PC104 platform and the firmware for the ramp generator (developed in VHDL to configure an FPGA) was also finalized. The controllers and ramp generators were completed. The documentation for each part/component is being produced. Most laboratory calibration tests in the laboratory have been performed.

To accommodate the new KG10 diagnostic a complete new arrangement of the quasi-optical connection was implemented and the equipment of the KG8b system was re-allocated.

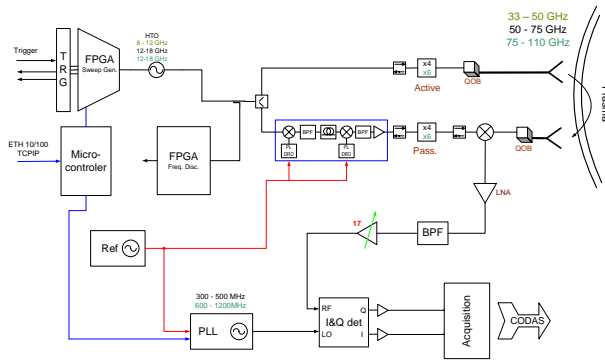


Figure 3.23 – Schematic configuration of the JET KG10 reflectometry system.

3.4.3.2. Further improvements

With the objective of further improving the performance of the reflectometry diagnostics for future large size machines like DEMO while reducing the access to the machine an advanced coherent reflectometer beyond the state of art is being pursuit. This will be able to make frequency hopping fast enough to measure density plus plasma fluctuations which is presently obtained with separate diagnostics using different microwave technologies. To achieve the above goal, coherent emission/detection schemes have to be developed along with highly coherent and phase-stable signals. This has a great number of technological difficulties and for this reason it is a development with several intermediate stages and associated prototypes. In 2008 the prototype of a fast FPGA ramp generator was developed and is being implemented the JET KG10 system. The prototype includes a FPGA frequency controlled source and associated fast digital hardware and software as well as refinements in IPFN’s own design of I and Q detection system.

3.4.4. Data acquisition for the neutron camera diagnostics and for the gamma ray spectroscopy

The following tasks were performed: (i) implementation and test of a 8-channel transient recorder board with 400 MSPS, 14-bit resolution for GRS (Figure 3.24); (ii) implementation of the codes for the acquisition boards (final FPGA code and FireSignal drivers); (iii) production of the required boards, assembling and test of the a 24-channel@250MSPS system for DNGG and 8-channels@400MSPS for GRS; (iv) implementation and simulation of the real-time pulse analysis algorithms for PHA, PSD, pile-up

detection/recover/rejection and for PMT correction, as well as its comparison with previous systems; (v) tests of the real-time pulse analysis algorithms on the DNGG diagnostic and evaluation of signal/noise ratio; (vi) production of 8 channels settable gain pre-amplifiers with 15 MHz bandwidth; (vii) tests of the GRS data acquisition system in JET and Milan (portable unit); (viii) implementation and test of the CODAS interface and (ix) installation of the DNG-G data acquisition at JET.

IST also provides the Project Leader for the data acquisition for the neutron camera diagnostics project.

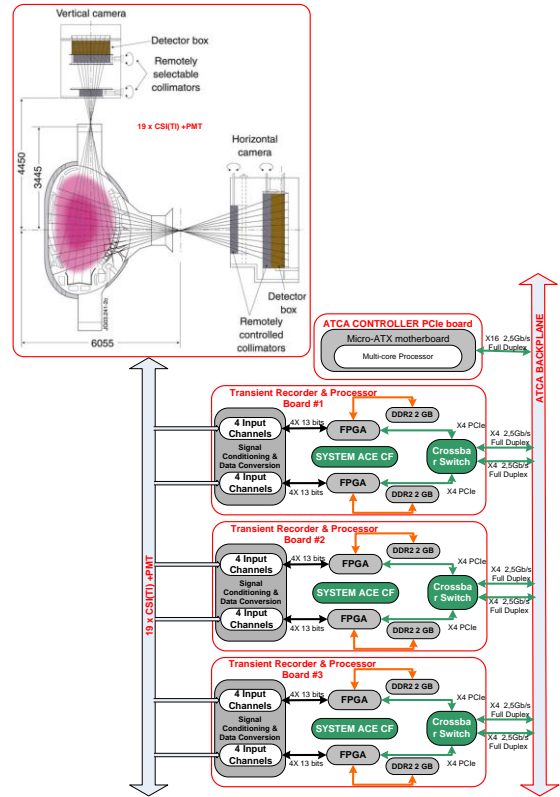
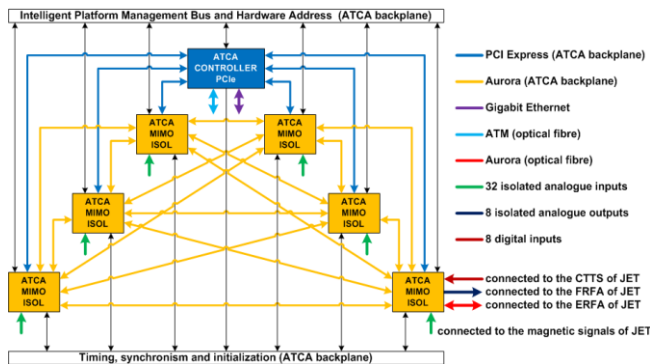


Figure 3.24 - DAQP system diagram block. Three TRP boards to cope with 19 lines of sight, 19 channels are being acquired simultaneously and data will be retrieved either after each 4 GB of memory of each board is full or in real time, in a data processed operation mode. The controller is responsible to arm the acquisition and to retrieve data to the system hard disk.

3.4.5. ATCA hardware platform for the plasma control upgrade

The following tasks were performed: (i) production and test of the complete control system hardware providing 192 ADC channels sampling at 2MSPS@18-bit, 24 channel DAC and 48 digital I/O channels (Figure 3.25); (ii) development of the FPGA codes including the PCIe interface, ADC interface, memory controller and decimation filters; (iii) development and test of codes for the host computer PCIe device drivers, hardware/data acquisition test program and multiprocessor support; (iv) implementation and test (latency and jitter measurements

with heavy-load processing, reliability of operation over several-day without rebooting and ability of remote diagnose of software faults) of an RTAI-LINUX real-time operating system platform including the multi-platform libraries BaseLib2 and MARTe; (v) testing of the system performance including noise, cross-talk and linearity, through the comparison with the existing KC1/KC1D/KC1E systems and (vi) integration with CODAS and commissioning at JET. The system is currently operational and proved able to control JET tokamak discharges. A second development phase required for the new power supplies commissioning will take place in 2009.



3.25 - System hardware architecture

3.4.6. Digital link for the vertical stabilization controller

Targeting an error-free link between the VS controller (Figure 3.26) and the new power supplies, the following tasks were performed: (i) specification of the Digital Link hardware and communications protocol (T3P); (ii) implementation of a PCI based test-bench unit for test purposes and (iii) implementation of a specification package for the Vertical Stabilization power supply designers.

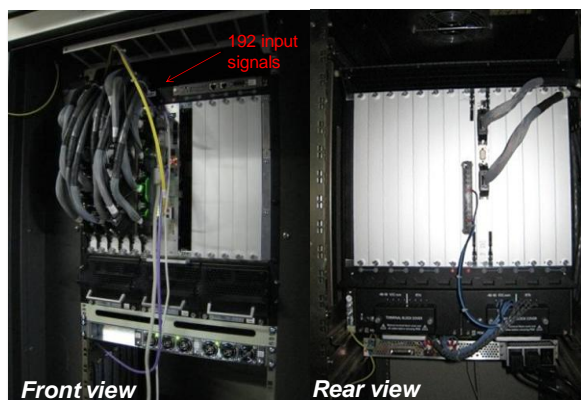


Figure 3.26 - Vertical stabilization controller system installed at JET with the 192 input signals connected

3.4.7. Real-time measurement & control diagnostics & infrastructure

The goal of this project is to expand the JET real-time diagnostics and control capabilities required to fulfill the programmed objectives of JET in the proposed FP7 phase of operation dedicated to the preparation of ITER.

The contract signed in December 2008 specifies the following tasks to be developed, which are already in progress: (i) improvement of the real-time measurement capabilities of FIR Interferometry (KG1); (ii) improvement of the real-time measurement capabilities of some of the Neutron Diagnostics (Total Neutron rate KN1, Hard X-ray rate KH1, 14 MeV neutron rate-KM7); (iii) expansion of the real-time JET Network Infrastructure to accommodate the extra real-time Diagnostics required for FP7 either by exploiting recent network technologies or by extending existing ATM, including the development and implementation of a Real-Time Network prototype.

IST also provides the Project Leader.

3.5. MANAGEMENT

The Association EURATOM/IST has collaborated on the management of the use of the JET Facilities by the EFDA Associate with: (i) one scientist at the Close Support Unit team, in the Operations Department from October 2008 onwards; and (ii) one scientist as Deputy Task Force Leader for Task Force D (Diagnostics).

4. PARTICIPATION IN THE ITER PROJECT¹

C.A.F. Varandas (Head), B. Gonçalves (Deputy Head), J. Belo, J.P. Bizarro, L. Cupido, H. Fernandes, M.E. Manso, M.I. Ribeiro, J. Santos, F. Serra, A. Silva, A. Vale, P. Varela, R. Igreja, R. Patrício, J. Ricardo.

4.1. INTRODUCTION

Following the increase of the activity of both the ITER International Legal Organization (ILO) and the European Joint Undertaking for ITER and the Development of Fusion Energy (“Fusion for Energy” (F4E)) as well as the transfer of the EURATOM Fusion Technology Programme from EFDA to F4E, IPFN has increased significantly its ITER-related activities, namely in the areas of:

- Diagnostics;
- Control and Data Acquisition;
- Heating systems;
- Remote Handling.

Besides the research and development activities mentioned in the following sections, it is important to underline the following events:

- Organization of a meeting at IST, on March 31st 2008, with the ITER Principal Deputy Director (Norbert Holtkamp), the F4E Director (Didier Gambier) and the F4E Chief Engineer (Maurizio Gasparoto) for discussion of the Portuguese participation in the ITER Project;
- Nomination of an ITER Industrial Liaison Officer;
- Elaboration of a website (<http://iter.cfn.ist.utl.pt/Empresas/news>) concerning the participation of Portuguese firms in ITER construction.

4.2. DIAGNOSTICS

4.2.1. Introduction

IPFN has been working in the development of four diagnostics for ITER in the frame of EFDA tasks:

- Plasma position reflectometer;
- Equatorial visible/IR wide angle viewing system;
- Core LIDAR Thomson scattering diagnostic;
- Diagnostic neutral beam.

4.2.2. Plasma position reflectometer

In task TW6-TPDS-DIADES, IPFN: (i) led the Cluster of Associations (IPFN, CIEMAT, CEA and CNR-Milan) that carry out the task activities; (ii) coordinated the development design activities for the plasma-position reflectometer diagnostic (PPRD); (iii) elaborated the Project Plan; (iv) studied the routing of the ex-vessel waveguides; and (v) collaborate in the engineering design

of the in-vessel critical components such as the antennas and first-bends.

IPFN prepared the intermediate and final reports displaying the results of the overall work as well as the identification of urgent R&D tasks which are already part of the full development of the PPRD for ITER and are integrated in the Project Plan for ITER Procurement Package 1. Figure 4.1 it is depicted the simulated attenuation and return losses of a section of waveguide with an hyperbolic secant bend model (120 mm), showing the resonance-free behaviour at frequencies within the operation range of the plasma-position reflectometers. It was identified as an urgent R&D task the development of a mock-up of in-vessel transmission lines plus antennas and surrounding blanket structures to provide essential data complementary to the numerical results.

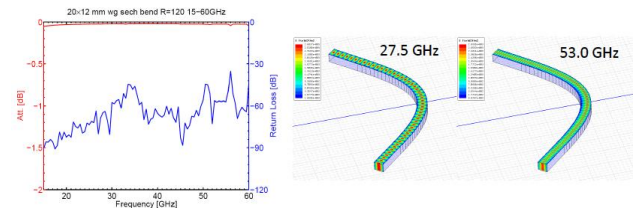


Figure 4.1 - Simulation of the electromagnetic performance of a waveguide section using a hyperbolic secant bend model (120 mm), showing resonance-free behaviour at two frequencies ($F1=27.5$ GHz and $F2=53$ GHz) within the operation range of the plasma-position reflectometers.

4.2.3. Equatorial visible/IR wide angle viewing system

IPFN was the leading unit for the CODAC integration. The requirements for data acquisition, CODAC interfacing and local control systems were defined, and the Final Report was produced.

A Consortium Agreement was signed (between CEA, CIEMAT, HAS, ENEA and IST) to promote the elaboration of a proposal to the likely next call by F4E on the “Implementation of the Diagnostics Procurement Package –11 for ITER”

4.2.4. Core LIDAR Thomson scattering diagnostic

IPFN was in charge of the specification of the LIDAR control and data acquisition sub-system. Two Work Packages were finished and the final reports issued:

¹Activities carried out in the frame of the Contract of Association EURATOM/IST and the Contract of Associated Laboratory, by staff of the Groups of Experimental Physics, Microwave Diagnostics, Theory and Modelling and Control and Data Acquisition, in collaboration with Instituto de Sistemas e Robótica (ISR) and Active Space Technologies (AST). Contact Person: Maria Isabel Ribeiro (ISR) and Ricardo Patrício (AST).

- Control System Interface Definition aiming at defining the interface from the local control system to the measurement and controlling points as well as to the ITER global control system.

- Control System aiming at designing the specifications of the key components of the CODAC control sub-system.

4.2.5. Diagnostic neutral beam²

IPFN has participated in the thermo-mechanical modelling and thermal radiation analysis of the diagnostic neutral beam cryopump.

The mechanical analysis and modelling was done using Msc.Patran/Nastran. The calculation of radiation heat loads to the cryogenic circuits (radiation shields and cryosorption panels) was computed via Monte Carlo algorithm using ESARAD. Design recommendations were made based on the performed mechanical stress analysis. In particular it was found that the overall stress level is not acceptable, as the predicted maximum Von Mises stress level is nearly four times the yield strength threshold in all six load cases analyzed. The need for substantial design changes over the DNB cryopump support structure was identified.

Furthermore, it was identified that the stress levels detected in the structure ribs that support the cooling pipes are of the same magnitude as yield strength. A redesign will be necessary in order to obtain a more rigid structure that can better withstand the very sharp gradients that will be observed when the fluid at 80 K will pass through the pipes.

4.3. CONTROL AND DATA ACQUISITION

4.3.1. Introduction

This research line included work on:

- Mini-CODAC;
- High performance networks;
- Plant system simulator and fast control plant system

4.3.2. Mini-CODAC

A proposal has been submitted to F4E and ITER for the development of a mini-CODAC and autonomous piece of hardware and software to simulate the behavior of the ITER CODAC in order to test and certify Plant systems functional integration. The mini-CODAC should: help testing concepts foreseen for ITER CODAC; provide a proof-of-concept of the overall design of the CODAC system using state-of-art technologies; help the consolidation of ITER CODAC specifications through a real implementation of the conceptual design.

The proposed mini-CODAC implementation included

- Data storage;
- Central Data management functions;
- Supervisory functions for global and plant operating states management as a project wide and interface specifications between CODAC and Plant Systems. Plasma Control is machine dependent and is out of the scope of this project;
- Synchronous DataBus;
- Plant monitoring (including Human Machine Interface: tools) with remote experiment handling capabilities and alarm and interlock handling functions;
- Basic CODAC systems with overall supervisory role;
- Network implementation;
- Authentication and hierarchical authorization software including different authentication levels for access control.

Special care was given to make the design of the Mini-CODAC implementation modular and for it to contemplate Dual Redundancy. The presented solution, based on ATCA, is scalable and can be adapted in the future to several applications (e.g. ITER test facilities). The different modules are self-consistently implemented in order to provide an adequate Minimum CODAC implementation.

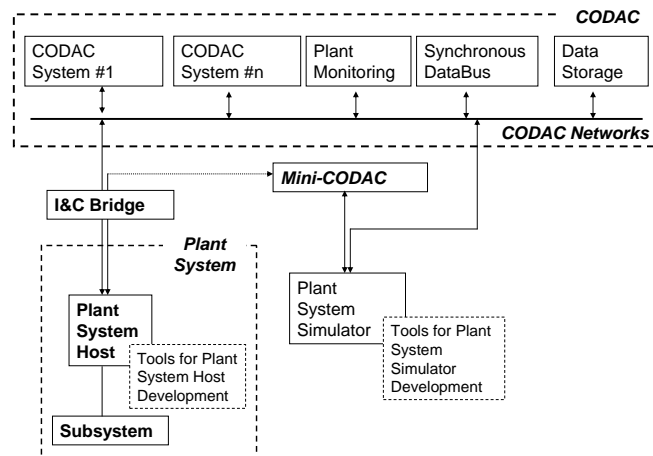


Figure 4.2 - Schematic representation of the modules composing the project and interfaces between them

²Work made in collaboration with Active Space Technologies.

4.3.3. High performance networks

A proposal to assess and prototype ITER High Performance Networks (HPN), able to transport Synchronous Data, Audio/Video, Time and Events for the Plant sub-systems was elaborated and sent to ITER Organization. The work to be performed consisted of the following key tasks: Perform a market survey to identify possible COTS product or existing systems fulfilling or approaching the stated requirements; Identify requirements which cannot be fulfilled by today's or tomorrow's COTS; Build up demonstrators of COTS or existing systems and perform benchmarks to validate performance; Document all results including recommendations to ITER.

A test facility with 10 nodes was proposed to test the performance of the selected technologies according to the test methodology defined for the project (Figure 4.3) allowing benchmarking the different technologies. The proposed facility would use PCs to act as plant systems network interface units and generate the traffic from/to the network nodes. The selected high performance networks would be tested individually. From a preliminary analysis it was foreseen that the traffic in the demonstrator network would be generated as follows:

- Events will be generated by event generator module from/to nodes
- Timing will be generated by GPS or UTC boards or recurring to a NTP server and distributed to nodes
- Video/Audio will be streamed from cameras and distributed to nodes
- Synchronous data will be generated by a packet generator from/to the nodes

The test facility would also allow data archiving with time stamp. All nodes would be generating packets simultaneously to stress the network. Performance degradation would be assessed by extending the nodes in the network and by increasing the number of channels per

nodes. Also failure test recovery analysis would be performed. Remote configuration and management of the network and Network redundancy methods would also be explored. The proposed network test relied on standard COTS software but, where essential to the test of ITER requirements, custom made software would have been developed.

4.3.4. Plant system simulator and fast control plant system

This project aims at: (i) defining technologies for ITER Plant Systems; (ii) designing and implementing a Plant System Simulator to facilitate a test environment for the Plant System Host and CODAC Systems; (iii) exploring ATCA technologies and assess its viability for ITER; and (iv) prototyping technology for a fast high performance Plant System.

A preliminary study and first assessment on technologies was performed and possible solutions were proposed for the implementation of two Plant System Simulators (ATCA and PXI/PXIe) and a Fast Control Plant System (ATCA). The proposed equipments were designed to provide ITER with forefront solutions, maximizing the benefits of a modern technology.

4.4. HEATING SYSTEMS

4.4.1. Introduction

The activity of this research line was focused on:

- Conceptual studies on a LHCD system for ITER;
- Design studies of the ITER NBI cryopumps.

4.4.2. Conceptual studies on a LHCD system for ITER

Following the work performed for the TORE SUPRA programme, IPFN has participated in the conceptual studies of a lower-hybrid current drive system for ITER.

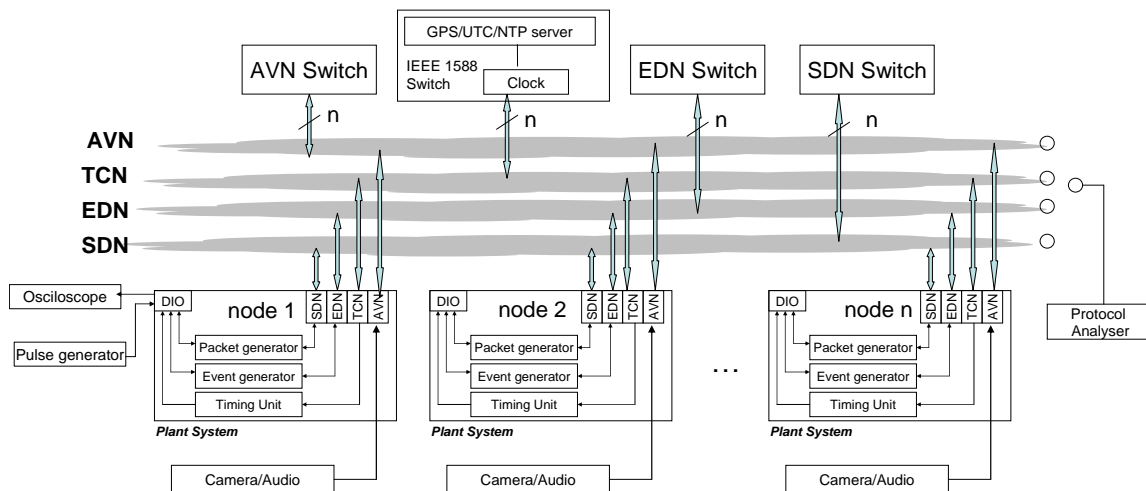


Figure 4.3 - Schematic view of proposed testing facility

4.4.3. Design studies of the ITER NBI Cryopumps

IPFN has been responsible for thermo-mechanical modelling and thermal radiation analysis of the Diagnostic Neutral Beam Cryopump. The mechanical analysis and modelling was done using Msc.Patran/Nastran. The calculation of radiation heat loads to the cryogenic circuits (radiation shields and cryosorption panels) was computed via Monte Carlo algorithm using ESARAD (Figure 4.4). Design recommendations were made based on the performed mechanical stress analysis.

In particular it was found that the overall stress level is not acceptable, as the predicted maximum Von Mises stress level is nearly four times the yield strength threshold in all six load cases analyzed. The need for substantial design changes over the DNB cryopump support structure was identified.

Furthermore, it was identified that the stress levels detected in the structure ribs that support the cooling pipes are of the same magnitude as yield strength. A redesign will be necessary in order to obtain a more rigid structure that can better withstand the very sharp gradients that will be observed when the fluid at 80 K will pass through the pipes.

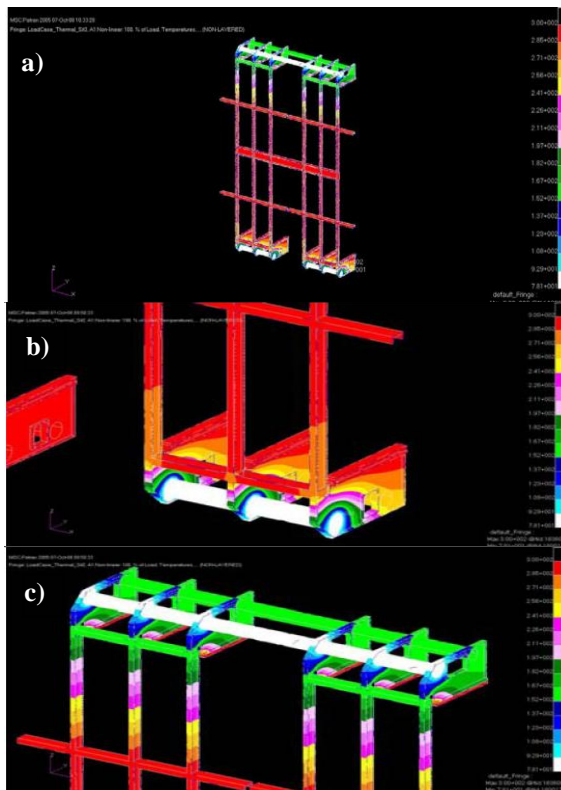


Figure 4.4 - Temperature distribution over the DNB: a) the whole structure; b) detail of the bottom part; c) detail of the top part. As expected, the two sections of considerably low temperatures achieve a steady state temperature with the pipe region at a temperature very close to 80 K, whereas all contact areas with the rest of the structure are at 300 K.

4.5. REMOTE HANDLING

4.5.1. Introduction

This research line included R&D activities related with:

- Design of gripper and sliding table mechanical sub-systems for the ITER DTP2 manipulator;
- Conceptual studies on the transfer cask system.

4.5.2. Design of gripper and sliding table mechanical sub-systems for the ITER DTP2 manipulator³

A detailed design of both subsystems was performed proposing, where possible, the use of commercial components. A pneumatic gripper (manufactured by Sommer Automatic) was selected, due to the fact that no contact between electric current and fluid is desired while providing the level of gripping force required. Removable Aluminium fingers (Figure 4.5), able to perform a set of certain gripping operations, were also designed. A FE static analysis was performed over one finger to assess its structural integrity under a distributed load equivalent to that provoked by a gripping force. A CTETRA 10-node solid elements mesh was prepared for the FEM with MSC.PATRAN (Figure 4.6), and the calculations were performed with MSC.NASTRAN. The post-processing was performed with MSC.PATRAN.

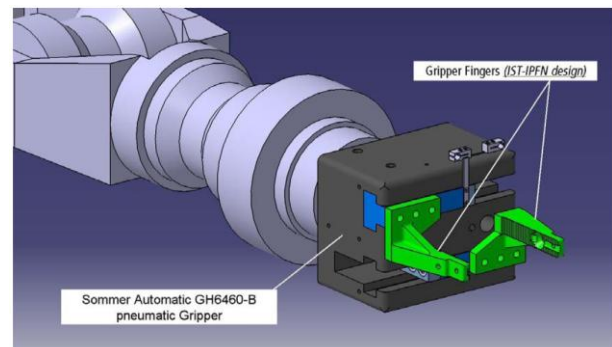


Figure 4.5 - Overall Gripper layout. WHMAN/Gripper interface and end of travel sensors of the fingers not shown.

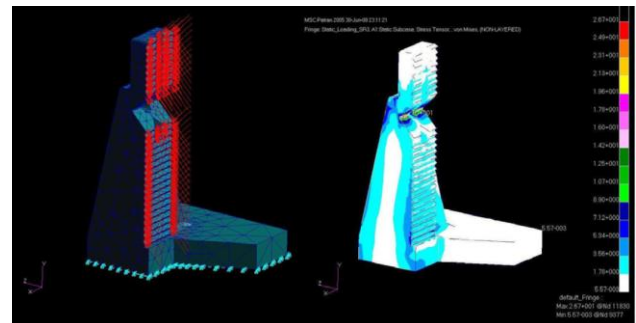


Figure 4.6 - FEM with loads and BC for the finger structural analysis (on the left) and Von Mises stresses distribution over the finger (on the right).

³Work carried out in collaboration with Active Space Technologies.

The sliding table and structural supports were also designed. An integrated static analysis was performed for the WHMAN, Sliding Table and Sliding Table supports system, in order to assess the overall structural performance of the system under static loads, namely the level of stresses over the supports and the level of deformations. The task also included an integration overview of both sub-systems, laying down procedures for its smooth assembly. The detailed 2D manufacturing and assembly drawings for both sub-systems were delivered.

4.5.3. Conceptual studies on the transfer cask system

Remote Handling (RH) is an absolutely required feature for ITER not only during nominal operation, but also during rescue and recovery situations. Among the various RH systems and sub-systems, a Transfer Cask System (TCS), including an Air Transfer System (ATS), has been adopted by ITER as the reference solution. The TCS will be used for the transportation of casks (containing divertors and blankets) to/from vacuum vessel ports in all levels of the Tokamak Building (TB) and ports in the Hot Cell Building (HCB).

Developments and studies in the topic of path planning and trajectory following of the TCS/ATS inside the Tokamak and Hot Cell Buildings have been performed including:

- A Matlab based simulator, with a Graphical User Interface, to support 2D path planning (trajectory design of the TCS/ATS between all vessel ports on all levels and hot cell ports), the definition of parking and maneuvering areas, the study of rescue and recover actions (possible involving a second ATS or other vehicle) and assessing the risk of motion in low clearance areas (Figure 4.7).

An interface between Matlab and CATIA aiming at providing an easy way of importing to the Matlab environment the CAD models of the different levels of ITER buildings.

- Trajectory optimization algorithms given the TCS dynamics/kinematics and the scenario configuration, resulting on free and smooth paths with the minimization of steering maneuvers and changes of direction.

- A proposal was presented to the F4E Call F4E Grant (F4E-2008-GRT-016): “Activities related to the development of an Air Transfer System prototype and Cask Transfer System Virtual Mock-up”. This proposal was approved to start in 2009.

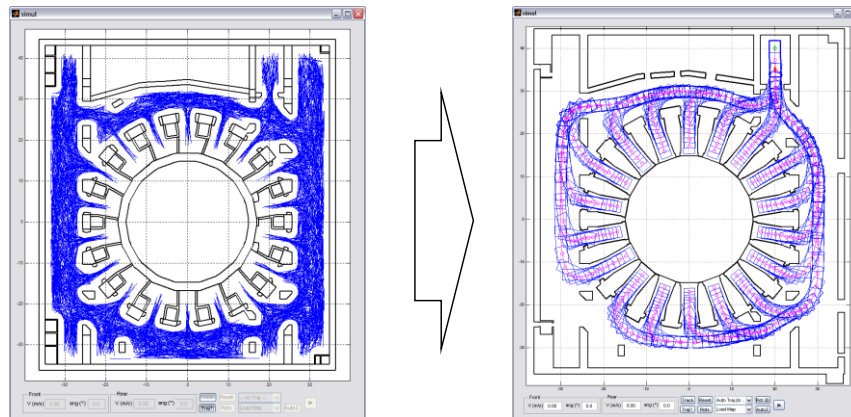


Figure 4.7 - ATS Trajectory optimization inside one of the levels of the tokamak building: a) Search space for trajectories; b) Trajectories between the lift and all VV in a level of the Tokamak Building

5. PARTICIPATION IN THE ASDEX UPGRADE PROGRAMME¹

M.E. Manso (Head), F. Serra (Deputy Head), D. Borba, R. Coelho, L. Cupido, L. Fattorini, I. Nunes, V. Plyusnin, T. Ribeiro, F. Salzedas, J. Santos, A. Silva, F. Silva, P. Varela, A. Combo, S. Graça, L. Guimarães, L. Meneses.

5.1. INTRODUCTION

This project included in 2008 activities related with the development, modelling and scientific exploitation of microwave reflectometry system as well as plasma physics studies on transport and MHD.

5.2. MICROWAVE REFLECTOMETRY

5.2.1. Operation and hardware issues

The fixed frequency and hopping systems for fluctuation measurements operate routinely but the operation of the FM-CW density profile system was limited because the diagnostic is not compatible with the increased levels of ECRH power used in AUG and has to be switched off during high power ECRH experiments. Figure 5.1 shows the millimeter wave shutters used to protect the system electronics from the ECRH radiation. Unfortunately those to not fully protect the diagnostic as ECRH radiation enters through the antenna apertures and has already damaged two of the in-vessel directional couplers of the HFS channels which antennas are more exposed to ECRH radiation. This damage prevented density profiles from the high field side to be obtained and associated HFS/LFS studies to be performed.

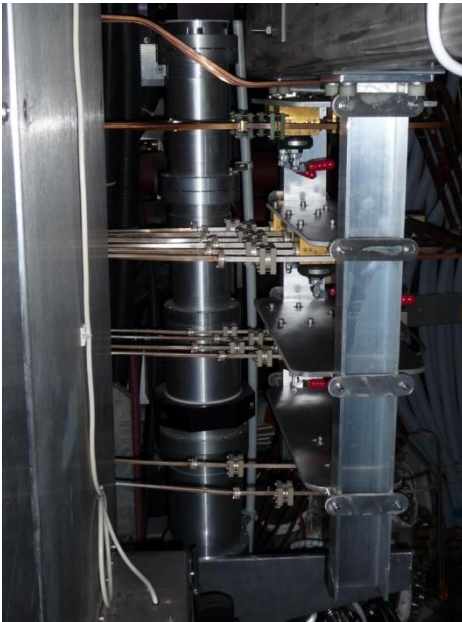


Figure 5.1 - Millimeter wave shutters used to protect the system electronics from the ECRH radiation.

Limited hardware developments and maintenance was performed since many microwave components in operation since 1991 need to be replaced by new ones. Millimetre wave shutters were installed in all channels to protect the electronics from high power ECRH radiation. It was also studied the re-allocation of the waveguides of the present system (HFS/LFS) in the CO6 port dictated by the installation of the new in-vessel control coils on AUG.

In view of difficulties to operate with ECRH, a new bi-static FM-CW broadband system using X mode operation was designed which avoids the use of critical in-vessel components. This option is essential for density profile measurements on ASDEX Upgrade not only to make the system compatible with present operating regimes on AUG but also to fit into the reduced access and in vessel space available for the waveguide routing after the installation of the in vessel coils for mode control. The system will in addition give the possibility to cover the complete density profile, the electromagnetic access to the plasma core being made from the HFS using the X lower cut off reflection, a technique proposed for ITER and never tested in any other fusion machine.

5.2.2. Data processing on density profile evaluation

Algorithms for statistical analysis of X-mode group delay data and detection of the first fringe in X-mode operation were developed and tested. Simulation studies covered the development of an X-mode code for density profile inversion including the ripple of the magnetic field and the study of algorithms that enable to obtain monotonic density profiles routinely.

5.2.3. Real time plasma position demonstration

The following main activities were carried out in 2009:

- Presentation of a proposal to EFDA that was awarded preferential support for the upgrade of the edge profile reflectometry system to be operated in real-time;
- Design of a real time acquisition and processing system adequate for real time evaluation of the plasma position;
- Procurement of key system components;
- Implementation of the web server for the project documentation;
- Development of the PCB interface board between the acquisition front ends and the FPGA board;
- Starting phase of the FPGA programming;
- RTAI patching of the host LINUX operating system;
- Integration of the UTDC timing board.

¹Activities carried out in the frame of the Contract of Association EURATOM/IST and the Contract of Associated Laboratory, by staff of the Groups of Microwave Diagnostics, Theory and Modelling and Control and Data Acquisition, in collaboration with the ASDEX-Upgrade Team. Contact Person: G. Conway

The debugging of the first prototype was initiated.

Figure 5.2 presents the simplified block diagram of the real-time data acquisition and processing system for the ASDEX Upgrade PPR demonstration. Also in the figure are indicated the project phases: I – Hardware development, II – Communication of the RT density profiles over Ethernet (high latency), III – Communication of the RT density profile and separatrix position estimates over a RT network (low latency).

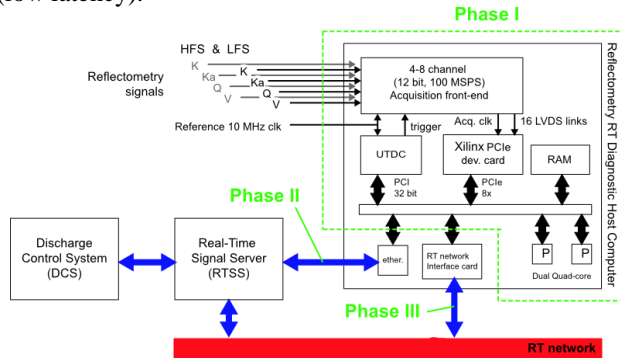


Figure 5.2 – Simplified block diagram of the real-time data acquisition and processing system for the ASDEX Upgrade PPR demonstration. Project phases are indicated: I – Hardware development, II – Communication of the RT density profiles over Ethernet (high latency), III – Communication of the RT density profile and separatrix position estimates over a RT network (low latency).

5.3. PLASMA PHYSICS STUDIES

5.3.1. Introduction

This research line included:

- Reflectometry-based plasma physics studies;
- Edge and SOL tokamak turbulence studies;
- ICRF-MC assisted tokamak start-up and current ramp-up.

5.3.2. Reflectometry-based plasma physics studies

Particular attention has been given to the following main topics:

- Investigation of HFS/LFS density profile changes during pellet induced ELM experiments and their impact on confinement;
- Analysis of edge MHD modes in H mode discharges with different heating power (ICRH and NBI) in LSN discharges. Due to the reduced number of USN and DN discharges the investigation in this area was very limited. The edge MHD modes are not yet identified, two possible candidates were considered: Washboard modes and quasi-coherent modes. It seems that the pressure and pressure gradient plays a role in the existence of these modes. It was observed that the mode disappears just after the ELM and reappears when the pressure becomes constant as it is the case in washboard modes. The radial structure of these modes at the edge was obtained using Lithium Beam and

reflectometer profiles. The profile of the density fluctuation level was estimated using two different models: the 1D Geometric Optics model and the Fanack's model. First measurements of the poloidal velocity of the edge modes were performed using poloidal correlation techniques. Figure 5.3 shows: (a) the temporal evolution of the poloidal velocity for two different poloidal separation (25 cm and 32 cm) for ASDEX Upgrade shot #21131; (b) the density fluctuation profile at the edge derived from 1D geometric optics model for ASDEX Upgrade shot #20354. Results seem to indicate that the ELM affects the modes poloidal velocity.

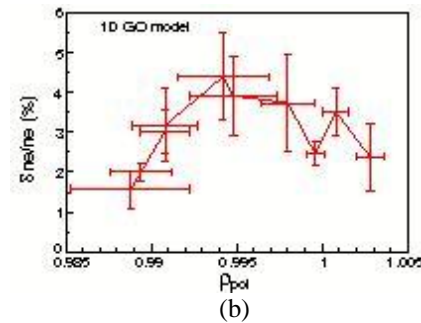
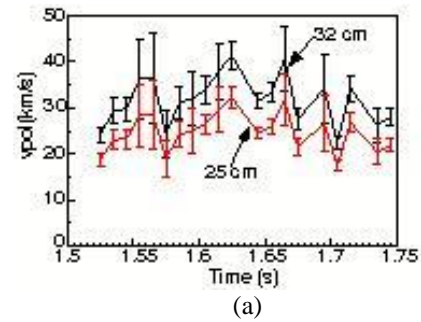


Figure 5.3(a) - Temporal evolution of the poloidal velocity for two different poloidal separation (25 cm and 32 cm) for ASDEX Upgrade shot #21131; (b) Density fluctuation profile at the edge derived from 1D geometric optics model for ASDEX Upgrade shot #20354.

5.3.3. Edge and SOL tokamak turbulence studies

In 2008 an analytical model for the X-point tokamak geometry was further developed.

The mathematics of X-point geometry was revisited to derive an analytical model for fluxtube gyrofluid simulations. The influence of this on the ballooning threshold was studied. In agreement with previous studies, the main effect of the magnetic flux surfaces shaping is to make the parallel gradient terms proportionally stronger in the equations. This is illustrated by the right frame of Figure 5.4, which shows the transport flux as a function of the collisionality. It is smaller for the red line, that corresponds to the simulations made with the X-point model. Further, the integration of the gyrofluid code GEM and the geometrical code METRICS was completed,

allowing self-consistent evolution of the turbulence with background profiles and an analytical X-point equilibrium model.

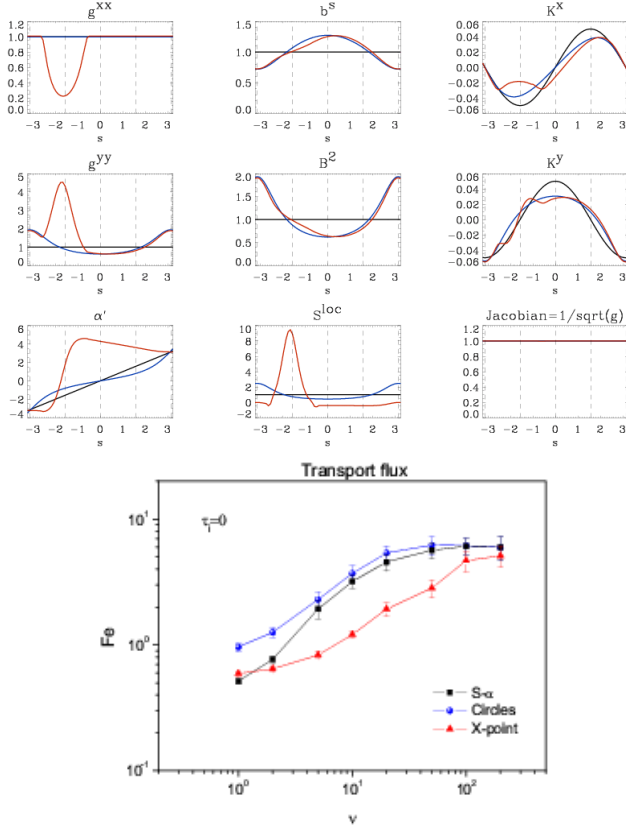


Figure 5.4 - (Top) Geometrical quantities that enter in the GEM model equations for different geometrical model for the tokamak magnetic field: S- α (black line), circular (blue line) and X-point (red line).

5.3.4. ECRH and ICRF-MC assisted tokamak start-up and current ramp-up

The participation in the ASDEX-Upgrade experiments on ECRH and ICRH plasma breakdown and current ramp-up for ITER simulations has been carried out in a frame of proposal ‘ICRF-MC Assisted Tokamak Start-up and Current Ramp-up’². In these experiments low voltage plasma initiation (breakdown) has been tested.

ASDEX-Upgrade typically starts the plasma at $E \sim 0.8$ V/m using resistor switches in the ohmic heating circuits. Switch-less operation was a new development for ASDEX-Upgrade, achieving $E \sim 0.25$ V/m. In comparison, ITER plans to use 0.32 V/m. At $E \sim 0.25$ V/m, ASDEX-Upgrade must use ECRH for pre-ionisation at either 2nd harmonic X-mode (105 GHz at 1.7 T, 140GHz at 2.3 T) or fundamental O-mode (105 GHz at 3.2 T). Alternatively, the ICRH mode conversion scheme was tested also. However, due to low hydrogen concentration (about 5%) several attempts to use ICRF-MC scheme did not reveal necessary

efficiency for start-up of ASDEX-Upgrade discharge. The resonance of ECRH was positioned on the high field side, making 105 GHz at 3.2 T similar to proposed 170 GHz at 5.2-5.3 T in ITER. Optimization of the stray fields at breakdown using multiple poloidal field coils, similar to configurations used in superconducting tokamaks like ITER or KSTAR for maximising the available loop voltage has been carried out.

Importance for the current rise studies is that at low voltage the initial current rise is slow (Figure 5.5.), with full control over the current rise rate by the transformer voltage in contrast to the high voltage breakdown cases with resistor switches where I_p rapidly rises to 300 kA.

The breakdown and current rise studies in AUG has shown the close correspondence to the similar experiments in JET. The main conclusions from these experiments is that: (i) low voltage breakdown works reliably at AUG using ECRH; (ii) ITER should use full bore plasmas just after plasma initiation with X-point formation as early as possible; (iii) additional heating during the current rise is required; and (iv) control of li with the heating systems is possible. In ITER, this would allow to provide different target plasmas for the burn phase at $q_{95}=3$ and advanced scenarios at $q_{95}=4$ and $q_{95}=5$.

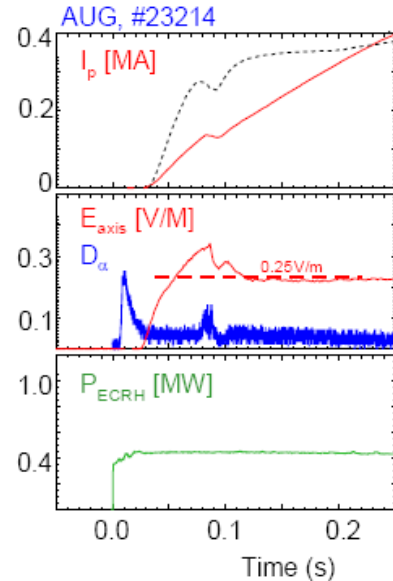


Figure 5.5 - Low voltage ($E \sim 0.25$ V/m) plasma initiation in ASDEX-Upgrade. D-alpha indicates plasma formation. Dashed lines (I_p) give reference cases at higher voltage.

²Elaborated in cooperation with A. Lysoivan, LPP-ERM/KMS, Brussels; J.-M. Noterdaeme, V. Bobkov, D.Hartmann, A. Sips, V.Mertens, J.Stober, IPP-Garching; Jong-Gu Kwak, Young-Dug Bae, Son-Jong Wang, KAERI (South Korea).

6. PARTICIPATION IN THE TJ-II PROGRAMME¹

C. Varandas (Head), M. Manso (Deputy Head), L. Cupido, H. Fernandes, I. Nedzelskij, A. Silva, C. Silva, A. Duarte, L. Guimarães, A. Neto, F. Oliveira.

6.1. INTRODUCTION

This Project had in 2008 three research lines: (i) microwave reflectometry; (ii) edge physics; and (iii) heavy ion beam diagnostic.

6.2. MICROWAVE REFLECTOMETRY

This research line included *studies based on data from the reflectometer hopping systems* aiming at investigating the parameters that control the radial electric field in the TJ-II stellarator leading to improved confinement. It was analyzed the parametric dependence of the perpendicular velocity shear layer formation in TJ-II plasmas. In those plasmas, the perpendicular rotation velocity of the turbulence changes from positive to negative (from ion to electron diamagnetic direction) inside the Last Closed Magnetic Surface (LCMS) when the line-averaged plasma density exceeds some critical value, this change being dominated by the inversion in the radial electric field. A parametric dependence of the critical density has been obtained studying plasmas confined in different magnetic configurations (different rotational transform and/or plasma volume) and heated with different ECH power levels. Figure 6.1 shows the critical line density values obtained experimentally versus the best fit on the corresponding predicted values. The studied data set shows a positive exponential dependence on heating power and a negative one on plasma radius, while the dependence on rotational transform has low statistical meaning. Besides,

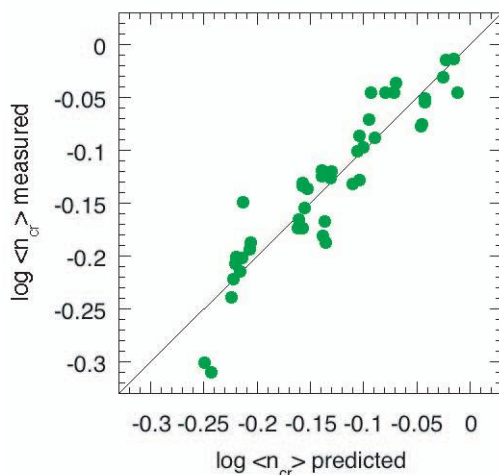


Figure 6.1 – Critical line-density values obtained experimentally versus the best fit found in the regression analysis, represented in a log-log scale

analysis of local plasma parameters points to plasma collisionality as the parameter that controls the inversion of the perpendicular rotation velocity of the turbulence. Figure 6.2 display the local values of plasma collisionality measured in plasmas with different ECH power and in the six magnetic configurations studied. This result explains the positive exponential dependence of the critical line-density on the ECH power.

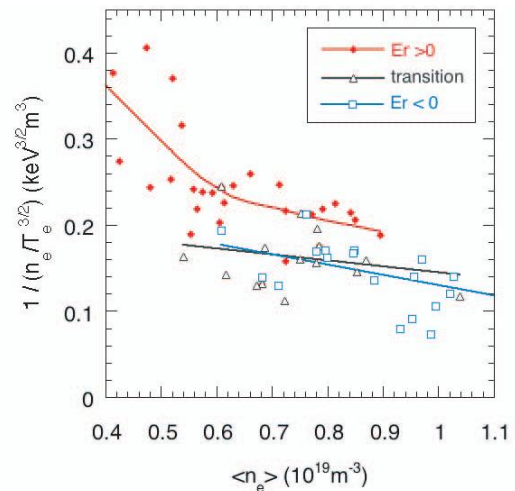


Figure 6.2 – Collision time as function of the line-density for plasmas heated with different ECH power and in the six different magnetic configurations. Plasmas with positive and negative radial electric field are represented in red and blue, respectively, while those in which the radial electric field transition is detected are shown in black.

6.3. EDGE PHYSICS

This research line included the following main tasks:

- *Characterization of large scale fluctuations in the TJ-II stellarator:* Large scale fluctuations have previously been identified on TJ-II using two probe systems. The dynamics of the long distance correlations has been studied during the edge shear layer development and in biased induced improved confinement regimes. The amplitude of the large scale fluctuations is observed to increase during the formation of the shear layer. Figure 6.3 shows the dependence of the long-range correlation on the line-averaged density. Large scale fluctuations are also observed to increase during the biasing period where an edge shear layer is externally imposed in the edge plasma.

¹Activities carried out in the frame of the Contract of Association EURATOM/IST and the Contract of Associated Laboratory, by staff of the Groups of Experimental Physics and Microwave Diagnostics, in collaboration with the TJ-II Team. Contact Person: Joaquin Sanchez

These findings show that the development of fluctuating perpendicular flows (with zonal flow-like structure) can be considered the first step in the transition to improved confinement regimes.

- *Development of a 5-channel Retarding Field Analyzer Probe:* A 5-channel RFA has been developed for edge ion temperature measurements on TJ-II. Tests of the RFA operation have been successfully performed on ISTTOK. Due to the TJ-II complex field line structure, the sensitivity of the RFA operation to magnetic field misalignments has been investigated. Figure 6.4 permits to conclude that no significant errors in the derived plasma parameters were found for misalignments below $\pm 15^\circ$. These observations could be explained by the ion pitch angle.

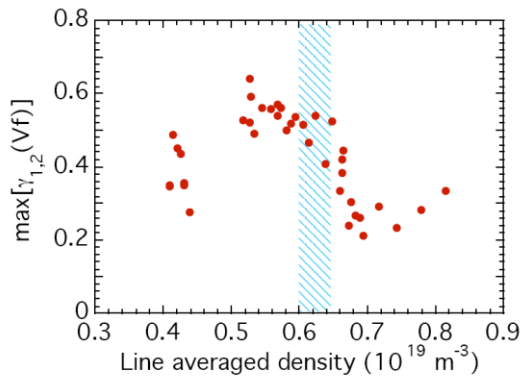


Figure 6.3 - Maximum value of the cross-correlation function between floating potential signals measured at approximately the same radial positions of both probes ($r/a \approx 0.9$) as a function of plasma density. Shaded area indicates the critical density region.

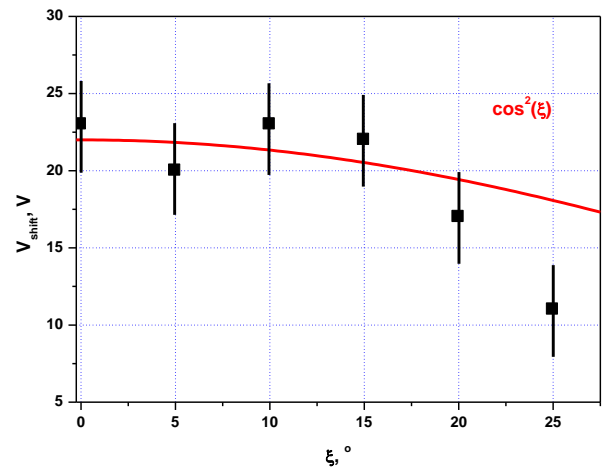


Figure 6.4 - Dependence of the derived ion temperature of the probe alignment.

6.4. HEAVY ION BEAM ANALYSER

This research line included the following main task:

- *Optimization of the HIBP diagnostic:* A strong reduction in the background signals of the Multiple Cell Array Detector (MCAD) has been achieved. An appropriate biasing of the two MCAD grids was proved to reduce the spurious plasma loading signal by a factor of 2.5.

7. PARTICIPATION IN THE TCV PROGRAMME¹

C. Varandas (Head), P. Amorim, A.P. Rodrigues, N. Cruz, T.I. Madeira, B. Santos.

7.1. INTRODUCTION

This project has two main research lines:

- X-ray diagnostics
- Advanced plasma control system.

7.2. X-RAY DIAGNOSTICS

7.2.1. Introduction

This research line had two main working lines:

- Improvement and scientific exploitation of the Pulse Height Analysis (PHA) X-ray diagnostics;
- Development of a real-time PHA X-ray diagnostic.

7.2.2. PHA X-ray diagnostics

7.2.2.1. Main activities

The following activities were performed in 2008:

- Commissioning and scientific exploitation of the vertical pulse height analysis (PHA) diagnostic;
- Demonstration of the throughput limit of the diagnostic;
- Calibration of the feedback system parameters;
- Increase of the temporal resolution (50 ms maximum, hardware and software limited);
- Participation in some TCV scientific campaigns.

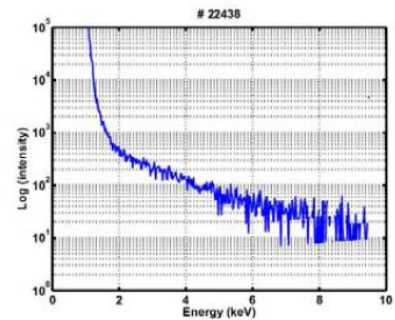
7.2.2.2. Main results

An alternative technique was developed, based on the comparison of experimental and simulation soft X-ray spectra, to extract the electron temperature from the experimental the PHA diagnostic, in particular when the emission is non-thermal and the classical linear fitting procedure is difficult to be employed.

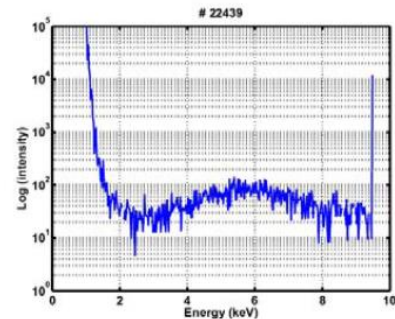
Observation of the behaviour of experimental *bremsstrahlung* data have shown that the maximum of this radiation is usually invisible (Figure 7.1A) but it can be visible (Figure 7.1B and C) and more or less pronounced depending on the combination of three factors: the RF power, the electron temperature and the beryllium filtering. Figure 7.2 enables to observe the moment where RF power starts to be injected ($t = 0.4$ s), when the power starts to increase and when it is removed ($t = 1.6$ s). The effect on the *bremsstrahlung* is quite clear. Sometimes the *bremsstrahlung* maximum shifts away from the V-PHA observation range, giving the impression that a tail is ‘going up’.

Simulations employing the theoretical model of *bremsstrahlung* X-ray spectrum and assuming a maxwellian distribution function for the electrons velocity distribution (Figure 7.3), have shown that:

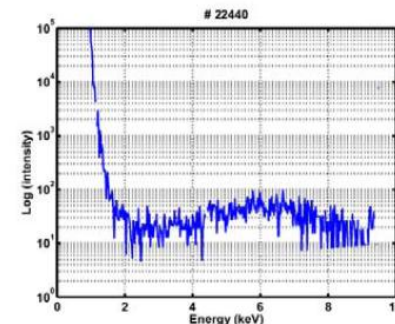
- The maximum of the *bremsstrahlung* curve shifts to the right as electron temperature increases, which is consistent with the experimental observations;
- The *bremsstrahlung* maximum seems to coincide with the electron temperature;
- The electron temperature and the endpoint of the *bremsstrahlung* seem to be related by a factor of 5.



A



B



C

Figure 7.1 – H-PHA results. Sequence of discharges showing what appears to be *bremsstrahlung* shifting.

¹Activities carried out in the frame of the Contract of Association EURATOM/IST and the Contract of Associated Laboratory, by staff of the Groups of Experimental Physics and Control and Data Acquisition, in collaboration with the TCV Team. Contact Person: Basil Duval.

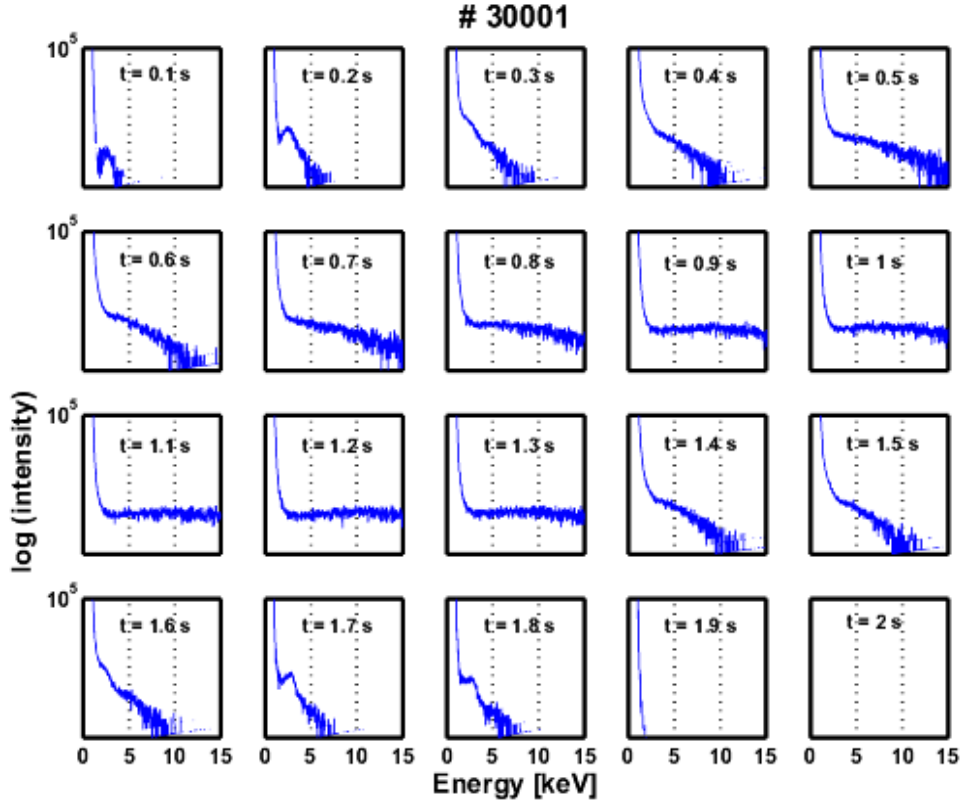


Figure 7.2 – Spectra obtained with the V-PHA diagnostic, in which it is possible to trace the instants the RF is switched on ($t = 0.4$ s) and off ($t = 1.6$ s), and the time intervals the RF power reaches its maximum and is held constant ($t = 0.9 - 1.3$ s).

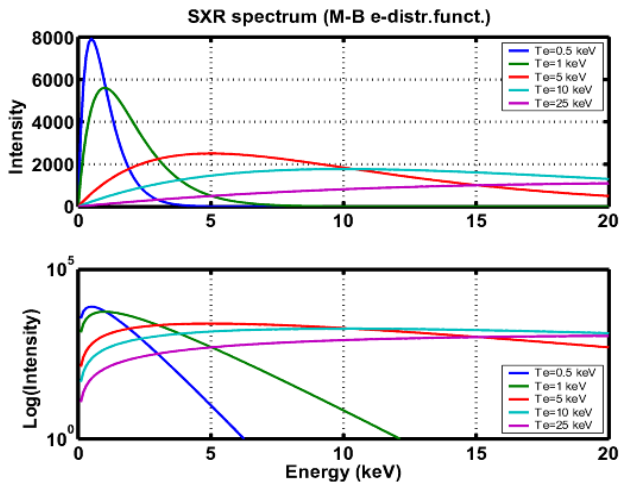


Figure 7.3 – Bremsstrahlung spectrum simulation for varying electron temperature.

These observations have suggested an alternative method to the traditional chi-square linear regression:

- Electron temperature could be estimated by searching for the maximum of the bremsstrahlung curve by performing a statistical fitting and calculating its null derivative (Figure

7.4). The Matlab function that produced the best results was a ‘spline’. By best results it is understood the ability to handle low statistics (>100 counts), robustness, stability and computation speed. The maximum of the bremsstrahlung did not coincide with the previously measured electron temperature by the chi-square linear fitting.

- It can happen that this maximum is not observed due to filtering (and the bremsstrahlung presents an exponential fall off) or because it lies outside the energy range accessible by the PHA diagnostics. In these cases one of the two parameters (bremsstrahlung maximum or bremsstrahlung end point) might be calculated from the 5 factor relation between both (as predicted by the simulations). The electron temperature should therefore be calculated from the relation,

$$-\frac{1}{T_e} = \text{bremsstrahlung slope} = \frac{y}{x} = t g \alpha$$

Figure 7.5 is just one example of the previous hypothesis in which all the geometrical relationships have been found and the results obtained from these trigonometric and proportionality relations agree well with the previous fitting procedure.

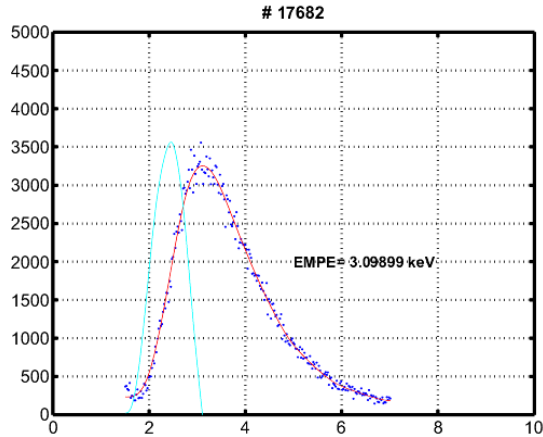


Figure 7.4 - Example of a 2s spectrum obtained with the H-PHA diagnostic in which the bremsstrahlung maximum was measured with the new fitting procedure.

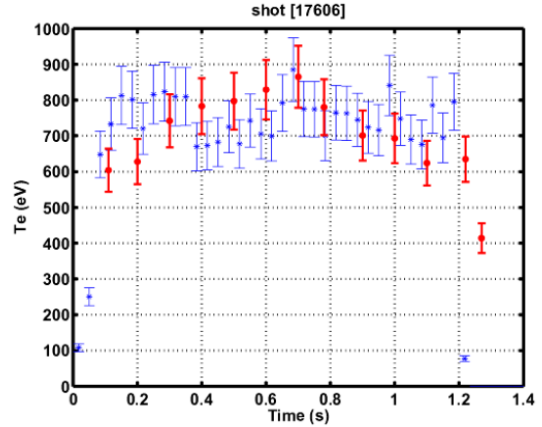


Figure 7.6 - Electron temperature evolution measured with the horizontal PHA diagnostic (•) and the Thomson scattering diagnostic (*), when maxwellian behaviour is observed.

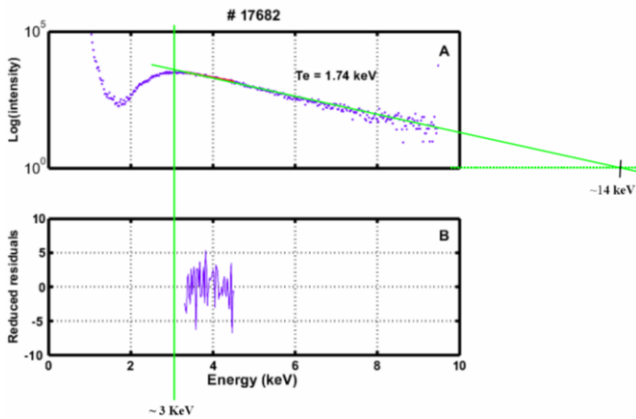


Figure 7.5 - Example of a 2s spectrum obtained with the H-PHA diagnostic in which the electron temperature is measured from the new fitting procedure together with the mathematical relation (5.8).

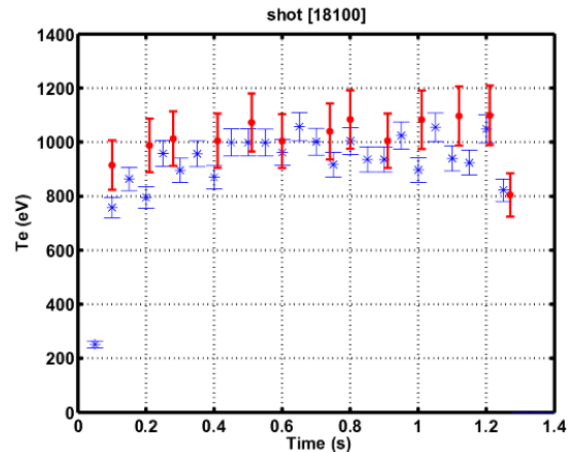


Figure 7.7 - Electron temperature evolution measured with the horizontal PHA diagnostic (•) and the Thomson Scattering diagnostic (*), when two populations of different energy are generated.

Figures 7.6 and 7.7 show good agreement between the electron temperature measurements made with the PHA and Thomson scattering diagnostics, even when two populations of different energies are generated.

7.2.3. Real-time PHA diagnostic

The main goal of the 2008 activities was the improvement of the data acquisition process by manufacturing a pre-amplifier pulse conditioner to the DSP input characteristics. This analog unit has three main objectives:

- (i) to restore the signal baseline;
- (ii) to amplify the input signal in order to use the total input voltage range of the ADC;
- (iii) to reduce the noise due to the DCDC converter of the preamplifier.

Figure 7.8 compares the results obtained before and after the development of this unit.

7.3. ADVANCED PLASMA CONTROL SYSTEM

The new Advanced Plasma Control System (APCS) has been successfully integrated in the main TCV control system and was routinely used during the TCV operation. Related to this second phase of the project several tasks were performed including:

- Preparation and beginning of the design of new algorithms for the plasma vertical control;
- Characterization of the APCS channels input and study of methods for noise reduction to improve control performance;
- Upgrade to the system control state machine with enhanced logging system and error states definition;
- Close support to the use of APCS by the TCV Control Group.

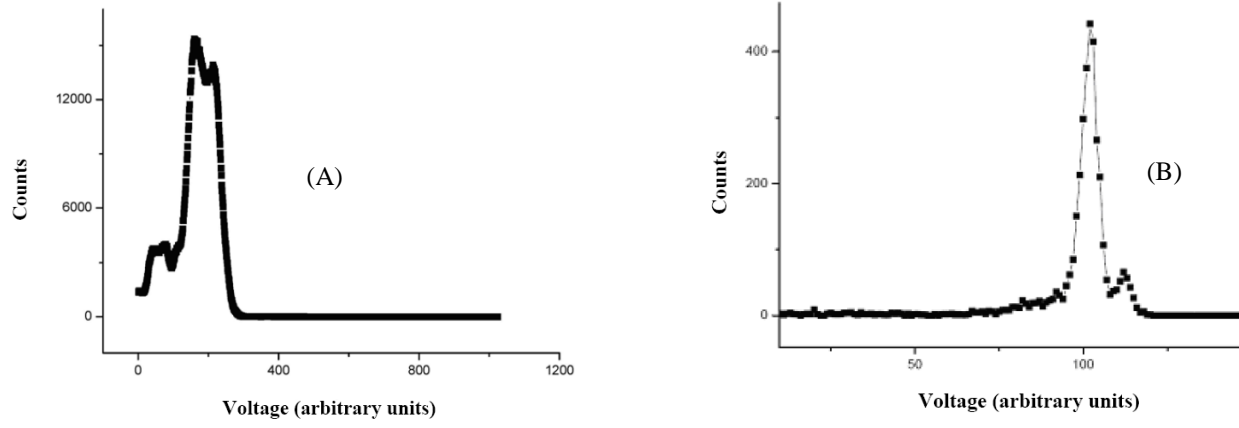


Figure 7.8 – Spectra measured before (A) and after (B) the analogue front-end development

8. PARTICIPATION IN THE COMPASS PROJECT¹

C. Varandas (Head), M.E. Manso and H. Fernandes (Deputy Heads), B. Carvalho, L. Cupido, A. Silva, C. Silva, J. Sousa, H. Alves, A. Batista, I. Carvalho, P. Carvalho, M. Correia, A. Duarte, A. Fernandes, J. Fortunato, R. Gomes, S. Magalhães, L. Meneses, A. Neto, N. Poolyarat, T. Pereira, D. Varcárcel.

8.1. INTRODUCTION

The research activities of this project have been focussed on:

- Tokamak systems;
- Microwave reflectometry;
- Control and data acquisition.

8.2. TOKAMAK SYSTEMS

IPFN staff collaborated in 2008 on:

- Implementation and testing of the vacuum systems;
- Definition of the characteristics of the power supplies.

8.3. FW-CW REFLECTOMETRY SYSTEM

The main activity was the elaboration of a technical proposal presented to EFDA Call 2008 for the development of the FM-CW reflectometer system for the Compass tokamak including cost and time schedule, in collaboration with IPP-CR. The schematic configuration of one of the Compass millimetre wave reflectometer channels to measure density fluctuations is depicted in Figure 8.1.

The reflectometry system should allow the measurement of density profiles as well as the correlation properties of plasma turbulence. It will be equipped with channels covering the K, Ka, U and E frequency bands. The mode of operation will be ordinary (O) mode in all channels. In addition a channel operating in extraordinary (X) mode will probe the outer edge of the plasma.

The system will be developed in the following three phases: (i) Density Profile Systems: K & Ka channels; (ii) Turbulence/Correlations: K & Ka Channels; (iii) Density Profile Systems and Turbulence/Correlations: U & E channels. In-vessel antennas and separate waveguides will be used for each of the four frequency bands. It is expected that the system will be developed in 2009/2010 in collaboration with IPP.CR under EFDA awarded preferential support.

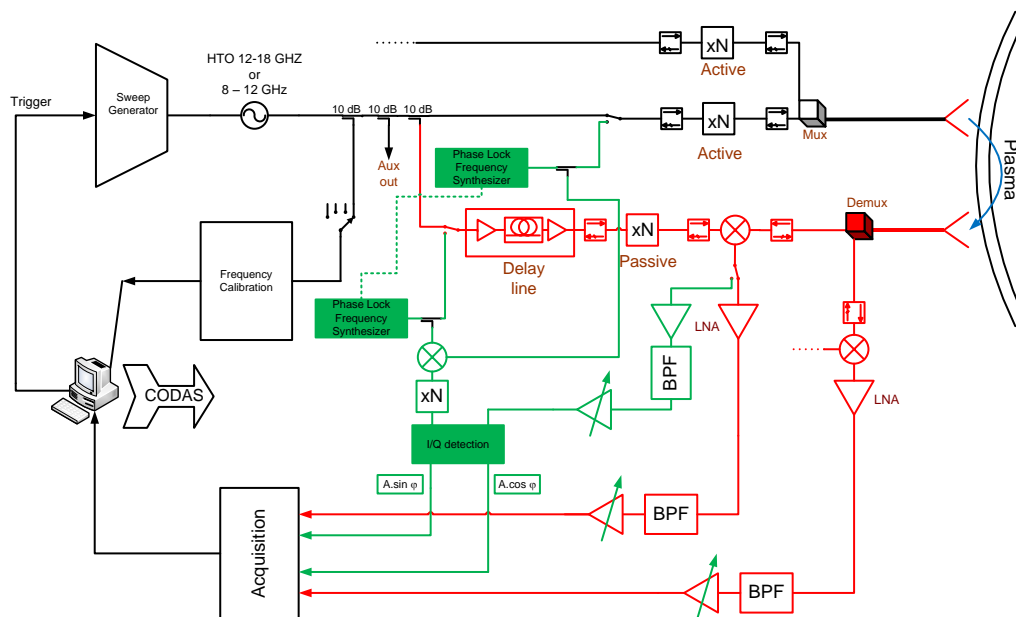


Figure 8.1 - Schematic configuration of the Compass millimetre wave reflectometer.

¹Activities carried out in the frame of the Contract of Association EURATOM/IST and the Contract of Associated Laboratory by staff of the Groups of Experimental Physics, Microwave Diagnostics and Control and Data Acquisition, in collaboration with the COMPASS team: Contact Person: Pavel

8.4. CONTROL AND DATA ACQUISITION

COMPASS control and data acquisition system is being redesigned and built from scratch based on the ATCA standard (Figure 8.2). The platform contains one ATCA controller with a Gigabit Ethernet interface, up to 12 ATCA Digitizer-Generator-Processor (DGP) cards and trigger and clock inputs, all on a 12U shelf. The multi-core x86-based General Purpose Processor (GPP) controller will be connected to the DGP cards by Peripheral Component Interconnect Express™(PCIe) point-to-point links through the ATCA backplane. Multiple-input multiple-output (MIMO) signal processing will be shared by the DGP cards using the built-in Field Programmable Gate Arrays (FPGA) and the controller's x86 general processor. Eleven Aurora™2.5 Gbit/s links allow further parallelization of the execution of code among several FPGAs. In order to guarantee real-time execution of the control codes a framework based on Linux and the Real-Time Application Interface (RTAI) will be used. This will explore the features provided by the new multi-core technologies. Synchronization between the subsystems will be guaranteed by a real-time event network.

The interface to the system will be provided by the FireSignal control and data acquisition system. This will allow the operators and diagnostic coordinators to configure the hardware, prepare the discharges, pre-program events of interest and follow results from the discharge. FireSignal will also orchestrate the data flow coming from the different diagnostics into the database and to registered data clients.

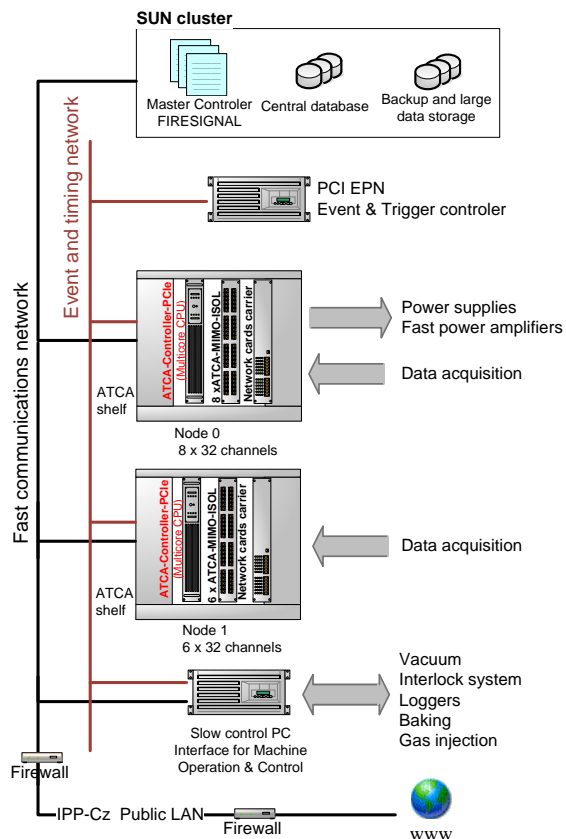


Figure 8.2 - Schematic of COMPASS tokamak control and data acquisition system.

9. COLLABORATION WITH THE ASSOCIATION EURATOM/CEA¹

J.P. Bizarro (Head), M. Manso and R.V. Mendes (Deputy Heads), J.H. Belo, F. Briolle, F. Cipriano, R. Coelho, F. Silva, D. Alves, J. Bernardo, S. Cortes.

9.1. INTRODUCTION

This project had four research lines:

- ITER-like PAM LH launchers;
- Microwave reflectometry;
- Motional Stark Effect diagnostic;
- Stochastic solutions of the Vlasov-Poisson and Vlasov-Maxwell systems.

9.2. ITER-LIKE PAM LH LAUNCHERS

9.2.1. Validation of Tore-Supra's (ITER-like) PAM LH launcher manufacture

Support to the validation of the C4's manufacture – Tore-Supra's upcoming (ITER-like) LH PAM launcher – has continued, addressing, via theoretical analysis/modelling, the impacts (on coupling, directivity and E-field inside its waveguides) of various defects that resulted from the fabrication process.

Detailed RF modelling of the C4's prototype module as well as of its 16 different modules (both with and without the TE₁₀ to TE₃₀ mode converters, besides the mode converter alone) was carried out also: the respective theoretical scattering matrices were computed over a wide range of frequencies aiming at the comparison with low-power RF measurements (tests on the mode converter alone and on the PAM prototype already showing very good agreement). An example of the E-field calculation inside such modules is shown in Figure 9.1.

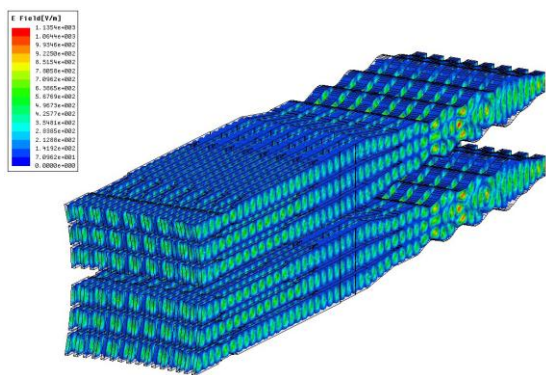


Figure 9.1 - "E-field amplitude computed inside the 16 modules of TS's PAM launcher"

9.2.2. Validation of the ALOHA LH coupling code

The validation/benchmarking of ALOHA, the most recent LH coupling code developed at DRFC/DEA, was carried

out by studying three multijunction based LH launchers with recourse to detailed RF modelling: the oldest currently in use at Tore Supra (dubbed C2), its successor (the C3) and the forthcoming PAM (the C4), each with 16 different modules. Comparisons have been made with the well established coupling code SWAN as well as with the experimental data base of the former two launchers.

9.2.3. LH launcher for ITER

The study of a LH launcher for ITER was started, namely initiating a re-evaluation of the existing project (the DDD of 2001) in view of the developments and changes brought to ITER since then (particularly in the port plug).

9.3. MICROWAVE REFLECTOMETRY

9.3.1. Modelling of experiments

The main studies performed were: (i) the contribution of the forward scattering to Doppler reflectometry using a FDTD code; (ii) Simulation studies using narrow band Kolmogorov and Gaussian spectra with identical correlation lengths, have been initiated to pursue the comparisons with a forward scattering theoretical model proposed by E. Gusakov. Simulation on the effects of forward scattering and Bragg back scattering were studied using a FDTD code illustrating in a very clear way some of the mechanisms which intervene in both Bragg backscattering and forward scattering. Simulations results show a good agreement with the behavior previewed by Gusakov theoretical model apart from the amplitude of the scattered signal that is under investigation.

9.3.2. Tomographic techniques for data analysis

Most natural and man-made signals are nonstationary and may be thought of as having a multi-component structure. Bat echolocation, whale sounds, radar, sonar and many others are examples of this kind of signals. The notion of nonstationarity is easy to define. However, the concept of signal component is not so clearly defined. A particular example quite relevant for plasma diagnosis is the separation of components (plasma reflection, wall reflection, multiple reflections, etc.) in reflectometry data. Based on previously developed (noncommutative) tomographic techniques (Figure 9.2), a method for component separation has been implemented. Later on, the separated components and the same method have been shown to be appropriate to obtain the phase derivative of the signal.

¹Activities carried out in the frame of the Contract of Association EURATOM/IST and the Contract of Associated Laboratory, by staff of the Groups of Microwave Diagnostic and Theory and Modelling.

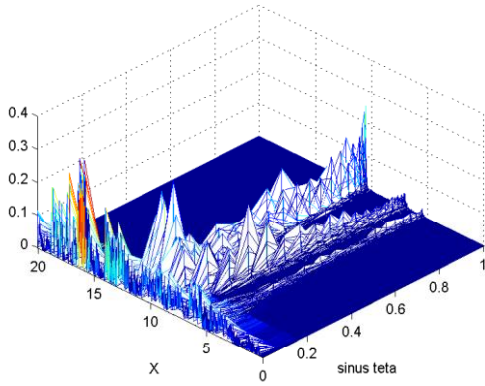


Figure 9.2 – Example of a tomographic reconstruction

9.4. MOTIONAL STARK EFFECT DIAGNOSTIC

9.4.1. Data processing

IPFN has proceed with the characterization of the spectral content of the raw MSE data (Figure 9.3) and the optimization of the amplitude estimation algorithm based on recursive filtering. This approach provides higher sampling rates and higher signal-to-noise ratios than the regular Fourier-based amplitude estimation (single-phase and dual-phase lock-in) algorithms.

9.4.2 Diagnostic simulation

An end-to-end MSE diagnostic synthetisation has been performed based on the Stokes description of polarised light as well as the Mueller matrices formalism used to describe the cumulative effect of relevant optical components. The intensities of linearly, circularly and non-polarised light are reconstructed for each channel based on the raw photomultiplier data. Preliminary investigation on channels exhibiting noticeable pitch angle drifts in time indicate that such drifts may not be accounted by current density transport but, instead, to vessel boundary effects that ultimately contaminate the measurements.

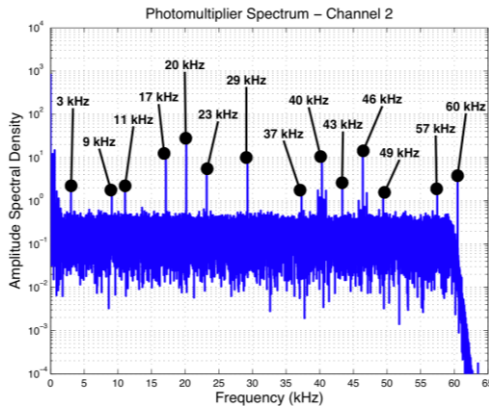


Figure 9.3 - Amplitude spectral density of the photomultiplier with the dominant frequencies.

9.5. STOCHASTIC SOLUTIONS OF THE POISSON-VLASOV AND MAXWELL-VLASOV SYSTEMS

Solutions of nonlinear partial differential equations (and in particular those describing plasma dynamics like Maxwell-Vlasov) may be expressed as mean-values of a stochastic process. This process is of multiplicative type, its realisations being represented by trees for which the branching is directly related to the nonlinearity in the equation (Figure 9.4). This approach is promising because it gives a natural characterisation of the solutions and leads to practical algorithms which, without the need for a phase space grid, provide localized solutions and are fully parallelizable. Moreover, by associating a stochastic process with the initial equation, it may give an intrinsic characterisation of the nature of the fluctuations exhibited by the physical system.

In addition, by examining the branching stochastic process, the method allows, in principle, to single out rare but efficient transport events such as intermittent bursts. This would provide a new method to characterise intermittency, relevant to the magnetic confinement of plasmas. So far this program has been successfully carried out for the Poisson-Vlasov equation and for a nonlocal version of the KPP equation.

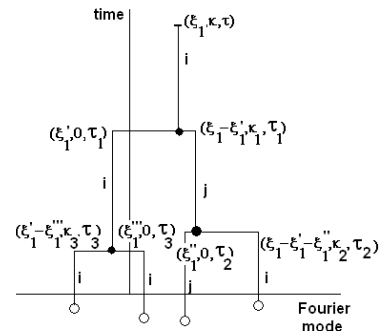


Figure 9.4 – Schematic of the branching process directly related to the nonlinearity in the equations

10. OTHER THEORY AND MODELLING STUDIES¹

J.P. Bizarro (Head), R. Coelho (Deputy Head), P. Belo, F. Nave, T. Ribeiro, J. Santos, F. Serra, A. Duarte, J. Ferreira and P. Rodrigues.

10.1. INTRODUCTION

This project included in 2008 seven research lines:

- Dynamical systems' description of ITB oscillations;
- Tokamak equilibria with toroidal current reversal;
- Noniterative reconstruction of tokamak equilibria;
- Signal processing;
- Integrated tokamak modelling task force;
- ITER scenario modelling;
- Other studies.

10.2. DYNAMICAL SYSTEMS' DESCRIPTION OF ITB OSCILLATIONS

The study of Internal Transport Barrier (ITB) oscillations within the framework of dynamical systems' theory was started. More precisely, the effort is being made to derive from the plasma transport equations in a tokamak a set of dynamical equations exhibiting limit-cycle behavior.

10.3. TOKAMAK EQUILIBRIA WITH TOROIDAL CURRENT REVERSAL

This activity was pursued, more precisely an exercise has been carried out to emphasize that several distinct equilibria (with and without current reversal) are consistent with the same set of experimental data, as illustrated in Figures 10.1 and 10.2 for JT-60U. So, one should be cautious before ruling out the existence of tokamak equilibria with negative current in the plasma core based on the present-day accuracy of MSE diagnostics (Figure 10.3).

10.4. NONITERATIVE RECONSTRUCTION OF TOKAMAK EQUILIBRIA

A noniterative algorithm to reconstruct tokamak equilibria has been extended to handle plasma configurations that are not symmetric with respect to the midplane and then used to compute equilibria solutions from experimental datasets (Figure 10.4). A number of issues concerning how available experimental data can be handled and provided as input to the GS solver in practical situations have also been made clear.

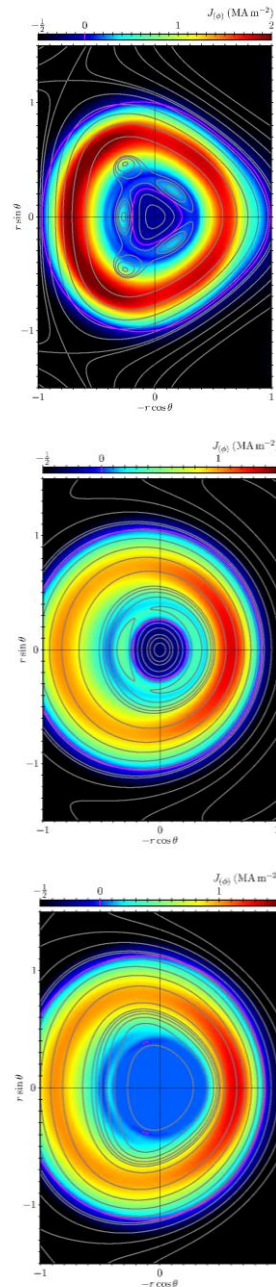


Figure 10.1 - Equilibrium reconstruction: flux surfaces (gray solid lines) and toroidal-current density distribution (colour map). The magenta contours indicate zero toroidal-current density.

¹Activities carried out in the frame of the Contract of Association EURATOM/IST and the Contract of Associated Laboratory, by staff of the Group of Theory and Modelling.

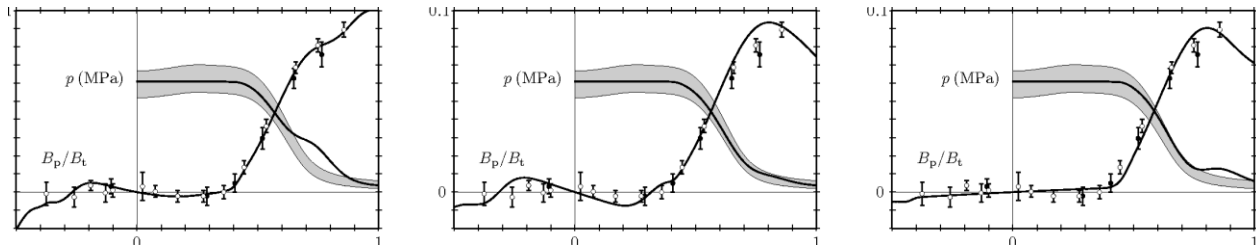


Figure 10.2 - Equilibrium reconstruction results (solid lines) vs. experimental data: field pitch from MSE diagnostics (circles) and plasma pressure (shaded area).

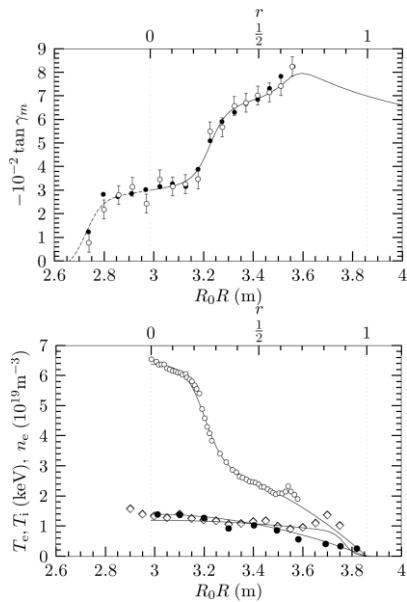


Figure 10.3 - Top panel - Polarization angle measured by motional Stark effect (open circles), predicted by an independent reconstruction technique (full circles), and given by a noniteratively reconstructed equilibrium (dashed line) built using the model along the low-field side (solid line) as an input profile. Bottom panel - electron density (open diamonds), electron temperature (open circles), ion temperature (full circles), and their respective input models (solid lines).

10.5. SIGNAL PROCESSING

Following the investigation of the time and frequency response of a lock-in amplifier scheme based on Kalman filter techniques, the prospects for the real-time estimation of the spectrum of plasma related signals (e.g. Mirnov coil signals) was explored. A parallel filter bank setup code, with possibly unevenly spaced probing frequencies, was devised and tested on both synthesized and actual experimental data. Preliminary results point to a trade-off between the frequency and time resolution that depends most notably on the ratio of the process and measurements error covariance's assumed in the filter but also on the instantaneous rate change of the signal's frequency (Figure 10.5).

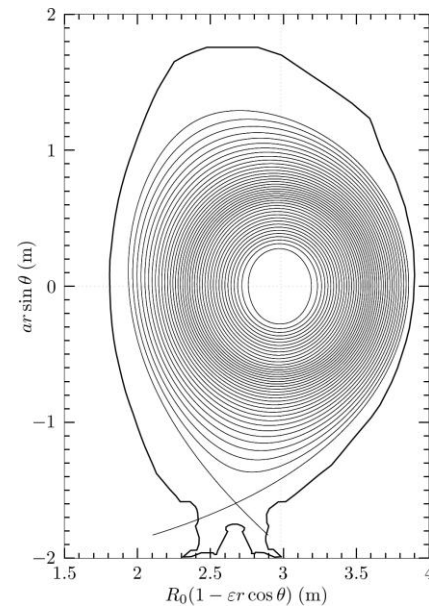


Figure 10.4 - Reconstructed equilibrium: closed flux surfaces and the separatrix.

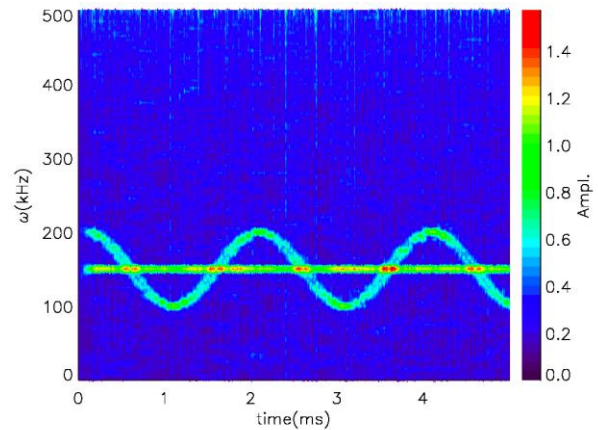


Figure 10.5 - Real-time (0.5μs sampling time) spectral distribution of synthesized signal using Kalman filter algorithm.

10.6. INTEGRATED TOKAMAK MODELLING TASK FORCE

10.6.1. Introduction

Activities in the framework of the ITM–TF Workprogramme covered three Task Agreements, namely in the TFL2, ISIP and IMP4 Integrated modeling projects respectively.

10.6.2. Task Agreement TFL2

Within TFL2, comprising tasks falling directly under the coordination of the Task Force Leadership, contributions focused on:

- Iter Scenario Modelling activities (see Section 10.7);
- Task Force Leadership (acting deputy Task Force Leader)².

Assistance to the task force leadership covered, among others, coordinating the overall ITM–TF activities, monitoring progress in the TF, defining and implementing the 2009 workprogramme and draft task agreements and providing the Annual report of ITM activities and the associated report tables. Coordination of the Experimentalists and Diagnosticians Resource Group, a privileged contact point for the ITM–TF with the European experiments, was initiated.

10.6.3. ISIP project

In the framework of the ISIP Project, the following activities were carried out:

- Formulation of the requirements for the simulations codes and data search databases and layout development. This layout was subsequently implemented on the ITM gateway as a MySQL relational database and a dedicated API was developed in C, enabling database accessing from the Universal Access Layer.
- Development of an higher level Java API dedicated to the interfacing of Java codes with the low level C API that communicates with the MySQL database.

10.6.4. IMP4 project

In the framework of the IMP4 – Transport processes and micro-stability Project, the following activities were carried out:

- Participation in the European turbulence codes benchmarking effort

The activities were part of the cross-verification study of several European edge turbulence codes. The GEM code was used to simulate the test cases defined within the joint study to realistically represent the edge turbulence regime in a generic medium tokamak L-mode base case. GEM had to be modified to comply with the data format agreed upon within the task force (HDF5 data format), in order to share the data between the codes involved in the benchmark activities. The edge turbulence results were found to agree

very well amongst the participating codes on collisionality scaling and acceptably well on beta scaling (below the MHD boundary) for cold-ion cases, also in terms of the non-linear mode structure. An example of the latter is illustrated by the spectra shown in Figure 10.6 for two of the participating codes.

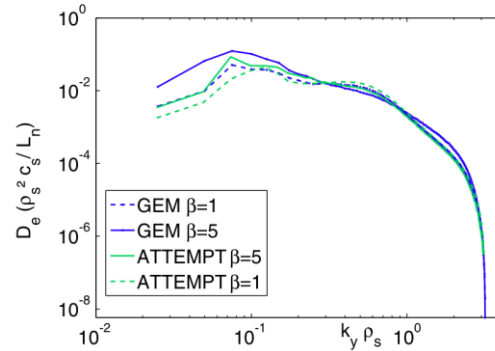


Figure 10.6 – Electron particle diffusivity spectra as a function of $k_y \rho_s$ (on logarithmic scale) for the flux-tube codes ATTEMPT and GEM, for the edge test case $C=7.65$, with normalized $\beta=1$ (---) and $\beta=5$ (—). Figure from the reference Falchetto et al, Plasma Phys. Control. Fusion, 50 (2008) 124015.

10.7. ITER SCENARIO MODELLING

To complement the assessment and validity of the available codes for neutral beam injection (NBI) heating & current drive (H&CD) modelling, more benchmarks were done, now including the code NEMO/SPOT. This new package, integrated in the transport code CRONOS and developed by the Association EURATOM-CEA, includes an improved module for neutral beam deposition, coupled to a monte carlo module for the fast ion dynamics, and can now be used for ITER scenario modelling. Envisaging the type of scenarios to be analyzed by the ISM, two particular JET discharges were chosen to benchmark the NBI H&CD codes. One was an ITER-relevant steady-state hybrid scenario with a non-inductive 20 sec flattop, the second an ITER-like current ramp-up. The agreement between NUBEAM, NEMO/SPOT and PENCIL is now within 10%. Some discrepancies between codes remain, specially concerning the charge-exchange losses (Figure 10.7).

Progress on ITER modelling for Ohmic, LH and NBI assisted current ramp up/down was accomplished with the validation of transport and LH codes using ITER-like plasmas recently obtain in JET. Reasonable agreement was obtained between CRONOS and JETTO although differences in LH current and power deposition are noticeable. Further work is needed to understand precisely the role of LH CD&H in shaping the q-profile in JET and ITER plasma (Figure 10.8).

²R. Coelho was nominated Deputy Task Force Leader by 1st August 2008.

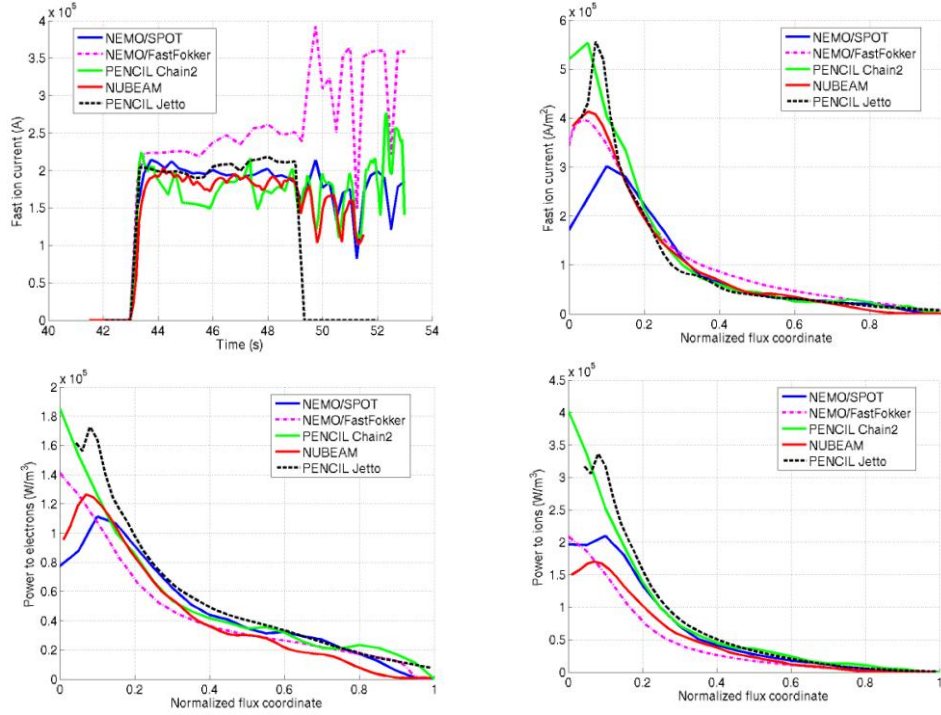


Figure 10.7 - JET #72517, timetraces and profiles (clockwise from top left) given by NEMO+SPOT, NEMO+FASTSOLVER, PENCIL, and NUBEAM, for fast ion current generation, fast ion current density, and power transferred to electrons and ions at 6,5 s by the action of 5 MW of Neutral Beam Injection.

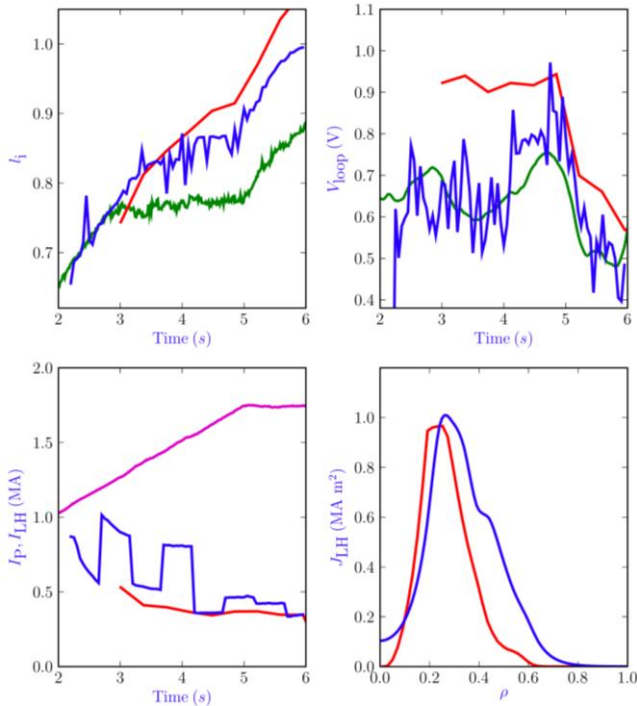


Figure 10.8 - JET#72823, timetraces of (clockwise from top left): internal inductance, loop voltage, total experimental, current and simulated LH current and LH current profile (green: experimental, magenta: total current, red: JETTO, blue: CRONOS).

10.8. OTHER STUDIES

Fundamental studies on the thermodynamics of irreversible processes with frictional dissipation were pursued, and expressions were obtained for entropy production in such cases. Eventually, this new framework will be applied to the thermodynamics of tokamak plasmas.

11. KEEP-IN-TOUCH ACTIVITIES IN INERTIAL FUSION ENERGY¹

J.T. Mendonça (Head), R. Bendoyro, J. Davies, J.M. Dias, M. Fajardo, G. Figueira, R. Fonseca, A. Guerreiro, C.P. João, C. Leitão, N. Lemos, N. Lopes, A.M. Martins, D. Resendes, L. Silva, J. Valente, J. Wemans.

11.1. INTRODUCTION

The main results obtained in 2008 in the context of keep-in-touch activities on inertial fusion energy are organized in the following themes:

- Fast ignition;
- High intensity photonics;
- Plasma accelerators and intense radiation sources;
- Fast electron transport theory for the HiPER project.

11.2. FAST IGNITION

A study of the laser-to-electrons energy transfer has been undertaken on the LULI2000 laser facility (Figure 11.1) at intensities relevant for the fast ignition scheme, in an international consortium of researchers from France, Italy, Portugal and the UK. In January/February 2008 we participated in an international experiment on the Vulcan PetaWatt laser in the UK, investigating electron transport for fast ignition. It was found that the number of laser-accelerated fast electrons increases when the laser contrast deteriorates, but the electron beam divergence angle ($\sim 30^\circ$) remains constant. Concerning code development and theory for fast ignition and IFE theory, in collaboration with UKAEA, CIEMAT, IPPLM, IPP.CR, and CEA we have worked on the definition of the requirements for the integration of the numerical tools for full scale simulation of a (fast) ignition scenario in IFE.



Figure 11.1 - LULI2000 target chamber

11.3. HIGH INTENSITY PHOTONICS

At the Laboratory for Intense Lasers, several ytterbium-doped hosts for high energy amplification at 1053 nm were tested, and Yb:KYW and Yb:CaF₂ were identified as most

adequate for this purpose. The aim is to obtain a Joule-level amplifier at this wavelength, with a high ($> \text{Hz}$) repetition rate, suitable for acting as an additional laser arm, or to pump a short pulse OPCPA-based source. Concerning the latter, work on supercontinuum generation through femtosecond filamentation and nonlinear effects in solid media has been started, with the purpose of creating an ultrabroadband optical source.

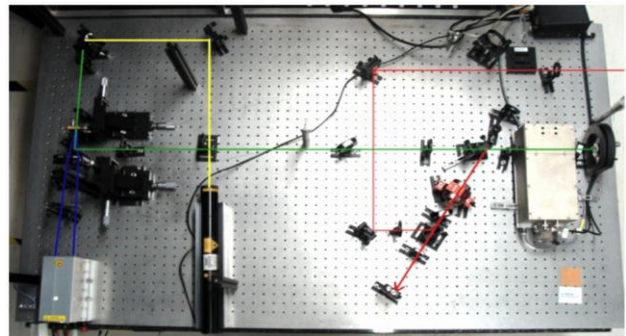


Figure 11.2 - Setup of diode-pumped Yb:glass regenerative amplifier

11.4. PLASMA ACCELERATORS AND INTENSE RADIATION SOURCES

Experiments on the demonstration of plasma channels for electron acceleration optimized for 2 cm lengths were carried out. Two prototypes were developed and tested, and the simmer discharge concept was demonstrated to produce reproducible and quality plasmas. Experiments were also performed for generating plasma channels in gas jets, in a collaboration with the Univ. Strathclyde (UK), involving the production and characterisation of plasma channels in argon, helium and hydrogen.

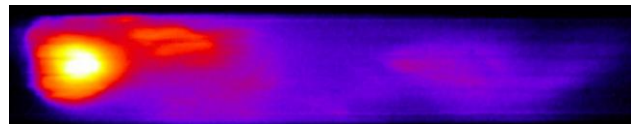


Figure 11.3 - Energy spectrum of the electrons generated in the so called bubble (or blowout) regime peaking at 400 MeV.)

11.5. FAST ELECTRON TRANSPORT THEORY FOR THE HIPER PROJECT

We are making an active contribution to the HiPER project on the critical problem of determining the laser parameters

¹Activities carried out in the frame of the Contract of Association EURATOM/IST and the Contract of Associated Laboratory, by staff of the Group of Lasers and Plasmas.

required for fast ignition, as part of the “requirements analysis for fusion programme” work package (WP 9). There exist a number of different results in common use for the stopping and scattering of fast electrons in plasmas, which lead to significant differences in the prediction of the laser parameters required for fast ignition. We have recently clarified this issue. These results have been implemented in a Monte Carlo energy deposition routine for the code DUEd, which has been used to repeat previous ignition calculations including more realistic energy deposition by fast electrons.

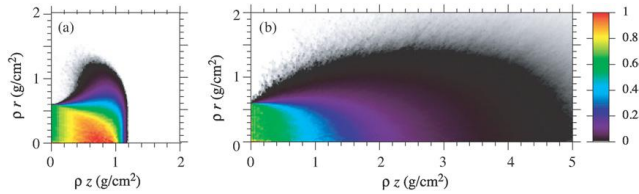


Figure 11.4 - Specific power deposited by (a) a beam of 1.5 MeV electrons and (b) a beam with exponential energy distribution (with average energy of 1.5 MeV)

12. PARTICIPATION IN THE FUSION TECHNOLOGY PROGRAMME UNDER EFDA¹

C. Varandas (Head), E. Alves², P. Ferrão³ and C.S. Silva³ (Deputy Heads), R. Mateus, J. Parente³, M.R. Silva, L. Alves, N. Barradas, J. Brito⁴, V. Livramento⁴, A. Mendes⁴.

12.1. INTRODUCTION

This project had two research lines in 2008:

- Characterization of fusion materials using nuclear techniques
- Socio-economics studies on nuclear fusion

12.2. CHARACTERIZATION OF FUSION MATERIALS USING NUCLEAR TECHNIQUES

12.2.1. Introduction

The activities of this research line have been focussed on:

- Study of new beryllide intermetallics;
- Study of Eurofer 97 ODS samples (TW5-TTMS-006);
- Studies of material erosion and redeposition in ITER-relevant divertor target temperatures, plasma impact energies and divertor chamber geometries (Task TW6-TPP-ERDEP).

12.2.2. Study of new beryllide intermetallics

A large number of techniques were used to determine the composition and homogeneity, Figure 12.1, (Ion beam techniques) and the structure (SEM and X-ray diffraction) of Titanium Be alloys (developed at FZK). In addition, the thermal stability and oxidation behaviour of the samples at high temperatures under controlled atmosphere was initiated.

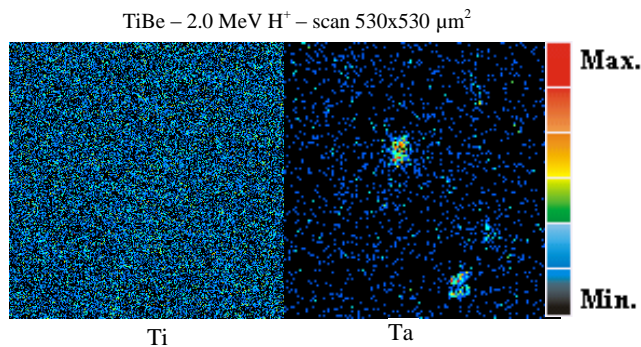


Figure 12.1 –Elemental distribution maps of Ti and Ta obtained by PIXE showing some Ta contamination present in the Be12Ti compounds and the homogeneity of Ti.

12.2.3. Study of Eurofer 97 ODS samples (TW5-TTMS-006)

Microindentation and nuclear and electronic microprobes were used to study four batches of Eurofer 97 ODS steel (produced at PLANSEE). The occurrence of carbide precipitation was identified in all samples, preferentially along the grain boundaries (commonly referred as ODS steels of first generation), and with entire globular shape precipitation (second generation). Microhardness measurements are strongly correlated with the presence of the two different precipitations. All the structural characteristics were related with the production parameters.

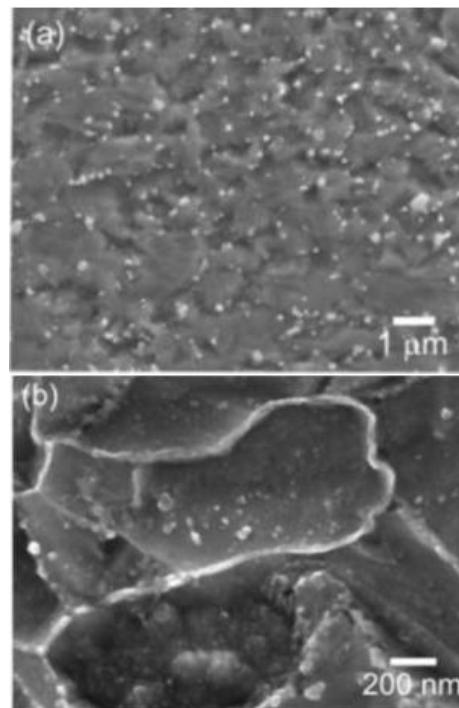


Figure 12.2 - Carbide morphologies observed in the Eurofer 97 ODS steels: (a) globular shape in Plate 16; (b) films along grain boundaries observed in Plate 6, Rod 20 and Rod 12.5.

¹Activities carried out in the frame of the Contract of Association EURATOM/IST by staff of the Group of Experimental Physics, in collaboration with Instituto Tecnológico e Nuclear (ITN), Centro de Estudos em Inovação, Tecnologia e Políticas de Desenvolvimento (IN+), Instituto Nacional de Energia e Geologia (INEG). Contact Persons: Eduardo Alves (ITN), José Brito (INEG) and P. Ferrão (IN+).

²Staff of ITN.

³Staff of IN+.

⁴Staff of INEG.

12.2.4. Studies of material erosion and redeposition in ITER-relevant divertor target temperatures, plasma impact energies and divertor chamber geometries (Task TW6-TPP-ERDEP)

The studies on tungsten tiles exposed to ITER relevant fluxes ($>10^{23} \text{ m}^{-2}\text{s}^{-1}$) were performed in collaboration with the Association Euratom-FOM. Tungsten targets (with 1 mm thick and 20 mm diameter) were exposed to deuterium plasma in the Pilot-PSI under different target conditions. This linear plasma generator produces plasma conditions that are expected to be typical at a detached ITER divertor strike point ($n_e \sim 10^{20} \text{ D}^+ \text{ m}^{-3}$, $T_e < 5 \text{ eV}$).

Fuel retention in the samples and its depth distribution was studied with Elastic Recoil Detection Analysis (ERDA) and Nuclear Reaction Analyses (NRA). The full picture of the samples surface condition after exposure was assessed with atomic force microscopy providing information on the erosion processes occurring during the plasma exposure.

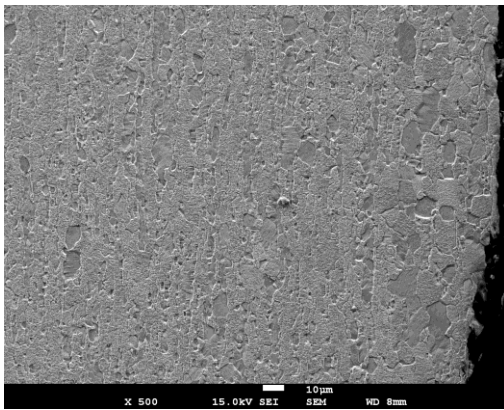


Figure 12.3 - SEM cross-section image of the central zone of a W surface. The temperature at the surface reached 1200-1300 C (W recrystallization temperatures) and induced a smooth grain growth during the deuterium plasma exposure.

12.3. SOCIO-ECONOMIC STUDIES ON NUCLEAR FUSION

12.3.1. Introduction

This section reports the progress of the tasks performed by IST until December 2008 under the EFDA workprogramme of 2008 and 2009 on Socio-Economic Studies:

- Integrated Framework;
- EFDA-TIMES & fusion economics.

The first task was developed with a slight delay according to the project plan, but it is expected that the delay is recovered during the year of 2009. The second task is being developed according to the plan.

12.3.2. Integrated Framework

Up to December 2008, IST had to three sub-activities:

- Characterization of the data and tools used by the Associations in their Socio-Economic Research;

- Assessment of the state-of-the-art concepts and methodologies and definition of a draft roadmap for an integrated framework;
- A SWOT analysis of the data and tools characterized in the first activity to address issues as defined in the second activity.

The first activity to be tackled was activity 2), in particular the assessment of the state-of-the-art concepts and tools. Only after a comprehensive understanding of the state-of-the-art, it was possible to make a deeper characterization of the data and tools used by the associations (activity 1) and the consequent SWOT analysis (activity 3). The draft roadmap for an integrated approach (second part of activity 2) will arise while completing of activities 1 and 3 during 2009. However, a preliminary approach was proposed for discussion with the other task associates (HAS and SCK-CEN).

The assessment of the state-of-the-art concepts and methodologies showed that, although all the different methodologies may bring new insights for socio-economic research of fusion systems, at this point is expected that the uncertainty and dynamics group of methodologies is the one that can be used more straightforward to the design of an integration framework, mainly for the design of energy scenarios under uncertainty.

At the moment, there is a slight delay on the schedule, since tasks 1), 2) and 3) should be finished. However, it is expected that the team catches up the work up to April 2009. Thus, the group expected to end this task within the proposed time frame.

12.3.3. EFDA-TIMES and Fusion Economics

IST has been helping developing the EFDA-TIMES model. Three specific work-packages were assigned to IST: check the CHP (combined heat and power) data for incorrect modelling of total efficiencies; check the PRC_CAPACT coefficients for new heat plants (ELC sector) for their consistency with the provided cost data; and check the UC constraint TUC_HydShr1 for its correctness and consistency.

For the duration of the year 2008, the group at IST working on this activity got acquainted to the tool, and have deeply studied the energy model. The group has already started to correct some of the problems that had been identified by the EFDA-TIMES modelling group.

13. OTHER FUSION-RELATED ACTIVITIES¹

C. Varandas (Head), M.P. Alonso, H. Fernandes, M.E. Manso, A. Silva, J. Sousa, A. Neto.

13.1. INTRODUCTION

This project concerns the collaboration of IST/IPFN with Brazilian Institutions and the W7-X project as well as activities on socio-economics, education and training, organization of scientific meetings, management of the EURATOM Fusion Programme and outreach.

13.2. COLLABORATION WITH BRAZILIAN INSTITUTIONS²

13.2.1. Introduction

IPFN has collaborated with:

- Laboratório de Plasmas do Instituto de Física da Universidade de São Paulo;
- Laboratório Associado de Plasmas do Instituto Nacional de Pesquisas Espaciais.

The research activities were focused on microwave reflectometry, control and data acquisition and Thomson scattering.

13.2.2. Microwave reflectometry for TCA/Br²

A broadband swept reflectometer system for the TCABr tokamak was developed. It is equipped with ultra-fast O-mode wave operation and has additional fixed frequency capability. The main activities were: (i) procurement of components; (ii) development and assembling of the system at IST; (iii) testing at the laboratory of the system blocks and calibration tests of the complete system in fast sweeping operation with a metallic mirror; assessment of the system accuracy. The diagnostic is in final phase of construction; the electronics is being mounted in the racks and is expected to be shipped January 2009 to Brasil. The front and rear views of the sub rack containing the TCABr K and Ka reflectometers (Figure 13.1).



Figure 13.1 - (a) - Front (a) and (b) views of the sub rack containing the TCABr K and Ka reflectometers.

13.2.3. Control and data acquisition

IPFN has proceeded with the development of control and data acquisition modules for TCA/Br and ETE³.

13.2.4. Thomson scattering (TS) diagnostic for TCA/Br

This diagnostic (Figure 13.2) will provide the radial profiles of the electron temperature and plasma density, with near 1 cm spatial resolution.

During the year 2008 the laser made of Neodymium-phosphate glass was refurbished with up to 10 J, 30 ns pulse duration and 1 pulse per minute, using one optical amplifier and a Faraday Isolator on a granitic table. The Nd:glass laser beam measured 25 mm in diameter and with a 1mrad divergence.

The laser pulse delivery system was concluded. In this way the four needed mirrors have a dichroic thin-film that maximizes the reflectivity (v shape) at 1053 nm and enclose simultaneously a 50% reflectivity for the 543 nm (green HeNe), booth laser beams (Nd:glass and green HeNe) are coaxial. The reduction of the laser stray light was made using anti reflection coating on the vacuum window and on the focusing lens, black painted steel pipes and with the critical positioning of few slightly oversize diaphragms made of industrial absorbing green glass.

The Thomson scattered light is analyzed at 90° by a simple collecting optics made with two plane concave lens. This collection lens was tested and positioned in place.

One fiber optic was installed from the collecting lens to the detector (a polychromator) following a particular long path in the laboratory.

The polychromator was tested for internal alignment and light response using a fast infrared photodiode feed by a comparable pulse generator.

The Optical ray-tracing analysis for stray-light was concluded using the software Zemax allowing to understand the best locations and dimensions for the diaphragms and to foresee the laser stray-light inside the vacuum vessel and in the laser dump.

Figure 13.3 presents the first raw data obtained with a digital oscilloscope. No stray-light has been observed in a plasma shot under irradiation from a 5 J, 20 ns laser pulse.

13.3. COLLABORATION WITH W7-X PROJECT

13.3.1. Introduction

This collaboration involved two research lines in 2008:

- Tomography diagnostics;
- Control and data acquisition.

¹Activities carried out in the frame of the Contract of Association EURATOM/IST and the Contract of Associated Laboratory.

²TCA/Br is a tokamak of the “Laboratório de Plasmas, do Instituto de Física, da Universidade de São Paulo”.

³ETE is a tokamak of the “Laboratório Associado de Plasmas do Instituto Nacional de Pesquisas Espaciais”.

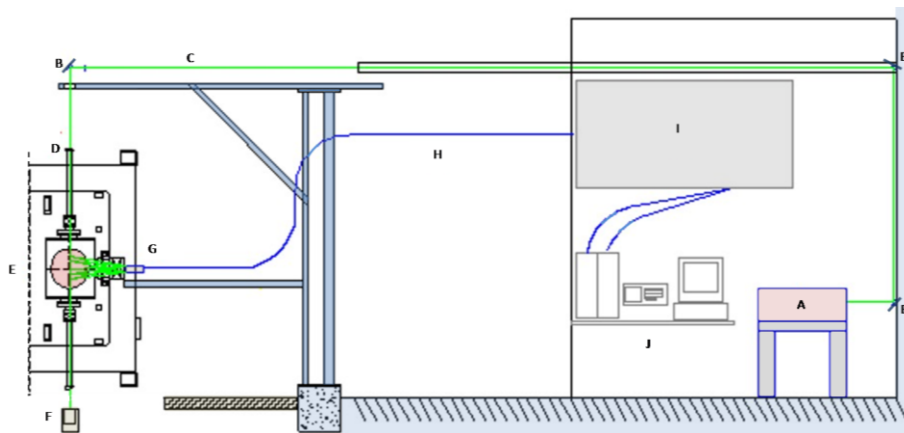


Figure 13.2 – Layout of the TS diagnostic: (A) Nd:glass laser, (B) Mirror, (C) Beam delivery system, (D) Input window, (E) Cross cut view of tokamak TCA/BR, (F) Laser pulse dump, (G) Collecting lens, (H) Fiber optic, (I) Delay and trigger lines and (J) Data acquisition system.

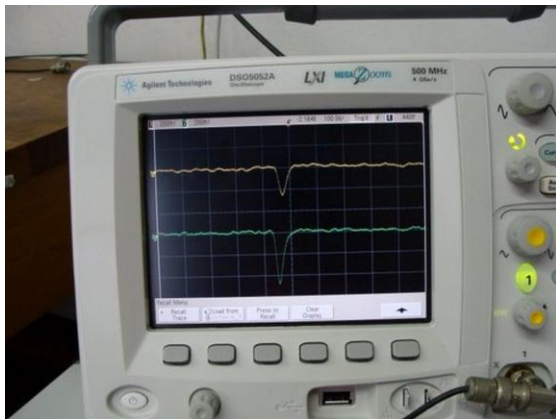


Figure 13.3 – First raw data from the TS diagnostic

13.3.1.1. Tomography

A new algorithm using the Fourier-Bessel technique on a noncircular geometry was implemented and proved to yield a better reconstruction than the circular Fourier-Bessel algorithm. This new method can be used with any kind of radial basis functions. The testes performed confirmed that the best results are achieved up to now with the Bessel functions. An alternate method for tomography was attempted that uses Support Vector Machines (SVMs). Much like Neural-Networks (NNs) SVMs require a training set of input and output data to determine the model of support vectors. Preliminary results yielded unacceptable results but further research is envisaged.

13.3.1.2. Control and data acquisition

The new ATCA proposal for data acquisition have been tested and evaluated by IPP staff to check the feasibility of its integration into the W7-X trigger and synchronization platform. The potentiality of the ATCA was demonstrated. The capabilities of FireSignal to be integrated on the W7-X data acquisition system (both developed natively in JAVA) were also assessed.

⁴This proposal was approved by the SOFT International Organizing Committee.

13.4. EDUCATION AND TRAINING

Besides the collaboration in Portuguese 2nd and 3rd cycle programmes, IPFN integrated the international network responsible for the first edition of the joint Ph.D. Programme on Fusion Science and Engineering, promoted by IST and the University of Padova and Munich.

13.5. ORGANIZATION OF SCIENTIFIC MEETINGS

The following tasks were performed in 2008:

- Publication of the Proceedings of the 17th IAEA Technical Meeting on Research Using Small Fusion Devices, held in Lisboa, on 22-24 October 2007;
- Organization, in collaboration with “Instituto Tecnológico e Nuclear”, of the International Conference on Emerging Nuclear Energy Systems, held in Ericeira, in June 2009;
- Presentation of a proposal for the organization of the Symposium on Fusion Technology (SOFT), in Porto, in September 2010⁴.

13.6. OUTREACH ACTIVITIES

The outreach activities included in 2008:

- Creation of the IPFN Outreach Group;
- Participation in the following events:
 - INOV-Innovation Fair, June;
 - Scientific Occupation of Students in Summer, Ciência Viva, July;
 - Portugal Tecnológico, 18-23 November.
- Organization of a meeting of the EFDA Committee Public Information, 8-9 May;
- Elaboration of the Annual Report;
- Organization of courses on Plasma Physics and Nuclear Fusion and Electronic Instrumentation, in collaboration with BEST and Athenes;
- Organization of seminars in secondary schools and visits to our laboratories;
- Elaboration of a video on Nuclear Energy;
- Publication of the following articles:
 - “Participar hoje na energia do amanhã”, B. Gonçalves, Revista Indústria (RI);

- “A opção nuclear”, B. Gonçalves, in RI;
- “IPFN: Projectos Internacionais”, C. Varandas, País Positivo.
- Participation in radio, television and newspapers:
 - Interviews with C. Varandas about “Nuclear: abertura do debate extremamente oportuna”, in four newspapers, 16-17 March.
- Invited Talks:
 - “A fusão nuclear no portfolio energético do séc. XXI”, B. Gonçalves, Associação Comercial de Lisboa;
 - “Fusão nuclear: uma tecnologia energética para o futuro”, C. Varandas, University of Porto;
 - “Novas Soluções para a Energia Nuclear”, C. Varandas, Meeting of the Associated Laboratories (MAL), Fundação Gulbenkian, Lisboa;
 - “Apresentação das Linhas de Actividades em Projectos internacionais de grande dimensão do IPFN-LA”, C. Varandas, F. Serra, L.O. Silva, MAL;
 - Portuguese strategy and R&D programmes on energy, C. Varandas and M. Alonso, EPS/SIF Energy Meeting, Varenna, Italy;
 - Nuclear fusion, H. Fernandes, Encontro Nacional de Estudantes de Física;
 - “O futuro energético em Portugal: pode a energia nuclear ser parte da solução?”, C. Varandas, Geração de Ideias, Setúbal.
- Participation of H. Fernandes in debates about Nuclear Energy:
 - “1º debate da plataforma de reflexão estratégica construir ideias”, Lisboa, September;
 - “Energia e inovação: o desafio do século, Estoril, October;
 - XII Semana da Física, IST, November.
- ITPA (International Tokamak Physics Activity) Topical Group on Diagnostics;
- Ad-Hoc Group from STAC for the COMPASS-D Project;
- International Board of Advisories of the COMPASS-D Project.
- José Tito Mendonça is member of the Inertial Fusion Energy Coordinating Committee.
- Profª Maria Emília Manso is:
 - Member of the Programme Committee of the ASDEX-Upgrade Project;
 - Chairperson of the International Advisory Board on Reflectometry;
 - Coordinator of the Cluster of EURATOM Associations for the development of the Plasma Position Reflectometer for ITER.

13.7. PARTICIPATION IN THE MANAGEMENT OF INTERNATIONAL FUSION PROGRAMMES AND PROJECTS

Several members of the Association EURATOM/IST have been involved in the management of the EURATOM Fusion Programme as well as on Ad-Hoc Groups and Scientific Committees of the EFP and other Fusion Programmes:

- Carlos Varandas is Chairman of the F4E Governing Board and member of:
 - Consultative Committee for the Research and Training Programme on Nuclear Energy-Fusion (CCE-FU);
 - Group of Chairmen (GoC);
 - Scientific and Technical Committee (STC);
 - EFDA Steering Committee;
 - EURATOM Delegation to the ITER Council;
 - EURATOM Delegation to the Steering Committee of the Broader Approach.
- Fernando Serra is member of:
 - F4E Governing Board;
 - Ad-Hoc Group from STAC for the Monitoring of W7-X Project;

14. PLASMA THEORY AND SIMULATIONS¹

L.O. Silva (Head), R.A. Fonseca, F. Peano, M. Marti, P. Abreu, L. Gargaté, J. Vieira, S.F. Martins, F. Fiúza, J.L. Martins, N. Shukla, P. Alves.

14.1. INTRODUCTION

The work in this field was developed along the following main topics:

- Laser-plasma accelerators with the next generation lasers;
- Radiation from self-injected beams of laser-plasma accelerators with the next generation lasers;
- One-to-one direct modeling of experiments and astrophysical scenarios: pushing the envelope on kinetic plasma simulations;
- Hardware acceleration of PIC codes: tapping into the power of state of the art processing units;
- Selective trapping and acceleration of charged particles;
- All-optical ultrafast muon acceleration;
- Monte Carlo simulations of relativistic collisions in plasmas;
- Laser-driven nuclear fusion in homonuclear and heteronuclear clusters;
- Laser plasma interaction in the regime of the Extreme Light Infrastructure;
- Migrating large output applications to Grid environments;
- Streaming the Boris Pusher: a CUDA implementation;
- Solar Energetic Particle acceleration in Coronal Mass Ejection shock fronts;
- Non-resonant magnetic field amplification in Supernova Remnant Shocks;
- One-to-one experimental modeling of self-guided propagation in LWFA;
- Generation of single cycle laser pulses in plasmas;
- Boosted frame PIC simulations of LWFA: towards the energy frontier;
- Ion dynamics and acceleration in relativistic shocks;
- High-brilliance synchrotron radiation induced by the plasma magnetic mode;
- Fast Ignition with Ultrahigh Intensity Lasers;
- Post-processing radiation modeling;
- Betatron radiation in laser-wakefield accelerators;
- Ion acoustic instability;
- Hybrid simulations of high-energy ion interaction with mini-magnetospheres.

14.2. LASER-PLASMA ACCELERATORS WITH THE NEXT GENERATION LASERS²

Motivated by the upgrade of the Vulcan laser system to 10 PW, we have performed a detailed theoretical and numerical study of the different scenarios of laser wakefield acceleration that can be explored with such systems, using as a baseline the design parameters of pulse durations of 30 fs with 300 J with an emphasis on relativistic laser intensities where blow-out can be achieved. For the matching conditions determined by the theory of Wei Lu et al we have demonstrated, through numerical simulations with OSIRIS and QuickPIC, the different possible regimes, with self-injected beams with energies in excess of 10 GeV, in laser self-guiding configurations (for distances on the 10s cm range) for moderately high intensities (corresponding to a normalized vector potential ~ 5), up to energies in the 50 GeV range for external guiding configurations with externally injected beams (with normalized vector potential ~ 2). Our results demonstrate the possibility to achieve energies close to the energy frontier with the next generation of ultra intense lasers.

14.3. RADIATION FROM SELF-INJECTED BEAMS OF LASER-PLASMA ACCELERATORS WITH THE NEXT GENERATION LASERS

Self-injected beams in laser wakefield accelerators are injected into an ion channel associated with the blow-out region, right behind the laser pulse. The oscillations of the self-injected electrons can generate betatron radiation. Estimates for the radiation in the 10 PW scenario, based on the post-processing of the tracks of the self-injected electrons extracted from the simulation, indicate an equivalent wiggler parameter for the betatron motion $K \gg 1$, with the total radiated energy reaching ~ 80 -mJ, the typical energy of the radiated photons in the 0.1-1~MeV range, and a beam divergence ~ 2 -5 mrad, placing these sources along the brightest sources for these range of energies.

14.4. ONE-TO-ONE DIRECT MODELING OF EXPERIMENTS AND ASTROPHYSICAL SCENARIOS: PUSHING THE ENVELOPE ON KINETIC PLASMA SIMULATIONS

There are many astrophysical and laboratory scenarios where kinetic effects play an important role. These range

¹Activities performed in the frame of the Contract of Associated Laboratory, out of the Contract of Association EURATOM/IST, by IPFN staff of the Group of Lasers and Plasmas

²W. B. Mori (UCLA), and P. Norreys, R. Trines (RAL).

from astrophysical shocks and plasma shell collisions, to high intensity laser-plasma interactions, with applications to fast ignition and particle acceleration. Further understanding of these scenarios requires detailed numerical modelling, but fully relativist kinetic codes are computationally intensity, and the goal of one-to-one direct modelling of such scenarios and direct comparison with experimental results is still difficult to achieve.

To perform one-to-one numerical experiments several issues had to be addressed. Present day HPC systems provide computing power in the PetaFlop scale, but this requires parallel scalability to tens of thousand of CPUs. Load balancing, communications and I/O were improved in OSIRIS [1,2], which now achieves a parallel efficiency of over 80% on 32k cpus IBM BlueGene system.

One-to-one modeling will also require very long simulations, with iteration counts in the order of $\sim 10^6$ and for such long simulations it is also crucial to insure that numerical issues don't interfere. This meant improving the simulation algorithm by implementing high order particle shapes and improving algorithm accuracy. This enhances energy conservation and greatly reduces simulation noise. Given the complexity of these algorithms, we chose to develop a code generation program, that can now generate Fortran code for any level of interpolation required.

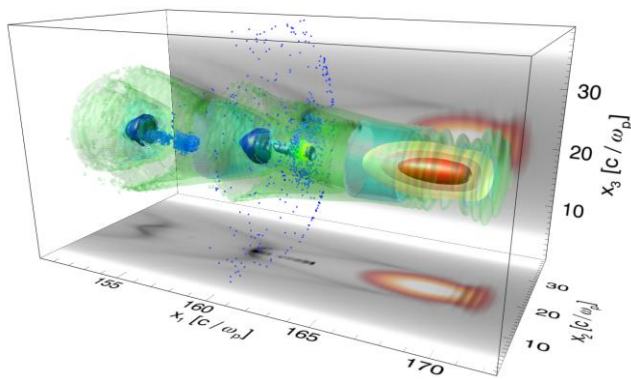


Figure 14.1 - 3D simulation of Laser Wakefield acceleration showing 2 bunches of injected particles.

14.5. HARDWARE ACCELERATION OF PIC CODES: TAPPING INTO THE POWER OF STATE OF THE ART PROCESSING UNITS

The total CPU hours required by full scale numerical experiments range in the order of $10^3 - 10^4$. Explicitly using available hardware resources such as SIMD units (AltiVec/SSE3), cell processors or graphics processing units (GPUs) may allow us to significantly boost performance of our codes and make better use of HPC systems. However, for most cases, the processing units are limited to single precision arithmetic, and require specific C/C++ code to be used.

We performed a comparison between double precision and single precision results, focusing both on performance and on the effects on the simulation in terms of algorithm

properties. We found that using single precision in the standard PIC algorithm would fail for most simulations. To overcome this we implemented an alternate particle description technique that indexes particle positions to the cell they are in. Although requiring $\sim 20\%$ more memory, this technique has a very small performance impact, allows for a much larger precision in particle interpolation, thus enabling the use of single precision for most scenarios. However, there are situations where we want to observe a small fluctuation on top of much larger phenomena; in these cases double (or even quad) precision will still be required.

We have also began vectorizing OSIRIS for SSE3 units. Since for a typical simulation the code will spend over 90% of the time in only 2% of the code, we focused only on these routines. Specialized C code was written for these routines, and Fortran wrappers were created so they could be called from the main OSIRIS code. In 2D this resulted in performance benefits of up to 65%, making the speedup from standard double precision runs of about ~ 2.5 . There is however much room for improvement since memory access is critical in this programming model and the algorithm may benefit from a different strategy from the one used for the Fortran version.

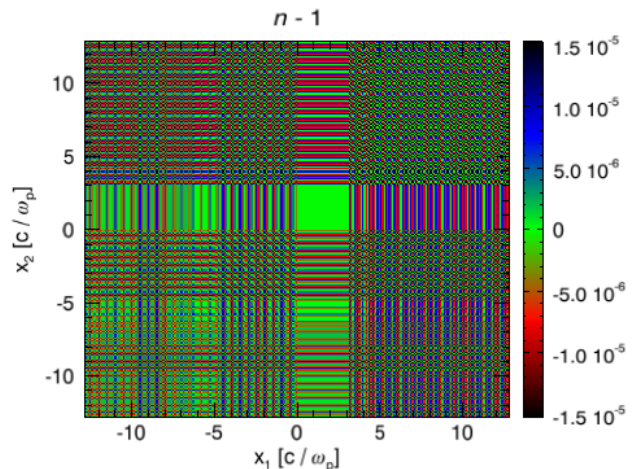


Figure 14.2 - Charge interpolation error for standard simulation algorithm in single precision.

14.6. SELECTIVE TRAPPING AND ACCELERATION OF CHARGED PARTICLES

All optical trapping and acceleration of charged particles can be obtained using the ponderomotive beat wave created by the superposition of counterpropagating EM waves having variable frequency. This technique can be used to separate species with different charge-to-mass ratios by tuning the chirp rate so as to trap only a given species. The scheme exhibits extreme sensitivity to low mass differences, thus suggesting new possibilities for isotope separation.

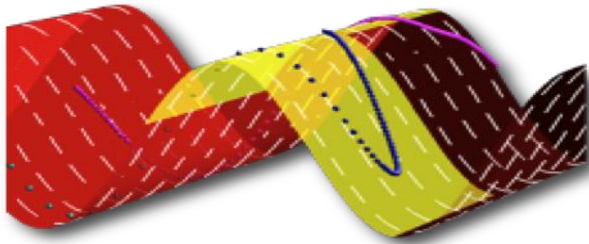


Figure 14.3 - Selective trapping of the heaviest of two isotopes (blue spheres), while the light isotope (magenta spheres) loses the wave.

14.7. ALL-OPTICAL ULTRAFAST MUON ACCELERATION³

High-quality muon beams would provide unprecedented capabilities for fundamental-physics experiments in cutting-edge topics, ranging from investigations on neutrino-oscillation physics in neutrino-factory machines to energy-frontier studies in TeV-level muon-antimuon colliders. However, accelerating muons a challenging task, mainly due to the short muon life-time. A novel method for ultrafast, ultracompact muon acceleration has been investigated, wherein muons are trapped in a variable-speed ponderomotive beat wave driven by two counterpropagating, chirped EM waves. The method could be important to provide prompt energy gains in the first stages of the overall acceleration process, during, or right after, muon cooling.

14.8. MONTE CARLO SIMULATIONS OF RELATIVISTIC COLLISIONS IN PLASMAS⁴

A consistent statistical description of relativistic binary collisions in dilute many-particle systems has been obtained using a Monte Carlo approach, based on the standard relativistic kinetic theory, wherein collisions are simulated by changing the momenta of appropriate samples of particle pairs. Results show that rigorous constraints hold on the way particle pairs are chosen for collision, and that nonrelativistic approximations (such as a uniform collision probability) are forbidden. By breaking the relativistic invariance of the number of collision events in a given space-time region, these approximations lead to unphysical results, notably wrong equilibrium distribution functions that differ from the Juttner function (i.e., the stationary solution of the relativistic Boltzmann equation). The study provides the framework for relativistically consistent Monte Carlo simulations of the statistical properties of multi-dimensional, collisional systems in the relativistic regime.

³In collaboration R. Mulas and G. Coppa (PoliTo); R. Bingham (RAL).

⁴In collaboration with: G. Coppa (PoliTo).

⁵In collaboration with: I. Last and J. Jortner (Tel Aviv University).

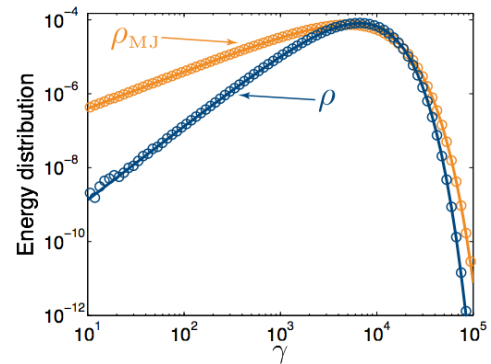


Figure 14.4 - Energy spectra at equilibrium: the blue curve is relativistically consistent and follows the Juttner distribution, while the red curve, obtained with a semi-relativistic algorithm, represents a modified equilibrium repeatedly appeared in the literature.

14.9. LASER-DRIVEN NUCLEAR FUSION IN HOMONUCLEAR AND HETERONUCLEAR CLUSTERS⁵

Molecular clusters exposed to ultraintense laser fields turn into nanoplasmas that undergo rapid expansion (when electrons are heated but remain bound to the cluster) or ultrarapid Coulomb explosion (when electrons are expelled from the cluster). In homonuclear deuterium clusters, mixed expansion-explosion regimes, as driven by appropriate sequences of two laser pulses, result in ion overtaking and prompt intracluster fusion. The intracluster fusion yield under different irradiation conditions has been computed resorting to 3D scaled-molecular-dynamics simulations confirming and refining previous estimates from 1D analyses and PIC simulations. The intracluster fusion occurring in deuterium-tritium clusters with single pulse irradiation has also been simulated. In both the homo- and hetero-nuclear case, the peculiar signature of intracluster reactions, which should be amenable to experimental verification, have been identified.

14.10. LASER PLASMA INTERACTION IN THE REGIME OF THE EXTREME LIGHT INFRASTRUCTURE

The Extreme Light Infrastructure (ELI) is an european project with the aim to provide a high intensity laser facility allowing for fundamental studies in laser matter interaction in a relativistic regime. Expected laser intensities for this facility range from 10^{23} W/cm² up to over 10^{25} W/cm² with ultra short pulses of 10^{-18} s to 10^{-15} s thus allowing for advanced research topics in medicine, nuclear energy and even nuclear waste processing.

Computer simulations play an important role in the preparatory phase of such a ground breaking project, allowing us to get important insides into physical processes and providing reliable numerical estimates for the future experiments and it's environment. Simulation therefore serve as an important tool in the conception and design of the infrastructural facility, the safety requirements and

protective measures as well as in the conception of the actual experiments.

We have conducted a set PIC simulations using the osiris framework in order to model high intensity matter interaction in the ELI regime: A solid hydrogen slab with varying thicknesses ranging from 1 up to over 30 μm at a density of $5.3 \cdot 10^{22} \text{ cm}^{-3}$ is exposed to a linear or circular polarized laser field with a wavelength of 0.8 μm , a pulse length of 15 fs and the dimensionless vector potential between 300 and 700.

We have found that in this setup the relativistic proton energy can reach values of up to 6 GeV which is well above the activation energy of oxygen in air. This finding has a severe impact on the design and dimensioning of the radiation shielding to be installed at the ELI facility. We have also shown that the transverse energies strongly depend on the laser beam quality as well as on the exact target geometry.

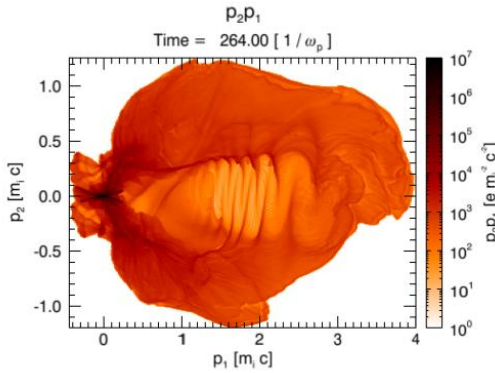


Figure 14.5 - Proton $p_2 p_1$ phase-space resulting from a tightly focused laser beam when impacting a solid hydrogen target. This graph shows the angular spread of the proton energies in the resulting ion beam.

14.11. MIGRATING LARGE OUTPUT APPLICATIONS TO GRID ENVIRONMENTS

As the Grid infrastructure and middleware matures, it is becoming increasingly attractive to different kinds of user applications than it was initially planned for. In particular, it starts to attract users of the application paradigm where, from a relatively small input data set, a large set of data is produced, like it is common in several types of simulations.

We have developed a simple library based on EGEE Grid middleware function calls that handles the transfer of large data file sets from the local storage of the Worker Node to an EGEE Storage Element in a way that is simple, robust, transparent to the user and minimizes performance impact. The library is very easy to integrate into non-Grid/legacy code and it is flexible enough to allow for overlapping of several data transfers and computation. Large data sets produced by running simulations on the Grid are thus immediately available to the user, that no longer has to wait for the whole simulation to finish before he can explore the result data.

This library was tested in a real case scenario, where it was used in a high-performance plasma simulation code: OSIRIS 2.0.

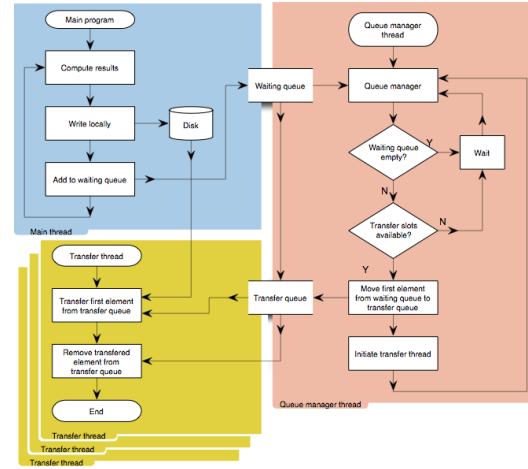
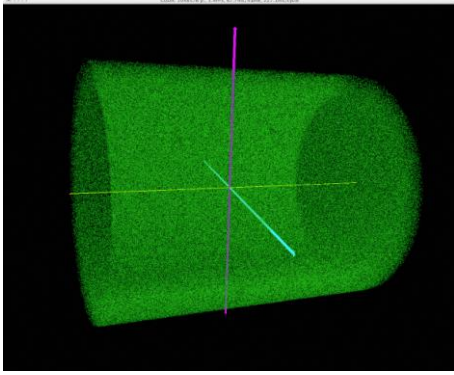


Figure 14.6 - Fuxogram of the library algorithm that allows for simultaneous Grid simulation and network transfer of results.

14.12. STREAMING THE BORIS PUSHER: A CUDA IMPLEMENTATION

CUDA is both a hardware and software architecture for creating GPGPU programs. At the hardware level, it is available for some NVIDIA's GeForce series (8000 and better), the Tesla systems and some Quadro equipment. At the software level, it has a software stack composed by the hardware driver, the C-like API and its runtime, and several higher-level mathematical libraries (CUFFT, CUBLAS).

We have implemented a 3D Boris Particle Pusher algorithm in CUDA. Speed gains were significant when compared to the fastest processor we had available (the Intel T9300). Specially relevant is the almost $2\times$ gain with the 8800GT: this GPU is already outdated and nonetheless is able to have twice the performance of a recent CPU, including the memory transfers penalty, for a price of $\approx \$200$. An interesting advantage of this implementation is the ability to interactively display the results. Since they are stored on the GPU memory, they can be displayed with a minimal penalty, simply by changing the frame buffer context.



14.7 - CUDA implementation of the Boris Pusher algorithm.

14.13. SOLAR ENERGETIC PARTICLE ACCELERATION IN CORONAL MASS EJECTION SHOCK FRONTS⁶

We perform hybrid simulations of a super-Alfvénic quasi-parallel shock, driven by a Coronal Mass Ejection (CME), propagating in the upper Solar Corona. The hybrid treatment of the problem enables the study of the shock propagation on the ion time scale, preserving ion kinetics and allowing for a self-consistent treatment of the shock propagation and particle acceleration.

Our results show that electromagnetic Alfvén waves are generated upstream of the shock. The waves propagate towards the shock front in the downstream frame of reference, and are produced by the two counter-streaming ion populations in the upstream foreshock region: the solar wind ions and a low density ion beam produced at the shock front. The electromagnetic waves generate turbulence in the foreshock region and downstream of the shock, providing the mechanism for efficient Fermi acceleration.

Diagnostics from the hybrid simulations show a $\sim 2\%$ fraction of the particles with supra-thermal energies above 64 times the mean solar wind ram energy, and with particle energies extending up to 144 the initial energy. The tracks of a sample of the most energetic particles show multiple shock crossings, and highly efficient acceleration zones in the foreshock and downstream regions of the shock. Also, a fraction of the particles gains energy by direct interaction with the shock front: they drift in the shock propagation direction at the velocity of the shock, and gain energy in the perpendicular directions, increasing their Larmor orbits.

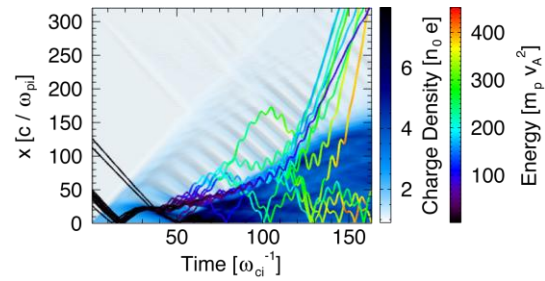


Figure 14.8 - Charge density of the background plasma, showing the propagation of the shock front in the x direction with time. The tracks of some of the most energetic particles in the simulation are superimposed, colored by their energy at a given time.

14.14. NON-RESONANT MAGNETIC FIELD AMPLIFICATION IN SUPERNOVA REMNANT SHOCKS⁷

Cosmic rays are observed up to a energy of 10^{18} eV, and such energies are not compatible with the magnitude of the magnetic field inferred from synchrotron radiation of Supernova Remnant shocks, which are the most likely source for these particles. A mechanism for beam driven non-resonant magnetic field amplification has been

⁶In collaboration with R. Bingham (RAL/UK).

⁷In collaboration with J. Niemiec (Instytut Fizyki Jadrowej PAN/Poland), R. Bingham (RAL).

⁸In collaboration with C. Huang, and W. B. Mori (UCLA).

presence of a background plasma. The fastest-growing wavelength predicted by linear theory is much smaller than the Larmor radius of the beam ions, and thus the excited magnetic field does not affect the beam ions significantly.

Using *dHybrid*, the non-linear saturation mechanism for this instability has been studied. Results show that the magnetic field growth rate is close to the prediction of the linear theory, in the linear phase of the instability. As the magnetic field grows to values $\delta B > B$, the background plasma starts to drift with the beam, and non-linear effects dominate. The typical scale-length of the electromagnetic turbulence generated increases up to a level close to the ion beam Larmor radius, and the beam distribution becomes isotropic. Also, simulations support other recent full particle simulations that show similar saturation mechanisms. The magnitude of the magnetic turbulence grows up to $\delta B/B \sim 10$ for the simulation parameters, which is still not sufficient for the acceleration of CR particles up to the observed energies. Further studies in this area are still being conducted since the exploration of the realistic astrophysical parameters is very computational-intensive, and thus requires the use of scaled-down parameters.

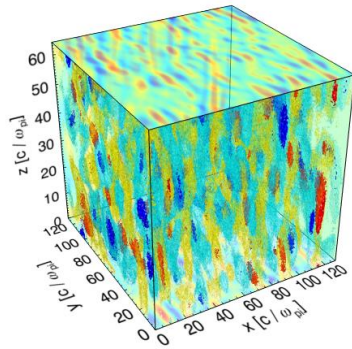


Figure 14.9 - Iso-surfaces and projections of the magnetic field along the z direction (perpendicular to the beam propagation), for a instant in time in the linear phase of the beam instability.

14.15. ONE-TO-ONE EXPERIMENTAL MODELING OF SELF-GUIDED PROPAGATION IN LWFA⁸

The use of reduced codes which are optimized for wakefield acceleration are beginning to assume a key role in experimental design and interpretation. QuickPIC is one of such codes. It is a spectral particle-in-cell (PIC) code which works under the quasi-static approximation, and which is two-three orders of magnitude faster than standard full PIC codes. The fourier space analysis introduces, however, imprecisions in the plasma response which are more relevant in the blowout regime of laser wakefield accelerators (LWFA). Therefore it is important to explore alternative schemes to increase the accuracy of the simulations. The possibility of using finite difference schemes in QuickPIC was investigated, showing that

accurate plasma responses could be retrieved. One-to-one simulations to model experiments such as those using the astra-gemini laser system were also performed. In order to better understand the experiments, different plasma density profiles, higher-order gaussian laser beams, and different beam energies were used.

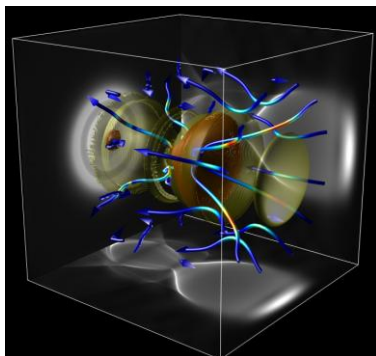


Figure 14.10 - Intensity isosurfaces and field lines of the plasma currents in the blowout regime of laser wakefield acceleration using the quasi-static PIC code.

14.16. GENERATION OF SINGLE CYCLE LASER PULSES IN PLASMAS⁹

Plasma waves provide ideal structures for the generation of single cycle laser pulses. This process is characterized by a strong self-steepening at the front of the laser, which is characteristic of relativistic regimes. In these regimes, the plasma electrons are violently pushed at the front of the laser and create a density void (the so-called bubble). Thus, while the back of the laser propagates in a vacuum like region, the front of the laser propagates in a steep density gradient which causes both the steepening and downshift of the laser front. As the pulse front downshifts, it loses energy to the generation of the plasma wave, leading to the formation of single cycle laser pulses. At the same time, the self-steepening of the front of the laser increases the laser ponderomotive force, and sustains the amplitude of the plasma wave during the propagation length which is required for single cycle laser pulse generation. The early self-steepening was then examined in the light of photon kinetics. This work showed that self-steepening plays a relevant role in state-of-the-art laser-underdense plasma experiments. The conditions where self-steepening is more important than self-focusing were also identified. A set of one dimensional PIC simulations (using OSIRIS and QuickPIC) confirmed the key predictions of the model.

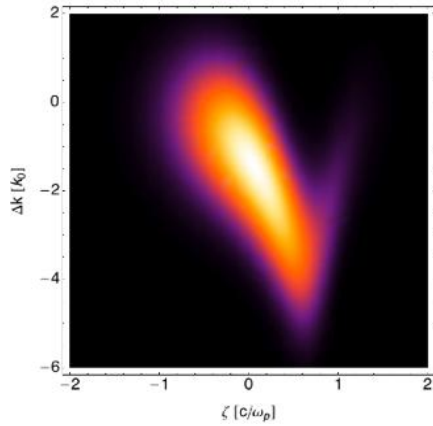


Figure 14.11 - Wigner transform of laser pulse which propagates in an underdense plasma. The front of the laser is downshifted with respect to its back, indicating that front of the laser is self-steepened.

14.17. BOOSTED FRAME PIC SIMULATIONS OF LWFA: TOWARDS THE ENERGY FRONTIER¹⁰

Increased laser power is driving laser wakefield accelerators (LWFA) as a prospective substitute for conventional particle accelerators. In the near future, a new generation of laser systems will be deployed to experimental teams, and LWFAs will be pushed to unexplored regimes. The optimal configurations for particle acceleration with these upgraded laser sources are not yet completely known, both due to the impossibility of developing a self-consistent theoretical model, and to the extreme computational requirements of one-to-one numerical simulations. We have shown that it is possible to perform ultra-fast LWFA simulations with all the relevant physics in these regimes, and we concluded on the path to follow in terms of the physical parameters and configuration to go beyond 10GeV acceleration. As a consequence, a new generation of numerical simulations is now available to perform parameter testing and scanning for the setup and optimization of future experiments.

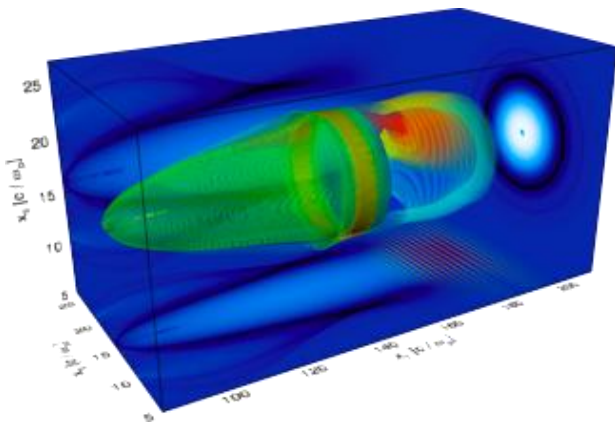


Figure 14.12 - Structure of a LWFA in a boosted frame. The laser (yellow and light blue iso-surfaces) propagates to the right and generates an ion column in the plasma density (green iso-surfaces) where electrons can be injected and accelerated.

14.18. ION DYNAMICS AND ACCELERATION IN RELATIVISTIC SHOCKS¹¹

We have performed an ab-initio numerical study of collisionless shocks in electron-ion unmagnetized plasmas with fully relativistic particle in cell simulations. The main properties of the shock have been obtained, and the implications for particle acceleration have been analyzed, comparing with previous simulations of other scenarios with relativistic shocks. We have then used particle tracking to analyze in detail the particle dynamics and the acceleration process, and we observed an energy growth in time that can be reproduced with a generalized Fermi mechanism, in which the time between collisions increases linearly as the particle gains energy, and the average acceleration efficiency is not ideal. This in depth analysis of the underlying physics is relevant to understand the generation of high energy cosmic rays, the impact on the astrophysical shock dynamics, and the consequent emission of radiation.

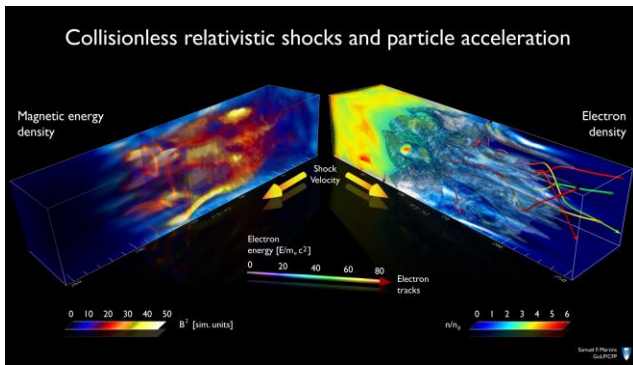


Figure 14.13 - Simulation results for a three-dimensional relativistic shock. On the left, the magnetic energy density shown, depicting the filamentation that occurs when two plasma clouds collide. On the right, the electron density illustrates the compression that constitutes the shock, and includes trajectories for a set of relevant particles.

14.19. HIGH-BRILLIANCE SYNCHROTRON RADIATION INDUCED BY THE PLASMA MAGNETIC MODE¹²

The existence of a plasma magnetic mode (PMM), or picket-fence mode, excited in the collision of a light pulse with a relativistic ionization front, has been predicted theoretically, but a mechanism or experimental setup for a clear evidence of this fundamental plasma mode is still missing. We have proposed, and demonstrated in particle-in-cell (PIC) simulations, a new scheme for the experimental evidence and characterization of the PMM. Using the PMM as a short-wavelength plasma undulator, the propagation of a moderate-energy electron beam through this structure will generate ultrashort-wavelength radiation.

We have shown the possibility for controlled generation of radiation, in the PMM, with unprecedented brilliance, equivalent to a compact all-optical gamma-ray synchrotron source, providing a clear evidence of the main experimental properties of this plasma mode.

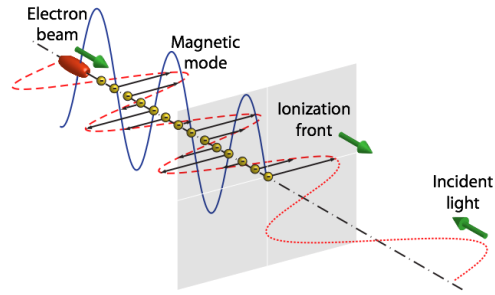


Figure 14.14 - Scheme for the generation of synchrotron radiation and experimental evidence of the plasma magnetic mode.

14.20. FAST IGNITION WITH ULTRAHIGH INTENSITY LASERS¹³

One of the critical issues for fast ignition of fusion targets is to understand the coupling of the ignition laser to the fast particles, and the transport of the accelerated particles in the mildly dense region of the target. It is generally assumed that the energy spectrum of the fast electrons follows the ponderomotive scaling found by Wilks et al., which together with the fact that electron energies within 1-3 MeV are preferred to deposit most of the energy in the core, have limited previous studies to laser intensities $I < 5 \times 10^{19} \text{ W/cm}^2$.

We have performed a series of two-dimensional (2D) PIC simulations in order to investigate the feasibility of using ignition lasers with ultrahigh intensities, up to $5 \times 10^{21} \text{ W/cm}^2$, for fast ignition. We have examined the absorption of such intense laser pulses in overdense targets with 50 to 100 times the critical density, and the subsequent energy transport. Our results, revealed that most of the energy transport is in a hot bulk, and not in the super-hot tail of the electron distribution as would be expected from the ponderomotive scaling. The heat flux through the overdense target is mostly carried by 1-3 MeV electrons. At the front of the target, the generated hot electrons drive turbulence in the collisionless plasma background, followed by a region with strong magnetic fields generated by the Weibel instability, due to the return current that builds up. At these ultrahigh intensities, we observed the formation of a relativistic collisionless shock, which is mediated by the Weibel driven magnet fields, in a similar fashion to relativistic shocks in astrophysics. The dynamics of the Weibel/streaming instabilities leads to the slow down of the accelerated electrons and to a strong isotropization, allowing for high efficiencies in the 1-3 MeV energy range.

¹¹In collaboration with W. Mori (UCLA).

¹²In collaboration with C. Joshi (UCLA).

¹³In collaboration with J. Tonge, J. May, and W. B. Mori (UCLA), C. Ren (University of Rochester).

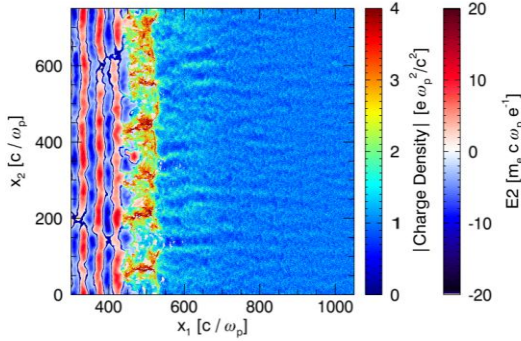


Figure 14.15 - Filamentation and shock formation at the front of a solid target irradiated by an ultra-intense laser pulse.

14.21. POST-PROCESSING RADIATION MODELING

Particle-in-cell (PIC) codes can only model the radiation whose wavelength the grid can resolve. However, in some scenarios, the radiation emitted by the accelerated charges beyond the grid resolution does not significantly affect the plasma and the particle dynamics itself. If in addition, the wavelength of the radiation emitted by particles is much smaller than the other spatial scales of the simulation, the use of a post-processing diagnostic to model this radiation, instead of lowering the cell size, can reduce the computational requirements in terms of memory and run time. To achieve this, a post-processing diagnostic was implemented that takes the information of the position and momentum of the particles as a function of time and calculates the energy deposited into a “virtual detector” chosen by the user. It is also able to provide spectral information on the emitted radiation.

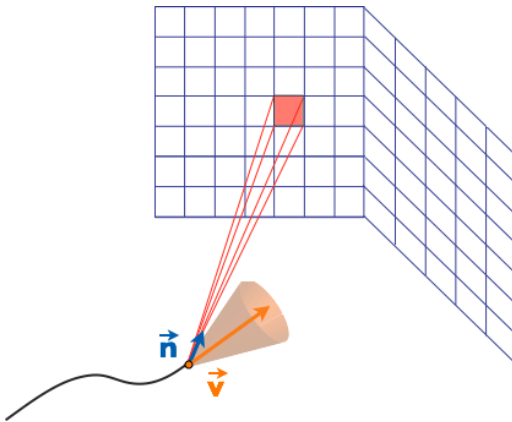


Figure 14.16 - Post-processing diagnostic scheme: particle trajectory with the cone of radiation depicted and the “virtual detector” grid; the vector n points in the direction of observation and the vector v is the particle velocity.

Particle trajectory data (position and momentum over time) is available directly from the track files obtained thanks to the particle tracking feature of OSIRIS 2.0, the PIC code used in this work.

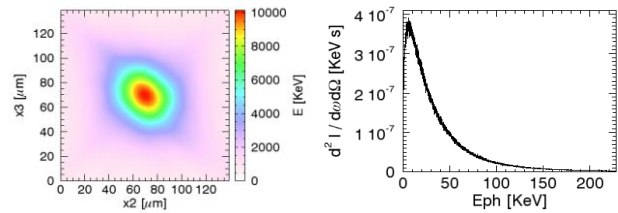
14.22. BETATRON RADIATION IN LASER-WAKEFIELD ACCELERATORS¹⁴

This post-processing diagnostic has been applied to the study of the emission of radiation by electrons in LWFA. In these scenarios, the electrons that get injected into the ion cavity are subject to a radial force that causes them to oscillate, which in turn results in radiation emission, the so called betatron radiation. This radiation can easily reach the VUV or the X-ray regime, while the plasma and the laser wavelength are usually much bigger.

A 1.5 and a 12 GeV laser-wakefield stages have been modeled. A sample of the electron tracks from each of these simulations was post-processed to obtain the energy deposited at a plane placed in the direction of the propagation of the laser.

In both scenarios, it was found that the electron bunch emits a collimated beam of radiation in the direction of propagation, as expected for relativistic charged particles. By placing a second “detector” parallel to the first but further away and then measuring the full width at half maximum (FWHM) of the radiation beam in both planes, it was possible to calculate its angular divergence. The values obtained were within the theoretical estimations in terms of order of magnitude. To evaluate precise theoretical values for the angular divergence the energy distribution of the beam electrons should be taken into account.

By calculating at different times the energy deposited in a plane placed perpendicular to the direction of propagation and parallel to one of the sides of the simulation box, it was possible to observe the radiation emission associated with the self-injection of the electrons in the ion cavity, in the 1.5 GeV LWFA stage. This was found to be orders of magnitude lower than in the propagation direction.



14.17 - Energy deposition at a plane perpendicular to the propagation direction of the electron beam (left panel) and spectrum at the center point of this detector (right panel). The detector was placed approximately 1.7 cm away from the region where the electrons reach an energy of approximately 1 GeV.

Spectral information on the betatron radiation was also analyzed. Analysis of this data showed that the position of the peak of the spectrum can be strongly influenced by the specific electron energy and amplitude of oscillation distributions.

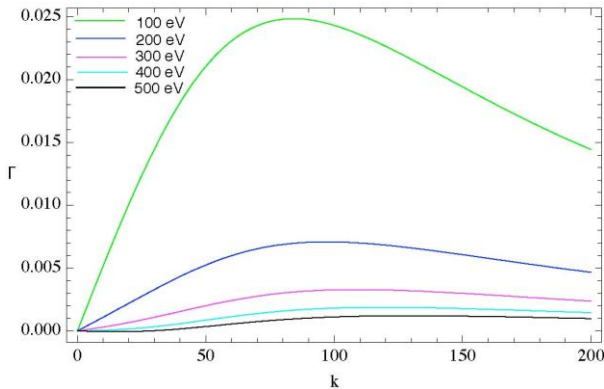
Even though the diagnostic has been applied so far mostly to LWFA scenarios, it is based on general formulas and can be applied to many other scenarios, provided that there is no significant effect of the radiation emission on the dynamics of the plasma particles, such as ionization,

¹⁴In collaboration with C. Joshi

bunching of the particles due to this radiation or strong deceleration from radiative damping.

14.23. ION ACOUSTIC INSTABILITY

Ion heating in ultra intense laser plasma interactions has been previously studied, analyzing the excitation of an electron two-streaming instability driven by the fast electron beam. These low frequency waves are then strongly damped by the ion collisions in the dense plasma thus exhibiting preferential heating of the bulk ion population. Recently, numerical simulations of collisionless beam–plasma instabilities to electron stopping and plasma heating have been performed in laser plasma in fast ignition target. Ion acoustic mode was studied analytically and numerically in a fast ignition scenario. The dispersion relation is derived by using the Vlasov equation for Maxwellian distribution functions for the collisionless electron beam and for the cold plasma. An example of the parameter sum of the growth rate for the ion acoustic mode and for two streaming instability is presented in the figure.



14.18 - Different colors show the different values of the temperature of the beam T_b , where T_b is 100, 200, 300, 400, and 500 eV. The cold plasma temperature is kept fixed, with $T_e = 10$ eV. The density ratio between the beam and the plasma is $n_{b0} = 0.1 n_{e0}$, where n_{e0} is the background electron density and $n_{i0} = n_{b0} + n_{e0}$.

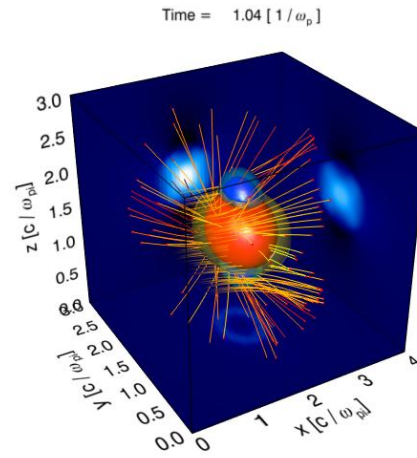
14.24. HYBRID SIMULATIONS OF HIGH-ENERGY ION INTERACTION WITH MINI-MAGNETOSPHERES

Space is an hazardous environment for astronauts and spacecraft equipment. Besides the abundant UV and gamma radiation, there are high-energy charged particles produced by the sun, the Solar Energetic Particles (SEP). These particles, mainly protons with energies up to 1 GeV, routinely reach the Earth environment at 1 AU and are deflected or captured by the magnetosphere. With this work we explore the possibility of using such small-scale magnetospheres for satellite and spacecraft protection.

We have studied the characteristics of mini-magnetospheres formed by a dipolar magnetic field and a plasma source via hybrid simulations (where ions are kinetic and electrons are fluid-like). Results have shown

that the distance between the edge of the magnetosphere (magnetopause) and the centre of the dipolar magnetic field, rmp, agree qualitatively with the theoretical prediction of MHD (magnetohydrodynamics). Deviations from the MHD model originate in the kinetic behavior of the particles, mainly finite-Larmor radius effects.

In our latest simulation scenario, we inject a plasma (simulating the solar wind) towards a dipolar magnetic field to form a mini-magnetosphere. Having obtained a stable magnetosphere we fire low-density, high-energy ions (simulating the SEPs), and study their deflection. Preliminary results show that particles with energies up to 0.1 MeV are effectively deflected by a dipolar magnetic field with a maximum intensity of 1.26 T.



14.19 - Tracks of 0.1 MeV ions that are deflected by the mini-magnetosphere. The bubble-like structure in the middle is the z component of the dipolar magnetic field.

15. LASER-PLASMA ACCELERATORS AND APPLICATIONS¹

L.O.Silva (Head), N.C. Lopes (Principal Investigator), J.M. Dias, C. Russo, N. Lemos, R. Bendoyro, M. Hilbert, J. Jiang, J. Berardo.

15.1. INTRODUCTION

The work in this field was developed along the following main topics:

- Pre-formed plasma channels using discharges in structured gas cells;
- The use of a simmer discharge to improve the quality of plasma channels;
- The use of a simmer discharge to improve the quality of plasma channels;
- Improvements of the gas cell design and experimental setup;
- Compact free-electron-lasers (FEL);
- Transverse dynamics of a plasma column created by field ionization.

15.2. PRE-FORMED PLASMA CHANNELS USING DISCHARGES IN STRUCTURED GAS CELLS

Pre-formed plasma channels are plasma targets with a radially growing parabolic density profile, able to guide intense laser pulses by a distance adequate for efficient electron acceleration. They act as graded index optical fibers and are able to keep laser pulse focused to high intensity by a distance much longer than the Rayleigh length. In order to avoid ionization-induced-defocusing of the laser, the plasma needs to be close to fully ionized. Using a discharge, high ionization levels can be achieved by using a low Z gas (H₂ or He). Several methods have been tested to create this plasmas. They used specially shaped laser beams or electric discharges to ionize a line of gas and heat the plasma. Normally, an electrical discharge between two points doesn't result in a plasma line between these points, but in a irreproducible more or less zig-zag type path. Different techniques can be used to force this path to a straight line. The most obvious method consists in forcing the discharge through a capillary tube of very small diameter. The other one was to use a discharge with a fast rising voltage and trigger the plasma by ionizing a small portion of the plasma line with an intense laser pulse. This last method was developed in our laboratory (2001-2003). We have produced and characterized one centimeter plasma channels. However, the time required for the plasma line to expand and form the parabolic shape channels is about 100 ns. This time is not practical for a delay line of an intense pulse (since part of the same pulse need to be used to trigger the plasma). The free plasma expansion using fast discharges clearly result in low-

density plasma channels adequate for guiding intense laser pulses. The low axial plasma density is especially important for increasing the acceleration length.

In order to avoid the laser triggering and keep the free expansion of the plasma we have developed a new method for creation of plasma channels. This method keep the hollow conical electrodes used in the previous work but the discharge is forced through a sequence of small diameter dielectric apertures that are coaxial with the propagation axis (defined by the electrodes). In this way we keep the free radial expansion and produce a straight plasma channel. Since the method require the use of light gases (H₂ or He) the ionization and heating of the plasma need to be done by a high-power pulse with a duration in the order of the expansion time (100 ns). Besides, in order to reduce the jitter and improve the quality of the plasma this pulse need to have a short rise time to high-voltage. The high-voltage pulse generator, described in, delivers up to 125 kV, 1kA pulses with 20 ns rise time. The rise time can be reduced to less than 4 ns by adding a magnetic compression stage to the main transmission line.

The use of short rise-time pulses, after the introduction of the magnetic compression in the setup, improved the discharge reproducibility. However the plasma uniformity and symmetry were strongly affected. The almost explosive start of the discharge produced hot spots of lower resistivity resulting in strong distortions of the plasma channel density profile.

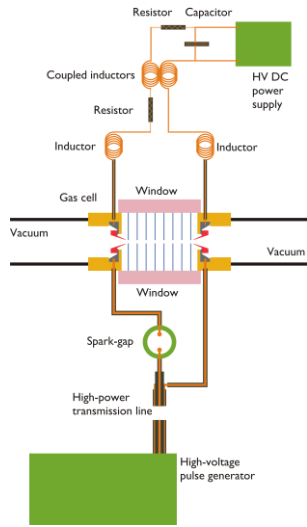
During 2008 the work on plasma channel development was focused in reducing the plasma channel diameter, increase the length, improve the smoothness and symmetry, and improve the stability of the experimental setup. The gas cells and the experimental setup where improved, a simmer discharge to pre-ionize the axial region of the gas cell was tested and demonstrated to strongly improve the plasma channels quality, and a gas cell for 8 cm long plasma channels was designed and assembled.

15.3. THE USE OF A SIMMER DISCHARGE TO IMPROVE THE QUALITY OF PLASMA CHANNELS

The use of ultra-short rise-time, high-voltage pulses to create jitterless plasma channels produces irreproducible hot-spots in the initial plasma line resulting in a non-symmetric and non-smooth plasma channel. In order to

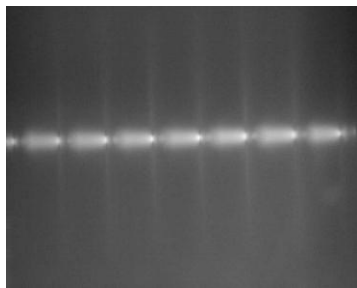
¹Activities performed in the frame of the Contract of Associated Laboratory, out of the Contract of Association EURATOM/IST, by IPFN staff of the Group of Lasers and Plasmas.

overcome this problem we have tested the use of a low current discharge to produce a uniform plasma background on the channels axis. A simplified setup of the plasma channel is presented in the Figure 15.1.



15.1 - Simplified schematic of the electrical setup used to test the use of a simmer discharge to improve the quality of the channel

A commercial high-voltage DC power supply producing 15 kV, at about 1 mA is used to produce the discharge. The DC power supply is activated by the trigger system a few milliseconds before the main discharge. In future we intend to install a solid-state switch to precisely control this discharge. The high-voltage pulse generator is connected to the conical electrodes in the gas cell through a spark-gap. The spark gap avoids the short circuit of the DC long (milliseconds) discharge since the pulse generator is a short circuit for pulses longer than 200 ns. When the gas is injected inside the gas cell (about 20 ms before the main discharge) a discharge is clearly visible in the channel axial region. A typical picture is presented in Figure 15.2.



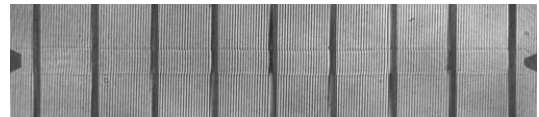
15.2 - Picture of the light emitted by the low current pre-discharge. This picture was made by imaging the plasma channel axis through on of the gas cell windows

One of the most interesting features in this picture is the symmetry of the plasma, which is a fundamental characteristic of a plasma channel. Since a mA current is

used for a long time (about 10 ms) the pre-discharge partially ionized plasma is very uniform and reproducible.

When the main discharge pulse, with up to 125 kV and 1 kA, is applied to the electrodes over such a pre-plasma, the result is also a uniform plasma with a high level of ionization. Figure 15.3 presents a typical interferometry picture of such a uniform plasma channel.

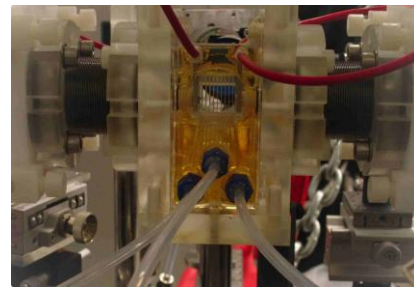
The pre-discharge opens the way for reproducible and useful plasma channels for electron acceleration. This technique can be used in longer channels and probably will extend this technique for multi-GeV compatible devices with a modest cost. The setup used in this experiment need to be improved to in order to control the pre-discharge parameters (voltage, current and duration) so it can be compatible with devices as long as 10 cm.



15.3 - Interferometry picture taken after plasma channel development. This picture was taken using a low energy ultra-short pulse produced by the L2I laser system about 100 ns after the rise of the main high-voltage pulse.

15.4. IMPROVEMENTS OF THE GAS CELL DESIGN AND EXPERIMENTAL SETUP

The design of the structured gas cell as well as the experimental setup for testing the plasma channels received important improvements in order to make possible the planned experimental work. A picture of one of the new gas cells is presented in Figure 15.4.



15.4 - Picture of a new structured gas cell prototype being installed in the testing setup.

The new features in the gas cell consist on a design optimized for stereophotolithography and individual injection of gas for the extreme end cells in order to reduce the probability of the pre-discharge through the gas feeding channels. The new prototypes are using now 150 micron diameter apertures on the dielectric plates and cones.

A new trigger system, for the millisecond and microsecond precision triggers, based on a configurable FPGA board running under LabView was installed to allow more the more complex operation of the experiment with the pre-discharge. In future this new trigger system

will evolve in order to fully control the experiment in a single and autonomous system.

The two main diagnostics on the experiment, laser guiding and interferometry, were equipped with 14 bit CCD cameras. An interface fully based in fiber optics was implemented in those cameras to make this diagnostics more compatible with the extreme electromagnetic noise produced in the experiments.

The first prototype of a “keep-aligned” system was tested with partial success. This system is intended to keep the beam aligned with the plasma channel by compensating the pointing instability with thermal origin. In future the CCD cameras and the mirror actuators in the “keep-aligned” system need to be upgraded with full fiber-optic interface for electromagnetic noise immunity.

15.5. COMPACT FREE-ELECTRON-LASERS (FEL)

FELs are adaptable light sources which can produce high-power coherent radiation across virtually the entire electromagnetic spectrum (from Microwaves (1m~1mm) to hard X-rays (<1nm)) in contrast with the discrete or narrow band conventional lasers. Furthermore, a free-electron laser is capable of efficiencies as high as 80% (efficiencies of 40% have already been demonstrated in the laboratory). In essence, a FEL is a kind of laser, produced by interaction among three basic elements: a bunch of electrons, electromagnetic wave traveling in the same direction as the electrons and periodic magnetic fields. The FEL convert part of the kinetic energy of the electrons into coherent electromagnetic radiation through the synchrotron motion of electrons. This conversion, usually takes place in the periodic magnetic field that is produced by a magnetic device called an undulator or wiggler. The discrete energy levels existing in the conventional lasers are not a trait in FELs, where electron energy transitions occurs in a continuum. Therefore FELs are classical rather than quantum-mechanical conventional lasers.

Because of FELs' unique set of properties: (i) Possibility to work at any frequency in the continuous range from microwaves to hard X-rays with extreme short pulse duration(fs) ; (ii) Extremely high levels of generated power (MW-TW) ; (iii) High electron efficiency (>40% with no limitation to100%) , Multiple valuable applications of free-electron lasers come to schedule, ranging from experiments in the solid-state physics, time-resolved chemistry to molecular biology, and novel designs also under development for such diverse purposes as lithography, communications, radar and ballistic missile defense, thus attract significant effort of scientists and engineers all over the world directed towards the FELs field .

Recent advances in laser-plasma-based electron accelerators (LPA) have demonstrated generation of low energy spread, small diameter, high current, low scattering, GeV electron beams within centimetres laser-plasma interaction length. In addition, the electron bunches emerging from a laser-plasma accelerator have naturally short durations (fs), and are intrinsically synchronized to the short-pulse laser driver, making LPA a source ideal for

a new method of compact, low cost, high-peak flux XFELs.

We have started the evaluation/design of a compact multipurpose single-pass FELs at saturation as the further application of our existing advantages on LPA. The whole set-up of our scheme including: high quality electrons beams source from our developing LPA; Laser-Plasmas High Harmonic Generation (HHG) radiation seeding device; Compact tunable electromagnet wiggler(within metres long); Necessary magnetic devices for beam concentration; Diagnostic systems. Finally, we expect our set-up becomes a standard scheme for the stable high brilliance coherent light resources at XUV&X-ray with extreme short pulse duration.

15.6. TRANSVERSE DYNAMICS OF A PLASMA COLUMN CREATED BY FIELD IONIZATION

The guiding of intense laser beams in plasmas is of great relevance for applications such as plasma accelerators, x-ray lasers and high-harmonic generators. These applications require laser pulses propagating at high intensity, generally above the ionization threshold of atoms. Although with current laser technology, such intensity can be achieved in a tightly focused beam, the subsequent spreading of the beam due to diffraction imposes a severe limitation on the total interaction length. There are several schemes to increase the interaction length from which the most promising is the use of a preformed plasma waveguide. Several methods have been implemented, including thermally driven laser-induced plasma expansion where a laser pulse with hundreds of picoseconds heats the plasma enough to expand and generate density depletion in the center of the plasma column. Until recently it was thought that ultra-short intense pulses (sub-picosecond) were inefficient at creating plasma channels through heating, since the collision frequency is reduced for large quiver velocities. Recent results show that due to stochastic heating and the Weibel instability tunneled ionized gases can heat enough the plasma to create a good plasma channel.

In this work, we will present a detailed study of the transverse dynamics of a plasma column created by an ultra-short laser pulse. By focusing a 500 fs pulse of the L2I laser chain on a 8 mm gas jet a uniform plasma column was created, that expanded after a few nanoseconds. The breakdown spark creates the plasma column that expands at the local sound speed, and ion-ion and ion atom collisions lead to the formation of a shock wave at the boundary between the hot plasma and the neutral or weakly ionized gas on the periphery. The cylindrical expansion of the shock wave results in radially increasing plasma density, thereby forming a waveguide suitable for optically guiding intense laser pulses. A detailed characterization of the evolution of the shock wave was done for three different gases. The evolution of the shock wave was approximated to a Self similar adiabatic expansion of a cylindrical blast wave as seen in Figure 15.5 where as expected it was observed a higher expansion rate for lighter gases.

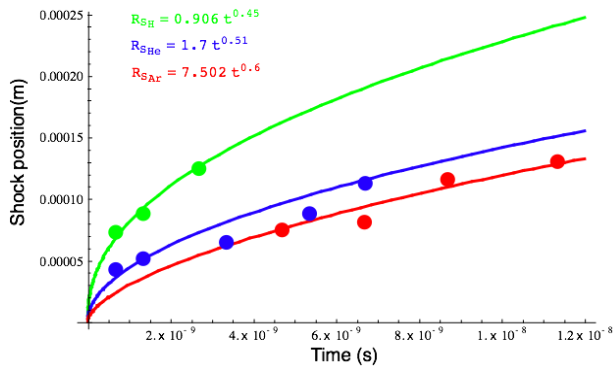


Figure 15.5 - Time evolution of the shock wave for the three gases that were used (Hydrogen, Helium and Argon)

16. HIGH INTENSITY LASER SCIENCE AND TECHNOLOGY¹

L.O. Silva (Head), G. Figueira (Principal Investigator), T. Imran, L. Cardoso J. Wemans, M. Fernandes, H. Pires, C. João

16.1. INTRODUCTION

The work on High Intensity Laser Science and Technology was focused on three main topics:

- Spatio-temporal distortion from beam propagation in grating compressors;
- Full front-end characterization;
- Supercontinuum generation in solid state media.

16.2. SPATIO-TEMPORAL DISTORTION FROM BEAM PROPAGATION IN GRATING COMPRESSORS

A matricial formalism known as the Kostenbauder matrices was used to determine the spatial-temporal distortions present in a Gaussian beam as it travels through optical elements. Based on this simple and versatile approach, we determined the distortions present in some common systems based on compressor gratings. The obtained results (Figure 16.1) were all in concordance with some already present in literature, furthermore, in the case of a system based on a double pass compressor the obtained result was in fact an extension of the already existing one due to the consideration of a Gaussian beam.

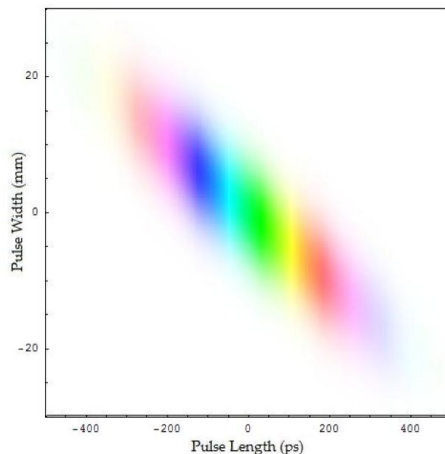


Figure 16.1 - Spectrally-resolved spatial profile of a Gaussian beam after a grating pair

16.3. FULL FRONT-END CHARACTERIZATION

This work is framed in the initiative to develop an OPCPA-based, ultra broadband, diode-pumped high energy laser system. Diode-pumping, in particular when associated with ytterbium-doped amplifying materials, allows a high efficiency, high repetition rate operation, therefore being ideal as a primary pump source for an

OPCPA system. However, the working wavelength for such a system may be different from the one regularly used at the laboratory (1053 nm). On the other hand, using a common seed for both the pump and the signal in a parametric amplification configuration allows jitter-free operation, ensured by the optical synchronization between the two. For this purpose, we performed a study of the tunability characteristics of the front-end of our chirped pulse amplification system.

This work consisted in the complete characterization of the performance of the mode-locked Ti:sapphire oscillator, the Ti:sapphire-based regenerative amplifier, and the Offner stretcher, under a variety of configurations. In the case of the oscillator, the operating wavelength was changed over the range 990-1080 nm. The spectral transmittance of the stretcher into the regenerative amplifier was clipped either at long or short wavelengths. The regenerative amplifier was tuned in wavelength, and the amplified pulse characteristics were measured.

The obtained data (Figure 16.2) shows good wavelength flexibility in the front-end, allowing a convenient choice of the operating wavelength for the full diode-pumped OPCPA system.

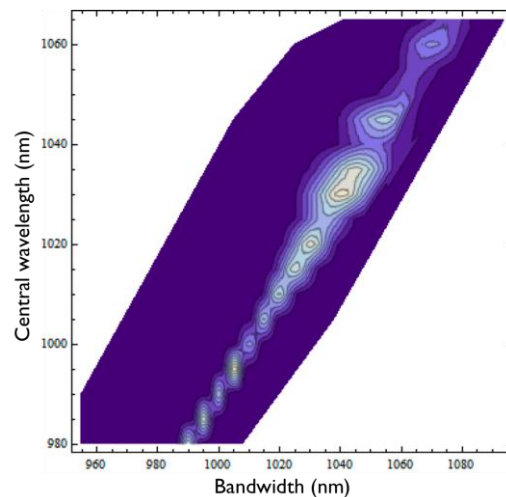


Figure 16.2 - Available bandwidth vs. operating wavelength of modelocked oscillator.

16.4. SUPERCONTINUUM GENERATION IN SOLID STATE MEDIA

Propagation of intense ultrashort laser pulses in transparent solid state media can induce ultrabroadening of the original

¹Activities performed in the frame of the Contract of Associated Laboratory, out of the Contract of Association EURATOM/IST, by IPFN staff of the Group of Lasers and Plasmas.

spectrum, which is called supercontinuum (SC) or white light generation. This broadband source of SC raises much interest for its wide applications such as characterization of optical components, interferometry or optical coherence tomography, and the generation of few-cycle pulses.

Development of a broadband laser source using the equipment and parameters of IPFN's Laboratory for Intense Lasers (L2I) was proposed, which would represent a new research field at this facility. We studied and evaluated the suitability of several techniques and it was decided that we should consider white-light generation in bulk media such as sapphire and fused silica, either at the first or second harmonic, and investigated the required parameters. We designed and implemented a low-energy double pass pulse compressor to be used in this experiment. This compressor has also been successfully used for high-harmonic generation experiments at L2I (see elsewhere in this report).

Preliminary experiments in 2008 using a new grating compressor showed the feasibility of generating supercontinuum (SC) radiation from the interaction of mJ-level, ~ 200 fs, 10 Hz pulses at 1053 nm using fused silica. The laser pulses used in the present experiment are generated using a conventional chirped pulse amplification (CPA) system. The L2I laser system comprises of an oscillator (Mira, Coherent Inc.) that delivers a ~ 150 fs, 76 MHz pulse train with pulse energy of 4 nJ at 1053 nm. The pulse train from the L2I oscillator is directed into a homemade regenerative amplifier pumped at 10 Hz by a Q-switched Nd:YAG laser (Spectra Physics Inc.). After compression we obtained pulses of ~ 200 fs duration with output energy of up to the mJ-level. In this typical SC generation experiment, pulse with energies up to 2 mJ are focused by a 400 mm focal length lens into a 12 mm thick fused silica plate. The generated continuum is detected by a CCD camera, and a white screen was also inserted in the far field in order to observe the diverging colorful pattern associated with SC generation (Figure 16.3). The white-light continuum beam has a central white part, which is surrounded by colored rings. These rings do not extend continuously from the central white-light, but occur as distinct rings of red, green, and blue light, often separated from the central white light beam and from each other by dark rings. The higher frequency light appears in the outermost ring, and the lower frequency light forms the ring nearest the white light continuum. An example of such a ring structure generated in fused silica is shown in the figure below.



Figure 16.3 - Continuum generated in fused silica

The white-light continuum after the fused silica plate is made to pass through an iris to cut off the outer unwanted portion of the beam (Figure 16.4).

The flip-type mirror mount is used after the fused silica plate to send the focused beam to the spectrometer to study and characterize the SC spectrum. The next step will be to apply this experimental setup to a pulse compression setup in order to generate ultrashort (sub-50 fs) laser pulses.

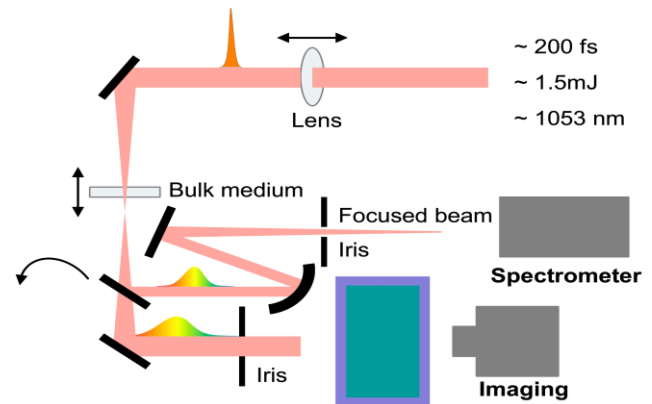


Figure 16.4 - Experimental setup for white light continuum generation

17. COHERENT SOFT-X-RAY SOURCES¹

L.O. Silva (Head), M. Fajardo (Principal Investigator), N.C. Lopes, E. Abreu, A. Sardinha and J. Miranda.

17.1. INTRODUCTION

The work in this project was focused on:

- Online tuning of the quasi-phase matched order;
- Polarization of high order harmonics in two-colored fields;
- Tunability of spectrally narrow High Order Harmonics;
- Optimization of soft x-ray amplifiers for seeded X-ray lasers.

17.2. ONLINE TUNING OF THE QUASI-PHASE MATCHED ORDER

During the HHG process a phase mismatch arises between the harmonic and the fundamental radiation. For high ionization fractions in the gas, the phase mismatch Δk is proportional to the harmonic order and the gas density. The generated harmonic radiation adds up constructively along the medium, as long as the propagation distance is smaller than the laser coherence length. For low ionization fractions, Δk can be set to zero, through a parameter adjustment leading to phase matching. High ionization fractions make phase matching impossible. Quasi-phase matching (QPM) techniques try to overcome this problem.

The interference of two coherent laser beams leads to a fringe pattern where the spacing depends on the angle between the beams. We achieve a periodic and easily tunable modulation of the electron density of the gas, by line focusing the pattern on the gas jet. The line focus can be obtained from two cylindrical lenses (Figure 17.1).

We calculated the expected enhancement for 1053nm, 300 fs pulses. Each of the interfering beams carries an energy of 110mJ, which means a maximum intensity of $1,2 \cdot 10^{13} \text{ Wcm}^{-2}$. As for the harmonics generating beam, it carries an energy of 7mJ, i.e. a $3,0 \cdot 10^{14} \text{ Wcm}^{-2}$ intensity. As shown in Figure 17.2, enhancements up to two orders of magnitude are achieved.

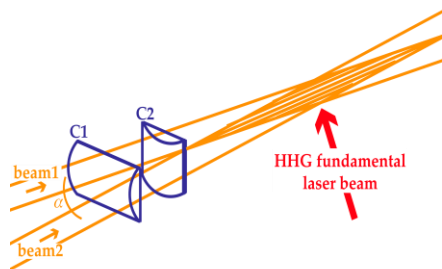


Figure 17.1 - Setup for the creation of a tunable density modulation in the gas, through the interference of two laser beams

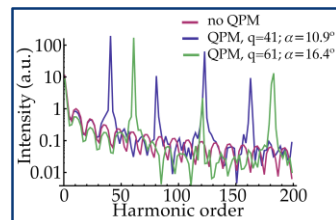


Figure 17.2 - Predicted intensity enhancement of harmonic orders 41 and 61 of a 1053nm, 300fs pulse, due to a laser interference based density modulation in the gas.

17.3. POLARIZATION OF HIGH ORDER HARMONICS IN TWO-COLORED FIELDS²

The most used combination for the enhancement of harmonic emission has been that of 2 fields with frequencies ω and 2ω propagating in the same direction, with linear polarizations (parallel or orthogonal or adjustable) with an adjustable phase difference. Standard models for the calculation of the harmonic generation efficiency (Corkum e Lewenstein) provide a detailed description of single atom response for the case of a monochromatic laser field with linear polarization.

However, the generalization for mixed fields is not trivial in the sense that the calculations (both analytical and numerical) become increasingly difficult and prevent from giving a clear picture of the physical mechanisms at stake. A simplified model for the atomic potential in which the calculation of the HHG spectrum is almost fully analytical would enable the explicit evaluation of the effect of two-color field mixing.

One prediction that is exact and is straightforward from the model above is that: in a mixed ω - 2ω field in which both fields are linearly and orthogonal polarized, the odd harmonics of the fundamental frequency ω will have the polarization of the ω field while the even harmonics will have the polarization of the 2ω field. This phenomenon should be independent from the relative phases or intensities of the two fields.

The main goal of this experience is, therefore, to confirm experimentally the polarization rules one can predict from the δ_3 potential model concerning HHG in mixed fields. Due to the great simplicity of the model, we find that it's important to measure the agreement with experience, in order to use the δ_3 potential, as first approach, when doing theoretical calculations of HHG in mixed fields.

¹Activities performed in the frame of the Contract of Associated Laboratory, out of the Contract of Association EURATOM/IST, by IPFN staff of the Group of Lasers and Plasmas.

²In collaboration with G.Lambert, J. Gautier, Ph. Zeitoun (LOA, France)

A Laserlab beamtime proposal was successfully submitted by our team to verify the difference in two-field mixing in the case of parallel and perpendicular polarization. Beamtime was awarded in November 2008. The goal was to measure the influence of the IR laser polarization on the emitted spectrum in the XUV region reflected by a broadband multilayer mirror. This will enable us to confirm either, as predicted, in a mixed ω - 2ω field in which both fields are linearly and orthogonal polarized, the odd harmonics of the fundamental frequency ω will have the polarization of the ω field while the even harmonics will have the polarization of the 2ω field.

We will correlate those measurements with the parallel and perpendicular cases, using a multilayer-coated XUV mirror at Brewster angle as shown above. Analysis of the experimental data is under way.

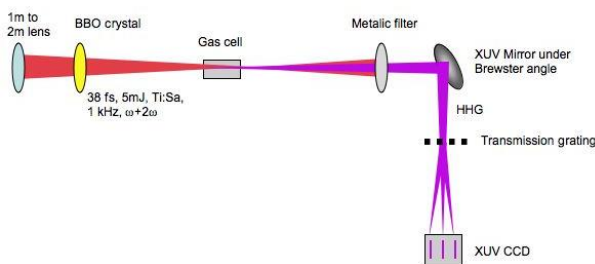


Figure 17.3 - Experimental set-up. HHG are generated in a Gas cell with varying IR beam polarization. Discrimination of polarization between odd and even harmonics is made via a polarizing XUV mirror.

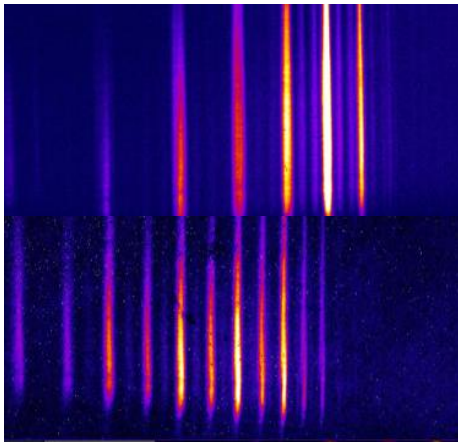


Figure 17.4 - High Harmonics from an 800 nm beam (above) and a mixed field at 800 nm and 400 nm (below) of orthogonal polarization. No polarizer is added to these shots.

17.4. TUNABILITY OF SPECTRALLY NARROW HIGH ORDER HARMONICS³

High order harmonics of narrow spectral bandwidth are generated when the driving IR laser is ps-range, as in our

case at the Laboratorio de Lasers Intensos (L2I). Indeed, we have shown last year in the first experimental campaign of High Harmonic Generation at L2I that a spectral bandwidth below 10^{-3} was obtained up to harmonic order 51, while conventional HHG from Ti:Sa lasers have a bandwidth of $\sim 10^{-2}$.

This characteristic enables the use of HHG for seeding a laser-produced X-ray laser with a much higher efficiency coupling than previously thought, as the XRL bandwidth is typically 10^{-4} . However, due to the limited X-ray laser lines available for seeding, HHG produced using such long pulses must be tunable, so that matching between a given harmonic and the closest available X-ray laser line is possible.

In 2008 we have built in collaboration with the Laser team a new, tabletop pulse compressor, for a low energy beam at L2I. It has the advantage over the main vacuum compressor to be of flexible adjustment, and to allow a variable spacing between gratings. Varying the spacing between compressor gratings around the optimum for minimum compression is a well-known technique for HHG wavelength tuning for short-pulse lasers.

The experimental interaction chamber suffered from a major overhaul in 2008 due to the installation of a clean vacuum pumping system. We took the opportunity to reconfigure the geometry inside the main interaction chamber, and install a motorized gas cell with variable gas pressure. In an experimental campaign in May-June 2008, we have measured the absolute wavelength of the generated harmonics in an argon gas cell.

The optimum for harmonic emission was found in two configurations of length and argon pressure for different laser energy regimes. The absolute wavelength calibration of HHG was obtained for the high energy case, where the laser nonlinear propagation effects are most critical. We found a correlation between the harmonics wavelength and the compressor length, and could produce HHG shifts above 2\AA , sufficient for matching relevant X-ray laser lines in the 20-30 nm range.

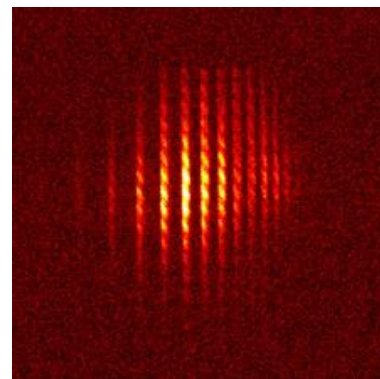


Figure 17.5 - Raw High Harmonic Spectrum from 2008 Campaign. The small-scale structure originates from the metallic mesh on a 1500Å aluminum filter blocking the IR beam.

³In collaboration with Ph. Zeitoun (LOA, France)

17.5. OPTIMIZATION OF SOFT X-RAY AMPLIFIERS FOR SEEDED X-RAY LASERS⁴

An experimental run at PALS (with IST beamtime from Laserlab) was dedicated to possible geometries and active medium for amplification of short wavelength lasers. We were careful to keep the compatibility of the geometry to long delays between pulses (10 ns between prepulse and pulse), to understand the effect of the 2D hydro expansion on the laser-produced plasmas, making XUV radiographs of the expanding plasma at delays as long as 16 ns.

The experiment was performed in the same geometry as in 2006: a long plasma (1-2 mm) produced by a long line focus was probed along the focus by an x-ray laser, and a 2D image of the expanding plasma, perpendicular to the probing axis, was obtained. This ensured that the 3D effects were constrained to the edges of the target and negligible compared to the main 2D geometry.

We also studied the effect of the prepulse on the homogeneity of the plasma with gain. For this, we probed through X-ray radiography the state of the density profile at the time the main pulse heats the target (with the main pulse off). Raw images for Zn and Au plasmas are shown above, for a prepulse intensity of 10^{10} W/cm². The structure of the pre-plasma is completely different for both cases, and although the plasma is small and confined for the Zn case, it has suffered a large expansion with structured jets in the Au case. This example of the influence of a prepulse as small as 10^{10} W/cm² at as long as 10 ns after it hits the solid shows that careful monitoring of the plasma profile at the main pulse time will be necessary for each new X-ray laser configuration.

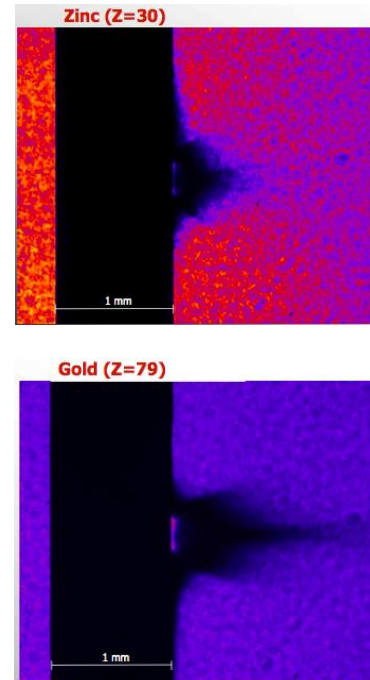


Figure 17.6 - Plasma profile at 10ns after heating the solid with a 10^{10} W/cm² prepulse in the hollow focus configuration. Notice the difference in expansion geometry for different Z elements

⁴ In collaboration with B. Rus, M. Kozlova, T. Mocek (PALS, Czech Republic)

18. GENERATION OF ELECTROMAGNETIC RADIATION IN PLASMAS AND DIAGNOSTICS¹

L.O. Silva (Head), J.M. Dias (Principal Investigator), N.C. Lopes, N. Lemos and J. Berardo.

18.1. INTRODUCTION

The work in this project was focused on:

- THz characterization and generation;
- Radiation sources based on a GeV laser wakefield accelerator and electron beam characterization.

18.2. THE CHARACTERIZATION AND GENERATION²

By focusing a high power and ultra-short laser pulse in a gas jet it is possible to generate relativistic ionization fronts. As it propagates through the jet, the laser beam ionizes the background gas by tunneling ionization, thus creating a relativistic plasma-gas interface (ionization front) that co-propagates with the laser pulse. As previously proposed, and recently observed, these relativistic ionization fronts can be used to strongly up-shift the frequency of colliding laser pulses, mainly determined by the density, shape and velocity of the front. However the difficulty of producing a total reflection at the ionization front is the low cutoff frequency given by relativistic factor of γ mirror for the typical plasma densities. Now with the ability of generating low frequency THz radiation sources produced by femtosecond laser pulses opens the possibility to achieve the reflection conditions needed to obtain a relativistic mirror using ionization fronts.

This way to produce and characterize the relativistic mirror it was assembled an experimental setup at the TOPS laboratory at Strathclyde University (Glasgow). The ionization front was generated focusing the laser in a 4mm supersonic gas jet and was characterized using a Mach-Zehnder interferometer. The THz radiation was created applying a high-voltage and irradiating the surface of the semi-conductor (GaAs) with the fs laser pulse. The resulting THz radiation was then characterized spatially and temporally.

For the temporal characterization of the THz pulse it were used two electro-optic techniques namely the Spectral encoding and the Cross-correlation. In wither one of the two techniques a THz and a chirped laser pulse were focused into an electro-optic crystal (ZnTe). The electric field of the THz changes the refractive index of the crystal on one axis, producing a birefringence in the crystal, changing the polarization of the chirped laser pulse. This way the THz electric field leaves a “fingerprint” on the chirped laser pulse. The results of both methods revealed

that the pulse duration is 500fs and the central frequency is 0.2 THz. The spatial characterization of the THz makes use of the same birefringence principle has the temporal characterization. The main modification is that the chirped laser pulse is not focused on to the electro-optic crystal, but remains collimated such that it overfills the THz spot at the crystal plane. Thus the THz spatial imprint is recorded in the chirped laser pulse and collected by a CCD (Figure 18.1) where the measured spot size of the THz beam was around 1.6mm.

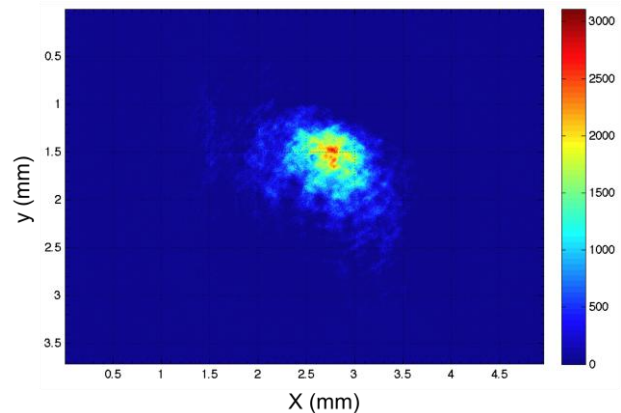


Figure 18.1 - THz spot at the interaction zone

In order to test the relativistic mirror concept it was determined the best position for the collision between the ionization front and the THz pulse over the gas jet. To determine this position it was used the THz characterization setup to detect the THz transmitted across the plasma. This way when the transmission signal reaches a minimum it can indicate that the reflection is at its maximum. In Figure 18.2 it is possible to see that there is a minimum in the region when the collision happens inside the gas jet region. This way if the ionization front arrives after the THz (longer delays) the signal transmission starts to go up. But the observed rising of the transmission is not so steep has it should be probably because of the crossing of the gas jet.

¹Activities performed in the frame of the Contract of Associated Laboratory, out of the Contract of Association EURATOM/IST, by IPFN staff of the Group of Lasers and Plasmas.

²In collaboration with J. G. Gallacher, J. Sun, R.C. Issac, D.A. Jaroszynski (Strathclyde)

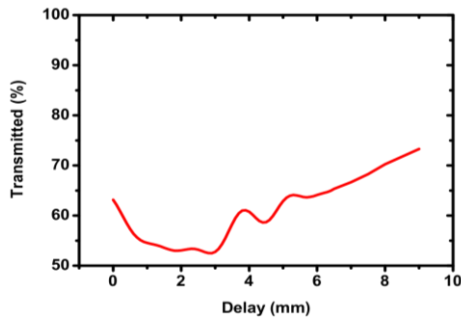


Figure 18.2 - THz pulse transmitted through the ionization front

18.3. RADIATION SOURCES BASED ON A GEV LASER WAKEFIELD ACCELERATOR AND ELECTRON BEAM CHARACTERIZATION³

It has been many years since laser created plasmas have been proposed to accelerate electrons. Their interest relies on the fact that plasmas can produce large acceleration gradients, on the order of 100 GV/m compared to 100 MV/m for conventional radio-frequency linear accelerators. Both three dimensional particle-in-cell simulations and experiments have shown that it is possible to generate electron beams with energies up to GeVs. An important application of these energetic particles is the production of x-ray radiation. When an ultra-intense laser is focused into a gas jet, the ponderomotive force pulls the electrons away from the strong field regions leaving a ion

cavity almost free of background electrons in its wake (this regime is usually designated by the bubble regime). As the relativistic electrons propagate in the bubble, they experience a longitudinal accelerating field and a transverse restoring force, which makes them undergo betatron oscillations. This way a collimated beam, of synchrotron radiation is originated from this relativistic oscillatory motion.

To produce and characterize the betatron radiation an experimental setup was assembled at the Rutherford Appleton Laboratory where it was used the Astra-Gemini laser with an energy of 3J and a pulse duration of 50fs. The beam was focused to a spot size of 30 μm into a plasma channel (created by a discharge inside a capillary) where it was guided for 3cm. Due to the high intensities reached inside the plasma channel ($2 \times 10^{19} \text{ W/cm}^2$) it was possible to enter the bubble regime and produce electron bunches and betatron radiation. The energy of the electron bunches was characterized using an electron spectrometer that measured energies around 400 MeV. The characterization of the bunch duration was done measuring the spectrum of the transition radiation of the electron bunch when crossing a metal, but because the spectrometers were affected by the laser amplifiers electrical noise it was impossible to have any good readings. The betatron radiation was measured with a silicon solid-state detector (Medipix2) that revealed radiation with a maximum energy of around 1MeV (gamma rays).

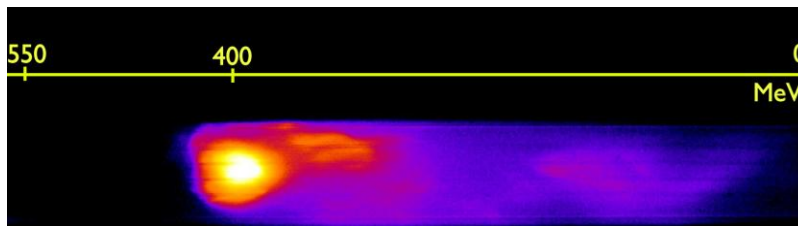


Figure 18.3 - Energy spectrum of the electrons generated by the bubble regime

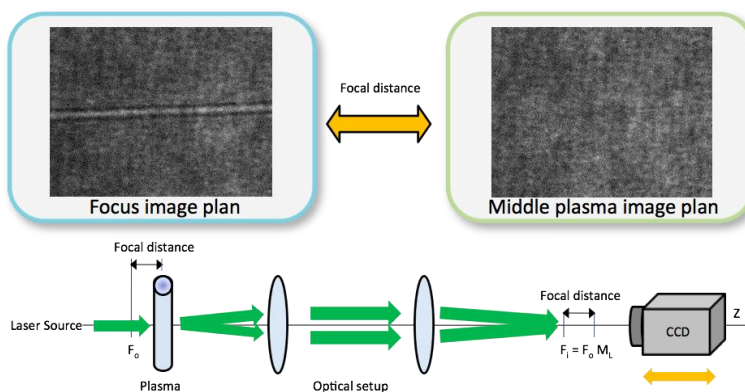


Figure 18.4 - The distance between plasma image plan and focus image plan

³In collaboration with S.Cipiccia, M.Wiggins, R.Shanks, G.Vieux, D. A. Jaroszynski (Strathclyde) and the Oxford team

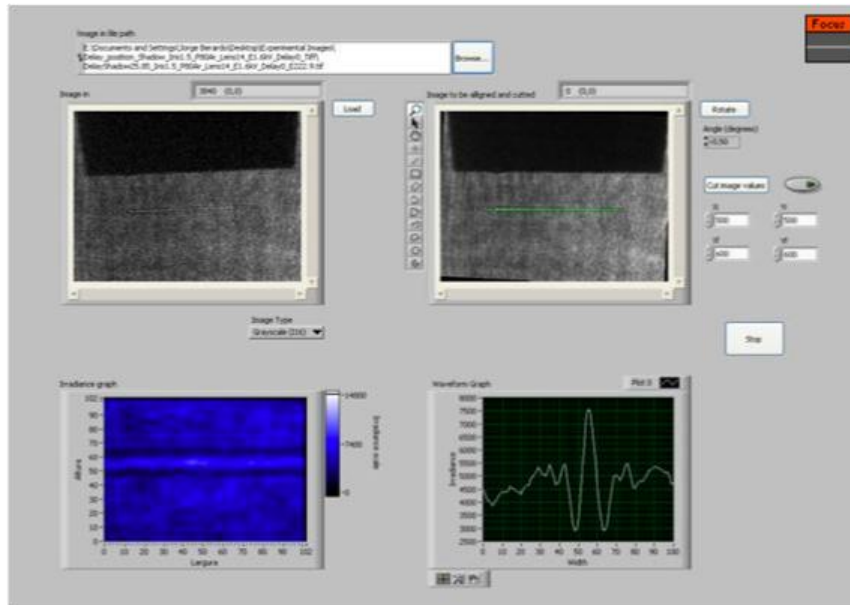


Figure 18.5 - Data measurement software developed

To execute this study was developed a theoretical description, a ray-tracing simulation and at last an experimental proof of principal of a diagnostic based on the refraction of a laser beam propagating through a plasma. Considering the curvature of the wavefront, induced by the different optical paths for each beam ray, the focal distance of the plasma lens can be determined. Using a shadowgraphy imaging setup we were able to measure the position of the focal spots of the plasma lens, and using a simple theoretical model, we have estimated the plasma density for a given plasma profile and width. A Labview software was developed to minimize the focal spot position error. In order to prove this diagnostic reliability, its quantitative values for the plasma density were compared with values obtained simultaneously from the interferometry diagnostic.

19. HIGH DENSITY LASER-PLASMA PHYSICS¹

L.O.Silva (Head), J. Davies (Principal Investigator) and J. Valente.

19.1. INTRODUCTION

The work in this field was developed along the following main topics:

- Fast electron transport theory for the HiPER project;
- Laser-Solid Experiments.

19.2. FAST ELECTRON TRANSPORT THEORY FOR THE HIPER PROJECT²

We are making an active contribution to the HiPER project on the critical problem of determining the laser parameters required for fast ignition, as part of the “requirements analysis for fusion programme” work package (WP 9).

There exist a number of different results in common use for the stopping and scattering of fast electrons in plasmas, which lead to significant differences in the prediction of the laser parameters required for fast ignition. We have recently clarified this issue. These results have been implemented in a Monte Carlo energy deposition routine for the code DUED, which has been used to repeat previous ignition calculations including more realistic energy deposition by fast electrons.

We have made an extensive compilation of numerical and experimental results on laser absorption, in the context of fast ignition. This work was presented as an invited review at the 10th International Fast Ignition Workshop and published in *Plasma Physics and Controlled Fusion*.

We have submitted a report to the coordinators of the “experimental verification” work package (WP 10) reviewing fast electron generation and identifying critical experiments that need to be carried out in this area in the next two years.

We are organizing the benchmarking of fast electron transport codes. We convened a meeting of those involved in this work in December 2008 and the first code comparison has been agreed upon.

19.3. LASER-SOLID EXPERIMENTS³

Two experiments were carried out at two of the world’s leading high power laser laboratories in 2008.

The first was carried out on the Vulcan PetaWatt laser at the Rutherford Appleton Laboratory (UK). The aim of the experiment was to reduce the divergence of the fast electron beam, which from our previous results [5] appears to be too high for efficient fast ignition. A pre-pulse with an intensity of 10^{18} W cm⁻² was used to try to form a collimating magnetic field inside the target before the arrival of the main pulse, with an intensity $> 10^{19}$ W cm⁻². Preliminary analysis of the data carried out by us and the RAL/Imperial group indicates that the scheme did not work as expected. These results have been included in a paper submitted to *Nuclear Fusion*.

The second experiment was carried out on the PICO2000 laser at LULI (France) in the HiPER dedicated slot. The aim of the experiment was to investigate the dependence of laser absorption into fast electrons on the extent of the pre-plasma. The duration of the ASE pre-pulse was varied to vary the pre-plasma. The analysis of these results is still underway, but preliminary results indicate a significant increase in absorption with scale length.

Proposals for further experiments were submitted, one of which has been accepted and scheduled for 2/3/2009 till 10/4/2009 on Vulcan TAW, in the HiPER dedicated slot. The analysis of two previous sets of experiments was completed and published. The analysis of transition radiation results from experiments on Vulcan TAP and TAW has been started.

¹Activities performed in the frame of the Contract of Associated Laboratory, out of the Contract of Association EURATOM/IST, by IPFN staff of the Group of Lasers and Plasmas.

²In collaboration with S. Atzeni and A. Schiavi (Rome)

³In collaboration with P. A. Norreys, K. L. Lancaster, J. S. Green and R. H. H. Scott (STFC, RAL), J. J. Santos (Bordeaux) and S. Baton (LULI).

20. ENVIRONMENTAL ENGINEERING PLASMA LABORATORY¹

C. M. Ferreira (Head), E. Tatarova (Principal Investigator), F. M. Dias (principal Investigator), V. Guerra, J. Henriques, M. Pinheiro, E. Felizardo.

20.1. INTRODUCTION

The research work in the Environmental Engineering Plasma Laboratory covered the following topics:

- Plasma torches for environmental issues;
- Extraordinary phenomena in hydrogen plasmas;
- Improvement of plasma diagnostic techniques.

20.2. PLASMA TORCHES FOR ENVIRONMENTAL ISSUES²

Having in view environmental issues, the activity of the “Environmental Plasma Engineering Laboratory” (EPEL) during 2008 consisted of experimental and theoretical investigations of various microwave molecular plasmas over a wide range of operating conditions.

Recently, there has been a growing interest in potential applications of microwave plasmas. High-density plasma torches provide suitable conditions to dissociate molecules in abatement systems and burn out chemical and biological warfare agents as well as to atomize and synthesize materials in carbon nanotubes forming systems. One of the main advantages of such microwave discharges at atmospheric pressure is that they make it possible to inject large power densities into the plasma and thus achieve high population densities of active species. The work carried out on microwave plasma torches and their applications included the following main fields of investigation:

- Further improvement of the experimental set-up;
- Development of new experimental techniques for spectral diagnostics of molecular plasmas - 2D mapping of the plasma torch structure;
- Further development of a theoretical model for the air-water plasma torch as a tool for optimization of the plasma source operation;

The waveguide-surfatron based set-up has been further improved in order to ensure stable operation of the torch when increasing the water percentage in the mixture. A new system for plasma dilution with water has been incorporated in the principal gas flow system, providing conditions for water heating before reaching the discharge zone. The new system provides gas flow rates from 100 to 2000 sccm under laminar gas flow conditions.

The air-water plasma emission in the 250 – 850 nm range has been investigated. Emission spectroscopy has been used to detect the following emission lines: the 777.4 nm, 844.6 nm and 630 nm atomic oxygen lines,

$O(3p^5P \rightarrow 3s^5S)$, $O(3p^3P \rightarrow 3s^3S)$ and $O(2p^1D \rightarrow 2p^3P)$, corresponding to the transitions respectively, and the $NO(\gamma)$ band in the range 230-260 nm (0-1, 0-2 and 0-3 vibrational transitions). The relative emission intensities of the Q_1 -branch of the OH rotational band within the (0 – 0) vibrational transition (in the range 306 – 315 nm) have been used to determine the gas temperature variation when the water percentage in the plasma increases (Figure 20.1). Infrared sensitive measurements using an optical thermometer provide data on the wall temperature. The gas temperature shows weak dependence on the water percentage in the mixture as in Figure 20.2.

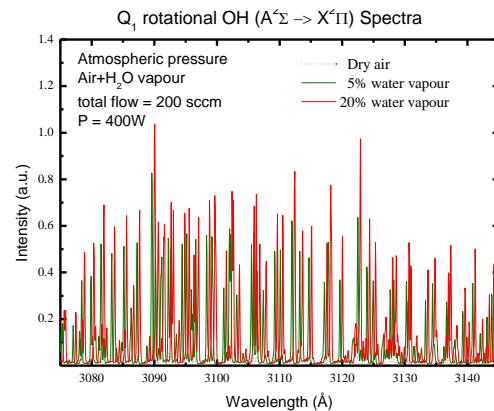


Figure 20.1 - OH spectra for various water percentages.

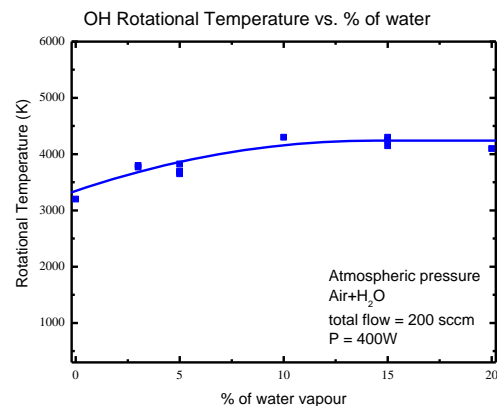


Figure 20.2 - Gas temperature vs water percentage.

¹Activities performed in the frame of the Contract of Associated Laboratory, out of the Contract of Association EURATOM/IST, by IPFN staff of the Group of Gas Discharges and Gaseous Electronics.

A self-consistent model for a microwave plasma torch using air mixed with water was further developed. The system of equations considered to describe the plasma source includes:

- Maxwell's equations;
- The dispersion equation for the azimuthally symmetric TM surface mode;
- The rate balance equations for vibrationally excited states of electronic ground state molecules $N_2(X^1\Sigma_g^+, v)$;
- The rate balance equations for the excited states of molecules and atoms $N_2(A), N_2(B), N_2(a'), N_2(a), N_2(C), N_2(a''), N(^2D), N(^2P), O_2(a), O_2(b), O(^1D), O(^1S)$;
- The rate balance equations for ions and electrons $N_2^+, N_4^+, O^+, O_2^+, O_4^+, NO^+, NO_2^+, H_2O^+, H_3O^+, H_2^+, H_3^+, HN_2^+, NH_3^+, NH_4^+, O^-, O_2^-, O_3^-, H, OH^-, NO_2^-, NO_3^-$;
- The rate balance equation for ground state molecules and atoms (N, O, O₃, NO, N₂O, NO₂, NO₃, N₂O₅, H₂O, H, H₂, OH, HO₂, H₂O₂, NH₃, NH₂, NH, HNO, HNO₂, HNO₃);
- The gas thermal balance equation;
- The equation of mass conservation for the fluid as a whole.

The improved model provides a complex, detailed description of the entire plasma source, i.e. discharge and post-discharge zones. The model predictions have been experimentally validated. A small change in UV radiation due to the NO(γ) band in the range 230 – 260 nm has been detected. However a significant increase in the UV radiation at about 300 nm has been obtained when the percentage of water increases up to 10 % in the mixture as can be seen in Figures 20.3 and 20.4.

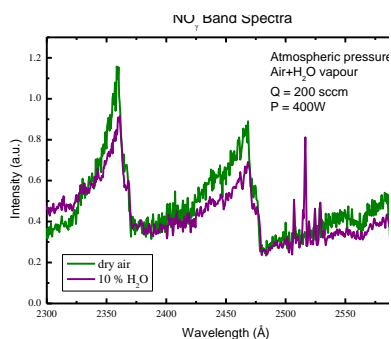


Figure 20.3 - NO(γ) spectra for various water percentages

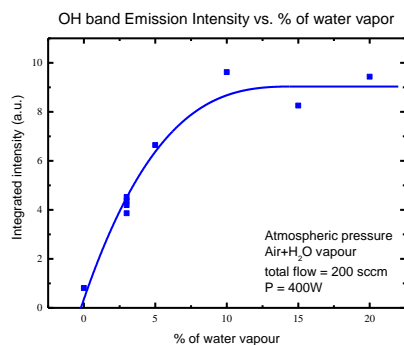


Figure 20.4 - OH intensity vs water percentage

The measured axial variations of the wave axial wavenumber (β) and attenuation coefficients (α) are in agreement with the theoretical axial variation of the dispersion characteristics of an azimuthally symmetric surface mode (Figures 20.5 and 20.6). Thus, the generated plasma torches are surface waves driven plasmas.

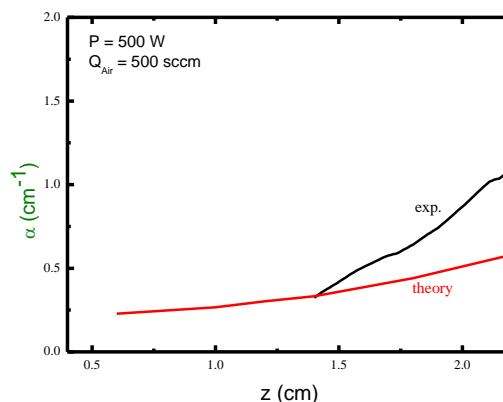


Figure 20.5 - Attenuation coefficient vs axial distance

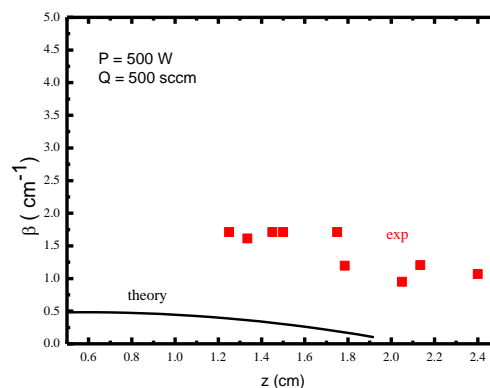


Figure 20.6 - Axial wavenumber vs axial distance

Furthermore, the spatial structure of an N₂ (80%) – Ar (18%) – H₂ (2%) plasma torch driven by an azimuthally symmetric surface mode (2.45 GHz) has been investigated by 2D imaging measurements. To this end, a spectroscopic imaging system able to couple the plasma-emitted radiation into a SPEX 1250M spectrometer, equipped with a nitrogen cooled CCD camera, was used to measure $2D(r, z)$ profiles of emission intensities and line profile parameters (Figure 20.7). Abel inversion has been applied to translate the side-on measurements into true radial profiles.

An analysis of the H β line main broadening mechanisms was performed. The measured Balmer line profiles have been fitted by a Voigt function, which results from the convolution of a Gaussian profile (due to Doppler and instrumental broadening) with a Lorentzian

one (due to Stark and van der Waals broadening). A GRAMS/32[®] software has been used to this end. Therefore, the Lorentzian ($\Delta\lambda_L$) and Gaussian ($\Delta\lambda_G$) full widths at half maximum have been separated. The resulting H_β Gaussian profile was employed to evaluate translational temperatures assuming a Maxwellian distribution. The measured atomic temperature reaches values up to 8000 K at the torch axis close to the launcher (Figure 20.8). The results demonstrate a strong radial gradient of the atomic temperature, which decreases to about (1000 K) close to the walls near the plasma column end. Gas temperatures were estimated from OH rotational emission bands in the 300-310 nm range. The radially averaged values of the gas temperature vary from about 3500 to about 1000 K close to the plasma torch end. Thus, *superthermal* hydrogen atoms with temperatures as high as twice the gas temperature have been detected. The hot H atoms may be created from reactions involving H^+ , H_2^+ , H_3^+ in H_2 or in Ar. The measured electron densities are in the range 10^{14} cm^{-3} close to the launcher and decrease to about 10^{13} cm^{-3} in the post discharge zone of the plasma torch (Figure 20.9).

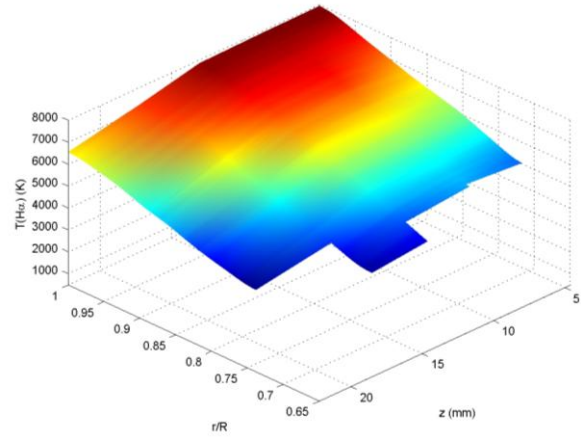


Figure 20.8 - 2D profile of H atom temperature

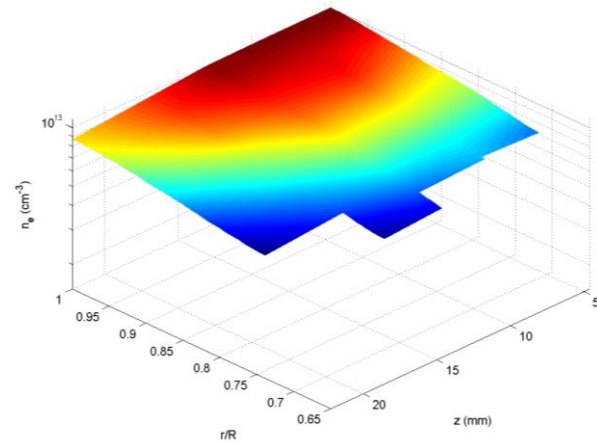


Figure 20.9 - 2D profile of electron density

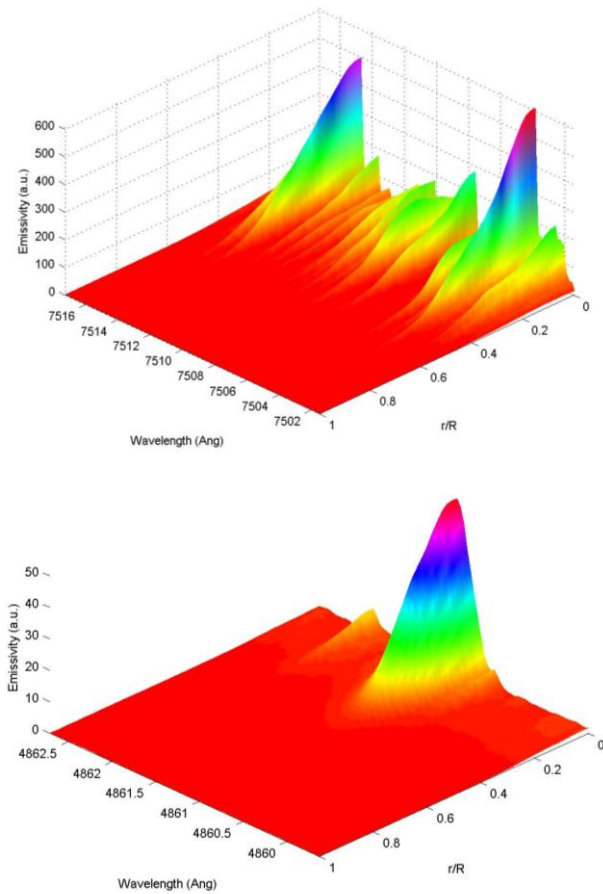


Figure 20.7 - Radially resolved profiles of Ar, N and H atomic lines at $z = 4 \text{ cm}$ (N_2 -Ar- H_2).

20.3. EXTRAORDINARY PHENOMENA IN HYDROGEN PLASMAS

Selective hydrogen line broadening has been detected when there is no significant broadening of noble gas lines or hydrogen molecular lines in a number of plasmas excited via DC, RF or microwave electric fields. In this context, we conducted an experimental study on the spectral broadening of the hydrogen Balmer lines in hydrogen and H_2 -Ar microwave plasmas at low pressure conditions ($p = 0.01 - 0.35 \text{ mbar}$). A surface wave sustained discharge operating at 500 MHz has been used as a plasma source. This plasma source has been chosen in order to avoid Stark effect influence (i.e., lower electric field intensities and electron densities than those occurring in 2.45 GHz discharges under the same operational conditions). The spectral profiles of the H_α , H_β , H_γ , H_δ , H_ϵ , lines, corresponding to the transitions $H [(n=3-8) \rightarrow (n=2)]$ in the 350 – 700 nm range, have been measured. At low-pressure, the Balmer profiles exhibit a bi-Gaussian structure (Figure 20.10), indicating the presence of *super hot* excited H atoms with energy higher

than 4.5 eV. The shape of the profiles changes to single Gaussian with increasing pressure ($p = 0.2$ mbar), the

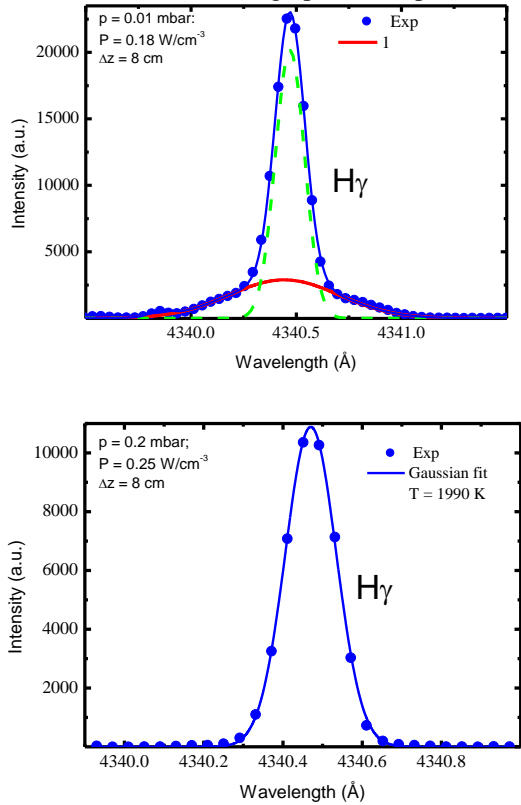


Figure 20.10 - Changes of $H\gamma$ profile with pressure.

corresponding temperature being about 2000 K. The rotational temperature corresponding to the Q-branch of the Fulcher- α band rotational spectrum [$d^3\Pi_u(v=0) \rightarrow a^3\Sigma_g^+(v=0)$], in the 600 – 610 nm wavelength range, has been determined as a measure of the background gas temperature. It varies between 400 and 600 K under the present conditions. Notably, at low

pressure conditions excited hydrogen atoms are hot, with a kinetic temperature greater than the background gas temperature. Two different mechanisms leading to generation of *super hot* and *warm* excited H atoms have been considered, viz. acceleration of H^+ ions in the radial potential well and recombination processes. Moreover, a weird behavior of excited H atoms is observed. The temperature of hydrogen atoms increases as the upper level quantum number increases in pure hydrogen, i.e., atoms at higher electronic levels are hotter. This effect deserves further investigation.

20.4. IMPROVEMENT OF PLASMA DIAGNOSTIC TECHNIQUES

In order to improve the measurements of the emission lines and to obtain 2D resolution a new telecentric imaging optical system has been developed (Figure 20.11).

The new imaging system is able to couple the plasma-emitted radiation into a SPEX 1250M spectrometer equipped with a nitrogen cooled CCD camera. The above system includes: i) an objective lens with a 3:1 ratio, which matches the plasma and the fibre sizes; ii) an imaging optical fibre, which rotates the image by 90 degrees; iii) an 1:1 inverse-telecentric lens, which effectively couples light into the input slit of the spectrometer and ensures the most possible uniform spatial response. The above inverse-telecentric arrangement is made possible using an iris at an appropriate position. The optical system was designed using a high resolution, flexible Schott optical fibre (model IG-567-36) made of 10 micron individual fibres with an extended UV transmission. The cryogenic, back-illuminated UV sensitive CCD camera has a 2048 x 512 matrix, with 13.5 micron pixel-sizes, and provides high spatial and spectral resolutions.

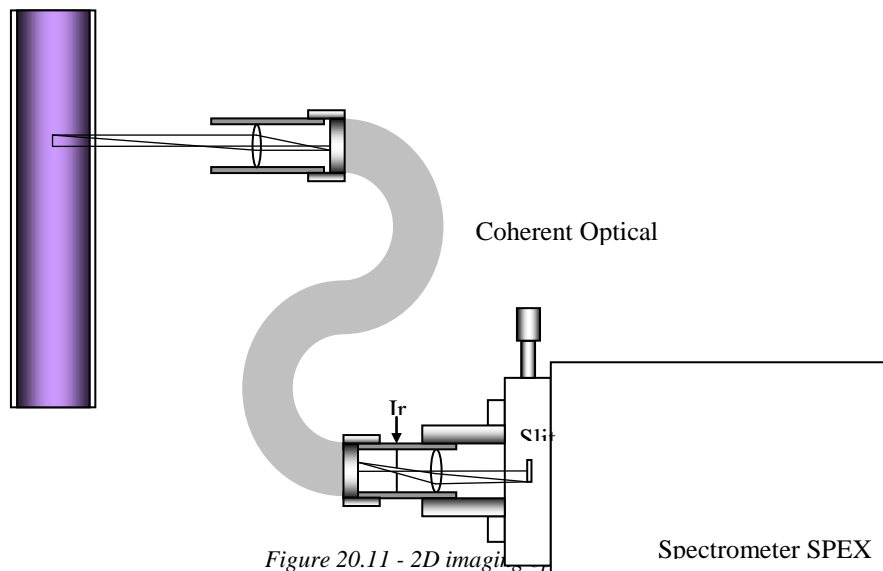


Figure 20.11 - 2D imaging

21. NON-EQUILIBRIUM KINETICS AND SIMULATIONS OF PLASMAS AND AFTERGLOW PLASMAS¹

C.M. Ferreira (Head), J. Loureiro (Principal Investigator), V. Guerra, P.A. Sá, C.D. Pintassilgo, M. Lino da Silva and K. Kutasi.

21.1. INTRODUCTION

The research work carried out in 2008 falls into the following main lines of investigation:

- Modelling of fundamental kinetic and radiative processes in low-pressure, high temperature plasmas;
- Study of N₂-O₂ afterglow plasmas for plasma sterilization of thermosensitive medical instruments;
- Study of Ar-O₂ afterglow plasmas for plasma sterilization and insight into elementary processes;
- Simulation of surface atomic recombination;
- Kinetic modelling of low-pressure dc discharges in air;
- Study of N₂-O₂ post-discharges when oxygen is added downstream a pure nitrogen microwave discharge;
- Simulation of Titan's atmosphere using a N₂ afterglow plasma with CH₄ addition in the post-discharge;

21.2. MODELLING OF FUNDAMENTAL KINETIC AND RADIATIVE PROCESSES IN LOW-PRESSURE, HIGH TEMPERATURE PLASMAS

The modelling of fundamental kinetic and radiative processes at high temperatures ($T > 10,000$ K) is a topic of renewed interest, driven by applications such as the simulation of plasma processes during spacecraft high-speed entries (5–10 km/s). Such kind of plasmas are created through heavy particle-impact reactions, downstream from a strong shockwave which converts the flow coherent energy (drift velocity) into random energy (species translational mode), for temperatures $T = 10,000$ – $100,000$ K. Such high temperatures favor dissociation, ionization and radiation processes, which in turn will influence the heat fluxes whistanded by the spacecraft thermal protections.

Our research group has been developing models and approaches for the simulation of collisional-radiative processes in such high-temperature ranges. Arising theoretical issues have also been addressed, helping to clarify the elementary physics of energy transfer processes among the internal modes of atoms and molecules.

21.2.1. Kinetic processes

The research undertaken has been initiated with the application of the Forced Harmonic Oscillator (FHO) theory to yield transition rates valid for higher collision velocities and transition rates for arbitrary multiquantum transition, unlike First-Order Perturbation Theory (FOPT) models, which only yield single-quantum rates. In the

preceding years, accurate datasets have been produced and validated for nitrogen. In 2008, we have additionally investigated the inclusion of rotational effects to improve the accuracy of such models, and we have discussed the concept of detailed balance for yielding accurate transfer rates for backward (recombination) processes.

21.2.2. Modelling of Translation-Rotation exchange processes

A model describing the translational-rotational exchanges in N₂ has been developed. The overall manifold of rotational and vibrational levels of N₂ has been calculated using the Rydberg-Klein-Rees (RKR) method to yield accurate molecular potentials. The energies for the corresponding rovibrational levels have been then calculated by solving the radial Schrödinger equation. The solutions so obtained allow for the existence of quasi-bound states, i.e. for states that can spontaneously dissociate through quantum tunnelling. The overall bound and quasi-bound states have been obtained using a potential reconstruction method.

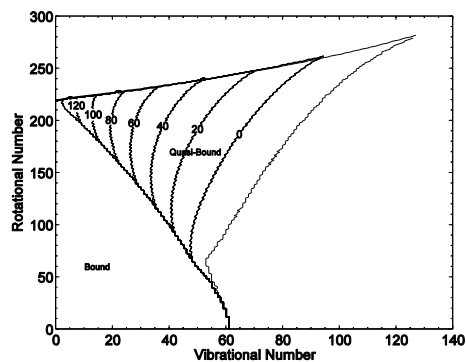


Figure 21.1 - Predicted bound and quasi-bound levels for N₂(X). The contour plot of the lifetimes (in log units) are reported for the quasi-bound states.

The large number of existing rotational states renders an explicit state-to-state calculation impractical, and it is customary to consider that the low energy spacing of such levels allows them to follow an internal rotational equilibrium at a characteristic rotational temperature T_r . Accordingly, T–R processes are calculated using the Landau-Teller equation with an effective collision number

¹Activities performed in the frame of the Contract of Associated Laboratory, out of the Contract of Association EURATOM/IST, by IPFN staff of the Group of Gas Discharges and Gaseous Electronics.

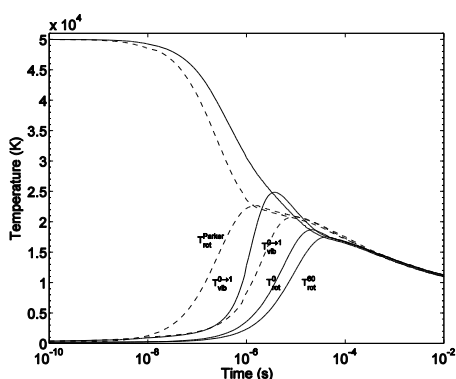


Figure 21.2 - Relaxation behind a Shockwave at 50,000K in the typical conditions of an Earth re-entry. Dashed lines show the temperatures calculated using the Parker rotational relaxation number. Full lines show the temperatures calculated using our calculated rotational relaxation number

Zr, except that the calculation is carried with our more precise manifold of rovibrational levels, and that a different Zr is calculated for each vibrational level. Traditional state-to-state models (accounting solely for vibrational and electronic modes) can then be updated utilizing such vibronically specific T-R weighted rates.

21.2.3. Modeling of recombination processes

The validity of using state-to-state three-body recombination rate coefficients obtained throughout the detailed balance has been investigated under non-equilibrium conditions. In basic trends, the state-to-state equilibrium dissociation-recombination rates, as well as the recombination rate coefficients, obtained for a situation of thermodynamic equilibrium remain valid under non-equilibrium conditions provided the translational modes of different species are given by Maxwellian distributions at a common temperature T . On the contrary, the total weighted dissociation rates depend on the distribution of molecules along the vibrational manifold so that the rates calculated in equilibrium cannot be obviously used out of equilibrium. However, this is not the case of the total weighted recombination rates where once again they depend only of the temperature of the translational mode. Based on actual data for V-V-T and V-T rates in N_2 , the magnitude of the total dissociation and recombination rates has been evaluated for typical conditions of both high (shock-heated flows) and low translational temperatures (gas discharges). Whereas at high temperatures the V-V and V-T mechanisms fully determine the dissociation-recombination balance, at moderate and low temperatures, typical of an electrical discharge, the dissociation and recombination processes preferentially populate the upper electronic states with energies close to the ground-state dissociation limit - $N_2(B)$ and $N_2(a)$ - rather than the electronic ground state.

21.2.4. Radiative processes

Investigations on radiative processes have proceeded in the scope of the programs defined in the latest years, with a major focus on the update and application of CO_2 radiation databases. The Line-by-Line code SPARTAN has also been applied to the simulation of the radiative tail of the NASA PHOENIX spacecraft, during its entry in Mars atmosphere, in a collaborative effort with the European Space Agency (ESA) who tracked the spacecraft entry with the MARS EXPRESS spacecraft, orbiting Mars.

21.2.5. Development of an updated CO_2 radiative database

Several improvements for the Line-by-Line modeling of CO_2 radiation have been carried out. Firstly, a theoretical model for the simulation of CO_2 chemiluminescence radiation, which results from the transition from an electronic bent state of CO_2 to the ground linear state of CO_2 , has been investigated. Radiative features from this system are found in the 300–700 nm spectral region, and although not dominant they are sufficiently ubiquitous to warrant their inclusion in N_2 complete radiative models for CO_2-N_2 plasmas. Secondly, the non-equilibrium spectral database for the calculation of Infrared CO_2 in the SPARTAN code has been updated. Departing from the CDS database, which provides accurate data for high-temperature CO_2 radiation, a more general database, allowing the simulation of non-equilibrium radiation (with different vibrational and rotational temperatures) has been produced.

21.2.6. Support to Mars exploration missions

Tracking of the PHOENIX spacecraft Martian Entry

The past 25th of May, the PHOENIX spacecraft successfully entered Mars atmosphere. In a collaborative effort, it was decided to track the PHOENIX entry with the Mars EXPRESS onboard cameras, thanks to a change of orbit. Prior to this, a Computational Fluid Radiative Dynamics simulation of the PHOENIX atmospheric entry has been carried out in order to predict the intensity, wavelength, spatial length, and timeline of the PHOENIX radiative plume.

CFD simulations were carried with a Monte-Carlo numerical code, for the 5 more critical entry points, and radiation was calculated over the whole VUV-IR range, including radiation from CO_2 , accounting for thermal nonequilibrium.

This allowed predicting which Mars EXPRESS instruments were likely to detect any radiation from the PHOENIX entry. Although no radiation was actually detected by the Mars EXPRESS orbiter, such calculations also provide an upper limit for the radiative intensity of the PHOENIX radiative plume.

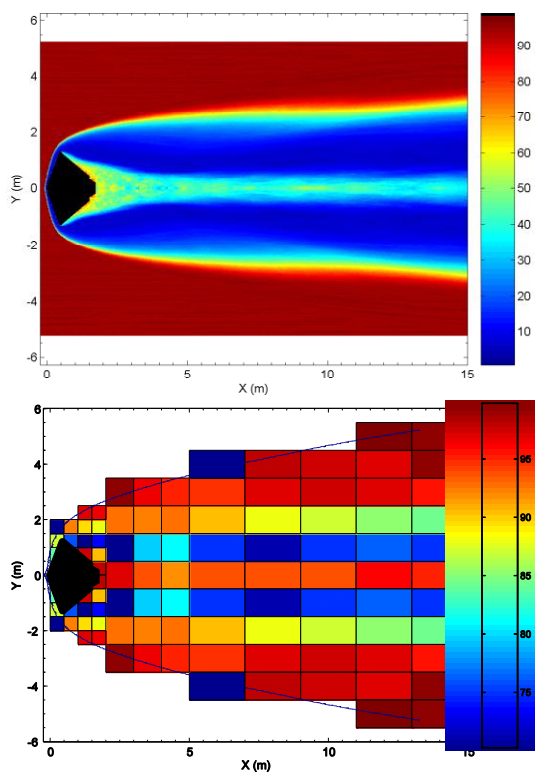


Figure 21.3 - CO_2 molar fraction (in %) of the flow around the PHOENIX spacecraft at $t = 223$ s (top), and contribution from CO_2 radiation to the overall plume radiative intensity (bottom)

21.3. STUDY OF $\text{N}_2\text{-O}_2$ AFTERGLOW PLASMAS FOR PLASMA STERILIZATION OF THERMOSENSITIVE MEDICAL INSTRUMENTS

In the last decade the use of polymer based heat sensitive tools in the medical praxis or pharmaceutical industry have brought the need of new low temperature sterilization and decontamination methods, which ensure complete inactivation or removal of all possible infectious microorganism: e.g. bacterial spores, viruses, or other potentially harmful biological residuals: e.g. endotoxins and proteins present on the used instruments. For the heat sensitive medical devices the most common sterilization methods in use are based on chemical treatment, which imply toxic active agents, or exposure to ionizing radiation, which may alter the bulk properties of polymers being sterilized. A new method, which overcomes these drawbacks, implies the use of low-temperature plasmas.

The investigations on this topic have been pursued in collaboration with the group of Plasma Physics in the Physics Department of the University of Montreal (Canada). Since previous investigations have demonstrated that almost total inactivation of *Bacillus Subtilis* spores may be achieved through a conjoint action of UV photons emitted by NO(A) and NO(B) states and O-atoms, the investigations have been focussed now on the role played by these two emitting NO-states.

Within this aim a post-discharge reactor placed

downstream from a $\text{N}_2\text{-O}_2$ flowing microwave discharge has been studied by modelling. The model for the discharge and early afterglow is constituted by a 1-D kinetic model for the species coupled to the electron Boltzmann equation, while the species distributions on the reactor are followed with a 3-D hydrodynamic model. The latter is composed of equations for the total mass conservation, momentum conservation, energy conservation and species continuity. The calculations have been performed for different discharge conditions by varying the discharge tube radius, excitation field frequency, total gas pressure and initial gas mixture composition. These calculations make possible to choose optimal conditions from the application point of view. For plasma sterilization in a $\text{N}_2\text{-O}_2$ system the important species are the O atoms and the UV emitting molecules NO(A) and NO(B).

Figure 21.4 shows the density of UV emitting molecules at the end of discharge column as a function of O_2 percentage at 2 Torr and 2.45 GHz. The densities of these two molecules behave similarly with the O_2 percentage, however the NO(B) density is about three orders of magnitude lower than that of NO(A). This difference occurs since they are populated by different processes. Whereas the NO(A) state is exclusively populated through $\text{N}_2(\text{A}) + \text{NO}(\text{X}) \rightarrow \text{NO} + \text{NO}(\text{A})$, the production of NO(B) takes place via the three-body mechanism $\text{N}(\text{S}) + \text{O} + \text{N}_2(\text{O}_2) \rightarrow \text{NO}(\text{B}) + \text{N}_2(\text{O}_2)$. Moreover, whereas the destruction of NO(A) occurs by radiative decay to NO(X), responsible for the emission of UV bands of NO γ system, and by quenching with O_2 and NO(X), whose contribution increases with pressure and O_2 percentage, the NO(B) is exclusively lost by radiative transfer, responsible for the emission of NO β system. Figure 21.5 shows the evolution of NO(A) and NO(B) densities in the early-afterglow as they fly through it. While in the discharge the NO(A) molecule dominates, in the afterglow the NO(A) density rapidly decreases to a lower value than NO(B). This decrease is explained by the reduction of $\text{N}_2(\text{A})$ state density along the early-afterglow. The model makes possible to determine the optimal length of the early-afterglow, which ensures that no ions and metastables, which are believed to induce damage to the materials to be sterilized enter the reactor. Meanwhile the densities of sterilizing agents do not decrease considerably. As long as the species enter the reactor their densities are also determined by the gas flow. The calculations have shown that the density distributions of species in the reactor become more homogeneous with decreasing pressure and increasing gas flow rate. Figure 21.6 shows the density distribution of NO(A) in the x - z plane at $y = 150$ mm in the reactor chamber at 1000 sccm N_2 and 8 sccm of O_2 gas flow rate at 2 Torr. At these conditions the NO(A) density decreases with about a factor of 2 from the entrance to the bottom wall allowing hence to obtain a quasi-homogeneous distribution. The distribution of the NO(A) density is mainly influenced by the N atoms density through the NO(A) creation process, since the O-

atoms density distribution is practically constant along the reactor.

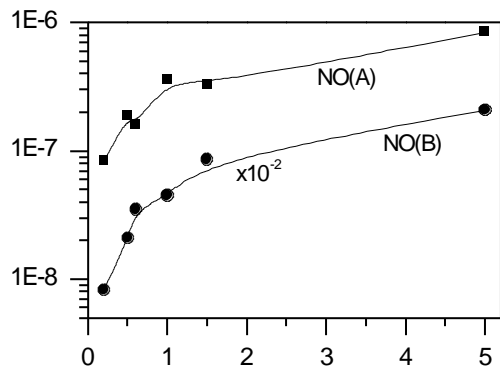


Figure 21.4 - Calculated NO(A) and NO(B) densities (relative to gas density) at the end of the discharge column as a function of O_2 percentage added to N_2 at 2 Torr and 2.45 GHz.

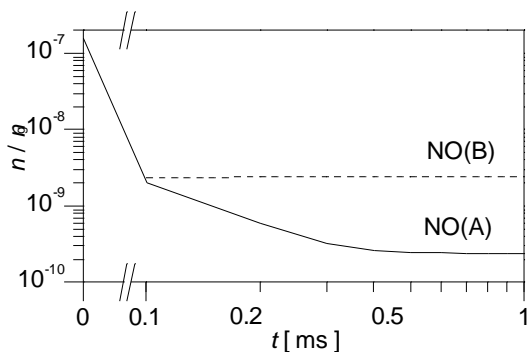


Figure 21.5 - Calculated densities of UV emitting molecules as a function of the species flight-time in the early afterglow region in the same conditions as in Figure 19.4.

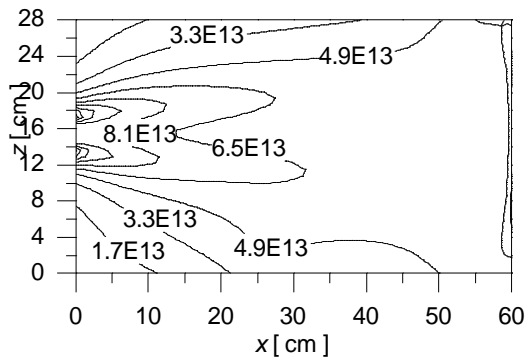


Figure 21.6 - Calculated density distributions of NO(A) in the x - z plane at $y = 150$ mm in the reactor chamber at 1000 sccm N_2 and 8 sccm of O_2 gas flow rate at 2 Torr.

21.4. STUDY OF AR- O_2 AFTERGLOW PLASMAS FOR PLASMA STERILIZATION AND INSIGHT INTO ELEMENTARY PROCESSES

Studies on the Ar- O_2 system have also been initiated for plasma sterilization purposes and for an insight in the understanding of elementary kinetics processes. Here, the species with importance for sterilization are the VUV emitting resonant states of Ar atoms and the O atoms. Our study has shown that the resonant and metastable Ar(4s) states are quickly depleted in the early-afterglow region. As a matter of fact, they are very effectively quenched by O atoms via $Ar(4s)+O \rightarrow Ar(^1S_0)+O$ reaction and by O_2 molecules through $Ar(4s)+O_2 \rightarrow Ar(^1S_0)+O+O$. Another relevant aspect is that O_2 is strongly dissociated, both by electron impact with $O_2(X,a,b)$ states and by Ar(4s) atoms, being the latter contribution of about 15% to the total dissociation rate. The results of the hydrodynamic model have shown that the metastable and resonant states of Ar are almost totally depopulated in the vicinity of the reactor's entrance. This result suggests that, contrary to earlier suppositions, the Ar resonant states cannot contribute to the VUV/UV emission in the reactor. At 2 Torr the O atoms density in the reactor decreases from the entrance towards the walls for about one order of magnitude. The loss of O atoms is due to surface recombination. A more homogeneous density distribution, which is more favorable for applications, can be achieved using Pyrex reactors, in which the atomic recombination on the surface is less efficient.

21.5. SIMULATION OF SURFACE ATOMIC RECOMBINATION

A dynamical Monte Carlo method to study heterogeneous recombination has been developed. The kinetic scheme comprises physisorption, thermal desorption from physisorption sites, chemisorption, Eley-Rideal recombination, surface diffusion of physisorbed atoms and Langmuir-Hinshelwood recombination. The efficiency of the algorithm and schemes to reduce statistical fluctuation were studied at first. It was found the efficiency and accuracy of the method can be improved by averaging on several realizations of the system. The effect of collisions between physisorbed atoms, often neglected in recombination studies, was subsequently investigated. The results were compared with experimental data and with the calculations from a mean-field model previously developed, which does not take into account these effects. It was shown these collisions can be important at high coverage of physisorption sites, in case they lead to recombination. However, it was shown this is unlikely for the case of nitrogen recombination in silica.

21.6. KINETIC MODELLING OF LOW-PRESSURE DC DISCHARGES IN AIR²

We have developed a time-dependent kinetic model to study low-pressure (133 Pa and 210 Pa) pulsed discharges

²Joint work with of Laboratoire de Physique et Technologie des Plasmas (LPTP), Ecole Polytechnique, France. Contact Person : Dr. Antoine Rousseau.

in air for DC currents ranging from 20 to 80 mA with a pulse duration from 0.1 up to 1000 ms. The model provides the temporal evolution of the heavy species along the pulse within this range time, where the coupling between vibrational and chemical kinetics is taken into account. The present work shows that the predicted values for NO(X) molecules and O(³P) atoms reproduce well previous measured data at the *Laboratoire de Physique et Technologie des Plasmas, École Polytechnique* for the absolute concentration of these two species, obtained, respectively, during a plasma pulse using time resolved tunable diode laser absorption spectroscopy in the infrared region and by using time resolved measurements by actinometry.

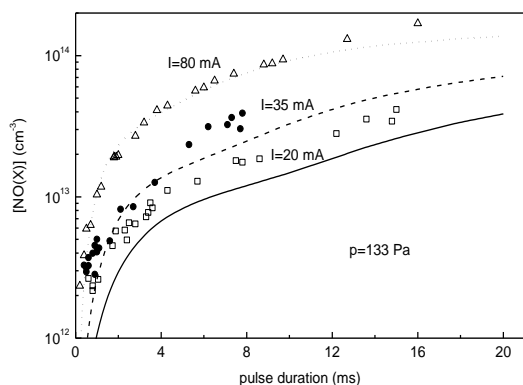


Figure 21.7 - $[NO(X)]$ as a function of the pulse duration of a N_2 -20% O_2 discharge with $p=133$ Pa and for the following currents: 20 mA (full curves, \square); 35 mA (dashed curves, \bullet) and 80 mA (dotted curves, Δ). The curves are the results of our calculations, whereas the symbols correspond to experimental data.

21.7. STUDY OF N_2 - O_2 POST-DISCHARGES WHEN OXYGEN IS ADDED DOWNSTREAM A PURE NITROGEN MICROWAVE DISCHARGE³

With the purpose to better understand the role of homogeneous reactions in N_2 - O_2 mixtures, we have been working with colleagues from Masaryk University, Brno, Czech Republic, that have developed an experimental set-up where oxygen is added downstream from a pure nitrogen microwave discharge via a capillary. By using electron paramagnetic resonance, it was observed that the absolute concentration of atomic nitrogen was measured for several gas pressures.

In order to understand this behaviour, we have considered a detailed model of the kinetic processes, in which the discharge region is described by the self-consistent determination of the active species concentrations for pure N_2 , considering the Boltzmann's equation for the electrons coupled to a set of rate balance

equations for the various molecular and atomic species produced in the discharge. Once the concentrations of the various neutral and ionic species at the end of the discharge are obtained, the relaxation of the most populated heavy species is studied in the afterglow by considering a system of coupled time-varying kinetic master equations, where the electron impact processes are neglected. This is done in two steps: first we calculate the heavy species concentrations in the near afterglow in which only N_2 exists; then we consider the introduction of a small oxygen percentage into the post-discharge, at different distances downstream from the end of the discharge, depending on the gas flow.

21.8. SIMULATION OF TITAN'S ATMOSPHERE USING A N_2 AFTERGLOW PLASMA WITH CH_4 ADDITION IN THE POST-DISCHARGE

This study involves a new perspective for the simulation of Titan's atmosphere, which consists in considering an afterglow instead of a discharge plasma in N_2 - CH_4 mixtures, which are commonly recognized to be an important tool in laboratory simulation of Titan's atmosphere. However, in these systems the electrons play a central role in determining the overall heavy species abundance, which is not the case of Titan's stratosphere and troposphere, where the electrons play only a minor role. Moreover, the typical temperature values in gas discharges have the order of 500-1000 K, whereas in the case of Titan's atmosphere the temperature is extremely lower.

With these facts in mind, we have developed a kinetic model to simulate the afterglow of a flowing N_2 microwave discharge operating in the range 26.6-106.4 Pa, in which the methane is introduced downstream from the discharge with 2% percentage at 10^{-5} - 10^{-3} s. This pressure range corresponds to Titan's stratosphere, at altitudes 250-180 km, in which the contribution of electron processes is negligibly small. In this study, the CH_4 is primarily dissociated in CH_3 and CH_2 in the post-discharge, due to collisions with the metastable $N_2(A)$, and the most populated species from methane dissociation are then formed.

The self-consistent kinetic model used for the microwave discharge is based on the coupled solutions for the electron Boltzmann equation and a set of rate balance equations for the populations of the various neutral and charged heavy species. Once the stationary concentrations are obtained the post-discharge is considered by cutting off the excitation by electron impact in the system of master equations for the species. CH_4 is then introduced with 2% percentage at 10^{-2} -1 ms.

³Joint work with Masaryk University, Brno, Czech Republic.

22. MODELING OF PLASMA SOURCES¹

C. M. Ferreira (Head), L.L. Alves (Principal Investigator), R. Álvarez, L. Marques, C. Pintassilgo, J. Gregório, and J.S. Sousa.

22.1. INTRODUCTION

This project has focused on the modeling of different plasma sources, used in various applications (mainly with material processing and environmental control). The general goal was the development of sophisticated simulation tools describing the operation of these sources, in view of their optimization. The research work in this field studied the following devices:

- Microwave-driven plasma reactor operated by an axial injection torch;
- Micro-plasma reactors;
- Capacitively coupled plasma reactors;
- Surface-wave plasma reactors.

22.2. MICROWAVE-DRIVEN PLASMA REACTOR OPERATED BY AN AXIAL INJECTION TORCH²

We have continued the study of a microwave-driven (2.45 GHz) plasma reactor (cylindrical chamber with 55mm radius and 150mm height), operated by an Axial Injection Torch³ (Figure 22.1), used for the destruction of industrial sub-products (VOC's and BEXT aromatic hydrocarbons). The torch (connected to a coaxial waveguide with 5.3mm and 14.5mm inner and outer radii, respectively) creates atmospheric plasmas in different pure gases (argon, helium, nitrogen) or gas mixtures (e.g. air), over a wide range of powers (300–3000W) and flow-rates (0.5–13 L min⁻¹), producing very hot flows of plasma species (electron temperatures around 20000K and gas temperatures between 2000–6000K).



Figure 22.1 - Plasma reactor operated by the axial injection torch

We have concluded the development of a hydrodynamic model for the gas-plasma flowing system (including its thermal description), yielding the two-dimensional distribution of mass density, pressure, velocities (Figure 22.2), and temperature (Figure 22.3).

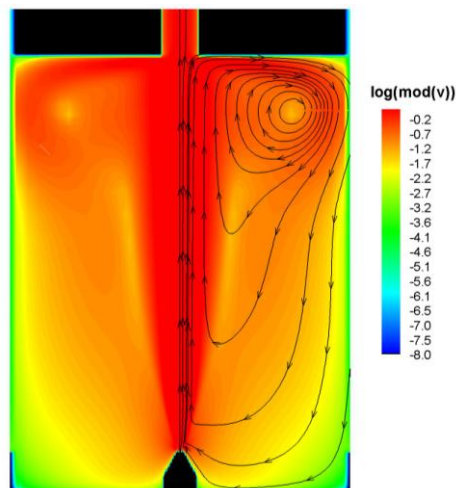


Figure 22.2 - Contour-plot of the logarithm of the modulus of the total velocity (normalized to its maximum value), for the AIT-reactor system at an input gas flow of 10³ sccm. The colour gradients in background are for the velocity modulus, whereas the streamlines are for its direction

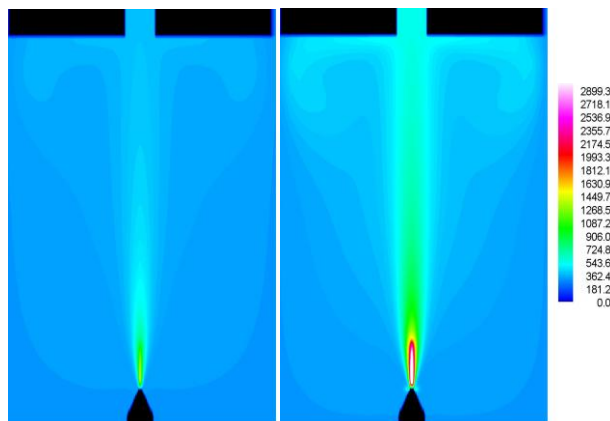


Figure 22.3 - Contour-plots of the gas temperature for the AIT-reactor system at 10³ sccm input gas flow, 300 K wall temperature, and the following maximum values of the electron density (in 10¹⁴ cm⁻³): 1 (left), 20 (right).

¹Activities performed in the frame of the Contract of Associated Laboratory, out of the Contract of Association EURATOM/IST, by IPFN staff of the Group of Gas Discharges and Gaseous Electronics.

²Work supported by FCT (Scholarship BPD/26420/2005 and Project PTDC/FIS/65924/2006) and Spanish MEC (Project CTQ2005-04974/PPQ), performed in collaboration with M.C. Quintero and A. Rodero (Departamento de Física, Universidad de Córdoba, Spain).

³AIT. Spanish patents P200201328 and P200302980.

The model solves the Navier-Stokes transport equations (mass, pressure and energy, the latter including the influence of plasma in gas heating, due to electron-neutral collisions), which are discretized onto two-dimensional staggered cell-centered grids, by using a finite volume method based on surface integrals. The equations are solved using an algorithm Semi-Implicit Method for Pressure-Linked Equation (SIMPLE) algorithm. Simulations used an input surface (about 1% of the output surface) with a radius of 0.5 mm, and were carried out in helium at atmospheric pressure, for input gas flows in the range 100-10000 sccm.

Simulations, which are highly dependent on the input flux, yield: (i) an interaction between the flowing gas and the reactor upper wall, which creates a re-circulation pattern inside the reactor (Figure 22.2); (ii) a hollow spatial distribution (in both axial and radial directions) of the gas temperature near the nozzle's tip, whose depth relates to the energy relaxation length with the plasma-gas heat transfer; (iii) a variation of the gas temperature distribution with the electron density (Figure 22.3), the wall temperature, and the input gas flow. A good agreement was found between simulations results and experimental measurements for the gas temperature profile (Figure 22.4).

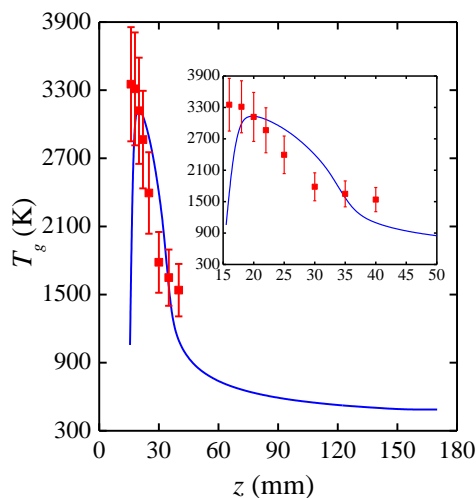


Figure 22.4 - Gas temperature axial distribution (at $r = 0$) at 10^3 sccm input gas flow, 300 K wall temperature, and 10^{15} cm^{-3} maximum electron density. The points are experimental results (divided by a factor of 1.3 for representation purposes), obtained at 600 W incident power. The inset is just a zoom of this figure over the plasma region.

22.3. MICRO-PLASMA REACTORS⁴

We have continued the study of atmospheric pressure micro-plasmas, created by electric discharges in very small

geometries (100's μm) without glow to arc transition, in view of developing portable devices for flue gas treatment, biological decontamination or detection of heavy metal gaseous traces, in ambient air or aerosols.

22.3.1. Microwave Micro-Plasma (MWMP) source⁵

We have pursued the study of an innovative plasma source for the production of atmospheric pressure micro-plasmas, in view of environmental applications. The device produces high-density ($>10^{15}$ cm^{-3}), low-power (~ 10 W) plasmas in ambient air or in controlled environments (argon, xenon, nitrogen, oxygen,.) within the 100-300 μm end-gap of a microwave (2.45GHz) micro-strip, by using a continuous wave excitation (thus guaranteeing a steady-state discharge regime).

We concluded the design and construction of (i) version-2 with the device (Figure 22.5), which features a reduction in both reactor dimensions (10 cm x 6 cm) and plasma size (6 mm wide and 50-200 μm between the blades), aiming portability and a reduction in power consumption; (ii) a system that allows to operate the MWMP source in controlled atmospheres (Ar, He, N₂, ...), at atmospheric pressure.



Figure 22.5 - Version-2 of the MWMP source

The MWMPs produced with this source in ambient air and in argon (Figure 22.6) were characterized by (i) electrical diagnostics of the power reflection coefficient, as a function of gap size and transmission line length (with and without plasma), and as a function of the incident power P_{inc} (with plasma); (ii) spatially-resolved emission spectroscopy measurements, to obtain translational temperatures $T_g \sim 900$ -1400 K and vibrational temperatures $T_{\text{vib}} \sim 4200$ -5000 K in air (via a spectral analysis of the rotational and the vibrational bands of nitrogen, respectively), translational temperatures $T_g \sim 550$ -700 K in argon (via a spectral analysis of the rotational band of OH), excitation temperatures between 0.45-0.56 eV in argon (measured from the Boltzmann plot of Ar emission lines), and electron densities between 10^{13} - 4×10^{13} cm^{-3} (measured by Stark broadening of the H β emission profile, Figure 22.7). In air, measurements were

⁴Work performed in collaboration with C. Boisse-Laporte and V. Puech (Laboratoire de Physique des Gaz et des Plasmas, Orsay, France) and L. Pitchford (Laboratoire Plasmas et Conversion d'Énergie, Toulouse, France).

⁵Work performed in the frame of the PhD thesis of J. Gregório and supported by FCT (Scholarship SFRH/29294/2006 and Project PTDC/FIS/65924/2006).

made for gap sizes between 50-100 μm at $P_{\text{inc}} \sim 37\text{-}55\text{ W}$, whereas in argon they were made for gap sizes between 50-200 μm at $P_{\text{inc}} \sim 9\text{-}14\text{ W}$.

We have also developed a one-dimensional stationary fluid code, to perform systematic simulations of the MWMPs produced, as a function of the axis electron density, gap size, and gas temperature (Figure 22.8). The following calculation modules compose the numerical code:

- Charged particle transport module, solving the continuity and momentum equations for electrons and Ar^+ , Ar_2^+ ions, the electron mean energy transport equations, and Poisson's equation for the space charge electrostatic field.
- Electromagnetic module, solving Maxwell's equations for the microwave field (or, alternatively, the plasma dispersion equation).
- Kinetic module for argon, solving the balance equation for the 4s levels as well as the electron Boltzmann equation, written under the homogeneous and stationary two-term approximation.

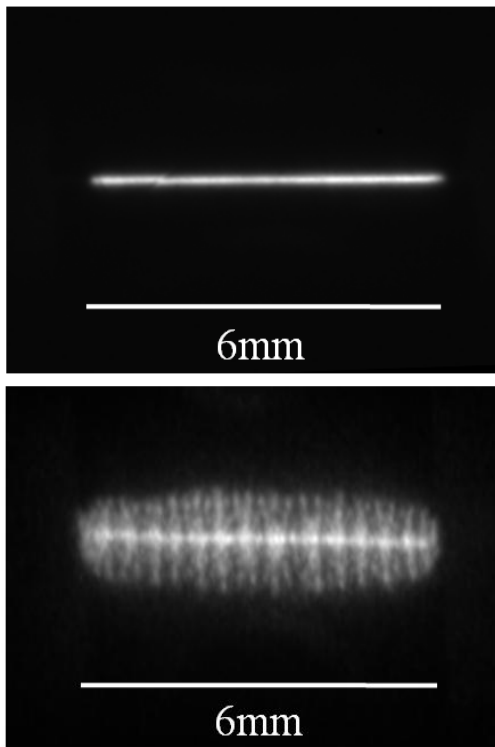


Figure 22.6 - Atmospheric pressure MWMPs in air (top, at 50 mm gap size and 31 W coupled power), and in argon (down, at 50 mm gap size and 12 W coupled power)

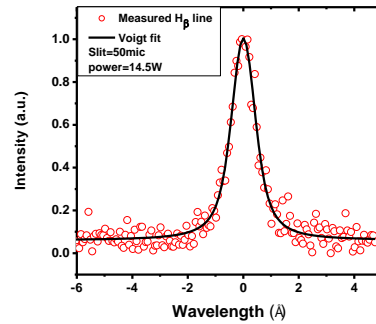


Figure 22.7 - H_{β} line in atmospheric pressure argon at 50 mm gap size and 14.5 W coupled power

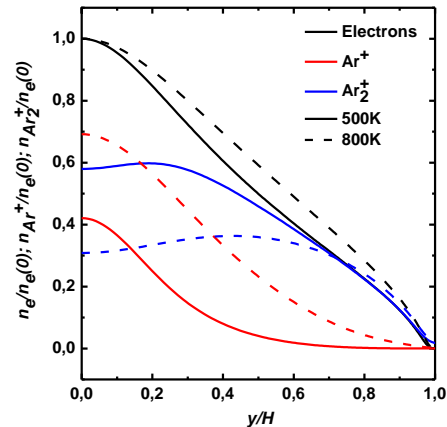


Figure 22.8 - Calculated particle density axial distributions for electrons (black), Ar^+ (red) and Ar_2^+ (blue). Simulations were made in argon at atmospheric pressure at $n_{e0} = 10^{14}\text{ cm}^{-3}$ and $H=50\text{ }\mu\text{m}$ gap size, for gas temperatures of 500K (solid line) and 800K (dashed line).

22.3.2. Micro-Cathode Sustained Discharge (MCSD)⁶

We have carried on the systematic study of a micro-discharge reactor, which uses a micro-hollow cathode discharge (MHCD), running in rare gas/oxygen mixtures, to generate a stable glow discharge of larger volume between the MHCD and a third electrode, placed at a distance of some mm's from the MHCD. This 3-electrode configuration is the so-called micro-cathode sustained discharge (MCSD), which is basically a positive column with a low value of the reduced electric field, allowing, therefore, the production of intense fluxes of $\text{O}_2(a^1\Delta)$ metastables (Figure 22.9).

By using optical emission spectroscopy and ultra-violet absorption spectroscopy, we have measured the electron density in the MCSD, and the $\text{O}_2(a^1\Delta)$ and O_3 densities in the afterglow, at $\sim 25\text{ cm}$ downstream. These measurements made it possible to study the production of $\text{O}_2(a^1\Delta)$ states as a function of pressure, flux, gas mixture composition, and energy deposited per oxygen molecule. For binary

⁶ Work performed in the frame of the PhD thesis of J. Santos Sousa and supported by FCT (Scholarship SFRH/BD/28668/2006).

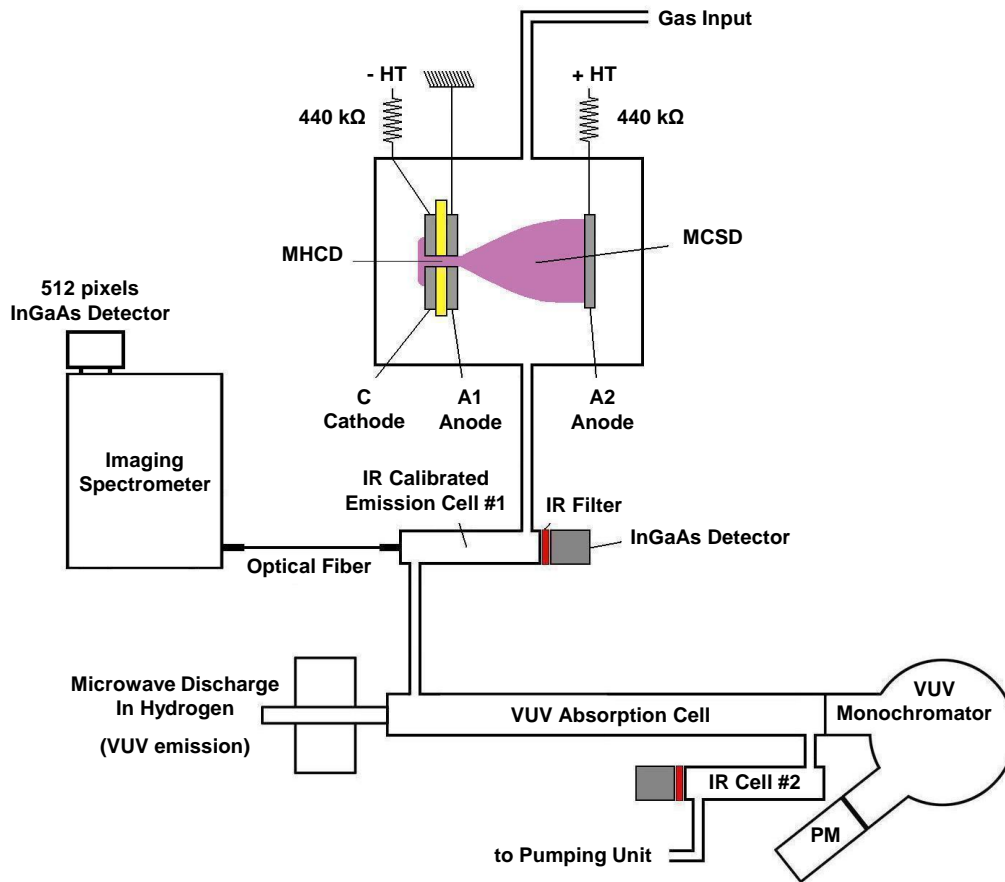


Figure 22.9 - Schematics of the MHCD-MCSD experimental setup, with diagnostics

He/O₂ mixtures at atmospheric pressure, the MCSD allowed the production of a O₂(a¹Δ) density of about 10¹⁵ cm⁻³, whenever the helium flow was higher than 15000 sccm. As the O₂(a¹Δ) molecules are effectively quenched by atomic oxygen (O-atom), one solution to increase the O₂(a¹Δ) number density is to add, in the He/O₂ mixture, an O-atom scavenger. As so, we have studied the influence of adding NO molecules, at low concentration, to the He/O₂ mixture at atmospheric pressure. Results show a large increase of the O₂(a¹Δ) number density (up to 50 times more), (Figure 22.10).

Indeed, O₂(a¹Δ) number densities higher than 10¹⁶ cm⁻³ were obtained at atmospheric pressures in He/O₂/NO mixtures and transported over some tens of cm for helium flows in the range 2000-30000 sccm. This opens the opportunity for a large spectrum of new applications requiring large amounts of O₂(a¹Δ) states and operation at atmospheric pressure, namely biological applications. Preliminary experiments were conducted showing that the developed system is particularly useful to study in detail the reactivity of O₂(a¹Δ) with biological molecules such as DNA constituents⁷.

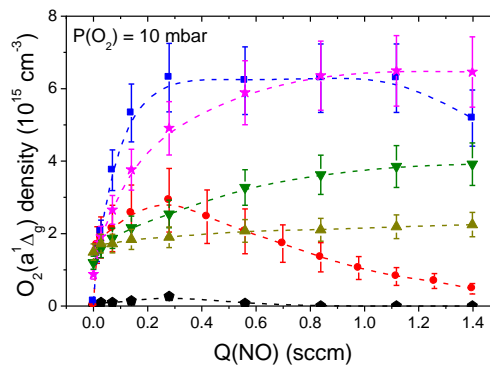


Figure 22.10 - O₂(a¹Δ) number density, as a function of NO flow, at 10 mbar O₂ pressure, 3mA current, and for the following He flows (in sccm): 1000 (black points), 2000 (red), 4000 (blue), 8000 (magenta), 16000 (green), 32000 (dark yellow).

⁷Work performed in collaboration with the Laboratoire des Lésions des Acides Nucléiques, CEA Grenoble, France).

22.4. CAPACITIVELY COUPLED PLASMA REACTORS⁸

We have continued to study low-pressure (0.05-2 Torr) capacitively coupled radio-frequency (CCRF) nitrogen discharges (13.56 MHz), produced within cylindrical parallel-plate reactors (~6cm radius and ~3-5cm height) (Figure 22.11).

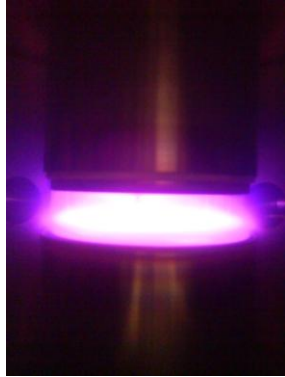


Figure 22.11 - CCRF nitrogen plasma (ICMSE, Spain)

Simulations used a hybrid calculation code, coupling a two-dimensional time-dependent fluid model (that solves the charged particle and the electron mean energy transport equations together with Poisson's equation), the two-term homogeneous electron Boltzmann equation (yielding the electron energy distribution function in the presence of inelastic and superelastic collisional events, involving both electronically and vibrationally excited states), and a quasi-homogeneous collisional-radiative model for the populations of electrons, positive ions N_2^+ , and N_4^+ , vibrationally excited ground-state molecules $N_2(X^1\Sigma_g^+, v=0-45)$, and 7 electronically excited states of the N_2 molecule, accounting for the production of electrons via associative ionization mechanisms involving the $N_2(A)$ and $N_2(a')$ metastables (Figure 22.12).

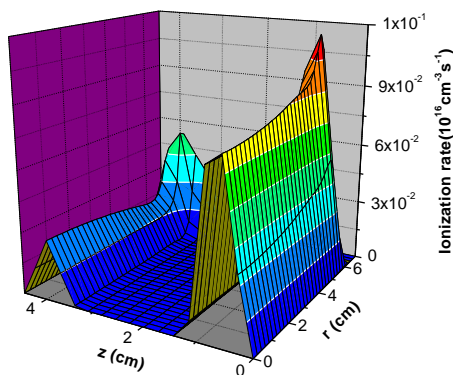


Figure 22.12 - Time-average two-dimensional profile of the electron ionization rate in a CCRF discharge in pure nitrogen, at 0.5 mbar pressure and 10W coupled power

The model was also used to study CCRF nitrogen discharges for material processing applications. Nitrogen and nitrogen-mixture plasmas are increasingly used for plasma-assisted processing applications, such as the modification and functionalization of materials like polyethylene terephthalate (PET), low-density polyethylene (LDPE), nanotubes, polymer surfaces used in the biomedical field in view of improving their biocompatibility, and for the deposition of N_2 containing functional groups in textiles, among others. In these applications the dissociating and ionizing properties of these plasmas are used to produce large fluxes of radicals with a high chemical reactivity, at ambient temperature and low pressure (< 1 Torr). The optimization of these procedures requires a deep knowledge of the mechanisms controlling the kinetics of nitrogen, which can be achieved with help of the simulation model developed. For this purpose, we have upgraded the simulation code as to extend its calculation domain beyond the plasma chamber (up to the reactor metal walls, Figures 22.13 and 22.14). Simulation results were compared with experimental measurements of the self-bias voltage (Figure 22.15) and power coupled, for various pressures and rf applied voltages.

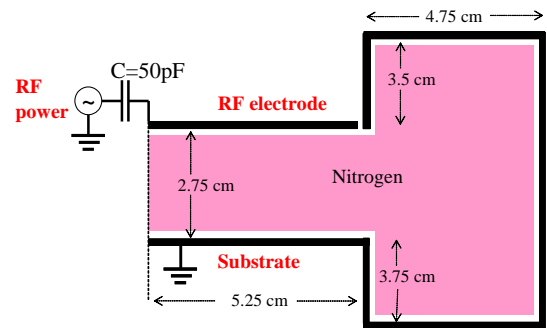


Figure 22.13 - Schematics of the calculation domain adopted in simulations of CCRF discharges

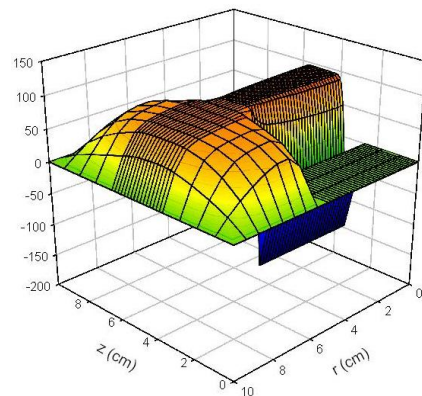


Figure 22.14 - Time-average two-dimensional profile of the plasma potential in a CCRF discharge in pure nitrogen, at 0.75 Torr pressure and 400V rf applied voltage

⁸ Work performed in collaboration with G. Cernogora (Université de Versailles St-Quentin, Service d'Aéronomie, Vêrières, France), and J. Cotrino and C. Lopez (Instituto de Ciencias de los Materiales de Sevilla, Consejo Superior de Investigaciones Científicas, Sevilla, Spain).

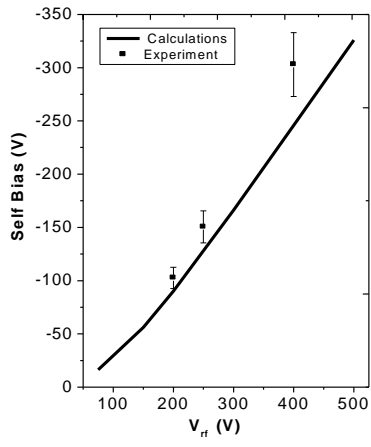


Figure 22.15 - Self-bias potential, as a function of the rf applied voltage, for CCRF discharges in pure nitrogen at 0.2 Torr pressure.

23. FUNDAMENTAL PHYSICS IN SPACE¹

L.O. Silva (Head), O. Bertolami (Deputy Head), T. Barreiro, C. Carvalho, A.M. Martins, J. Paramos, C. Bastos.

23.1. INTRODUCTION

The research activity of this project was focused in 2008 on:

- Generalized Chaplygin gas model;
- Braneworld models and Lorentz invariance;
- $f(R)$ extensions to General Relativity;
- Non-commutative quantum mechanics;
- Mission design of fundamental physics tests;
- Thermal modelling of the Pioneer anomaly.

23.2. GENERALIZED CHAPLYGIN GAS MODEL

The recent discovery of the accelerated expansion of the Universe has led to several efforts aiming to fit this new observation into the general scheme of the Big-Bang cosmological model. These attempts include models of dark energy and modified models of gravity.

An active line of research in GFFE consists in studying and testing the unified model of dark energy and dark matter, the generalized Chaplygin gas model. Theoretical work has been carried out to understand the origin of this unification and to devise new observational strategies. These include the use of gravitational lensing techniques, cosmic microwave background radiation properties, supernovae data, correlations extracted from the observation of gamma-ray bursts and some features in the process of structure formation. Despite the progress, some key questions remain open, especially in what concerns the issue of gravitational collapse.

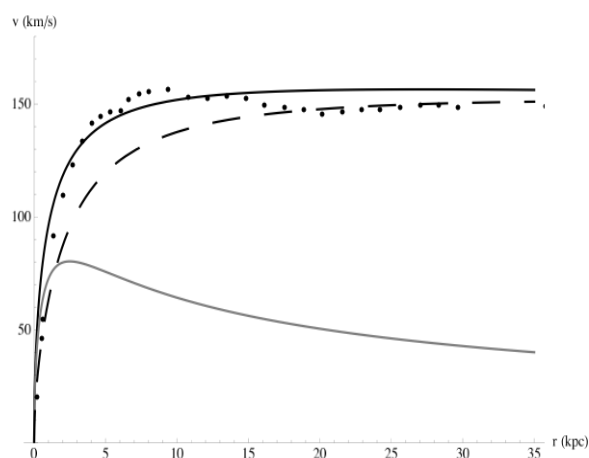
23.3. BRANEWORLD MODELS AND LORENTZ INVARIANCE

Another area of recent interest in the group is the development of braneworld models to understand gravity in four dimensions, and hence the problem of the accelerated expansion of the universe. In this respect, we are also interested in brane models that can bring some insight on the nature of fundamental symmetries such as Lorentz invariance.

23.4. $F(R)$ EXTENSIONS TO GENERAL RELATIVITY

On the theoretical front, we are actively investigating fundamental and phenomenological implications of yet another extension to General Relativity, where the space-time curvature displays a non-minimal coupling to matter. This could be relevant at several scales, influencing solar equilibrium and possibly playing a part at an astrophysical

setting, namely through the mimicking of a dark matter profile that could explain the flattening of the galaxy rotation curves.



23.1 - NGC 3198 galaxy rotation curve (points), with fit (full line) arising from a power-law coupling of matter with curvature.

23.5. NON-COMMUTATIVE QUANTUM MECHANICS

Another interesting prospect lies in the possibility of quantum effects arising due to the manifestation of a meaningful non-commutative quantum mechanics. This could lead to relevant modifications at several scales, including within a cosmological context.

23.6. MISSION DESIGN OF FUNDAMENTAL PHYSICS TESTS

Recent success of observational missions in space, mainly in the area of observational cosmology, has prompted the interest in conducting experiments in space to test the fundamental underlying principles of physics. Prospective experiments include tests of the general theory of relativity, Lorentz invariance, Equivalence Principle and confirming the observed anomalous acceleration of the Pioneer 10 and 11 spacecraft.

Our work has also dealt with the theoretical aspects of models that extend our current knowledge of gravity and unification models and the conceptual development of missions and strategies to select the most suitable observables to test these models.

¹Activities performed in the frame of the Contract of Associated Laboratory, out of the Contract of Association EURATOM/IST, by IPFN staff of the Group of Lasers and Plasmas.

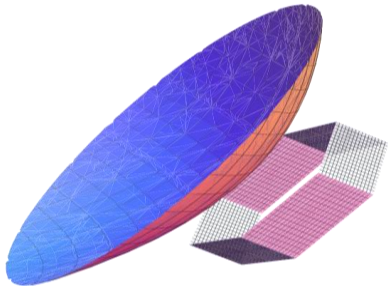


Figure 23.2 - Pioneer spacecraft model geometry considered in the thermal analysis of the Pioneer anomaly

23.7. THERMAL MODELLING OF THE PIONEER ANOMALY

Our contributions also include a thermal model to explain the Pioneer anomaly and the design of a mission to test the salient features of most of the proposals put forward to account for the anomaly. We are also studying ways to generalize our techniques to other spacecraft, such as *e.g.* Cassini probe and the so-called Fly-by anomalies.

24. QUANTUM PLASMAS¹

J.T. Mendonça (Head), A.M. Martins, D. Resendes, S. Mota, H. Terças.

24.1. INTRODUCTION

The work on Quantum Plasmas was focused in 2008 on four main topics:

- Plasma effects in Magneto-Optical Traps (MOT);
- Waves in Quantum Plasma;
- Theoretical Methods;
- Electromagnetic diagnostics for weakly ionized plasma flows

24.2. PLASMA EFFECTS IN MAGNETO-OPTICAL TRAPS (MOT)

We have launched a new area of research in 2008, leading to the installation of a magneto-optical trap (abbreviated MOT) in IST. A MOT is a device that cools down and stores neutral atoms by using the optical force of laser light combined with a magnetic field. A typical MOT for alkali atoms can trap and cool the atoms down to few μK . A major application of this technique is the achievement of Bose-Einstein condensation. Due to the competition between light forces (absorption and re-scattering), MOTs are a perfect stage to observe plasma-like phenomena, provided that the effective collective force is similar to the Coulomb force present in plasma systems. It is therefore possible to study the existence of collective oscillations, based on the usual plasma techniques, and explore some complexity that it is very hard or even impossible via a typical atomic physics approach. On the other hand, it opens the door to new and exotic regimes of plasma physics.

The first results of our theoretical investigation reveal the possibility of exciting hybrid plasma waves, a collective mode with both plasma and acoustic features, given by a simple dispersion relation

$$\omega^2 = \omega_{P,\text{eff}}^2 + u^2 k^2, \quad (24.1)$$

where $\omega_{P,\text{eff}}^2$ is the effective plasma frequency in the MOT. As a consequence of the finite size of the cloud, such hybrid modes are steady waves, envisaging the occurrence of modified Tonks-Dattner (TD) resonances, given by the following new relation

$$\omega_{v,l}^2 = \omega_{P,\text{eff}}^2 \left[1 + \left(z_{v,l}^2 \frac{\lambda_D}{a} \right)^2 \right] \quad (24.2)$$

Recent experiments performed in collaboration with the Institute Non-Lineaire de Nice, strongly suggest the possible observation such Tonks-Dattner oscillations for the first time. A fluorescence spectroscopy of the MOT surprisingly shows resonances approximately at the same values predicted by our theory.

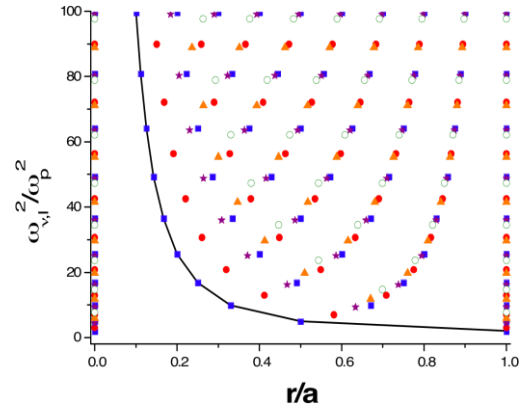


Figure 24.1 - Normalized modes plotted against the nodes.

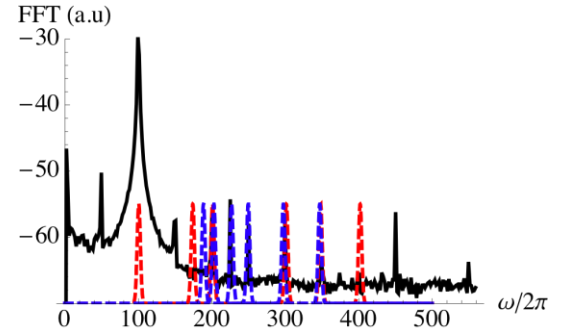


Figure 24.2 - Experimental spectrum vs the predicted Tonks-Dattner resonances. Red lines correspond to the effective plasma frequency $\omega_{P,\text{eff}}^2$ and respective harmonics. Blue lines correspond to the lowest order TD modes.

This agreement, if confirmed in future experiments planned for 2009, will open way to a new diagnostic tool for cold atoms in a MOT, namely the gas temperature, which is one of the basic parameters of the system. Considerations on how the collective behavior of the system is related to different cooling mechanisms may also be in order within this approach.

¹Activities performed in the frame of the Contract of Associated Laboratory, out of the Contract of Association EURATOM/IST, by IPFN staff of the Group of Lasers and Plasmas.

24.3. WAVES IN QUANTUM PLASMA

In recent years, special attention has been paid to the quantum effects in plasmas. The advent of miniaturization techniques, the progress on the understanding of the quantum properties of dense astrophysical media, experiments on extreme physics like laser plasmas, and the recent progress in producing ultra cold plasmas in terms of Rydberg states, have envisaged the application of plasma physics to dense plasmas systems with typical inter-particle distances are frequently comparable to the de Broglie wavelength. Hence, quantum mechanical effects, as electron tunneling, non-locality and interference, are expected to play an important role in the dynamics of such dense systems.

In a recent publication², we have considered the propagation of electrostatic waves, with frequency near the electron plasma frequency, in a magnetized plasma column. We derive the dispersion relation for the quantum version of the well-known Trivelpiece-Gould (TG) modes. We show that, in the classical limit, $\hbar \rightarrow 0$, the dispersion relation reduces to the expression derived in the past by Cabral et al. Our results establishes the following dispersion relation for the TG waves

$$\omega_{l,m}^2 = \omega_p^2 \frac{k^2}{k^2 + k_{\perp(l,m)}^2} + v_F^2 k^2 + \frac{\hbar^2}{4m^2} k^2 \quad (24.3)$$

We have also shown the possible existence of Trivelpiece-Gould solitons in magnetized quantum plasma.

24.4. THEORETICAL METHODS

Other important results published in 2008 by the Group of Quantum plasmas include the quantum theory of free electron lasers³, the orbital angular momentum of neutrino beams in a dense plasma⁴, gamma ray sources using imperfect mirrors⁵, time- refraction of both electrostatic and electromagnetic waves in expanding or contracting plasma bubbles, quantum automata, and several other subjects.

In particular, a model of a quantum automaton (QA), a transducer, working with n qubits was proposed⁵. The quantum states of the automaton are represented by *density operators*. The linearity of the QA and of the *partial trace* operator, jointly with the properties of invariant subspaces and of the quotient spaces, are used to minimize the dimension and the cardinality of the state set of the QA. Two main results are obtained in this paper: (a) The conditions that the unitary evolution operators, representing the quantum gates of the QA, must obey in order to reduce its dimension and its state set. (b) An

algorithm is developed to find the minimal QA and its complexity is computed. We show that the necessary and sufficient conditions for minimization depend uniquely in the structure of the unitary evolution operators, and they are independent of the initial quantum state of the QA.

24.5. ELECTROMAGNETIC DIAGNOSTICS FOR WEAKLY IONIZED PLASMA FLOWS

The 2008 activity in this area has focused on the upgrade of the plasma reflectometer for operation in a specific plasma environment, namely the Von Karman Institute (VKI) plasmatron. Operation in the VKI plasmatron requires increasing system sensitivity and time resolution. Interfering signals, of the order of the signal of interest, must be eliminated for improved system sensitivity. This has been implemented with range gating through the implementation of a frequency band filter. Since the VKI plasma shows rapid oscillations (at 600 and 1200 Hz) increased sampling capability must be incorporated. This has imposed a complete revision of the design.

²Physics Plasmas 15, 072109 (2008).

³Physics Plasmas 15, 013110 (2008).

⁴Europhysics Letters 84, 41001 (2008).

⁵Physics Plasmas 15, 113105 (2008).

⁵Physical Review A, 78, 062326 (2008).

25. OTHER ACTIVITIES OF THE RESEARCH LINE ON INTENSE LASERS AND PLASMAS TECHNOLOGIES¹

25.1. INTRODUCTION

The members of the research line on intense lasers and plasma technologies have also been involved in outreach activities, organization of scientific meetings, and have participated in the management of international programmes and projects.

25.2. OUTREACH ACTIVITIES

The IPFN members involved in outreach activities in 2008 are:

- G. Figueira is the Assistant Editor of “Gazeta de Física”, the journal of the Portuguese Physics Society; he co-edited Nos. 1-4 of Vol. 31 (2008), and contributed with several columns, interviews, and book reviews;
- G. Figueira, representing the Portuguese Physics Society, is one of the contributors of the “Physics Blog” hosted by the portuguese weekly newspaper “Expresso” in its “Science Blogs” section;
- G. Figueira and N.C. Lopes, participated in the scientific exhibit “Fórum Ciência Viva”;
- A. Sardinha and J. Berardo, participated on the exposition “Ville Européene des sciences” – Paris – Grand Palais em Paris, November de 2008 ;
- G. Figueira and J. M. Dias are Scientific Consulting for an Exposition in Parque Mineiro do Lousal to be inaugurated in 2009;
- J.A. Rodrigues participated in the 4th International Particle Physics Masterclasses 2008: Hands on Particle Physics at the Faculdade de Ciências e Tecnologia da UAlg, 5 de Março de 2008;
- J.A. Rodrigues was involved in the Ciencia Viva Programme of Science for Youths in the Summer at the Faculdade de Ciências e Tecnologia da UAlg, 1 a 5 de Setembro de 2008.

25.3. ORGANIZATION OF SCIENTIFIC MEETINGS

During 2008, the following IPFN members participated in the organization of scientific meetings:

- E. Tatarova, Chair of the Organizing Committee, 1st Workshop on “Plasma for Environmental Issues, Kiten, Bulgaria, July 2008;
- V. Guerra, Member of International Scientific Committee, ESCAMPIG, Granada, Spain 2008;
- M. Fajardo, Member of the Local Organizing Committee XVII International Symposium on Gas Flow and Chemical Lasers & High Power Lasers, Lisbon, September 2008;
- M. Fajardo, Beam Particles and Inertial Fusion Panel on Scientific Committee and Session Chairman, EPS Conference on Plasma Physics and Controlled Fusion, Hersonissos, Crete, June 2008;

- M. Fajardo, Scientific Program Committee and Session Chairman, Radiative Properties of Hot Dense Plasmas, Santa Barbara, USA, November 2008;
- G. Figueira coordinated the preparation of a portuguese thematic network on lasers and photonics, whose first meeting took place at the Calouste Gulbenkian Foundation, Lisbon, Oct. 2008;
- L.O. Silva, member of the Organizing Committee of XVII International Symposium on Gas Flow and Chemical Lasers and High Power Lasers, Lisbon, Sep. 2008;
- L.O. Silva, Member of the Programme Committee of the 35th European Physical Society Conference on Plasma Physics, July 2008;
- L.O. Silva, Member of the Scientific Programme Committee of the 5th International Conference on Physics of Dusty Plasmas, May 2008;
- L.L. Alves, Member of the Program Committee, 21st ICNSP, International Conference on the Numerical Simulation of Plasmas, Lisbon, 6-9 October 2009;
- L.L. Alves, Member of the International Scientific Committee, International Colloquium on Plasma Processes (next edition: Marseille, 22-26 June 2009);
- R.A. Fonseca, Chairman of the 21st International Conference on the Numerical Simulation of Plasmas, ICNSP’09, to be held in Lisbon in October of 2009;
- L.O. Silva, member of the International Scientific Committee of the 21st International Conference on the Numerical Simulation of Plasmas, ICNSP’09, to be held in Lisbon in October of 2009;
- L.O. Silva, Member of the Selection Committee of the John Dawson PhD Thesis Prize on Laser and Plasma Accelerators 2009;
- L.O. Silva, Member of the International Advisory Committee of Coulomb 09 - Ions Acceleration with high Power Lasers: Physics and Applications, Senigallia (Italy), June 2009;
- L.O. Silva, Member of the Programme Committee, Harnessing Relativistic Plasmas Waves as Novel Radiation Sources from THz to X-rays and beyond SPIE Europe Conference, Prague (Czech Republic), April 2009;
- L.O. Silva, Member of the Programme Committee of the 2nd Symposium on Laser-Driven Relativistic Plasmas applied to Science, Industry and Medicine, Kyoto (Japan), January 2009;

25.4. PARTICIPATION IN THE MANAGEMENT OF INTERNATIONAL PROJECTS AND PROGRAMMES

Several members of IPFN were also involved in the coordination and the management of international projects and programmes, namely:

- J.T. Mendonça is member of the HiPER Council;

¹Activities carried out in the frame of the Contract of Associated Laboratory.

- L.O. Silva, is member of the Participants Council of HiPER;
- O. Bertolami was Chairman of the Astroparticle Physics section at the 37th COSPAR (Committee for Space Research) Assembly in Montreal, July 2008.

26. PUBLICATIONS, LABORATORIAL PROTOTYPES, PRIZES AND AWARDS

26.1. MAGNETIC FUSION

26.1.1. Publications in Books

- Alonso A., P. Andrew, A. Neto, J.L. de Pablos, E. de la Cal, H. Fernandes, J. Gafert, P. Heesterman, C. Hidalgo, G. Kocsis, A. Manzanares, A. Murari, G. Petravich, L. Rios, C. Silva and P.D. Thomas, "Fast visible camera installation and operation in JET", Burning Plasma Diagnostics: International Conference. (Eds) G. Gorini, F.P. Orsitto, E. Sindoni, M. Tardocchi, AIP Conference Proceedings Vol. 988. American Institute of Physics, Merville, NY, 185, 2008.
- Alonso MP, JH Severo, FO Borges, JI Elizondo, LA Berni, M Machida, CAF Varandas, RMO Galvão, "Multipoint Thomson scattering diagnostic for the TCABR tokamak with centimeter spatial resolution". Plasma and Fusion Science: 17th IAEA Technical Meeting on Research Using Small Fusion Devices. (Eds.) C. Varandas, C. Silva. AIP Conference Proceedings, Vol. 996, American Institute of Physics, Melville, NY, 192, 2008.
- Carvalho PJ, H Thomsen, S Gori, U Toussaint, J. Geiger, A Weller, R Coelho, and H Fernandes, "Comparison of fast tomographic methods for application on the Soft X-ray tomography system on Wendelstein 7-X stellarator". Plasma 2007: The International Conference Research and Application of Plasmas; 4th German-Polish Conference on Plasma Diagnostics for Fusion and Applications; 6th French-Polish Seminar on Thermal Plasma in Space and Laboratory (Eds.) H.-J. Hartfuss, M. Dudeck, J. Musielok, M.J. Sadowski, AIP Conference Proceedings, Vol. 993, American Institute of Physics, Melville, NY, 167, 2008.
- Carvalho PJ, H Thomsen, S Gori, U Toussaint, A Weller, R Coelho, A Neto, T Pereira, C Silva and H Fernandes, "Fast tomographic methods on the tokamak ISTTOK". Plasma and Fusion Science: 17th IAEA Technical Meeting on Research Using Small Fusion Devices. (Eds.) C. Varandas, C. Silva. AIP Conference Proceedings, Vol. 996, American Institute of Physics, Melville, NY, 199, 2008.
- Coelho R, D Alves and C Silva, "Time scale analysis of ISTTOK probe data". Plasma and Fusion Science: 17th IAEA Technical Meeting on Research Using Small Fusion Devices. (Eds.) C. Varandas, C. Silva. AIP Conference Proceedings, Vol. 996, American Institute of Physics, Melville, NY, 207, 2008.
- Figueiredo J, RB Gomes, H Fernandes, A Sharakovski, "Plasma Spectroscopy in ISTTOK". Plasma and Fusion Science: 17th IAEA Technical Meeting on Research Using Small Fusion Devices. (Eds.) C. Varandas, C. Silva. AIP Conference Proceedings, Vol. 996, American Institute of Physics, Melville, NY, 213, 2008.
- Gomes RB, H Fernandes, C Silva, A Sarakovskis, T Pereira, J Figueiredo, B Carvalho, A Soares, P Duarte, C Varandas, O Lielausis, A Klyukin, E Platadis and I Tale, "Interaction of a liquid Gallium jet with ISTTOK edge plasmas". Plasma and Fusion Science: 17th IAEA Technical Meeting on Research Using Small Fusion Devices. (Eds.) C. Varandas, C. Silva. AIP Conference Proceedings, Vol. 996, American Institute of Physics, Melville, NY, 151, 2008.
- Livramento V, JB Correia, D Nunes, PA Carvalho, H Fernandes, C Silva, K Hanada, N Shohoji, E Osawa, "Novel approach to plasma facing materials in nuclear fusion reactors". Plasma and Fusion Science: 17th IAEA Technical Meeting on Research Using Small Fusion Devices. (Eds.) C. Varandas, C. Silva. AIP Conference Proceedings, Vol. 996, American Institute of Physics, Melville, NY, 166, 2008.
- Nedzelskiy IS, A Malaquias, Yu Tashchev, C Silva, H Figueiredo, B Goncalves, H Fernandes, CAF Varandas, "Development of a multichannel time-of-flight technique for plasma potential profile measurements by heavy ion beam diagnostic on the tokamak ISTTOK". Plasma and Fusion Science: 17th IAEA Technical Meeting on Research Using Small Fusion Devices. (Eds.) C. Varandas, C. Silva. AIP Conference Proceedings, Vol. 996, American Institute of Physics, Melville, NY, 185, 2008.
- Oost G. Van, M. Gryaznevich, E. Del Bosco, A. Malaquias, G. Mank, M. Berta, J. Brotankova, R. Dejarnac, E. Dufkova, I. Duran, M. Hron, P. Peleman, J. Sentkerestiova, J. Stöckel, B. Tál, V. Weinzettl, J. Zajac, S. Zoletnik, V. Budaev, N. Kirneva, G. Kirnev, B. Kuteev, A. Melnikov, M. Sokolov, V. Vershkov, I. El Chama Neto, J. Ferreira, R. Gonzales, C.R. Gutierrez Tapia, H. Hegazy, P. Khorshid, A.W. Kraemer-Flecken, L.I. Krupnik, Y. Kuznetsov, A.M. Marques, A. Ovsyannikov, L. Ruchko, E. Sukhov, A. Singh, V. Soldatov, A. Talebitaher and G.M. Vorobjev. "Joint experiments on the tokamaks CASTOR and T-10". Plasma and Fusion Science: 17th IAEA Technical Meeting on Research Using Small Fusion Devices. (Eds.) C. Varandas, C. Silva. AIP Conference Proceedings, Vol. 996, American Institute of Physics, Melville, NY, 24, 2008.
- Santos J.H., F. Reis, H. Fernandes, A. Neto, A. Duarte, F. Oliveira and W.P. de Sá "Fusion talk: a remote participation tool". Plasma and Fusion Science: 17th IAEA Technical Meeting on Research Using Small Fusion Devices. (Eds.) C. Varandas, C. Silva. AIP Conference Proceedings, Vol. 996, American Institute of Physics, Melville, NY, 3, 2008.
- Silva C, H Fernandes, CAF Varandas, D Alves, P Balan, BB Carvalho, I Carvalho, P Carvalho, PA Carvalho, R Coelho, JB Correia, A Duarte, P Duarte, J Ferreira, H Figueiredo, J Figueiredo, J Fortunato, R Galvão, R Gomes, B Gonçalves, C Hidalgo, C Ionita, O Lielausis, V Livramento, T Lunt, A Klyukin, I Nedzelskiy, A Neto, T Pereira, E Platadis, V Plyusnin, R Schrittwieser, A Sharakovski, I Tale, D Valcárcel, "Overview of recent ISTTOK results". Plasma and Fusion Science: 17th IAEA Technical Meeting on Research Using Small Fusion Devices. (Eds.) C. Varandas,

C. Silva. AIP Conference Proceedings, Vol. 996, American Institute of Physics, Melville, NY, 3, 2008.

- Valcárcel DF, IS Carvalho, BB Carvalho, H Fernandes, C Silva, P Duarte, A Duarte, PJ Carvalho e T Pereira, "Validation of ISTTOK Plasma Position Controller". Plasma and Fusion Science: 17th IAEA Technical Meeting on Research Using Small Fusion Devices. (Eds.) C. Varandas, C. Silva. AIP Conference Proceedings, Vol. 996, American Institute of Physics, Melville, NY, 291, 2008.

26.1.2. Publications in refereed scientific journals (publications in ISI)

- Alonso MP, ACA Figueiredo, LA Berni and CAF Varandas, "Simulation images of Doppler broadening for the Thomson scattering diagnostic of the TCABR tokamak", IEEE Transactions on Plasma Science, 36, 4, 1094, Aug. 2008
- Andrew Y, TM Biewer, K Crombe, D Keeling, E de la Luna, C Giroud, NC Hawkes, M Kempenaars, A Korotkov, A Meigs, YR Martin, A Murari, I Nunes, R Sartori, T Tala and JET EFDA contributors "H-mode access on JET and implications for ITER", Plasma Physics and Controlled Fusion, 50, 12, 124053, 2008
- Antar GY, M Tsalas, E Wolfrum, V Rohde and the ASDEX Upgrade Team, "Turbulence during H- and L-mode plasmas in the scrape-off layer of the ASDEX Upgrade tokamak", Plasma Physics and Controlled Fusion, 50, 9, 095012, 2008
- Asunta O, T Kurki-Suonio, T Tala, S Sipilä, R Salomaa and JET-EFDA contributors, "Comparison of fusion alpha performance in JET advanced scenario and H-mode plasmas", Plasma Physics and Controlled Fusion, 50, 12, 125008, 2008
- Behler K., H. Blank, H. Eixenberger, A. Lohs, K. Lüddecke, R. Merkel, G. Raupp, G. Schramm, W. Treutterer, M. Zilker and ASDEX Upgrade team, "Real-time diagnostics at ASDEX Upgrade – Architecture and operation", Fusion Engineering and Design, 83, 304-311, 2008
- Belo JH, P Bibet and D Guilhem, "Images of the TE wave inside Tore Supra's LH PAM launcher", IEEE Transactions on Plasma Science, 36, 4, 1096, Aug. 2008
- Belo JH, P Bibet and D Guilhem, "Images of the RF stability of a lower hybrid PAM launcher", IEEE Transactions on Plasma Science, 36, 4, 1098, Aug. 2008
- Belo JH, P Bibet and D Guilhem, "Images of the power splitting stability of a lower hybrid PAM launcher", IEEE Transactions on Plasma Science, 36, 4, 1100, Aug. 2008
- Belo P, W Fundamenski, V Parail, G Corrigan, C Giroud, J Spence and JET EFDA contributors, "Numerical simulation of hydrogenic and impurity flows in the boundary plasma on JET", Plasma Physics and Controlled Fusion, 50, 8, 085003, 2008
- Belonohy E., O.J.W.F. Kardaun, T. Fehér, K Gál, S. Kálvin, G. Kocsis, K. Lackner, P.T. Lang, J. Neuhauser and ASDEX Upgrade Team, "A high field side pellet penetration depth scaling derived for ASDEX Upgrade", Nuclear Fusion, 48, 065009, 2008
- Beurskens M.N.A., G. Arnoux, A.S. Brezinsek, C.D. Challis, P.C. de Vries, C. Grioud, A. Huber, S. Jachmich, K. McCormick, R.A. Pitts, F.G. Rimini, A. Alfier, E. de la Luna, W. Fundamenski, S. Gerasimov, E. Giovannozzi, E. Joffrin, M. Kempenaars, X. Litaudon, T. Loarer, P. Lomas, J. Mailloux, R. Pasqualotto, V. Pericoli-Ridolfini, R. Pugno, E. Rachlew, S. Saarelma, E. Solano, M. Walsh, L. Zabeo, K.-D. Zastrow and JET-EFDA Contributors, "Pedestal and ELM response to impurity seeding in JET advanced scenario plasmas", Nuclear Fusion, 48, 095004, 2008
- Bizarro JP, ACA Figueiredo and JET EFDA Contributors, "Time-frequency analysis of fusion plasma signals beyond the short-time Fourier transform paradigm: An overview", Fusion Engineering and Design, 83, 350, 2008
- Bizarro JP, XL Litaudon, TJJ Tala, and JET EFDA Contributors, "Computational images of internal-transport-barrier oscillations in tokamak plasmas", IEEE Transactions on Plasma Science, 36, 4, 1090, Aug. 2008
- Bizarro J.P.S., "Entropy production in irreversible processes with friction" Physical Review E, 78, 021137 1-5, 059903 1 (2008).
- Carlen E and R. Vilela Mendes, "Signal reconstruction by random sampling in chirp space", Nonlinear Dynamics, doi:10.1007/s11071-008-9394-7
- Carvalho BB, Batista AJN, Patricio F, et al., "Multi-rate DSP/FPGA-based real-time acquisition and control on the ISTTOK tokamak", IEEE Transaction on Nuclear Science, 55, 1, 54-58, 1, 2008
- Carvalho PJ, R Coelho, T Pereira, P Duarte, C Silva, A Neto, DF Valcárcel, ACA Figueiredo and H Fernandes, "Tomographic visualization for plasma position control in ISTTOK", IEEE Transactions on Plasma Science, 36, 4, 1102, Aug. 2008
- Carvalho P. J., B.B. Carvalho, A. Neto, A. Duarte, R.Coelho, H. Fernandes, J. Sousa and C. Varandas "A real-time tomography diagnostic and control system in ISTTOK", Rev. Sci. Instruments 79, 10F329 (2008)
- Castro R., J. Vega, A. Portas, A. Pereira, S. Balme, A. Duarte, H. Fernandes, J. Kadlecik, P. Lebourg, A. Neto, F. Oliveira, K. Purahoo, F. Reis, C. Rodriguez, J. Signoret, J.M. Theis, K. Thomsen, "EFDA-fed: European federation among fusion energy research laboratories", Campus-Wide Information Systems, 25, 5, 359, 2008
- Chaari S., F. Cipriano, S. Gheryani and H. Ouerdiane, "Sanov's theorem for white noise distributions and application to the Gibbs conditioning principle", Acta Appl. Math.,104, (2008) 313-324

- Chapman IT, I Jenkins, RV Budny, JP Graves, SD Pinches, S Saarelma and JET EFDA Contributors, “Sawtooth control using off-axis NBI”, Plasma Physics and Controlled Fusion, 50, 4, 045006, 2008
- Coelho R. and D. Alves, “Real-time estimation of the poloidal wavenumber of ISTTOK tokamak magnetic fluctuations”, Rev. Sci. Instruments 79, 10F121 (2008)
- Conway G.D. and the ASDEX Upgrade Team, “Amplitude behaviour of geodesic acoustic modes in the ASDEX Upgrade tokamak”, Plasma Physics and Controlled Fusion, 50, 8, 085005, 2008
- Conway G.D., C. Tröster, B. Scott, K Hallatschek and the ASDEX Upgrade Team, “Frequency scaling and localization of geodesic acoustic modes in ASDEX Upgrade”, Plasma Physics and Controlled Fusion, 50, 8, 055009, 2008
- Corre Y, E Joffrin, P Monier-Garbet, Y Andrew, G Arnoux, M Beurskens, S Brezinsek, M Brix, R Buttery, I Coffey, K Crombe, E de La Luna, R Felton, C Giroud, S Hacquin, J Hobirk, A Huber, F Imbeaux, S Jachmich, M Kempenaars, X Litaudon, H Leggate, T Loarer, G Maddison, E Rachlew, J Rapp, O Sauter, A Savchukov, G Telesca, A Widdowson, KD Zastrow, O Zimmermann and JET-EFDA collaborators. “Hybrid H-mode scenario with nitrogen seeding and type III ELMs in JET”, Plasma Physics and Controlled Fusion, 50, 11, 115012, 2008
- Cruz N, AP Rodrigues, B Santos, CAF Varandas, BP Duval, J-M Moret, J Berrino, Y Martin, X Llobet, “The Integration of the New Advanced Digital Plasma Control System in TCV”, Fusion Engineering and Design, 83 (2008) 215–219.
- Cupido L., A. Cardinali, R. Igraja, F. Serra, M.E. Manso, A. Murari and JET EFDA Contributors, “High resolution Fast Wave Reflectometry: JET design and implications for ITER”, Review Scientific Instruments, 79, 10, 10F106 (2008)
- Del-Castillo-Negrete D, P Mantica, V Naulin, JJ Rasmussen and JET EFDA Contributors, “Fractional diffusion models of non-local perturbative transport: numerical results and application to JET experiments”, Nuclear Fusion, 48, 7, 75009, 2008
- Duarte A.S. et al., “Firecalc: An XML-based framework for distributed data analysis”, Fusion Engineering and Design, 83, 458 (2008)
- Dumbrajs O., V. Igochine, H. Zohm and ASDEX Upgrade Team., “Diffusion in a stochastic magnetic field in ASDEX Upgrade”, Nuclear Fusion, 48, 024011 (2008)
- Duval BP, A Bortolon, A Karpushov, RA Pitts, A Pochelon, O Sauter, A Scarabosio, G Turri, the TCV Team, “Spontaneous L-mode plasma rotation scaling in the TCV tokamak”, Physics of Plasma, 15, 5, 056113, 2008
- Falchetto GL, BD Scott, P Angelino, A Bottino, T Dannert, V Grandgirard, S Janhunen, F Jenko, S Jolliet, A Kendl, BF McMillan, V Naulin, AH Nielsen, M Ottaviani, AG Peeters, MJ Pueschel, D Reiser, TT Ribeiro and M Romanelli, “The European turbulence code benchmarking effort turbulence driven by thermal gradients in magnetically confined plasmas”, Plasma Physics and Controlled Fusion, 50, 12, 124015, 2008
- Fattorini L, PT Lang, ME Manso, J Santos, LD Horton, GD Conway and the ASDEX Upgrade Team, “High temporal and spatial resolution reflectometry investigations of type-I ELMs induced edge barrier collapse at ASDEX Upgrade”, Plasma Physics and Controlled Fusion, 50, 12, 125001, 2008
- Figueiredo ACA, JS Ferreira, R Coelho and D Alves, “A signal processing tool to compute and visualize the Choi-Williams distribution and the Hilbert-Huang transform of nonstationary signals in fusion research”, Fusion Engineering and Design, 83, 354, 2008
- Figueiredo ACA, A Fonseca, L Meneses, and JET-EFDA Contributors, “Systematic and routine analysis of radial correlation reflectometry data in JET”, Review of Scientific Instruments, 79 (2008).
- Fischer R, E Wolfrum, J Schweinzer and the ASDEX Upgrade Team, “Probabilistic lithium beam data analysis”, Plasma Physics and Controlled Fusion, 50, 8, 085009, 2008
- Floriani E, R. Lima and R. Vilela Mendes, “Poisson-Vlasov: stochastic representation and numerical codes” European Physical Journal D 46, 295-302, 2008
- Fortunato JC, Batista A, Sousa J, et al., “Event and pulse node hardware design for nuclear fusion experiments” IEEE Transactions on Nuclear Science, 55, 2, 679-682, 2008
- Fundamenski W., D.P. Coster, M. Airila, P. Belo, X. Bonnin, A. Chankin, G. Corrigan, S.K. Erents, O.E. Garcia, S. Glowacz, B. Gulejova, A. Kirschner, V. Naulin, A. Nielsen, G. Kirnev, V. Kotov, C. Konz, J.J. Rasmussen, R.A. Pitts, D. Reiter, T. Ribeiro, B.D. Scott, J.D. Strachan, F. Subba, E. Tsitronel, D. Tskhakaya, S. Wiesen, M. Wischmeier, R. Zagorski and EFDA-JET Contributors, “Progress in Edge Plasma Transport Modeling on JET”, Plasma Physics, 48, 1-3, 190, 2008
- Gál K., E. Belohnohy, G. Kocsis, P.T. Lang, G. Veres and ASDEX Upgrade Team, “Role of shielding in modelling cryogenic deuterium pellet ablation”, Nuclear Fusion 48, 085005, 2008
- Ghendrih Ph., R. Lima and R. Vilela Mendes, “Reduction and approximation in guiding-center dynamics”, J. Phys. A: Math. Theor. 41, 465501, 2008
- Gomes R, H. Fernandes, C. Silva, A. Figueiredo, “Fast Camera images of surviving gallium droplets during plasma-liquid gallium Jet interaction experiments in ISTTOK”, IEEE Transactions on Plasma Science, 36, 4, 1086, Aug. 2008
- Gomes R. B., H. Fernandes, C. Silva, A. Sarakovskis, T. Pereira, J. Figueiredo, B. Carvalho, A. Soares, C. Varandas,

- O. Lielausis, A. Klyukin, E. Platacis, I. Tale “*Interaction of a liquid gallium jet with the tokamak ISTTOK edge plasma*”, Fusion Engineering and Design, 83, 102 (2008)
- Gonçalves B, “*Participar hoje na energia de amanhã*”, Revista Indústria, 68, 38, Mar/Abr. 2008
 - Gonçalves B., “*A opção Nuclear*”, Revista Indústria (CIP), Nº 70, Julho/Agosto 2008
 - Gryaznevich MP, TC Hender, DF Howell, CD Challis, HR Koslowski, S Gerasimov, E Joffrin, YQ Liu, S Saarelma and JET-EFDA contributors “*Experimental studies of stability and beta limit in JET*”, Plasma Physics and Controlled Fusion, 50, 12, 124030, 2008
 - Guimarães L, T Estrada, E Ascasibar, ME. Manso, L. Cupido, T Happel, E Blanco, F Castejon, R Jimenez-Gomez, MA Pedrosa, C Hidalgo, I Pastor and A Lopez-Fraguas “*Parametric Dependence of the Perpendicular Velocity Shear Layer Formation in TJ-II Plasmas*” Plasma and Fusion Research, 3 S1057, 2008
 - Hölzl M., S. Günter and ASDEX Upgrade Team, “*Heat diffusion across magnetic islands and ergodized plasma regions in realistic tokamak geometry*”, Physics of Plasmas, 15, 072514, 2008
 - Hynönen V, T Kurki-Suonio, W Suttrop, A Stäbler and the ASDEX Upgrade Team, “*Effect of radial electric field and ripple on edge neutral beam ion distribution in ASDEX Upgrade*”, Plasma Physics and Controlled Fusion, 50, 3, 035014, 2008
 - Igochine V., O. Dumbrajs, H. Zohm and ASDEX Upgrade Team, “*Transition from quasiperiodicity to chaos just before sawtooth crash in the ASDEX Upgrade tokamak*”, Nuclear Fusion, 48, 062001, 2008
 - Johnson M. Gatu, L. Giacomelli, A. Hjalmarsson, J. Kallne, M. Weiszflog, E. Andersson Sundén, S. Conroy, G. Ericsson, C. Hellesen, E. Ronchi, H. Sjostrand, G. Gorini, M. Tardocchi, A. Combo, N. Cruz, J. Sousa, S. Popovichev, JET-EFDA contributors, “*The 2.5-MeV neutron time-of-flight spectrometer TOFOR for experiments at JET*”, Nuclear Instruments and Methods in Physics Research A, 591 (2): 417-430, 2008.
 - Kallenbach A., R. Dux, T. Eich, R. Fischer, L. Goannone, J. Harhausern, A. Herrmann, H. W. Müller, G. Pautasso, M. Wischmeier and ASDEX Upgrade Team “*Divertor power and particle fluxes between and during type-I ELM in the ASDEX Upgrade*”, Nuclear Fusion, 48, 085008, 2008
 - Kiptily G, D. Borba, F.E. Cecil, M. Cecconello, D. Darrow, V. Golobrod'ko, K. Hill, T. Johnson, A. Murari, F. Nabais, S.D. Pinches, M. Reich, S.E. Sharapov, V. Yavorskij, I.N. Chugunov, D.B. Gin, G. Gorini, A.E. Shevelev, D.B. Syme and V. Zoitam, “*Fast ion JET diagnostics: confinement and losses*”, AIP Conference Proceedings 988, American Institute of Physics, Melville, NY, 283-290, 2008
 - Klein A, H Carfantan, D Testa, A Fasoli, J Snipes and JET EFDA Contributors, “*A sparsity-based method for the analysis of magnetic fluctuations in unevenly-spaced Mirnov coils*”, Plasma Physics and Controlled Fusion, 50, 12, 125005, 2008
 - Kotov V, D Reiter, RA Pitts, S Jachmich, A Huber, DP Coster and JET-EFDA Contributors, “*Numerical modeling of high density JET divertor plasma with the SOLPS4.2 (B2-EIRENE) code*”, Plasma Physics and Controlled Fusion, 50, 10, 105012, 2008
 - Kramer GJ, GY Fu, R Nazikian, RV Budny CZ Cheng, NN Gorelenkov, SD Pinches, SE Sharapov, K-D Zastrow and JET-EFDA Contributors, “*Reversed shear Alfvén eigenmodes in the frequency range of the triangularity induced gap on JET*”, Plasma Physics and Controlled Fusion, 50, 8, 082001, 2008
 - Krupnik, L.I., A.D. Komarov, A.S. Kozachek, A.V. Melnikov, I.S. Nedzelskiy, “*High intensity thermionic alkali ion sources for plasma diagnostic*”, IEEE Transactions on Plasma Sci., 36, 4(2), 1536 (2008)
 - Lang P.T., K. Lachner, M. Maraschek, B. Alper, E. Belonohy, K. Gál, J. Hobirk, A. Kallenbach, S. Kálvin, G. Kocsis, C.P. Perez von Thun, W. Suttrop, T. Szepesi, R. Wenninger, H. Zohm, ASDEX Upgrade Team and JET-EFDA Contributors “*Investigation of Pellet-triggered MHD events in the ASDEX Upgrade*”, Nuclear Fusion, 48, 095007, 2008
 - Lerche EA, D Van Eester and JET EFDA contributors, “*Improved break-in-slope analysis of the plasma energy response in tokamaks*”, Plasma Physics and Controlled Fusion, 50, 3, 035003, 2008
 - Marques T. G., A. Gouveia, T. Pereira, J. Fortunato, B. B. Carvalho, J. Sousa, C. Silva, and H. Fernandes, “*Real-time digital heterodyne interferometer for high resolution plasma density measurements at ISTTOK*”, Rev. Sci. Instrum. 79, 10E711 (2008)
 - Martins JF, J. A. Dente, A. J. Pires and R. Vilela Mendes, “*From controlled dynamical systems to context-dependent grammars: A connectionistic approach*”, Engineering Applications of Artificial Intelligence, doi:10.1016/j.engappai.2008.05.005
 - McDonald DC, L Laborde, JC DeBoo, F Ryter, M Brix, CD Challis, P de Vries, C Giroud, J Hobirk, D Howell, E Joffrin, TC Luce, J Mailloux, V Pericoli-Ridolfini, ACC Sips, K Thomson and JET-EFDA contributors, “*JET confinement studies and their scaling to high β_N ITER scenarios*”, Plasma Physics and Controlled Fusion, 50, 12, 124013, 2008
 - Murari A, T Edlington, A Alfier, A Alonso, Y Andrew, G Arnoux, M Beurskens, P Coad, C Crombe, E Gauthier, C Giroud, C Hidalgo, S Hong, M Kempenaars, V Kiptily, T Loarer, A Meigs, R Pasqualotto, T Tala and JET-EFDA Contributors “*Innovative diagnostics for ITER physics*

addressed in JET”, Plasma Physics and Controlled Fusion, 50, 12, 124043, 2008

- Nazikian R, NN Gorelenkov, B Alper, HL Berk, D Borba, RV Budny, GY Fu, WW Heidbrink, GJ Kramer, MA Makowski, SD Pinches, SE Sharapov, WM Solomon, EJ Strait, RB White, MA Van Zeeland, JET-EFDA contributors, “Excitation of Alfvén eigenmodes by low energy beam ions in the DIII-D and JET tokamaks”, Physics of Plasmas, 15, 5, 056107, 2008
- Nedzelskiy I. S., R. Coelho, D. Alves, C. Silva, and H. Fernandes, “Observation of plasma density fluctuations by a heavy ion beam probe diagnostic with multiple cell array detector on the tokamak ISTTOK”, Rev. Sci. Instrum. 79, 10F319 (2008)
- Neto A., J. Sousa, B. Carvalho, H. Fernandes, R. C. Pereira, A. M. Fernandes, C. Varandas, G. Gorini, M. Tardocchi, D. Gin, A. Shevelev and K. Kneupner, “The control and data acquisition software for the gamma-ray spectroscopy ATCA sub-systems of the JET-EP2 enhancements” Fusion Engineering and Design, 83, IS 2-3, 346-349, 2008
- Neu R., R. Dux, A. Kallenbach and ASDEX Upgrade Team, “Plasma operation with high-Z environment” Journal of Physics: Conference Series, 100, 062001, 2008
- Neuhauser J., V. Bobkov, G.D. Conway, R. Dux, T. Eich, M. Garcia-Munoz, A. Herrmann, L.D. Horton, A. Kallenbach, S. Kalvin, G. Kocsis, B. Kurzan, P.T. Lang, M. Maraschek, H.W. Müller, H.D. Murmann, R. Neu, A.G. Peeters, M. Reich, V. Rohde, A. Schmid, W. Suttrop, M. Tsalas, E. Wolfrum and ASDEX Upgrade Team, “Structure and dynamics of spontaneous and induced ELMs on ASDEX Upgrade” Nuclear Fusion, 48, 045005, 2008
- Pedrosa M. A., C. Silva, C. Hidalgo, B. A. Carreras, R. O. Orozco, D. Carralero, and TJ-II team “Evidence of Long-Distance Correlation of Fluctuations during Edge Transitions to Improved-Confinement Regimes in the TJ-II Stellarator”, Phys. Rev. Lett., 100, 215003 (2008)
- Pereira R.C., J.Sousa, A.M. Fernandes, F. Patrício, B. Carvalho, A. Neto, C.A.F. Varandas, G. Gorini, M. Tardocchi, D. Gin, A. Shevelev, “ATCA Data Acquisition system for gamma ray spectrometry”, Fusion Engineering and Design, 83, IS 2-3, pg:341-345, 2008
- Perez von Thun CP, M Maraschek, S da Graça, RJ Buttery, A Herrmann, J Stober, G Conway, T Eich, JC Fuchs, LD Horton, V Igochine, A Kallenbach, A Loarte, HW Müller, I Nunes, G Saibene, R Sartori, ACC Sips, W Suttrop, E Wolfrum and the ASDEX Upgrade Team, “Identifying the MHD signature and power deposition characteristics associated with type-II ELMs in ASDEX Upgrade”, Plasma Physics and Controlled Fusion, 50, 6, 065018, 2008
- Piovesan P, V. Igochine, P. Lauber, K. Sassenberg, A. Flaws, M. Garcia-Munoz, S. Günter, M. Maraschek, L. Marrelli, P. Martin, P.J. McCarthy and AUG Team, “TAE internal structure through high-resolution soft x-ray measurements in ASDEX Upgrade”, Nuclear Fusion, 48, 065001, 2008
- Plyusnin V. V., L. Jakubowski, J. Zebrowski, H. Fernandes, C. Silva, K. Malinowski, P. Duarte, M. Rabinski, and M. J. Sadowski, “Use of Cherenkov-type detectors for measurements of runaway electrons in the ISTTOK tokamak”, Rev. Sci. Instrum. 79, 10F505 (2008)
- Poli FM, SE Sharapov, SC Chapman and JET-EFDA Contributors, “Study of the spectral properties of ELM precursors by means of wavelets”, Plasma Physics and Controlled Fusion, 50, 9, 095009, 2008
- Poli FM, M. Garcia-Munoz, H.-U. Fahrbach, S. Günter and ASDEX Upgrade Team, “Observation and modeling of fast trapped ions losses due to neoclassical tearing modes”, Physics of Plasmas, 15, 032501, 2008
- Pütterich T, R Neu, R Dux, AD Whiteford, MGO Mullane and the ASDEX Upgrade Team, “Modelling of measured tungsten spectra from ASDEX Upgrade and predictions for ITER”, Plasma Physics and Controlled Fusion, 50, 8, 085016, 2008
- Rapp J, W Fundamenski, LC Ingesson, S Jachmich, A Huber, GF Matthews, P Morgan, MF Stamp and JET-EFDA Contributors. “Septum assessment of the JET gas box divertor”, Plasma Physics and Controlled Fusion, 50, 9, 095015, 2008
- Ribeiro T.T. and B. Scott, “Gyrofluid turbulence studies of the effect of the poloidal position of an axisymmetric Debye sheath”, Plasma Physics and Controlled Fusion, 50, 5, 055007, 2008
- Rodrigues P, JP Bizarro, “Images of tokamak equilibria with toroidal-current reversal”, IEEE Transactions on Plasma Science, 36, 4, 1088, Aug. 2008
- Rodrigues AP, N Cruz, B Santos, CAF Varandas, J-M Moret, J Berrino, BP Duval, “TCV Advanced Plasma Control System Software Architecture and Preliminary Results”, IEEE Transactions on Nuclear Science, vol. 55, 316-321 (2008).
- Ryter F., J.C. Fuchs, W. Schneider, A.C.C. Sips, A. Stäbler, J. Stober and ASDEX Upgrade Team “H- mode confinement properties close to the power threshold in ASDEX Upgrade”, Journal of Physics: Conference Series, 123, 012035 (2008).
- Schmid A, A. Herrmann, HW Müller, and the ASDEX Upgrade Team, “Experimental observation of the radial propagation of ELM induced filaments on ASDEX Upgrade”, Plasma Physics and Controlled Fusion, 50, 4, 045007, 2008
- Schrittwieser R., C. Ionita, P. Balan, C. Silva et al, “Turbulence and transport measurements with cold and emissive probes in ISTTOK”, Plasma Phys. Control. Fusion 50, 055004 (2008)

- Silva C., C. Hidalgo, H. Figueiredo, P. Duarte, H. Fernandes, I. Nedzelskiy, and M. A. Pedrosa, “*Experimental evidence of coupling between local turbulent transport and large scale fluctuations in the ISTTOK edge plasma*”, Phys. Plasmas 15, 120703 (2008)
 - Silva F. da and S. Heurax, “*Study of ITER plasma position reflectometer using a two-dimensional full-wave finite-difference time domain code*” Review of Scientific Instruments, 79(10):1F104-1-10F104-4, 2008
 - Sips ACC, O Gruber and the ASDEX Upgrade Team “*Compatibility of ITER scenarios with an all-W wall*”, Plasma Physics and Controlled Fusion, 50, 12, 124028, 2008
 - Svensson J, A Werner and JET-EFDA Contributors, “*Current tomography for axisymmetric plasmas*”, Plasma Physics and Controlled Fusion, 50, 8, 085002, 2008
 - Tabarés FL, MA Ochando, F Medina, D Tafalla, JA Ferreira, E Ascasibar, R Balbín, T Estrada, C Fuentes, I Garcia-Cortés, J Guasp, M Liniers, I Pastor, MA Pedrosa and the TJ-II Team “*Plasma performance and confinement in the TJ-II stellarator with lithium-coated walls*”, Plasma Physics and Controlled Fusion, 50, 12, 124051, 2008
 - Tardocchi M., I.L. Proverbio, G.Gorini, G. Grosso, M. Locatelli, I.N. Chugonov, D.B. Gin, A.E.Shevelev, A.Murari, V.G.Kiptily, B.Syme, A.M.Fernandes, R.C.Pereira, J.Sousa, JET-EFDA Contributors, “*Gamma ray spectroscopy at high energy and high time resolution at JET*”, Review of Scientific Instruments, 79, IS 10, 2008
 - Told D, F Jenko, P Xanthopoulos, LD Horton, E Wolfrum and ASDEX Upgrade Team, “*Gyrokinetic microinstabilities in ASDEX Upgrade edge plasmas*”, Physics of Plasmas, 15, 102306, 2008
 - Treutterer W., K. Behler, L. Giannone, N. Hicks, A. Manini, M. Maraschek, G. Raupp, M. Reich, A.C.C. Sips, J. Stober, W. Suttrop and ASDEX Upgrade Team, “*Real-time diagnostics at ASDEX Upgrade – Integration with MHD feedback control*”, Fusion Engineering and Design, 83, 300-300-303, 2008
 - Udintsev VS, O Sauter, E Asp, E Fable, TP Goodman, G Turri, JP Graves, A Scarabosio, G Zhuang, C Zucca and the TCV Team “*Global plasma oscillations in electron internal transport barriers in TCV*”, Plasma Physics and Controlled Fusion, 50, 12, 124052, 2008
 - Valcárcel D.F., A. Neto, J. Sousa, B.B. Carvalho, H. Fernandes, J.C. Fortunato, A.S. Gouveia, A.J.N. Batista, A.G. Fernandes, M. Correia, T. Pereira, I.S. Carvalho, A.S. Duarte, C.A.F. Varandas, M. Hron, F. Janky and J. Pisacka, “*An ATCA Embedded Data Acquisition and Control System for the Compass Tokamak*”, Fusion Engineering and Design, 2008
 - Varandas C, “*EURATOM strategy towards fusion energy*”, Energy Conversion & Management, 49, 1803, 2008.
 - Varandas C, “*A física e a energia*”, Gazeta de Física, 31, 3, 12, 2008.
 - Varandas C.A.F., C. Silva, V.A. Gribkov, A. Malaquias and G. Van Oost, Summary of the 17th International Atomic Energy Agency Technical Meeting on “*Research Using Small Fusion Devices*”, Nucl. Fusion 48, 7, 077001(2008)
 - Vermare L., C. Angioni, A. Bottino, A.G. Peeters and ASDEX Upgrade Team “ *β dependence of micro-instabilities using linear gyrokinetic simulations*” Journal of Physics Conference Series, 123, 012040, 2008
 - Vilela Mendes R, Fernanda Cipriano, “*A stochastic representation for the Poisson-Vlasov equation*” Communications in Nonlinear Science and Numerical Simulation, 13 (2008) 221-226
 - Vries de PC, E Joffrin, NC Hawkes, X Litaudon, CD Challis, Y Andrew, M Beurskens, M Brix, J Brzozowski, K Crombé, C Giroud, J Hobirk, T Johnson, J Lönnroth, A Salmi, T Tala, V Yavorskij, K-D Zastrow and JET EFDA Contributors, “*Effect of toroidal field ripple on the formation of internal transport barriers*”, Plasma Physics and Controlled Fusion, 50, 6, 065008, 2008
- 26.1.3. Contributions in Conferences and Workshops**
- 26.1.3.1. Invited talks in conferences**
- Annual Meeting of the Special Expert Working Group “Transient Loads” September 2008, Culham, UK.**
- Plyusnin VV and JET-EFDA Contributors, “*Characterization of runaway electron generation process at major disruptions*”.
- 18th International Conference on plasma Surface Interactions Toledo, Spain, May 26 - 30, 2008.**
- Lehnen M., S.S. Abdullaev, G. Arnoux, S.A. Bozhenkov, M.W. Jakubowski, R. Jaspers, V.V. Plyusnin, V. Riccardo, U. Samm and JET EFDA Contributors and the TEXTOR team “*Runaway generation during disruptions in JET and TEXTOR*”
- Workshop on Runaway Electrons in ITER. Cadarache, July 15-17, 2008.**
- Plyusnin V.V. and JET-EFDA Contributors, “*Trends in runaway electron generation at disruptions in JET*”
- 26.1.3.2. Oral contributions**
- Materiais 2008, 5-8 April, Lisbon**
- Nunes D., V. Livramento, J.B. Correia, K. Hanada, P.A. Carvalho, R. Mateus, N. Shohoji, H. Fernandes, C. Silva, E. Alves, E. Osawa, “*Consolidation of Cu-nD nanocomposites; hot extrusion vs spark plasma sintering*”
- EFTSOMP2008 - 11th Workshop on Electric Fields, Turbulence and Self-Organisation in Magnetized Plasmas, Crete, Greece, June 2008**
- Figueiredo H., *Structure of the ISTTOK edge plasma fluctuations*

SPEEDAM - 19th International Symposium on Power Electronics, Electrical Drives, Automation and Motion, Ischia (Italy), 11-13 June 2008

- Carvalho I. S., et al., "Fast digital link for a tokamak current source control"

2º Encontro CIÊNCIA 2008, Fundação Calouste Gulbenkian, Lisboa, 2-4 July 2008

- Gonçalves B., "Instrumentação avançada para o ITER"
- Varandas C., F. Serra and L.O. Silva, "Apresentação das Linhas de Actividade em Projectos Internacionais de grande dimensão do IPFN – LA"

35th European Physical Society Conference on Plasma Physics, June 9-13, 2008, Hersonissos, Crete, Greece.

- Graça S. da, G.D.Conway, M.Maraschek, A. Silva, E. Wolfrum, R. Fisher, L.Cupido, F. Serra, M.E.Manso and the ASDEX Upgrade Team, "Studies of edge MHD modes in H-mode discharges in ASDEX Upgrade using reflectometry"

13th EU-US Transport Force Transport workshop 1-4 September 2008 Copenhagen, Denmark

- Nabais F. "Fast ion losses by Alfvén eigenmodes and fishbones in JET"
- Ribeiro T.T., "Gyrofluid turbulence simulations near the X-point: drift wave vs. interchange turbulence"
- Silva C., "Experimental evidence of local turbulent transport regulation by long-range correlations in the ISTTOK edge plasma"

18th IAEA Technical Meeting on Research Using Small Fusion Devices, Alushta, Ukraine, 25-27 September, 2008

- Nedzelskiy I. S., C. Silva, D. Alves, R. Coelho, H. Fernandes, "Plasma density fluctuations measurements by heavy ion beam probe with a multiple cell array detector on the tokamak ISTTOK"

22nd IAEA Fusion Energy Conference, Geneva, Switzerland, 13-18 October 2008, EX/3-3

- Tala T., J. Ferreira, P. Mantica, A.G. Peeters, G. Tardini, P.C. de Vries, K.-D. Zastrow, M. Brix, G. Corrigan, C. Giroud, I. Jenkins, V. Naulin, D. Stryntzi, T. Versloot e JET-EFDA contributors, "Experimental evidence on inward momentum pinch on JET and comparison with theory and modeling"
- C. Silva, H. Fernandes, C.A.F. Varandas, D. Alves, B.B. Carvalho, I. Carvalho, P. Carvalho, P.A. Carvalho, R. Coelho, A. Duarte, P. Duarte, H. Figueiredo, J. Figueiredo, J. Fortunato, R. Gomes, B. Gonçalves, I. Nedzelskiy, A. Neto, T. Pereira, V. Plyusnin, D. Valcárcel, "Overview of recent ISTTOK results"

Garching-Greifswald Theory Meeting, Ringberg, Germany, November 2008

- Ribeiro T.T., "Gyrofluid turbulence simulations near the X-point: drift wave vs. interchange turbulence"

MRS fall meeting, 1-5 December, Boston

- Mateus R., P.A. Carvalho, D. Nunes, L.C. Alves, N. Franco, J.B. Correia, H. Fernandes, C. Silva, R. Lindau, E. Alves, "Microstructure characterization of ODS-RAFMs steels"

"Ringberg" Programme Seminar, 27-31 October 2008, Ringberg Castle

- Silva A., IPFN reflectometry Group and ASDEX Upgrade Team, ASDEX Upgrade "Plans for the ASDEX Up reflectometry upgrades"

26.1.3.3. Poster Contributions

EPS/SIF Energy Meeting, Varenna, Italy 7-8 April 2008

- Varandas C and MP Alonso, "The Portuguese Strategy and R&D Programmes on Energy;"

18th International Conference on Plasma-Surface interactions, Toledo, 25-31 May 2008

- Alonso J.A., P. Andrew, A. Neto, J.L. de Pablos, E. de la Cal, H. Fernandes, W. Fundamenski, C. Hidalgo, G. Kocsis, A. Manzanara, A. Murari, G. Petravich, R.A. Pitts, L. Rios, C. Silva, EFDA-JET contributors, "Fast visible imaging of ELMs wall interaction on JET"
- Gomes R. B., H. Fernandes, C. Silva, A. Sarakovskis, T. Pereira, J. Figueiredo, B. Carvalho, A. Soares, P. Duarte, C. Varandas, O. Lielausis, A. Klyukin, E. Platacis, I. Tale and A. Alekseyev "Plasma-liquid gallium jet interaction studies in ISTTOK tokamak"
- Livramento V., J.B. Correia, D. Nunes, P.A. Carvalho, H. Fernandes C. Silva, K. Hanada, N. Shohoji, E. Osawa, "Development of W-nDiamond nanostructured composites for fusion devices"
- Nunes D., I. D. Nogueira, P. A. Carvalho, J.B. Correia, N. Shohoji, R. B. Gomes, H. Fernandes, C. Silva "On hydrogen diffusion in tungsten and copper probes at ISTTOK"
- Silva C., B. Gonçalves, C. Hidalgo, M.A. Pedrosa, W. Fundamenski, M. Stamp, R.A. Pitts and JET-EFDA contributors, "Intermittent transport in the JET far-SOL"
- Borges F.O., M.P. Alonso, L. A. Berni, J.I. Elizondo, L. C. Jeronino, R.M.O. Galvão, M. Machida, J.H. Severo, C.A.F. Varandas, "The multipoint Thomson scattering diagnostic for the TCABR tokamak"
- Carvalho P. J., B.B. Carvalho, A. Neto, A. Duarte, R. Coelho, H. Fernandes, J. Sousa and C. Varandas "A real-time tomography diagnostic and control system in ISTTOK"

- Coelho R. and D. Alves, “Real-time estimation of the poloidal wavenumber of ISTTOK tokamak magnetic fluctuations”
- Cupido L., A. Cardinali, R.Igreja, F.Serra, M.E.Manso, A.Murari and JET EFDA Contributors, “High resolution Fast wave reflectometry, system design challenges”.
- Figueiredo ACA, A Fonseca, L Meneses, and JET-EFDA Contributors, “Systematic and routine analysis of radial correlation reflectometry data in JET”
- Fonseca A., A.C.A. Figueiredo, J. Fessey, L. Cupido, B. Alper, N. Cruz, L. Meneses, A. Sirinelli, M.E. Manso, M. Walsh and JET EFDA contributors, “In-Situ Calibration of the Correlation Reflectometry Systems on the Joint European Torus Tokamak”
- Marques T. G., A. Gouveia, T. Pereira, J. Fortunato, B. B. Carvalho, J. Sousa, C. Silva, and H. Fernandes, “Real-time digital heterodyne interferometer for high resolution plasma density measurements at ISTTOK”
- Nedzelskiy I. S., R. Coelho, D. Alves, C. Silva, and H. Fernandes, “Observation of plasma density fluctuations by a heavy ion beam probe diagnostic with multiple cell array detector on the tokamak ISTTOK”
- Plyusnin V. V., L. Jakubowski, J. Zebrowski, H. Fernandes, C. Silva, K. Malinowski, P. Duarte, M. Rabinski, and M. J. Sadowski, “Use of Cherenkov-type detectors for measurements of runaway electrons in the ISTTOK tokamak”
- Silva F. da and S. Heurax “Study of ITER plasma position reflectometer using a two-dimensional full-wave finite-difference time domain code”
- Ionita C., R. Schrittwieser, C. Silva, P. Balan, H. Figueiredo, V. Naulin, J. Juul Rasmussen, “Turbulence measurements with cold and emissive probes in ISTTOK”
- Oost G. Van, R.B. Gomes, M. Gryaznevich, H. Fernandes, C. Silva, A. Malaquias, A.Czarnecka, M.Dreval, P.Duarte, H. Figueiredo, C. Gutierrez-Tapia, P.Korshid, A. Melnikov “Overview of results from the IAEA-CRP 3rd International Joint Experiment on the tokamak ISTTOK”
- Pedrosa M.A., C. Silva, C. Hidalgo, D. Carralero, B.A. Carreras, R.O. Orozco and the TJ-II team “Long-distance correlations of fluctuations and sheared flows during transitions to improved confinement regimes in the TJ-II stellarator”
- Plyusnin V. V., L. Jakubowski, J. Zebrowski, H. Fernandes, C. Silva, P. Duarte, K. Malinowski, M. Rabinski, M.J. Sadowski, “Detection of runaway electrons using Cherenkov-type detectors in the ISTTOK Tokamak”
- Ribeiro T.T., B. Scott, “Drift wave vs. interchange turbulence geometrical effects on the ballooning threshold”. Europhysics Conference Abstracts, Vol. 32D, P-5.039 (2008)
- Rodrigues P. and J. P. S. Bizarro, “Noniterative equilibria reconstruction without up-down symmetry”
- Silva C., H. Figueiredo, H. Fernandes, P. Duarte, G. Van Oost, A. Melnikov, C. Gutierrez-Tapia, “Structure of the ISTTOK edge plasma fluctuations”
- Sips A.C.C., P. Lomas, O. Gruber, J. Hobirk, G.M.D. Hogewij, L.D. Horton, F. Imbeaux, M. Mattei, F. Köchl, X. Litaudon, E. de la Luna, A. Lysoivan, Y-S Na, I. Nunes, V. Parail, V. Plyusnin, J. Kim, J. Romero, G. Saibene, J. Seol, J. Stober, L. Zabeo, and the AUG Team and JET EFDA contributors. “Current rise studies at ASDEX Upgrade and JET in preparation for ITER”
- Thomsen H., P.J. Carvalho, S. Gori, U. v. Toussaint, A. Weller, R. Coelho, H. Fernandes, “Application of Neural Networks for Fast Tomographic Inversion on Wendelstein 7-X,”

50th American Physical Society Division of Plasma Physics Meeting

- Nave M.F. F., T. Johnson, B. Alper, L.-G. Eriksson, C. Giroud, M.-L. Mayoral, J. Ongena, A. Salmi, K.-D. Zastrow, JET-EFDA Contributors, “The influence of magnetic field ripple on JET Intrinsic Rotation”

7th Iberian Vacuum Meeting (RIVA 7), Caparica, Portugal, June 2008

- Marques T. G., A. Gouveia, T. Pereira, J. Fortunato, B. B. Carvalho, J. Sousa, C. Silva, and H. Fernandes, “Study for the real-time control of the ISTTOK hydrogen injection system”

35th European Physical Society Conference on Plasma Physics, June 9-13, 2008, Hersonissos, Crete, Greece.

- Bizarro J. P. S. and P. Rodrigues, “Grad-Shafranov equilibria with negative core toroidal current vs. experimental data”, in Proceedings Europhysics Conference Abstracts, Vol. 32D, P-4.065 (2008).
- Eriksson L.-G, T. Hellsten, K. Holmström, T. Johnson, J. Brzozowski, F. Nave, J. Ongena, K.-D. Zastrow and JET EFDA contributors, “Simulation of Fast Ion Contribution to Toroidal Rotation in ICRF Heated JET Plasmas”

Calculus of Variations and its Applications from Engineering to Economy. Lisbon, 8 -10 September 2008

- Cipriano F., “Navier-Stokes equation and diffusions on the group of homeomorphisms of the torus”.

25th Symposium on Fusion Technology, Rostock, Germany, 15-19 September 2008

- Guilhem D., J. Achard, G. Agarici, A. Argouarch, A. Becoulet, J. H. Belo, G. Berger-by, B. Bertrand, E. Bertrand, Ph. Bibet, C. Brun, M. Chantant, E. Delmas, L. Delpuch, L. Doceul, S. Dutheil, A. Ekedahl, F. Faisse, C. Goletto, M. Goniche, J. C. Hatchressian, J. Hillairet, G. Houry, L. Jourd’heuil, F. Kazarian, M. Lipa, X. Litaudon, G. Lombard, S. Madeleine, R. Magne, A. Martinez, J. L. Mayerhoffer, M. Missirlian, S. Poli, C. Portafaix, D. Raulin, F. Samaille,

A. Saille, B. Soler, D. Thouvenin, K. Vulliez, "A new concept of a Passive Active Multi-junction launcher for Tore-Supra long pulse experiments"

- Hillairet J., M. Goniche, A. Ekedahl, D. Voyer, J. Belo, "Modelling of lower hybrid antennas using the ALOHA code, comparisons with Tore Supra experiments"
- Hron, M, F Janky, O Bilykova, J Havlicek, A Neto, H Fernandes, J Sousa, M Cavinato, J Pisacka, J Horacek, J Adamek, B Carvalho, D Valcarcel, J Fortunato, A Duarte, T Pereira, I Carvalho, A Batista, R Panek, and C Varandas "Control, data acquisition, and communication system for the COMPASS tokamak"
- Murari A., J.Vega, G.Vagliasindi, J.A.Alonso, D.Alves, R.Coelho, S.DeFiore, J.Farthing, C.Hidalgo, G.A.Rattá, and JET-EFDA Contributors, "Recent Developments in Data Mining and Soft Computing for JET with a view on ITER"
- Neto A, Silva C, Sousa J, et al., "ITER CODAC interface for the visible and infra-red wide angle viewing cameras"
- Neto A, H Fernandes, J Sousa, B Carvalho, D Valcarcel, A Batista, I Carvalho, A Duarte, J Fortunato, T Pereira, C Varandas, M Hron, F Janky, and J Pisacka "An ATCA embedded data acquisition and control system for the Compass tokamak"
- Neto A, Sartori F, Piccolo F, et al., "Linux Real Time Framework for Fusion Devices"

International Conference and School on Plasma Physics and Controlled Fusion Alushta-2008, Alushta, Ukraine, 22-27 September, 2008

- Nedzelskiy I.S., C. Silva, H. Fernandes, C. Hidalgo, "Retarding field energy analyzers for ion temperature measurements in the boundary plasmas of the tokamak ISTTOK and TJ-II stellarator"

29th Conference on Quantum Probability and Related Topics. Hammamet, Tunisia, 13-18 October 2008

- Cipriano F., "Stochastic solutions of a nonlinear fractional differential equation"
- Hoang G.T., A. Bécoulet, J.F. Artaud, B. Beaumont, J.H. Belo, G. Berger-By, J.P.S. Bizarro, P. Bonoli, J. Decker, L. Delpech, A. Ekedahl, J. Garcia, G. Giruzzi, M. Goniche, C. Gormezano, D. Guilhem, J. Hillairet, F. Imbeaux, F. Kazarian, C. Kessel, S.H. Kim, J.G. Kwak, J. Lister, X. Litaudon, R. Magne, S. Milora, F. Mirizzi, J.M. Noterdaeme, R. Parker, Y. Peysson, D. Rasmussen, P.K. Sharma, M. Schneider, E. Synakowski, A. Tanga, A. Tuccillo, Y.X. Wan, "A Lower Hybrid Current Drive system for ITER"
- Ongena J, Yu.Baranov, V.Bobkov, C.D.Challis, S.Conroy, A. Ekedahl, G.Ericsson, M.Goniche, Ph.Jacquet, I.Jenkins, L.Giacomelli, C.Hellesen, A.Hjalmarsson, J.Källne, V.Kiptily, K.Kirov, A.Krasilnikov, M.Laxåback, E.Lerche, J.Mailloux, M.L.Mayoral, I.Monakhov, M.Nave, V.Petrzilka, K.Rantamaki, E.Solano, D.Van Eester, A.Walden and JET

EFDA Contributors, "Heating optimization studies at JET in support of ITER"

- Mazzitelli G., M. L. Apicella, M. Marinucci, A. Alekseyev, G. Apruzzese, P. Buratti, R. Cesario, L. Gabellieri, V. Lazarev, I. Lyublinski, C. Mazzotta, S. Mirnov, V. Pericoli Ridolfini, A. Romano, O. Tudisco, A. Vertkov, R. Zagorski, FTU Team, ECRH Team, R. B. Gomes, H. Fernandes, C. Silva, C. Varandas, O. Lielausis, A. Klyukin and E. Platacis, "Status and Perspectives of the Liquid Material Experiments in FTU and ISTTOK"
- Nightingale M, F. Durodie, A. Argouarch, G. Berger-By, T. Blackman, J. Caughman, V. Cocilovo, P. Dumortier, D. Edwards, J. Fanthome, D. Frigione, R. Goulding, M. Graham, J. Hobirk, S. Huygen, S. Jachmich, P. Jacquet, P. Lamalle, T. Loarer, R. Maggiora, M.-L. Mayoral, A. Messiaen, D. Milanese, I. Monakhov, M. Nave, K. Nicholls, J. Ongena, F. Rimini, D. Stork, C. Sozzi, M. Tsalas, M. Vervier, M. Vrancken, A. Walden, A. Whitehurst, KD. Zastrow and JET EFDA contributors, "Development of the JET Ion Cyclotron Resonance Frequency Heating System in Support of ITER"
- Paley J.I., F.Felici, J.Berrino, S.Coda, N.Cruz, B.P.Duval, T.P.Goodman, Y.Martin, J.M.Moret, F.Piras, A.P.Rodrigues, B.Santos, C.A.F.Varandas and the TCV team, "Real Time Control of Plasmas and ECRH Systems on TCV"
- Parail V., P. Belo, P. Boerner, X. Bonnin, G. Corrigan, D. Coster, J. Ferreira, A. Foster, L. Garzotti, G.M.D. Hogewej, W. Houlberg, F. Imbeaux, J. Johner, F. Kochl, V. Kotov, L. Lauro-Taroni, X. Litaudon, J. Lonroth, G.Pereverzev, Y. Peysson, G. Saibene, R. Sartori, M. Schneider, G. Sips, P. Strand, G. Tardini, M.Valovic, S. Wiesen, M. Wischmeier, R. Zagorski, EU ITM Task Force and EFDA JET contributors, "Integrated Modelling for ITER in EU"

MRS fall meeting, 1-5 December, Boston

- Nunes D., P.A. Carvalho, R. Mateus, I.D. Nogueira, A. Moita de Deus, J.B. Correia, N. Shohoji, R.B. Gomes, H. Fernandes, C. Silva, N. Franco, E. Alves, "Effects of hydrogen permeation on W, Mo and Cu Langmuir probes at ISTTOK"
- Nunes D., V. Livramento, J.B. Correia, R. Mateus, P.A. Carvalho, N. Shohoji, H. Fernandes, C. Silva, E. Alves, K. Hanada, E.Osawa, "W-nDiamond/Cu-nDiamond nanostructured composites for fusion devices"

26.1.4. Internal Report

- Alonso MP and HD Stryczewska, *Draft for a proposal to measuring electron temperature in a industrial plasma using Thomson scattering technique for the Institute of Electrical Engineering and Electrotechnologies, Thecnical University of Lublin, Poland, IPFN, 17 April 2008.*
- Varela, P. and Manso, M., *Draft Final Report on EFDA Contract nr. 06-1449, June 2008.*

26.1.5. Other Publications

- Silva A., J. Zajac, M. Manso, "Design of a reflectometry system for the Compass-D Tokamak", February 2008.
- Silva A., M. Manso, P. Varela, G. Conway, "Proposal to upgrade the ASDEX Upgrade FMCW reflectometer", February 2008.
- Achard J. and J. Belo, "Réception électrique des composants prototypes de l'antenne C4", DRFC-CEA report CIMES/NTT-2008.001 (2008)
- Silva F. da, Stéphane Heurax and Evgeniy Gusakov "A Numerical Study Of Forward- And Back-Scattering Signatures On Doppler Reflectometry Signals", (Submetido em 20/8/2008 para apreciação como relatório interno).
- Alonso MP and F Serra, Fusion Expo Support Action Call for Participation – Fusion Expo, EFDA Reference: CfO WP08-PI June 20 2008

26.1.6. Laboratorial Prototypes

- Silva A, "Four channel high gain wideband voltage-controlled if detection amplifier"
- Silva A, " Two channel broadband millimeter wave reflectometer for the TCA/Br Tokamak"
- Figueiredo H., "Gundestrup probe for the determination of the poloidal and toroidal plasma velocity"
- Fortunato J, OGS L " (Optical gigabit serial link) hardware module in a 22cm 6U Eurocard format to be used as a communication link between the VS controller and the Fast Radial Field Amplifier (ERFA) in JET".
- -
- Silva C., "Array of electric probes with 20 pins for the study of the plasma poloidal asymmetries"
- TE₁₀ to TE₃₀ mode converter - A prototype of the TE₁₀ to TE₃₀ mode converter for Tore Supra's new LH PAM launcher was made. Low-level RF tests revealed performances in accordance with the predictions.
- PAM module - The prototype of a PAM module for Tore Supra's new LH launcher was completed. Low-level RF measurements were found to be in agreement with the numerical modelling of the device.

26.1.7. Computer codes

- Carvalho P., Tomographic reconstruction code: a code based on the Fourier-Bessel algorithm but taking into account the finite width of the viewing cone of each sensor and using different radial basis functions that can be adapted to different magnetic configurations
- Coelho R., D. Alves, Coherency spectrum implementation using Kalman filtering: This code is an implementation of the well known coherency spectral analysis with the innovation that the Fourier transform is replaced by the Kalman filter spectral estimation algorithm. This allows much higher output

estimation of the coherent spectrum characteristics (wavenumber vs time)

- Coelho R., D. Alves, Parallelised algorithm for the EMD-HHT: This code implements the Empirical Mode Decomposition and Hilbert-Huang Transform method for the time-frequency characterization of digitized signals. The parallelization is achieved using signal partition and SSH remote invocation
- Coelho R., D. Alves, Kalman Filter MSE amplitude estimator: The Kalman filter has been proposed as an amplitude estimation method of known frequency components in quasi-periodic signals. It provides an improved filtering capability as well as the minimization of the Edge Localized Modes (ELMs) impact and 50 Hz power grid component when compared with the conventional lockin-amplifier signal processing for the Motional Stark Effect (MSE) diagnostic signals
- Coelho R., D. Alves, Kalman Filter Synchronous Detector: This algorithm is basically a flexible, computationally efficient and with a high output rate Real-Time Non-Stationary BandPass Filter. It was developed to perform a real-time non-stationary spectral selection (in the time domain) for subsequent mode number analysis
- Figueiredo H., Turbulence characterization: This code evaluated the plasma particle and momentum transport based on electric probe measurements

26.1.8. Master thesis

- Carvalho I. S., "Amplificadores de potência comutados para o tokamak ISTTOK", Universidade Técnica de Lisboa, 2008
- Cruz N., "Sistema de Controlo e Aquisição de Dados do Reflectómetro de Correlação do JET", Universidade Técnica de Lisboa, 2008
- Duarte A., Implementação de Middleware genérico no CODAC do ISTTOK. Universidade Técnica de Lisboa, 2008
- Figueiredo J., "Espectroscopia e imagem no tokamak ISTTOK", Universidade Técnica de Lisboa, 2008
- Fortunato J.C., "Sistema de Temporização e Gestão de Eventos Rápidos" Universidade Técnica de Lisboa, 2008
- Marques T., "Real-Time measurement of the plasma electron density at ISTTOK and study of the ISTTOK hydrogen injection system" Universidade Técnica de Lisboa, 2008
- Ricardo P., "Software de Teste e de Desenvolvimento para Controlo e Aquisição de Dados em Fusão Nuclear". Universidade Técnica de Lisboa, 2008

- Valcárcel D.F., “*Controlo em Tempo-Real da Posição da Coluna de Plasma no Tokamak ISTTOK*”, Universidade Técnica de Lisboa, 2008

26.1.9. PhD. Thesis

- Santos J., “*Fast reconstruction of reflectometry density profiles on ASDEX Upgrade for plasma position feedback purposes*” Universidade Técnica de Lisboa, 2008

26.1.10. Organizing Committees of Conferences

The 8th EFDA Public Information Group Meeting, 8 - 9 May 2008, Lisbon

- Serra F and Alonso MP (Local Committee)

26.1.11. Public Information Activities

- Alonso MP and C Varandas, Talk's movie translation to portuguese of the movie “*Fusion Classroom 2100*” http://www.efda.org/download_pmlib/movies/Classroom_2100_English_low.mpg
- Alonso MP, C Varandas and F Serra, Translation to Portuguese of the EFDA Poster, *Fusion Energy - Cleaner Energy for the future*.
- Alonso MP, “Fórum Ciência Viva”, 22 - 23 November 2008, Participation in the "Science alive Forum", Lisbon, FIL (1 Stand).

26.2. TECHNOLOGIES OF PLASMAS AND LASERS

26.2.1. Publications in books

- Bertolami O., “*The mystical formula and the mystery of Khronos*”, Contribution to the volume ‘Minkowski Spacetime: A Hundred Years Later’ to be published by Springer in the series ‘Fundamental Theories of Physics’ edited by V. Petkov [arXiv:0801.3994 [gr-qc]]
- Bertolami O., T. Harko, F. S. N. Lobo and J. Páramos, “*Non-minimal curvature-matter couplings in modified gravity*”, Contribution to the anniversary volume “The Problems of Modern Cosmology”, on the occasion of the 50th birthday of Prof. S. D. Odintsov. Editor: Prof. P. M. Lavrov, Tomsk State Pedagogical University [arXiv:0811.2876 [gr-qc]]
- Felizardo E., F. M. Dias, E. Tatarova, G. Ferreira, J. Henriques and C. M. Ferreira, “*Microwave plasma torches driven by surface waves for bacteria treatment*”, Plasmas for Environmental Issues, ed. by E. Tatarova, A. Ricard and E. Benova
- Marques L., C.D. Pintassilgo, G. Alcouffe, L.L. Alves, G. Cernogora “*Modelling of a CCP-RF discharge used for the simulation of Titan's chemistry*”, Fifth International Conference on Physics of Dusty Plasmas, (T. Mendonça et al eds.), Ponta Delgada (Azores), Portugal, AIP Conference Proceedings (Multifacets of Dusty Plasmas) 1041, 169 (2008).

- Marti M., L. Gargaté, R.A. Fonseca, L.L. Alves, J.P.S. Bizarro, P. Fernandes, J.P.M. Almeida, H. Pina, F.M. Silva, L.O. Silva “*The IST Cluster: an integrated infrastructure for parallel applications in Physics and Engineering*”, IBERGRID'2008: 2nd Iberian Grid Infrastructure Conference (L. Ribeiro, T. Vieira et al eds.), Porto, Portugal 2008.

- Mendonça J. T., J. Loureiro, H. Terças and R. Kaiser, “*Plasma effects in cold atom physics*”, New Aspects of Plasma Physics (ed. Padma K. Shukla, Lennart Stenflo and Bengt Eliasson), World Scientific (Singapore) 2008, Proceedings of the 2007 ICTP Summer College on Plasma Physics, p.133-151.

- Mendonça J.T., D. Resendes and P.K. Shukla editors, “*Multifacets of Dusty Plasmas*”, American Institute of Physics, New York (2008)

- Mendonça J.T., “*Nonlinear optics of ultra-short laser pulses: cascades and sliding resonances*”, in “Atoms and Molecules in Laser and External Fields”, edited by Man Mohan, Narosa, New Delhi, pages 157-164 (2008)

26.2.2. Publications in refereed scientific journals

- Álvarez R., L.L. Alves, “*Numerical solution to an electromagnetic model with Neumann boundary conditions, for a microwave-driven plasma reactor*”, J. Phys. D: Appl. Phys. 41, 215204 (2008).
- Álvarez R., L.L. Alves, “*Images of the Electromagnetic-Field Distribution in a Microwave Reactor Excited by an Axial Injection Torch*”, IEEE Trans. Plasma Sci. 36(4), 1378 (2008).
- Annanatonne B.M., A. Biancalani, D. Bruno, M. Capitelly, F. Caccherini, E. Daly, P. Doiomedea, G. D'Ammando, A. Hilgers, S. Longo, S. Mercuccio, J.T. Mendonça, V. Naguibede, F. Pegoraro and J.R. Sanmartin, “*Plasma kinetics issues in an ESA study for a plasma laboratory in space*”, Plasma Phys. Control. Fusion, 50, 074016 (2008)
- Atzeni S., C. Bellei, J.R. Davies, R.G. Evans, J.J. Honrubia, Ph. Nicolai, X. Ribeyre, G. Schurtz, A. Schiavi, J. Badziak, J. Meyer-ter-Vehn, M. Olazabal, L. Silva and G. Sorasio, *Fast ignitor target studies for HiPER, Journal of Physics: Conference Series 112 022062 (2008)*
- Atzeni S., A. Schiavi, J. J. Honrubia, X. Ribeyre, G. Schurtz, Ph. Nicolai, M. Olazabal-Loumé, C. Bellei, R. G. Evans, and J. R. Davies, *Fast ignitor target studies for the HiPER project, Phys. Plasmas 15, 056311 (2008)*
- Bamford R, Gibson KJ, Thornton AJ, Bradford J, Bingham R, Gargate L, Silva LO, Fonseca RA, Hapgood M, Norberg C, Todd T, Stamper R, “*The interaction of a flowing plasma with a dipole magnetic field: measurements and modelling of a diamagnetic cavity relevant to spacecraft protection*”, *Plasma Phys. Control. Fusion, 50 (12): Art. No. 124025 Dec 2008*

- Barreiro T., O. Bertolami and P. Torres, *WMAP5 constraints on the unified model of dark energy and dark matter*, *Phys. Rev. D* 78 (2008) 043530 [arXiv:0805.0731 [astro-ph]]
- Bastos C., O. Bertolami, N. C. Dias and J. N. Prata, “Weyl-Wigner formulation of noncommutative quantum mechanics”, *J. Math. Phys.* 49, 072101 (2008) [arXiv: hep-th/0611257]
- Bastos C., O. Bertolami, N. C. Dias and J. N. Prata, “Phase-Space Noncommutative Quantum Cosmology”, *Phys. Rev. D* 78 (2008) 023516 [arXiv:0712.4122 [gr-qc]]
- Bastos C. and O. Bertolami, “The Berry phase in the noncommutative gravitational quantum well”, *Phys. Lett. A* 372, 5556 (2008) [arXiv:gr-qc/0606131]
- Bendoyro, RA; Onofrei, RF; Sampaio, J; et al., “Plasma channels for electron accelerators using discharges in structured gas cells”, *IEEE Transactions on Plasma Science*, 36 (4): 1728-1733 Part 4 AUG 2008
- Bernardini A. E. and O. Bertolami, “Stationary condition in a perturbative approach for mass varying neutrinos”, *Phys. Lett. B* 662 (2008) 97 [arXiv:0802.4449 [hep-ph]]
- Bernardini A. E. and O. Bertolami, “Perturbative approach for mass varying neutrinos coupled to the dark sector in the generalized Chaplygin gas scenario”, *Phys. Rev. D* 77 (2008) 083506 [arXiv:0712.1534 [astro-ph]]
- Bernardini A. E. and O. Bertolami, “Lorentz violating extension of the Standard Model and the Beta-decay endpoint”, *Phys. Rev. D* 77 (2008) 085032 [arXiv:0802.2199 [hep-ph]]
- Bertolami O., “Dark energy, dark matter and gravity”, *Int. J. Mod. Phys. D* 16, 2003 (2008) [arXiv:astro-ph/0608276]
- Bertolami O., “A Curvature Principle for the interaction between universes”, *Gen. Rel. Grav.* 40 (2008) 1891 [arXiv:0705.2325 [gr-qc]]
- Bertolami O., F. Francisco, P. J. S. Gil and J. Páramos, “Thermal Analysis of the Pioneer Anomaly: A method to estimate radiative momentum transfer”, *Phys. Rev. D* 78 (2008) 103001 [arXiv:0807.0041 [physics.space-ph]]
- Bertolami O., F. S. N. Lobo and J. Páramos, “Non-minimum coupling of perfect fluids to curvature”, *Phys. Rev. D* 78 (2008) 064036 [arXiv:0806.4434 [gr-qc]]
- Bertolami O. and J. Páramos, “On the non-trivial gravitational coupling to matter”, *Class. Quant. Grav.* 25 (2008) 245017 [arXiv:0805.1241 [gr-qc]]
- Bertolami O. and J. Páramos, “Do $f(R)$ theories matter?” *Phys. Rev. D* 77 (2008) 084018 [arXiv:0709.3988 [astro-ph]]
- Bertolami O. and R. Rosenfeld, “The Higgs portal and an unified model for dark energy and dark matter”, *Int. J. Mod. Phys. A* 23 (2008) 4817 [arXiv:0708.1784 [hep-ph]]
- Christophe B. et al., “Odyssey: a Solar System Mission”, *Exper. Astron.* 10.1007/s10686-0089084-y [arXiv:0711.2007 [gr-qc]]
- Coppa GGM, Dulla S, Peano F, Ravetto P, “Alternative forms of the time-dependent neutron transport equation,” *Progress in Nuclear Energy* 50: 934–938, 2008
- Faure J, Fonseca RA, Neely D., “Laser and plasma accelerators” *workshop 2007 editorial, IEEE Transaction Plasma Science* (2008) 36 (4): pp 1690-1693 AUG 2008
- Fonseca RA, Martins SF, Silva LO, Tonge JW, Tsung FS, Mori WB, “One-to-one direct modeling of experiments and astrophysical scenarios: pushing the envelope on kinetic plasma simulations”, *Plasma Physics and Controlled Fusion*, 50 (12): Art. No. 124034 Dec 2008
- Gargate L, Bingham R, Fonseca RA, Bamford R, Thornton A, Gibson K, Bradford J, Silva LO, “Hybrid simulations of mini-magnetospheres in the laboratory”, *Plasma Physics and Controlled Fusion*, 50 (7): Art. No. 074017 JUL 2008
- Gargate L, Fonseca RA, Bingham R, Silva LO, “Expansion of a plasma cloud into the solar wind”, *IEEE Transactions on Plasma Science*, 36 (4): 1168-1169 Part 1 Aug 2008
- Gautier J, Zeitoun P, Hauri C, Morlens AS, Rey G, Valentin C, Papalarazou E, Goddet JP, Sebban S, Burgy F, Mercère P, Idir M, Dovillaire G, Levec X, Bucourt S, Fajardo M, Merdji H and Caumes JP, “Optimization of the wave front of high order harmonics”; *Eur. Phys. J. D*, 48, 459-463 (2008)
- Glinec Y, Faure J, Lifschitz A, Vieira JM, Fonseca RA, Silva LO, Malka V., “Direct observation of betatron oscillations in a laser-plasma electron accelerator”, *EPL* 81 (6): Art. No. 64001 MAR 2008
- Green J. S., V. M. Ovchinnikov, R. G. Evans, K. U. Akli, H. Azechi, F. N. Beg, C. Bellei, R. R. Freeman, H. Habara, R. Heathcote, M. H. Key, J. A. King, K. L. Lancaster, N. C. Lopes, T. Ma, A. J. MacKinnon, K. Markey, A. McPhee, Z. Najmudin, P. Nilson, R. Onofrei, R. Stephens, K. Takeda, K. A. Tanaka, W. Theobald, T. Tanimoto, J. Waugh, L. VanWoerkom, N. C. Woolsey, M. Zepf, J. R. Davies, and P. A. Norreys, “Effect of Laser Intensity on Fast-Electron-Beam Divergence in Solid-Density Plasmas”, *Phys. Rev. Lett.* 100, 015003 (2008)
- Haas F and PK Shukla “Nonlinear stationary solutions of the Wigner and Wigner-Poisson equations”, *Physics of Plasmas*, 15, 11, 112302, 2008
- Henriques J., E. Tatarova, F. M. Dias, and C. M. Ferreira, “Spatial Structure of a N_2 -Ar Microwave Plasma Source”, *J. Appl. Phys.*, 103, 2008, 103304.
- Jovanovic D, PK Shukla and F Pegoraro “Effects of the parallel electron dynamics and finite ion temperature on the plasma blob propagation in the scrape-off layer”, *Physics of Plasmas*, 15, 11, 112305, 2008

- Kutasi K., B. Saoudi, C. D. Pintassilgo, J. Loureiro and M. Moisan, "Modelling the low-pressure N₂-O₂ plasma afterglow to determine the kinetic mechanisms controlling the UV emission intensity and its spatial distribution for achieving an efficient sterilization process", Plasma Process and Polymers, 5(9) (2008) 840-852.
- Lino da Silva M., V. Guerra, J. Loureiro and P. A. Sá, "Vibrational distributions in N₂ with an improved calculation of energy levels using the RKR method", Chemical Physics, 348 (2008) 187-194.
- Lino da Silva M., Vacher D., Dudeck M., Andre P., and Faure, G., "Radiation From an Equilibrium CO₂-N₂ Plasma in the [250-850 nm] Spectral Region: II. Spectral Modelling", Plasma Sources Science and Technology, Vol. 17, 035013, 2008, pp. 1-9.
- Marques L., H.M. Pinto, A.C. Fernandes, O. Banakh, F. Vaz, M.M.D. Ramos "Optical properties of titanium oxycarbide thin films", Appl. Surface Sci. (in press), <http://dx.doi.org/10.1016/j.apsusc.2008.08.022>
- Martins A.M., "Minimization of a quantum automaton: the transducer", Phys. Rev. A, 78, 062326 (2008), selected for publication on the Virtual Journal of Quantum Information, January 2009 at <http://www.vjquantuminform.org>
- Mendonça J. T., R. Kaiser, H. Terças and J. Loureiro, "Collective oscillations in ultra-cold atomic gas", Physical Review A, 78 (2008) 013408-1-8.
- Mendonça J.T. and L. Stenflo, "Radiation forces between dust grains in a plasma", J. Plasma Phys., 74, 145 (2008)
- Mendonça J.T., A. Serbeto and P.K. Shukla, "Wave kinetic description of Bogoliubov oscillations in the Bose-Einstein condensate", Phys. Lett. A, 372, 2311 (2008)
- Mendonça J.T., E. Ribeiro and P.K. Shukla, "Wave kinetic description of quantum electron-positron plasmas", J. Plasma Phys., 74, 91 (2008)
- Mendonça J.T. and P.K. Shukla, "Effective photon charge in relativistically hot electron-positron plasmas", Phys. Scripta, 77, 018201 (2008)
- Mendonça J.T., "Maxwell and the classical wave particle dualism", Phil. Trans. Royal Soc. A, 366, 1771 (2008)
- Mendonça J.T., R. Bingham and C. Wang, "A new approach to the Sachs-Wolfe effect", Class. Quant. Grav., 25, 095015 (2008)
- Mendonça J.T., R. Kaiser, H. Terças and J. Loureiro, "Collective oscillations in ultracold atomic gas", Phys. Rev. A, 78, 013408 (2008)
- Mendonça J.T., G. Brodin and M. Marklund, "Vacuum effects in a vibrating cavity: time refraction, dynamical Casimir and effective Unruh acceleration", Phys. Lett. A, 372, 5621 (2008)
- Mendonça JT, Serbeto A, Davies JR and Bingham R, Plasmon "kinetics and ion instabilities", Plasma Phys. Control. Fusion 50, 105009 (2008)
- Mendonça JT "Gamma ray sources using imperfect relativistic mirrors", Physics of Plasmas, 15, 11, 113105, 2008
- Nakatsutsumi M., R. Kodama, Y. Aglitskiy, K. U. Akli, D. Batani, S. D. Baton, F. N. Beg, A. Benuzzi-Mounaix, S. N. Chen, D. Clark, J. R. Davies, R. R. Freeman, J. Fuchs, J. S. Green, C. D. Gregory, P. Guillou, H. Habara, R. Heathcote, D. S. Hey, K. Highbarger, P. Jaanimagi, M. H. Key, M. Koenig, K. Krushelnick, K. L. Lancaster, B. Loupias, T. Ma, A. Macphee, A. J. Mackinnon, K. Mima, A. Morace, H. Nakamura, P. A. Norryes, D. Piazza, C. Rousseaux, R. B. Stephens, M. Storm, M. Tampo, W. Theobald, L. V. Woerkom, R. L. Weber, M. S. Wei, and N. C. Woolsey, "Heating of solid target in electron refluxing dominated regime with ultra-intense laser", Journal of Physics: Conference Series 112 022063 (2008)
- Nakatsutsumi M., J. R. Davies, R. Kodama, J. S. Green, K. L. Lancaster, K. U. Akli, F. N. Beg, S. N. Chen, D. Clark, R. R. Freeman, C. D. Gregory, H. Habara, R. Heathcote, D. S. Hey, K. Highbarger, P. Jaanimagi, M. H. Key, K. Krushelnick, T. Ma, A. MacPhee, A. J. MacKinnon, H. Nakamura, R. B. Stephens, M. Storm, M. Tampo, W. Theobald, L. Van Woerkom, R. L. Weber, M. S. Wei, N. C. Woolsey and P. A. Norreys, "Space and time resolved measurements of the heating of solids to ten million kelvin by a petawatt laser", New J. Phys. 10, 043046 (2008)
- Páramos J. and O. Bertolami, "Solar system tests of scalar field models with an exponential potential", Phys. Rev. D 77 (2008) 084014 [arXiv:0710.5702 [astro-ph]]
- Peano F, Vieira J, Silva LO, Mulas R, Coppa G, "All-optical trapping and acceleration of heavy particles", New Journal of Physics 10: Art. No. 033028 MAR 2008
- Peano F, Martins JL, Fonseca RA, Peinetti F, Mulas R, Coppa G, Last I, Jortner J, Silva LO, "Expansion of nanoplasmas and laser-driven nuclear fusion in single exploding clusters", Plasma Physics and Controlled Fusion, 50 (12): Art. No. 124049 DEC 2008
- Peano F, Vieira J., Fonseca R.A., Mulas R., Coppa G., Silva L.O. Direct acceleration of ions with variable-frequency lasers. IEEE Transactions on Plasma Science, 36 (4) pp. 1857-1865 Part 4 AUG 2008
- Santos Sousa J., G. Bauville, B. Lacour, V. Puech M. Touzeau, L.C. Pitchford, "O₂(a¹Δ_g) Production at Atmospheric Pressure by Microdischarge", Appl. Phys. Lett. 93, 011502 (2008)
- Serbeto, J.T. Mendonça, K.H. Tsui and R. Bonifacio, "Quantum wave kinetics of high-gain free electron lasers", Phys. Plasmas, 15, 013110 (2008)

- Shukla N, Shukla PK, Brodin G, Stenflo L “*Ion streaming instability in a quantum dusty magnetoplasma*”, Physics of Plasmas, 15 (4): Art. No. 044503 APR 2008
 - Sircombe M.J., R. Bingham, M. Sherlock, J.T. Mendonça and P.A. Norreys, “*Plasma heating by intense electron beams in fast ignition*”, Plasma Phys. Control. Fusion, 50, 065005 (2008)
 - Tatarova E., F. M. Dias, E. Felizardo, J. Henriques, C. M. Ferreira, and B. Gordiets, “*Microwave plasma torches driven by surface waves*”, Plasma Sources Sci. Technol. 17 024004, 7, (2008)
 - Terças H., J.T. Mendonça and P.K. Shukla, “*Quantum Trivelpiece-Gould waves in a magnetized dense plasma*”, Phys. Plasmas, 15, 072109 (2008)
 - Trines, R.M.G.M., Bingham R., Dunlop M.W., Vaivads A., Davies J.A., Silva L.O., Mendonca J.T., Shukla, P.K., “*Simulation of zonal flow excitation by drift mode turbulence: applications to tokamaks and the magnetopause*”, Plasma Physics and Controlled Fusion, 50 (12): Art. No. 124048 DEC 2008
 - Tzoufras M., Lu W., Tsung, F.S., Huang C., Mori W.B., Katsouleas T., Vieira J., Fonseca R.A., Silva L.O., “*Beam loading in the nonlinear regime of plasma-based acceleration*”, Physical Review Letters, 101 (14): Art. No. 145002 OCT 3 2008
 - Wolf P. et al., Quantum Physics Exploring Gravity in the Outer Solar System: The Sagas project, Exper. Astron. 10.1007/s10686-008-9118-5 [arXiv:0711.0304 [gr-qc]]
 - Vacher D., Lino da Silva M., Andre P., Faure, G., and Dudeck M., “*Radiation From an Equilibrium CO₂-N₂ Plasma in the [250-850 nm] Spectral Region: I. Experiment*”, Plasma Sources Science and Technology, 17, 035012, 1-8, 2008,
 - Valentin C, Gautier J, Goddet JP, Hauri C, Marchenko T, Papalazarou E, Rey G, Sebban S, Scrick O, Zeitoun P, Dovillaire G, Levecq X, Bucourt S, and Fajardo M, “*High-order harmonic wave fronts generated with controlled astigmatic infrared laser*”; JOSA B, Vol. 25, Issue 7, B161-B166 (2008)
 - Vieira JF, Martins SF, Fiuza F, Fonseca RA, Silva LO, Huang C, Lu W, Tzoufras M, Tsung F, Mori WB, Cooley J, Antonsen T, “*Three-dimensional structure of the laser wakefield accelerator in the blowout regime*”, IEEE Transactions on Plasma Science, 36 (4): 1124-1125 Part I Aug 2008
 - Vieira J, Fiuza F, Fonseca RA, Silva LO, Huang C, Lu W, Tzoufras M, Tsung FS, Decyk V, Mori WB, Cooley J, Antonsen T, “*One-to-one full-scale simulations of laser-wakefield acceleration using QuickPIC*”, IEEE Transactions on Plasma Science, 36 (4): 1722-1727 Part 4 Aug 2008
- 26.2.3. Proceedings of international conference**
- Abreu P, Fonseca R, Silva L, “*Migrating large output applications to Grid environments: a simple library for threaded transfers with gLite, Ibergrid — 2nd Iberian Grid Infrastructure Conference Proceedings, Fernando Silva, Gaspar Barreira, Lúgia Ribeiro (Eds), Netbiblo, Spain, 2008, ISBN: 978-84-9745-288-5*
 - Geddes CGR, Bruhwiler L, Cary JR, Mori WB, Vay JL, Martins SF, Katsouleas TC, Cormier-Michel E, Fawley WM, Huang CK, X Wang, B Cowan, Decyk VK, Esarey E, Fonseca RA, Lu W, Messmer P, Mullaney P, Nakamura K, Paul K, G R Plateau, Schroeder CB, Silva LO, Toth C, Tsung FS, Tzoufras M, Antonsen T, Vieira JF, Leemans WP, “*Computational studies and optimization of wakefield accelerators*”, Journal of Physics Conference Series 125: 12002 2008
 - Marti M, Gargaté L, Fonseca RA, Alves LL, Bizarro JPS, Fernandes P, Almeida JPM, Pina H, Silva FM, Silva LO, “*The IST Cluster: an integrated infrastructure for parallel applications in Physics and Engineering*”, Ibergrid — 2nd Iberian Grid Infrastructure Conference Proceedings, Fernando Silva, Gaspar Barreira, Lúgia Ribeiro (Eds), Netbiblo, Spain, 2008, ISBN: 978-84-9745-288-5
 - Peano F, Martins JL, Fonseca RA, Peinetti F, Mulas R, Coppa G, Last I, Jortner J, Silva LO, “*Expansion of nanoplasmas and laser-driven nuclear fusion in single exploding clusters*”, AIP Conference Proc. 1041: 127-130 2008
 - Peano F, “*Expansion dynamics of atomic clusters irradiated by ultraintense lasers*”, Multifacets of Dusty Plasma Book Series: AIP Conference Proc. 1041: 127-130 (2008).
 - Ren, C, Tonge J, Li G, Fiuza F, Fonseca, RA, May J, Mori, WB, Silva, LO, Wang TL, Yan, R, “*Particle-in-cell simulations for fast ignition*”, Journal of Physics Conference Series 125: 12046 2008
 - Sun JH, Gallacher JG, Limos N, Issac R, Dias JM, Huang ZX, Jaroszynski DA, “*High energy terahertz pulse emission from GaAs illuminated by a femtosecond laser*”, Proceedings of SPIE, 6840, 68401B (2008)
- 26.2.4. Invited talks**
- APS April Meeting, St. Louis (USA) April 2008**
- Silva LO, “*Weibel instability in colliding electron-ion-positron flows*”.
- Fifth International Conference on Physics of Dusty Plasmas, Ponta Delgada, Azores (Portugal), May 18 – 23, 2008**
- Peano F, “*Expansion dynamics of atomic clusters irradiated by ultraintense lasers*”.
- Workshop on Techniques for Scientific Mission Monitoring and Data Analysis, ZARM, Bremen, Germany, 21-23 May 2008**
- Bertolami O., F. Francisco, P.S.J. Gil and J. Páramos, “*Estimating radiative momentum transfer through a thermal analysis of the Pioneer Anomaly*”

Workshop PIC Simulations of Relativistic Collisionless Shocks, Dublin (Ireland) May 2008

- Silva LO, "Specific numerical issues in PIC simulations of relativistic shocks"

Institute of Physics Plasma Physics Meeting, London (UK), May 2008

- Silva LO, "From intense lasers to relativistic astrophysics: exploring extreme plasma physics scenarios with numerical simulations"

Calcolo Scientifico nella Fisica Italiana, Rimini (Italy) May 2008

- Silva LO, "From intense lasers to relativistic astrophysics: exploring extreme plasma physics scenarios with numerical simulations"

35th EPS Conference on Plasma Physics, Crete (Greece) June 2008

- Fonseca RA, "One-to-one direct modeling of experiments and astrophysical scenarios: pushing the envelope on kinetic plasma simulations".
- Peano F, "Expansion of nanoplasmats in ultraintense laser-matter interactions".

Workshop on Ultra High-Intensity Laser Nuclear and Particle Physics, ECT Trento, Italy, 23-27 of June 2008.

- Mendonça J.T. "Acceleration mechanisms in the Peta-Watt regime"

International Conference "Laser Optics 2008", St. Petersburg, Russia, 23-28 June 2008.

- Mendonça J.T., "Sliding resonances and photon cascades into the sub-cycle domain"

IWSSPP III "3rd International Workshop & Summer School on Plasma Physics", Kiten, Bulgaria, June 30 – July 5, 2008

- Alvarez R., L. Marques, L.L. Alves "Modeling of an axial injection torch"
- Guerra V., E. Tatarova, F. M. Dias, and C. M. Ferreira, "Kinetic modelling of surface wave discharges in molecular plasmas".

19th Europhysics Conference on the Atomic and Molecular Physics of Ionised Gases (ESCAMPIG XIX), Granada, Spain, 15-19 July, 2008 (hot topic lecture).

- Lino da Silva M., Guerra V., and Loureiro J., "Non-Equilibrium Rates for Atmospheric Entry Studies"
- Wijvliet R., E. Felizardo, E. Tatarova, F. M. Dias, C. M. Ferreira, S. Nijdam, E. Veldhuzen, G. Kroesen, "Exotic Phenomena in Hydrogen Containing Microwave Plasmas".

International Workshop on the Frontiers of Modern Plasma Physics, ICTP Trieste, Italy 14-25 July 2008.

- Mendonça J.T. "New topics in Quantum Plasmas".

DICE 2008, Castiglioncello, Italy, 22–26 September, 2008

- Bastos C., O. Bertolami, N. Dias and J. Prata. "Noncommutative quantum cosmology".

XVII International Symposium on Gas Flow and Chemical Lasers & High Power Lasers, Lisbon, Sep 2008

- Figueira G, "Towards high power, high repetition rate, ultrashort laser pulses"

International Congress on Plasma Physics Fukuoka 2008 (Japan) September 2008

- Silva LO, "White Light Parametric Instabilities"

Conference on Kinetic modeling of astrophysical plasmas Krakow (Poland) October 2008

- Silva LO, "Particle dynamics in relativistic shocks"

3rd US-Japan Workshop on Ultra-Intense Laser-Plasmas and Beam Plasma Interactions, Austin Texas (USA) November 2008

- Martins SF, "Boosted frame PIC simulations of LWFA: Towards the energy frontier".

VI International Workshop em Fisica Molecular e Espectroscopia, Sao Jose dos Campus, Brazil, 5–7 November, 2008

- Tatarova E., "Balmer Lines Broadening in Microwave Plasmas".

1st PRACE Scientific Workshop, ICT 2008, Lyon (France) November 2008

- Fonseca RA, "Full Scale Kinetic Modelling of Laboratory and Astrophysical Plasmas with Petascale Systems"

Workshop on Correlations and Coherence in Quantum Matter, Evora, Portugal, 10-14 November 2008

- Mendonça J.T., "Waves and oscillations in ultra-cold gas"

HEDSA Symposium - High Energy Density Laboratory Plasma Physics: Prospects for a Bright Future, Dallas (USA), November 2008

- Silva LO, "Relativistic shocks: from astrophysics to fast ignition"

Free Electron Laser Seeding Workshop, Frascati, December 2008

- Fajardo M, "High Harmonic Generation below 10 nm"

26.2.5. Regular talks in Conferences

XVII International Symposium on Gas Flow and Chemical Lasers & High Power Lasers, Lisbon, Sep 2008

- Cardoso L, H. Pires and G. Figueira, "Broadband optical parametric chirped pulse amplification with group velocity matching by angular dispersion of chirped pump pulses"
- Wemans J, C.P. João and G. Figueira, "Hybrid ytterbium-neodymium laser chain and scalability to petawatt peak powers"

3rd International Workshop and Summer School on Plasma Physics, Kiten, Bulgaria (2008)

- Álvarez R., L.L. Alves "Electromagnetic modeling of axis-symmetric microwave devices",

XIth International Symposium on High-Pressure Low-Temperature Plasma Chemistry, Oleron Island, France (2008).

- Santos Sousa J., G. Bauville, B. Lacour, V. Puech, M. Touzeau "Atmospheric Pressure Generation of $O_2(a^1\Delta_g)$ by Microplasmas"

61st GEC, Gaseous Electronics Conference, Dallas, Texas, USA (2008); Bull. Am. Phys. Soc. 53,10 (2008).

- Santos Sousa J., G. Bauville, B. Lacour, V. Puech, M. Touzeau, J.-L. Ravanat "Atmospheric Pressure Generation of High Fluxes of Singlet Oxygen for Biological Applications"

26.2.6. Poster contributions

SPIE 7th, International High-Power Laser Ablation, Taos, New Mexico, USA (2008)

- Puech V., G. Bauville, B. Lacour, J. Santos Sousa, L.C. Pitchford, M. Touzeau "Microplasmas as Efficient Generators of Singlet Delta Oxygen"

X^{ème} Congrès de la Division Plasmas de la Société Française de Physique, Paris, France (2008).

- Gregório J., P. Leprince, O. Leroy, L.L. Alves, C. Boisse-Laporte "Etude d'un microplasma micro-onde à pression atmosphérique"
- Santos Sousa J., G. Bauville, B. Lacour, V. Puech, M. Touzeau "Production d'Oxygène Singulet par Microdécharges"

7th Iberian Vacuum Meeting and 5th European Topical Conference on Hard Coatings (O.M.N.D. Teodoro e J.L. de Segóvia, eds.), Caparica, Portugal 2008

- Marques L., L.L. Alves "Modeling of capacitively coupled radio-frequency discharges in nitrogen"

IWSSPP III "3rd International Workshop & Summer School on Plasma Physics", Kiten, Bulgaria, June 30 – July 5, 2008

- Álvarez R., L.L. Alves "Construction of an electromagnetic model for axis-symmetric microwave devices"

- Guerra V., E. Tatarova, F. M. Dias, and C. M. Ferreira, "Kinetic modelling of surface wave discharges in molecular plasmas", Abstracts II.

19th ESCAMPIG, Europhysics Conference on the Atomic and Molecular Physics of Ionised Gases (F.J. Gordillo-Vázquez et al, eds.), Granada, Spain (2008).

- Álvarez R., L.L. Alves "Two-dimensional hydrodynamic model of a microwave plasma torch", CD-Proceed. and Book of Abstracts

- Felizardo E., E. Tatarova, F. M. Dias, C. M. Ferreira, S. Nijdam, E. Veldhuzen, G. Kroesen, "Exotic Phenomena in Hydrogen Containing Microwave Plasmas".

- Gregório J., R. Álvarez, C.Boisse-Laporte, L.L.Alves "Fluid modeling of a microwave micro-plasma at atmospheric pressure", CD-Proceed. and Book of Abstracts

- Gregório J., L.L.Alves, P. Leprince, O. Leroy, C.Boisse-Laporte "Study of a microwave micro-plasma reactor at atmospheric pressure", CD-Proceed. and Book of Abstracts

- Kutasi K., V. Guerra, P. A. Sá and J. Loureiro, "Active species in Ar-O2 microwave flowing post-discharges"

- Kutasi K., B. Saoudi, C. D. Pintassilgo, J. Loureiro and M. Moisan, "UV radiation spatial distribution in N2-O2 post-discharges used for sterilization"

- Lino da Silva M., V. Guerra and J. Loureiro, "Nonequilibrium dissociation rates for atmospheric entry studies"

- Lino da Silva M., V. Guerra and J. Loureiro, "Modelling of rotational nonequilibrium in low-pressure, high-temperature plasma flows",

- Marques L., C.D. Pintassilgo, G. Alcouffe, G. Cernogora, L.L. Alves "Modeling of nitrogen ccrf discharges used to study titan's atmosphere", CD-Proceed. and Book of Abstracts

- Pintassilgo C.D. and J. Loureiro, "Kinetic study of an afterglow plasma for simulation of Titan's atmosphere"

- Santos Sousa J., G. Bauville, B. Lacour, V. Puech, M. Touzeau "Singlet Oxygen Production at Atmospheric Pressure by Microplasmas", CD-Proceed. and Book of Abstracts

- Wijvliet R., E. Felizardo, E. Tatarova, F. M. Dias, C. M. Ferreira, S. Nijdam, E. Veldhuzen, G. Kroesen, "Exotic Phenomena in Hydrogen Containing Microwave Plasmas", Hot Topic HT1.

XIth International Symposium on High-Pressure Low-Temperature Plasma Chemistry, Oleron Island, France (2008).

- Santos Sousa J., G. Bauville, B. Lacour, V. Puech, M. Touzeau "Atmospheric Pressure Generation of $O_2(a^1\Delta_g)$ by Microplasmas"

- Makasheva K., G.J.M. Hagelaar, J.-P. Bœuf, Th. Callegari, J. Santos Sousa, V. Puech, E. Munoz-Serrano, L.C. Pitchford "Plasma Properties of Microcathode Sustained Discharges in Argon at Atmospheric Pressure"

61st GEC, Gaseous Electronics Conference, Dallas, Texas, USA (2008)

- Gregório J., P. Leprince, O. Leroy, L.L. Alves, C. Boisse-Laporte, "Study of a microwave micro-plasma reactor at

atmospheric pressure”, Proceed. Bull. Am. Phys. Soc. 53, 10 (2008).

- Gregório J., R. Álvarez, C. Boisse-Laporte, L.L. Alves “*Fluid modeling of a microwave micro-plasma at atmospheric pressure*”, Proceed. Bull. Am. Phys. Soc. 53, 10 (2008).
- Santos Sousa J., G. Bauville, B. Lacour, V. Puech, M. Touzeau, J.-L. Ravanat “*Atmospheric Pressure Generation of High Fluxes of Singlet Oxygen for Biological Applications*”, Proceed. Bull. Am. Phys. Soc. 53, 10 (2008).
- Santos Sousa J., B. Eismann, S. Pancheshnyi, L.C. Pitchford, V. Puech “*Experimental and Theoretical Investigations of Singlet Oxygen Production by High-pressure Microdischarges*”, Proceed. Bull. Am. Phys. Soc. 53, 10 (2008).

XVII International Symposium on Gas Flow and Chemical Lasers & High Power Lasers, Lisbon, Sep 2008

- Pires H, L. Cardoso, J. Wemans, C. João and G. Figueira, “*High efficiency diode-pumped parametric amplification of optically synchronized pulses*”
- Figueira G, N. Lopes, H. Pires, M. Fernandes, J. Wemans, L. Cardoso, T. Imran and N. Cornet, “*Focal spot improvement of a chirped pulse amplification laser by using a single actuator mechanical deformable mirror*”
- João C P, J. Wemans, G. Figueira, “*Numerical comparison of pulse amplification in ytterbium-doped media*”
- Fernandes M, G. Figueira, “*Spatio-temporal distortions in chirped pulse amplification grating compressors*”

3rd International Workshop on Radiation of High Temperature Gases in Atmospheric Entry, Heraklion, Greece, 30 Sep.-3 Oct. 2008

- LeQuang D., Lino da Silva M., Passarinho F., and Dudeck M., “*Simulation of High Enthalpy Flows With Non Equilibrium Effects (Earth, Mars and Titan Type Conditions)*”
- Lino da Silva M., “*A Reinvestigation of CO₂ Radiation in the UV-Visible and IR Range*”
- Lino da Silva M., Sobbia R., and Witasse O., “*MARS EXPRESS Onboard Tracking of the PHOENIX Entry Plasma Plume: Simulation and Mission Outcome*”

5th International Conference on the Physics of Dusty Plasmas, Ponta Delgada-Azores (Portugal) 2008

- Gattobigio G. L., F. Michaud, G. Labeyrie, J. Loureiro, J. T. Mendonça, T. Pohl, H. Terças and R. Kaiser, “*Long range interactions with laser cooled neutral atoms*”; AIP Conference Proceedings, vol. 1041, p. 17-20.

VI International Workshop em Física Molecular e Espectroscopia, São José dos Campus, Brazil, 5 – 7 November, 2008

- Tatarova E., “*Balmer Lines Broadening in Microwave Plasmas*”.

3rd European Planetary Science Congress, Munster (Germany) 2008.

- Loureiro J. and C. D. Pintassilgo, “*Production of N-containing hydrocarbon species in an afterglow plasma for simulation of Titan's atmosphere*”

26.2.6. Seminars

- Alves L.L., “*Modelisation d'une Torche à Injection Axiale*”, LPGP, Orsay, France, February 2008.
- Gregório J., “*Microwave micro-plasmas at atmospheric pressure*”, IPFN, Lisbon, Portugal, December 2008
- Santos Sousa J., “*Atmospheric pressure generation of singlet oxygen by micro-plasmas*”, IPFN, Lisbon, Portugal, December 2008

26.2.7. Numerical codes

- Alvarez R, Marques L, Alves LL, “*Two-dimensional hydrodynamic model (including heating module) for the transport of a neutral gas in high-flow regime*”
- Gregorio J, Álvarez R, Alves LL, “*One-dimensional fluid model for argon Microwave Micro-Plasmas*”

26.2.8. Laboratorial Prototypes

- Dias F.M., E. Tatarova, E. Felizardo “*Microwave plasma torch operating in air-water*”
- Dias F.M., E. Tatarova, E. Felizardo “*Atmospheric pressure plasma torch for bacteria sterilization*”
- Dias F.M., E. Tatarova, E. Felizardo “*500 MHz microwave discharges-spectroscopy and radiophysics investigations*”

26.2.9. Board of Scientific Journals

- Alves LL, European Physical Journal – Applied Physics (EDP Sciences, ed.), Associated Editor (Section “Plasmas discharges and processes”)

26.2.10. MSc thesis completed in 2008

- Hugo Manuel da Silva Pereira Pinto, “*Estudo das Propriedades Físicas do Oxicarboneto de Titânio Usando a Teoria do Funcional da Densidade*”, Universidade do Minho, Supervisor: Marques L.

26.2.11. Projects/Funding Awarded in 2008

- Alves LL, “*Simulation Tools for Atmospheric Pressure Microwave-Driven Mini-Plasmas*”, Fundação para a Ciência e a Tecnologia (Portugal), PTDC/FIS/65924/2006, starting date: September 2008

26.2.12. Supervision and training

- Rafael Álvarez, “Two-dimensional model of microwave plasma produced by an Axial Injection Torch”, Post-Doctoral researcher (FCT-SFRH/BPD/26420/2005), Supervisor: Alves LL
- José Gregório, “Micro-wave system for the production of mini-plasmas at atmospheric pressure”, PhD student (FCT-SFRH/BD/29294/2006), Supervisors: Alves LL and Boisse-Laporte C
- João Santos e Sousa, “Micro-hollow cathod discharges for the production of intense flows of reactive species”, PhD student (FCT-SFRH/BD/28668/2006), Supervisors: Alves LL and Puech V
- Hugo Manuel da Silva Pereira Pinto, “Estudo das Propriedades Físicas do Oxicarboneto de Titânio Usando a Teoria do Funcional da Densidade”, MSc student, Supervisor: Marques L.
- Tatarova E., C. M. Ferreira, Jose Munoz (Cordoba Spain) *Atmospheric pressure Ar plasma numerical simulation: a code for self-consistent description of electron kinetics, plasma thermodynamics, air-water chemical reactions and wave electrodynamics.*
- Tatarova E., C. M. Ferreira, B. Gordiets, *numerical simulation of water vapor plasma at low-pressure conditions.*
- Tatarova E., C. M. Ferreira, B. Gordiets, *numerical simulation of “hot” atoms generation in hydrogen plasmas at low-pressure conditions.*

26.2.13. Master thesis supervised

- Ruud Vijtvet “Spectroscopic Measurements of Low-Pressure Hydrogen Microwave Plasmas (2008) (Eindhoven University of Technology, Eindhoven, The Netherlands)

26.2.14. Courses

Alves LL, “Electron Kinetics in Atomic and Molecular Plasmas” (2.5h lecture) and “Fluid Modeling of Discharge Plasmas” (1.5h lecture), 13th European Summer School Low Temperature Plasma Physics: Basics and Applications, Bad Honnef, Germany, October 2008

26.2.15. Consulting

- Alves LL, Programme National en Nanosciences et Nanotechnologies (PNANO), consultant on Plasma modelling and simulation for material treatment, Agence National de la Recherche (ANR), France

26.2.16. Organizing Committees of Conferences

- Alves LL, member of the Program Committee with the 21st ICNSP, International Conference on the Numerical Simulation of Plasmas, Lisbon, 6-9 October 2009
- Alves LL, member of the International Scientific Committee with the CIP, International Colloquium on Plasma Processes (next edition: Marseille, 22-26 June 2009)

26.2.17. Computer Codes

- Felizardo E., E. Tatarova, M. Silva, *numerical code for simulation the fine structure of hydrogen lines and fitting of experiental emission profiles*
- Tatarova E., C. M. Ferreira, B. Gordiets, *Air-water plasma numerical simulation: a code for self-consistent description of electron kinetics, plasma thermodynamics, air-water chemical reactions and wave electrodynamics.each sensor and using different radial basis functions that can be adapted to different magnetic configurations.*

27. ANNEX I - COMPOSITION OF THE MANAGEMENT BODIES IN 2008

1. *Directive Board:*

C. Varandas (President), F. Serra and L.O. Silva (Vice-Presidents), B. Gonçalves and L.L. Alves.

2. *Scientific Commission (C4):*

C. Varandas, L.O. Silva, F. Serra, L.L. Alves, B. Gonçalves, H. Fernandes, M.E. Manso, J.P. Bizarro, J. Sousa, C.M. Ferreira, J.T. Mendonça, O. Bertolami and V. Guerra.

3. *External Advisory Panel:*

F. Wagner, W. Sandner and D.C. Schram.

4. *Steering Committee of the Contract of Association EURATOM-IST:*

Y. Capouet, R. Giannella, E. Rille, J. Sentieiro, C.M. Ferreira and J. Santos-Victor.